Identification of Structural Systems from Measured Response

By

Mohammad-Reza Banan

and

Keith D. Hjelmstad

A report to sponsors:
The Army Research Office
The National Science Foundation

Department of Civil Engineering
University of Illinois at Urbana–Champaign
Urbana, Illinois

May 1993

50272-101

REPORT DOCUMENTATION PAGE	1. REPORT NO. UILU-ENG-93-2002	2.	3. PB94-162567

4. Title and Subtitle

Identification of Structural Systems from Measured Response

5. Report Date: May 1993

6.

7. Author(s)

Mohammad-Reza Banan and Keith D. Hjelmstad

8. Performing Organization Rept. No: SRS 579

9. Performing Organization Name and Address

Department of Civil Engineering
University of Illinois
205 N. Mathews Avenue
Urbana, Illinois 61801

10. Project/Task/Work Unit No.

11. Contract (C) or Grant (G) No.
(G) *CES 86-58019 (NSF)*
DAAL-03-87-K-006 (ARO)
DAAL-03-86-G-0186 (ARO)
DAAL-03-86-K-0188 (ARO)

12. Sponsoring Organization Name and Address

National Science Foundation, Washington D.C.

Army Research Office, Washington D.C.

13. Type of Report & Period Covered

14.

15. Supplementary Notes

16. Abstract (Limit 200 words)

This report presents an approach to the problem of parameter estimation of finite element models of complex structural systems using measured response. The method computes the element constitutive parameters of a finite element model of a structure by finding a constrained nonlinear minimum of the difference between the measured response of the real structure and the computed response of a finite element model of the structure. Constraints are used to bound the constitutive parameters. The optimization problem is solved by the method of Recursive Quadratic Programming. A simple and straightforward method of computing the gradient of the loss function on an element-by-element basis is presented.

The method presented herein has been implemented as a general purpose parameter estimation program for structural systems. This program has all the flexibilities of a general purpose finite element package in that it can treat complex structures with different topologies, geometries. and element types. It is suited to static. modal dynamic. or forced dynamic response, sparsely sampled in space, time, and state. We consider both an equation-error estimator and an output-error estimator for the static and modal dynamic problems. and an equation-error estimator for the forced dynamic problem.

Monte Carlo simulation is used to study the behavior of the parameter estimation algorithms in the presence of noise in the measurements. Extensive simulations are carried out for both the static and forced dynamic cases. A case study, using real field measurements is presented for the modal dynamic case.

17. Document Analysis a. Descriptors

System identification, parameter estimation, optimization, least-squares. structures, dynamics

b. Identifiers/Open-Ended Terms

c. COSATI Field Group

18. Availability Statement	19. Security Class (This Report): Unclassified	21. No. of Pages: 176
	20. Security Class (This Page): Unclassified	22. Price

(See ANSI-Z39.18) see instructions on reverse

OPTIONAL FORM 272 (4-77)
(Formerly NTIS-35)
Department of Commerce

Acknowledgments

The authors thank Mahmoud-Reza Banan, the first author's brother, for his valuable contributions to this work on parameter estimation of structural systems. Without the thoughtful and provocative discussions that he not only participated in but often fostered, this work would be diminished. He has helped us immeasurably in charting our way through the difficult topographies of the loss functions associated with these minimization problems.

The research reported herein was supported by the U. S. Army Research Office, as part of a program at the University of Illinois Advanced Construction Technology Center (grant numbers *DAAL 03-87-K-006*, *DAAL 03-86-G-0186*, and *DAAL 03-86-K-0188*), and the National Science Foundation (grant number *CES 86-58019*). Joseph P. Murtha is the director of the Advanced Construction Technology Center and S.-C. Liu is the cognizant program officer at the National Science Foundation. The support of these agencies is gratefully acknowledged. The results, opinions, and conclusions expressed in this report are solely those of the authors and do not necessarily represent those of the sponsors.

TABLE OF CONTENTS

CHAPTER ONE

Introduction

Maintenance, inspection, and repair of existing structural systems is a multi-billion dollar industry. Dunker and Rabbat (1993) estimate that over forty percent of the nearly half million existing highway bridges in the United States are deficient. The projected cost of restoring all of these deficient highway bridges is about $90 billion. Housner, *et al* (1990) suggest that a single earthquake in California could cause in excess of $100 billion in damage to buildings, bridges, dams, and lifeline facilities. The construction and maintenance costs of pavements in the United States are more than $30 billion per year. These illustrations of the great costs associated with maintaining the integrity of our civil infrastructure are only the tip of the iceberg because they include only the direct costs of physical replacement or repair. Many billions of dollars are lost every year indirectly due to inadequate maintenance of structures; the cost of interrupted services after a natural disaster could be astronomical. New methods for the evaluation of structural condition need to be developed to help manage these maintenance problems.

A structural system must endure many different events during its lifetime that may not have been anticipated in its original design. It might experience new loads, modifications, or damage. In making decisions about the maintenance of a structure, one needs information about its past performance and its current condition. One also needs a method to create a likely scenario of its future performance. For rehabilitation of a structural system one often needs to model the current behavior of the system in order to successfully modify the structure to meet new design criteria. Engineering models of structural behavior have proven to be very useful in making such performance estimates.

Very few structural systems can be adequately modeled using theory alone; there are always parameters in an analytical model, particularly constitutive parameters, whose values must be assumed or empirically determined. Physical testing of a structure often provides valuable information that a theory cannot provide. However, test data are often incomprehensible without a theoretical framework to aid the data reduction. System identification and parameter estimation are the natural tools for bridging the gap between an analytical model and test data.

To build a mathematical model we begin with generally accepted physical laws. In structural mechanics these laws include balance of linear and angular momentum, kinematics of deformation, and the constitutive behavior of materials. The governing equations, based upon those things that we know well, provide the structure for our identification model. The aspects of the model that we do not know are parameterized and left to be estimated from the data. In the test we seek to excite the structure in a manner that will encourage a mode of response that will help the most in identifying the parameters of our model. Also, we try to measure

those quantities that are most indicative of the structural characteristics. It is often important to make those measurements as accurate as possible.

Here we shall limit our context to linear analytical models. Further, we assume that the structure is amenable to discretization using the finite element method. Even though we know that, in general, a real structural system will behave nonlinearly, one can often justify such a limitation by observing that a linear model is the first order approximation of any nonlinear system and that most structures respond linearly over some reasonably interesting range of excitation. Clearly, not all problems can be approached this way. For example, many kinds of damping cannot be represented with a linear model. Fortunately, a linear approximation yields valuable information for many structural systems .

One of the greatest challenges in performing a test on a large structural system lies in exciting the structure. There are probably as many choices of excitation as there are structures, but most would be examples of three general classes: *(a)* static, *(b)* modal dynamic, and *(c)* transient dynamic. In a static test loads are applied slowly so that inertial effects are negligible. The generation of large enough loads for certain types of structures is difficult, and thus static tests are probably most appropriate for laboratory experiments. A modal dynamic test relies on resonant excitation of the structure. The dynamic magnification at resonance for lightly damped structures is easily accomplished with a modest force. Such a force might be generated by rotating an eccentric mass at a fixed resonant frequency. Many modes can be excited by resonance, provided the integrity of the connection between the structure and the exciting device is not compromised by the motion. Some modal tests use free vibration data, generated, for example by imparting an initial displacement or an initial velocity to the structure. Imparting an initial displacement is easily done in a laboratory, but may be impossible in the field. Imparting an initial velocity can be accomplished using falling weights or by impulsive forces generated by explosive cartridges or small rockets. For most structures, only the lowest few modes of vibration can be excited in free vibration. A transient dynamic test relies on motion of the structure from some known cause. Motion of the structure can be induced by impact, by forced motion of an attached device, or by forced motion of the foundation. An earthquake can be used as a structural dynamic test if the record of the ground acceleration at the base of the structure is accurately known. Large explosions can also generate ground motions and therefore can be considered as possible dynamic tests excitations. The main problem in a transient dynamic test is accurately measuring the forcing function.

In this research study we focus on parameter estimation of linear structural systems and propose algorithms to minimize the gap between the measured response from the structure and computed responses of the parameterized analytical model of that structure. In particular, we focus on analytical models wherein the topology and geometry of the structure are assumed to be known, while the constitutive properties are parameterized and estimated from the test measurements.

1.1. System Identification: General Concepts

In the field of science and engineering, observing the behavior of a system and measuring its input-output pairs are fundamental tools for building a model for the system. In general, model building is a mapping problem from a data set of input-output pairs to a set of candidate models and is defined by the identification process (Ljung 1982). The identification process tries to construct a model for a system or improving the existing

model of a system based on some available observations, and any *a priori* knowledge about the system. The identified model provides physical insight about the system and consequently leads to simulating or predicting the response of the system.

System identification is defined by Zadeh (1962) as "the determination on the basis of input and output, of a system within a specified class of systems, to which the system under test is equivalent." Elements of the specified class of systems are models which have the same structure with different parameters. Equivalence is defined by an error or loss that is a function of the process and the model input and output. If the value of the loss function is the same for two models, then they are equivalent. *Parameter estimation* is defined as the determination of values of the parameters that govern the behavior of the model, assuming that the structure of the model is known (Eykhoff 1974).

The use of system identification for deformable mechanical systems dates back to the late 1950's. At that time the airplane industry was performing many tests on real airplanes to measure the overall behavior of an airplane as well as the behavior of various of its components. These experiments were very expensive and relatively time consuming. On the other hand, existing analytical models were not able to reconcile the test measurements to the desired level of accuracy. The gap between theory and experiment pushed the industry to look for methods to improve their analytical models. System identification had already been used in other fields of engineering and held great promise as a tool for simulating and/or predicting the behavior of deformable mechanical systems.

The most significant evolution in identification methods was initiated in the field of automatic control around 1960. At that time, existing control theories had solutions for many complicated control problems, but no one knew how to build mathematical models that contained the essential properties of the systems. Exploiting the concept of system identification afforded improvements in the mathematical models and thus paved the way for further progress in control. Since that time, system identification has evolved a great deal, and has been applied in many fields of science and engineering; from automatic control to seismic experiments and from speech recognition to social economic systems.

The process of system identification consists of three main stages; *(1)* defining a model and arranging some experiments to measure the response of the system (model selection), *(2)* using the chosen model and the measured response to estimate the unknown parameters of the model (parameter estimation), and finally *(3)* validating and refining the model if necessary (diagnostic check).

The choice of the model. A model is a representation of the essential aspects of a system that contains knowledge of that system in a usable form (Eykhoff 1974). Model selection is basically governed by three choices: *(1)* the candidate class of models, *(2)* the structure and size of the chosen model, and *(3)* parameterization of the chosen model. The intended use of the model usually dictates the class of the model. Choosing the size of the model is not a trivial problem because the model is often a representation of an unknown process. The model should include only the essential features of the real system to avoid introducing unnecessary complication. The parameterization of the model should be guided by three important objectives (Niedertinski and Hajdasinski 1979): *(1)* the parameterization should be universal, *i.e.* the model should be applicable to all systems in the same class, *(2)* the number of parameters should be in accord with the limited information

available, and *(3)* the model should be identifiable from the available information. Some of the well-known mathematical models used in system theory include autoregression (AR), moving average (MA), impulse response, Voltera series, Markov chains, autoregression-moving average (ARMA), matrix fraction description (MFD), state-space representations, the Hankel representation, and the transfer matrix representation (Hajdasinski, *et al.* 1982).

Experiment design. The main goal of designing an experiment is to provide maximum information about the parameters of the system to be identified. There are many factors involving in the design of an experiment. These include the intended application of the results, prior knowledge about the system, the structure of the model, the measure of equivalence to the real system, the parameter estimation method, and the operational constraints of the system. Many procedures for designing a good experiment have been suggested in the literature (Goodwin 1982).

Parameter estimation. The essence of building a model for a real system is its capability to simulate and/or to predict the behavior of the system. The performance of the model can be evaluated by an loss function that indicates how well the model fulfills the intended tasks. It is natural to minimize the discrepancy between the model and the system by tuning the parameters of the model. The essence of parameter estimation is to find parameters which minimize a scalar measure of discrepancy known as the criterion of equivalency or loss function. A procedure for estimating parameters is referred to as a parameter *estimator.* In the statistical literature, a number of different estimators have been developed. These methods differ predominantly in the criterion of equivalency and in the use of available prior information about the statistics of the measurements and the parameters. There are three popular estimators in the field of system identification: *maximum-likelihood, Bayesian,* and *cross-entropy* estimators. The famous class of *least-squares* estimators is the subset of maximum-likelihood estimators that does not require knowledge of the probability density of the measurements or the parameters. The class of weighted or Gauss-Markov least-squares estimators is a superset of the least-squares method that makes optimal use of the known variability of the measurements.

There are two basic approaches for estimating the parameters: the *off-line* or *batch* method and the *on-line* or *recursive* method. In the batch approach the computational operations are carried out on the complete set of measurements as a whole. Another way of processing the measurements is to continuously update the estimation of parameters while working serially through the measurements. The recursive approach generates an updated estimation as it receives new information. The batch method is computationally more efficient and robust than the recursive method. However, recursive methods are popular in the field of control and automation because they do not require the storage of raw data. Matko and Schumann (1982), and Goodwin (1984) reported on families of recursive methods namely: least squares, instrumental variable, maximum likelihood projection, output error, and stochastic methods.

Model validation. A model obtained from the identification process has to be validated to ensure that it describes the system suitably for its intended application. Model testing is the most difficult phase of the identification process and can be very subjective. In general, there are two approaches to examine the identified model. Compare the results of the model with the results of the best models from the other classes of models, or decide whether the properties of the model meet some reasonable requirements such as cross-val-

idation, residuals, and consistency with *a priori* knowledge not used in the estimation. Model validation is subjective and, regardless of the validation criteria, one must judge for one's self to what extend the model really explains the behavior of the system.

1.2. System Identification in Structural Mechanics

Model building is a fundamental concept in the natural sciences and engineering because of the importance of experiments and measurements in these fields. The procedure for building a mathematical model starts with the application of basic physical laws (*e.g.* the governing laws of mechanics) to the system or process being studied. From these laws, a number of relations among the inputs and outputs of the system follow and establish the structure of the mathematical model. These relations often take the form of algebraic equations, ordinary or partial differential equations, or integral equations. If all external and internal conditions of the system are quantitatively known and if the physical knowledge about the system is complete then, at least in principle, the numerical values of all parameters in those relations can be determined. For non-chaotic systems finding an appropriate mathematical model based on this procedure may be difficult even in a narrow field of application because information is limited by incomplete or uncertain knowledge of the environment or the physical aspects of the system.

System identification and parameter estimation in mechanical sciences and structural engineering have become increasingly important areas of research in the last three decades. Identification methods have been used to establish mathematical models or to improve existing models. Many nondestructive testing methods are based on the concepts of system identification and parameter estimation. Identification has been used for structural monitoring of load carrying systems such as aircraft, space structures, buildings, bridges, offshore platforms, and mechanical systems (Cawley 1985; Chen and Garba 1987; Stubbs, *et al.* 1989; Natke 1989; Hajela and Seiro 1990; Ismail, *et al.* 1990). In offshore structures, attempts have been made to assess structural damage from changes in the frequency spectrum of the structure to ambient excitations (Vandiver 1975; Duggan, *et al.* 1980; Kenley and Dodds 1980; Coppolino and Rubin 1980). Engineers have been attracted to such methods because of the extreme difficulty and expense of under-water inspection. The aerospace and automotive industries extensively use identification techniques to verify or improve mathematical models for subsequent use in simulation, design, and control studies (Thoren 1972; Collins, *et al.* 1974; Sheena, *et al.* 1982; Flannelly and Berman 1983; Hashemi-Kia 1988; Kammer, *et al.* 1988; Stubbs, *et al.* 1989; Jiang, *et al.* 1990; Holkamp and Batill 1991).

Mathematical model building has been used frequently for parameter estimation of buildings. Typically, system identification is used to model existing structures (Hart and Yao 1977; Torkamani and Ahmadi 1988), assess structural changes in buildings after earthquakes (Distefano and Pena-Pardo 1975 and 1976; Beck 1982; Distefano and Cakmak 1990), evaluate seismic vulnerability of existing buildings (Ho and Aktan 1989; Aktan and Ho 1990), and identify critical collapse mechanisms of structures (Ellis, *et al.* 1990). Parameter estimation has been used to evaluate performance of bridges from ambient, earthquake, and force transient responses (Melamore, *et al.* 1971; Douglas and Reid 1982; Flesch and Kernbichler 1988; Werner 1989; Raghavendrachar, *et al.* 1991). Another area of application for identification techniques is the condition monitoring of machines to enhance the efficiency of their maintenance and operation (Zimoch 1987; Tustin and Mercado 1985; Foster

and Mottershead 1990; Mottershead 1990). Mathematical models have been derived to describe the mechanical behavior of composite materials (Hashin 1983; Zhang and Evans 1988; Courage, *et al.* 1990; Soiero and Hajela 1990). These models try to deal with characteristic mechanical behavior including anisotropy, viscoelasticity, and deterioration phenomena like debonding or delamination.

1.3. Objectives and Scope

Although identification techniques have been extensively developed in system science, identification of complex structural systems presents many new problems. In particular, we often know a great deal about our systems, but we are often rather limited in our opportunities to observe their responses. Our models often contain regions that are inaccessible, but are important to the response. Data cannot be collected at those locations. Instrumentation is currently expensive and difficult to deploy. As a consequence data are usually sparsely distributed in space. Incompleteness of measurements and inadequacy of the model are enemies of any identification process. Incomplete measurement of the response with respect to time and space and noise in measurements reduce the amount and reliability of the available data (Young 1970; Berman and Flannelly 1971; Wang 1988; Lee and Chen 1989; Mottershead 1990). On the other hand, the approximate nature of the mathematical model and the inexact material modelling compromise the suitability of the model (Leonard and Khouri 1985).

While accurate and efficient numerical methods have been developed for the analysis of direct problems (*e.g.* given the model and the loading, estimate the response), analogous techniques for inverse problems (identification) have not yet achieved the same level of generality and reliability. In this research study we present a general approach for computing the constitutive parameters of finite element models of complex structural systems. We choose finite element models because finite element analysis is a well-established field that provides generality and flexibility in developing algorithms and civil engineers are familiar with this tool. We study the above-mentioned problems and develop algorithms suitable for complex structural systems with minimal required data.

This manuscript consists of nine chapters and two appendices. Chapter Two provides a general framework for our approach to parameter estimation of complex structural systems. We outline our least-squares formulation for all of the specific cases examined in this work; we describe the recursive quadratic programming algorithm, which we use throughout to solve our problems of constrained minimization; and we discuss the essential elements of simulation and statistics necessary to interpret the examples provided herein. In Chapter Three we develop and *equation-error estimator* and an *output-error estimator* for the static problem. We study the behavior of these estimators via simulation on a bowstring truss structure in Chapter Four. In Chapter Five, we modify the static estimators to treat modal data. In Chapter Six, the modal estimators are applied to the problem of building a mathematical model for a building that was damaged during the 1989 Loma Prieta earthquake, and for which forced vibration test results were available. In Chapter Seven, we present the theoretical foundations for an *equation-error estimator* for transient dynamic response. We study the behavior of this estimator through simulation in Chapter Eight. Chapter Nine is a summary. Appendix A covers the local optimization technique we have used in this study, and Appendix B covers the computation of element sensitivities necessary for all of the algorithms.

CHAPTER TWO

Structural Modeling Based on Test Data

For structural systems, a mathematical model can be constructed from conditions of equilibrium, kinematics of deformations, and material constitutive requirements. The mathematical model can be further processed by numerical tools such as the finite element method, the finite difference method, or the boundary element method. Because our structures generally comprise many interconnected elements we shall refer to them as *complex systems*. Using data from a static, forced transient, or free, undamped vibration experiment on the structure, parameter estimation techniques can be used to adjust the parameters of the model so that the model will best represent the actual performance of the structure during that evaluating experiment. The parameters may include the constitutive properties (stiffness, mass, and damping), the geometry of the structure (positions of the nodes), or the degree of boundary restraint. Here we will focus only on the identification of constitutive parameters.

In this study we will propose an approach to parameter estimation of finite element models of structural systems. We formulate the parameter estimation problem as one of constrained minimization of the difference between measured response and response estimated by the parameterized model. The first, and most fundamental, class of problems that we shall consider is the equilibrium of a structure subjected to static loads, (Chapters Three and Four). The second class is the equilibrium of a structure in free, undamped vibration, (Chapters Five and Six). And the third class is the transient, damped motion of a structure subjected to dynamic loads, (Chapters Seven and Eight). We have endeavored to develop a unified approach to these discrete inverse problems with a particular view toward evolving methods that are amenable to large-scale computation.

The primary goal of this chapter is to describe our approach to the parameter estimation of mathematical models of structural systems and to derive the relationships required for the proposed algorithms. We will refer back to these derived equations in the subsequent chapters.

We begin the chapter by presenting the equilibrium equations for a mathematical model of a structure for static excitation, for undamped free vibration, and for damped, forced dynamic motion. We then propose our basic approach, that is, nonlinear constrained optimization, to estimate the constitutive parameters of the model using some measured input-output pairs of the real structural system. Next, we present an algorithm, recursive quadratic programming, to solve the constructed optimization problem. Finally, we present a frame work for simulation to study the behavior of the proposed algorithm. We use this simulation environment in Chapters Four and Eight to investigate the statistical properties of the algorithm for the static and forced dynamic cases, respectively.

2.1. Governing Equations

Static equilibrium. The equation governing the static equilibrium of a structure with n_d degrees of freedom can be expressed as

$$K(x)u = f \tag{2.1}$$

where $K(n_d \times n_d)$ is the stiffness matrix, parameterized by vector x with n_p components, $f(n_d \times 1)$ is the vector of equivalent nodal forces, and $u(n_d \times 1)$ is the vector of nodal displacements. The direct problem (analysis) is characterized by knowing the parameter vector x (and thus the matrix K), and has the goal of determining unknown portions of displacement u and force f from known portions of u and f. The direct problem is well posed if the known and unknown portions of the force and displacement vectors are disjoint (one can only know force or motion *a priori* at a point, not both), and it has a unique solution if the matrix K is positive definite. The estimation problem is different from the direct problem in that we are given samples of u and f with the goal of determining x. In the inverse problem, a single pair (u, f) is usually not sufficient to uniquely determine the parameters x, even if those vectors are consistent with a unique solution to some direct problem; in fact, they will constitute solutions to an entire set of direct problems. The question of how much data (*i.e.* how many pairs of u and f, and how many components of each) are required to adequately determine x is a central issue in this work.

Free, undamped vibration. The governing equation for free, undamped vibration of a structure is an eigenvalue problem which can be stated in discrete form as

$$K(x)u = \lambda M(x)u \tag{2.2}$$

where the $(n_d \times n_d)$ matrices K and M represent structural stiffness and mass, respectively, and the eigenvalue λ represents the square of the natural frequency of the mode whose deformed shape is represented by the eigenvector u. Here, we assume that the mass and stiffness parameters are lumped in the parameter vector x. The direct eigenvalue problem gives rise to at most n_d independent solution pairs (λ, u), for a positive definite M and a positive semi-definite K. The inverse problem not only requires more than a single eigenpair (λ, u), but also needs an equality constraint on the parameters of the model, to yield a unique solution.

Transient, forced dynamics. The discrete form of the governing equation for the transient damped motion of a structure subjected to dynamic loads can be written as

$$M(x)\ddot{u}(t) + C(x)\dot{u}(t) + K(x)u(t) = f(t) \tag{2.3}$$

where, in addition to those terms already defined, $C(n_d \times n_d)$ is the damping matrix, and $\ddot{u}(t)$, $\dot{u}(t)$, and $u(t)$ are state vectors representing nodal accelerations, velocities, and displacements. Here, we assume that the mass, damping, and stiffness parameters are lumped in the parameter vector x. The direct and inverse problems are like the direct and inverse static problems, except that the response and loading are time dependent. The static inverse problem is much easier to formulate and solve than the dynamic inverse problem;

however, it is generally much easier to excite a structure dynamically than statically. Consequently, methods of testing based on dynamic excitation are much more practical and popular than those based on static excitation. From a theoretical point of view, the distinction is less clear. We will show that the static, modal dynamic, and transient dynamic inverse problems can be cast into a unified format as constrained nonlinear optimization problems.

2.2. Parameter Estimation as an Optimization Problem

To provide a unified approach toward the parameter estimation problem of models described by Eqns. (2.1), (2.2), and (2.3), we propose to cast the problem of parameter estimation into a constrained nonlinear optimization problem. Consider that we have subjected a structure (sometime referred to as the *real structure* even though we will often use a simulation model) to N different excitation cases and have observed the response at certain locations. We will refer to N as the number of *observation sets*: The number of independent load cases for the static problem, the number of measured modes for the free vibration problem, or the number of time points for the transient dynamic problem. Assume that we also have at our disposal a finite element model of the subject structure, parameterized by certain constitutive properties. We estimate the unknown parameters of the finite element model by minimizing a scalar loss function J subject to a set of constraints, where the loss function indicates how well the model equation is satisfied. The parameter estimation problem can then be expressed as follows

$$\begin{aligned} &\underset{(x,\bar{u})}{\textit{minimize}} && J(x,\bar{u}) = \frac{1}{2}\sum_{i=1}^{N} a_i \,\| e_i(x,\bar{u}_i) \|^2 \\ &\textit{subject to} && c(x) \le 0 \end{aligned} \tag{2.4}$$

The loss function J is the weighted summation of L_2 norms of the individual error functions e for the various observation sets. These error functions reflect the discrepancy between the estimated response of the mathematical model and the observations from the real structure, and are a function of the constitutive parameters x of the model as well as the unmeasured response $\bar{u}$ of the structure. For the sake of the general discussion of algorithms, we introduce s as the vector of unknown variables and assume that it contains both unknown parameters x and unmeasured degrees of freedom of the model $\bar{u}$. (We will demonstrate in subsequent chapters that not all parameter estimation algorithms require the estimation of the unmeasured response.)

The weight a_i in Eqn. (2.4) reflects the degree of confidence to the ith set of observations. For example, in a free vibration experiment, since the lower modes are easy to measure reliably, their weights might be chosen larger than the weights for the higher modes. In a statistical sense, the best values for the weights are the inverse of the variance of the error functions. The proposed estimator is in the class of weighted least squares estimators, a subclass of maximum likelihood estimators, and does not require *a priori* knowledge of the probability density of the parameters and measurements.

The constraints $c(x)$ are used to enforce *a priori* knowledge of the parameters. In this study we generally use only bounding constraints for the unknown constitutive parameters,

$$\underline{x} \leq x \leq \bar{x} \tag{2.5}$$

where $\underline{x}$ and $\bar{x}$ are the lower and upper bound vectors, respectively for the unknown parameters. These bounds define the feasible region and are important because they eliminate the possibility of converging to physically unreasonable solutions. For structural systems, if the constitutive, damping, and mass parameters are chosen to be the parameters of the model, the lower bound $\underline{x}$ might be chosen greater than or equal to zero because theory insists that these parameters be positive. The upper bound $\bar{x}$ is more difficult to select, but might, for example, be chosen in the neighborhood of the nominal design values (remember, no choice is ultimately irrevocable). We will give some guidance on the selection of parameters in Section 2.5.

2.3. Recursive Quadratic Programming

The proposed approach to estimating the parameters is an off-line (or batch) method and uses all sets of observations in the computation of the parameters. Because of the presence of constraints and the nonlinearity of the loss function, a batch approach is more robust than a recursive approach. The selected models (2.1) to (2.3) are linear in their response but the parameter estimation problem is inherently nonlinear. Thus linearity of the response presents no advantage. Furthermore, linearity of the constitutive model is not important (the structural matrices $\boldsymbol{K}$, $\boldsymbol{C}$, and $\boldsymbol{M}$ can be nonlinear with respect to the constitutive parameters x and no computational burden accrues). We assume that our models have lumped, time independent parameters. We further assume that the parameters are deterministic; however, we will study the behavior of the estimators with respect to random observation errors in a simulation environment.

To solve the constrained nonlinear optimization problem (2.4), we use the recursive quadratic programming (RQP) method. The recursive quadratic programming method is currently one of the most promising approaches to solving constrained nonlinear optimization problems. The RQP algorithm is attractive because it applies directly to problems with inequality as well as equality constraints, it is globally convergent, and it is amenable to large-scale computation. In this section, we briefly describe the RQP algorithm used in our study to solve optimization problems regarding parameter estimation of structural systems. An extensive discussion of recursive quadratic programming can be found in Appendix A.

A typical iteration of the recursive quadratic programming algorithm has only a few basic steps. One begins by selecting a feasible starting vector s_o. At the current estimate the objective function is quadratified and the inequality constraints are linearized. The resulting inequality-constrained, quadratic subproblem is then solved (*i.e.* the quadratic objective is minimized and the linearized constraints are satisfied) using an active set strategy. The search direction is then the solution to the quadratic subproblem. The length of the step in this direction is determined by minimizing a line search objective function (the sum of the original objective function and a penalty term that becomes positive whenever one or more of the constraints is violated). The line search procedure ensures the global convergence of the RQP method.

A general nonlinear optimization problem with both equality and inequality constraints can be written as follows

$$
\begin{aligned}
&\underset{s}{\text{minimize}} && J(s) \\
&\text{subject to} && c_i(s) = 0 \quad i = 1,\ldots,m' \\
& && c_i(s) \leq 0 \quad i = m'+1,\ldots,m
\end{aligned}
\tag{2.6}
$$

where the objective function J and/or some of the constrains c are nonlinear with respect to the unknown variables s. In our proposed parameter estimation problem (2.4), the loss function is the squared-error objective function, the vector of unknown variables s contains unknown parameters x and unmeasured degrees of freedom $\overline{u}$, and the constraints are simply bounding the unknown parameters as shown in Eqn. (2.5). The recursive quadratic programming algorithm can be stated in a compact form as follows:

Step 1: Start with an initial s_o and set the iteration index k to zero.

Step 2: Compute the search direction d_k by solving the quadratic subproblem

$$
\begin{aligned}
&\underset{d_k}{\text{minimize}} && \tfrac{1}{2} d_k^T H_k d_k + \nabla J(s_k) d_k \\
&\text{subject to} && \nabla c_i(s) d_k + c_i(s_k) = 0 \quad i = 1,\ldots,m' \\
& && \nabla c_i(s) d_k + c_i(s_k) \leq 0 \quad i = m'+1,\ldots,m
\end{aligned}
\tag{2.7}
$$

If the search direction d_k or the gradient vector $\nabla J(s_k)$ is small, then terminate and take the current iterate as the solution.

Step 3: Determine a step length β_k by solving the one-dimensional minimization problem

$$
\underset{\beta_k}{\text{minimize}} \; J(s_k + \beta_k d_k) + r\left[\sum_{i=1}^{m'} |c_i(s_k + \beta_k d_k)| + \sum_{i=m'+1}^{m} \max[c_i(s_k + \beta_k d_k),\ 0]\right] \tag{2.8}
$$

Step 4: Compute matrix H_{k+1} using a Gauss-Newton approximation (or a quasi-Newton update, or a full Newton computation of the Hessian). Set $s_{k+1} = s_k + \beta_k d_k$ and increment counter to $k = k+1$. Go to *Step 2*.

The Fletcher *active set strategy* is used to solve quadratic subproblem (2.7) as explained in Appendix A. The Fletcher algorithm is a robust iterative procedure and suitable for large-scale computation. The active set strategy converges to the solution of an inequality constrained problem using a sequence of equality constrained problems. At each phase of the strategy, a subset of the constraints of the original problem, named the *working set*, are treated as active constraints. The active set method starts with a given working set, the set of equality constraints, and begins minimizing the objective function over the working surface of constraints. If new constraints boundaries are encountered, they are added to the working set, however, no constraint is dropped. When a local minimum of the loss function with respect to the current working set is obtained, the Lagrange multipliers corresponding to the inequality constraints in the working set are determined, if they are all nonnegative, an optimal solution is found. Otherwise, the inequality constraint with the lowest negative Lagrange multiplier is dropped from the working set and the process is reinitiated with this new working set.

In the third step of the recursive quadratic programming algorithm, a line search is performed to compute a step length. The line search objective function (2.8) is an *absolute-value penalty function* which is compatible with the RQP method. The line search procedure ensures the global convergence of the optimization algorithm and promotes convergence from a poor starting point. The penalty parameter r in objective function (2.8) should be greater than all Lagrange multipliers at the solution to guarantee the global convergence (Coleman and Conn 1980). Since the absolute-value penalty function is not differentiable, the *golden section search* is used to minimize one-dimensional objective function (2.8) (Press, *et al.* 1990). The golden section search only requires the value of the objective function and is a robust, linearly convergent method.

The quadratic subproblem (2.7) needs the gradient of the objective function ∇J and the matrix H_k which is an approximation of the Hessian matrix of the Lagrangian associated to the original problem (2.6). In the following section, we compute the gradient of the loss function and the Hessian of the Lagrangian for parameter estimation problem (2.4).

2.4. Sensitivity of the Loss Function

For the sake of brevity in subsequent presentation of mathematical formulations, let us introduce some notational conveniences. From now on, the application of the gradient operator ∇ to an arbitrary scalar field $a(y)$, vector field $\boldsymbol{a}(y)$, and tensor field $\boldsymbol{A}(y)$ are defined to have components as follows

$$\begin{aligned} [\nabla a(y)]_i &= \frac{\partial a(y)}{\partial y_i} & [\nabla^2 a(y)]_{ijk} &= \frac{\partial^2 a_i(y)}{\partial y_j \partial y_k} \\ [\nabla \boldsymbol{a}(y)]_{ij} &= \frac{\partial a_i(y)}{\partial y_j} & [\nabla \boldsymbol{A}(y)]_{ijk} &= \frac{\partial A_{ij}(y)}{\partial y_k} \end{aligned} \tag{2.9}$$

where $\boldsymbol{y}$ is the dependent vector. The gradient of the loss function J, in the constrained nonlinear optimization problem (2.4), with respect to the unknown variables $\boldsymbol{s}$ has the expression

$$\nabla J(\boldsymbol{s}) = \sum_{i=1}^{N} \alpha_i \nabla^T \boldsymbol{e}_i(\boldsymbol{s}) \boldsymbol{e}_i(\boldsymbol{s}) \tag{2.10}$$

The Lagrangian function of optimization problem (2.4) takes the form

$$l(\boldsymbol{s}, \lambda) = J(\boldsymbol{s}) + \lambda^T \boldsymbol{c}(\boldsymbol{s}) \tag{2.11}$$

where λ is the vector of Lagrange multipliers and $\boldsymbol{c}(\boldsymbol{s})$ is the vector of constraints (2.5) bounding the unknown parameters $\boldsymbol{x}$ (which are a part of the unknown variables vector $\boldsymbol{s}$). These constraints are linear, therefore the Hessian of the Lagrangian l is simply the Hessian of the loss function J. From Eqn. (2.10), the Hessian matrix $\boldsymbol{H}$ is computed as follows

$$\boldsymbol{H} = \nabla^2 J(\boldsymbol{s}) = \sum_{i=1}^{N} \alpha_i [\nabla^2 \boldsymbol{e}_i(\boldsymbol{s}) \boldsymbol{e}_i(\boldsymbol{s}) + \nabla^T \boldsymbol{e}_i(\boldsymbol{s}) \nabla \boldsymbol{e}_i(\boldsymbol{s})] \tag{2.12}$$

where the components of the third order tensor $\nabla^2 \boldsymbol{e}_i(\boldsymbol{s})$ and those of the matrix $\nabla \boldsymbol{e}_i(\boldsymbol{s})$ are defined according to Eqn. (2.9). The Hessian matrix in Eqn. (2.12) requires the second derivative of the error function, which

is sometimes difficult to compute. Another difficulty with the exact Hessian matrix is that it may not be positive definite, complicating the numerical calculations. A sensible remedy is to neglect the first term in the parentheses of Eqn. (2.12) so as to ensure that the approximated Hessian is positive semi-definite. This approximation, called the Gauss-Newton approximation of the Hessian matrix H^{GN}, is constructed as

$$H^{GN} = \sum_{i=1}^{N} a_i \nabla^T e_i(s) \nabla e_i(s) \tag{2.13}$$

The H^{GN} matrix is computationally simpler than the exact Hessian matrix H and contains enough information about the second derivative of the loss function to be computed reliably if the residual errors are sufficiently small.

Another way to compute an approximation for the Hessian matrix is to use a low-rank update formulae as explained in Appendix A. Like Gauss-Newton, these update methods use only the first order derivatives of the loss function to update the Hessian matrix at each iteration. Unlike Gauss-Newton, they attempt to gather information necessary to approximate the exact Hessian. In our study we use the modified BFGS method developed by Han and Powell (Han 1976 and 1977). The Han-Powell approximation of the Hessian matrix H^{HP} is given in Appendix A.

2.5. The Selection of Parameters

To establish the parameter estimation algorithm we must specify the choice of parameter vector x needed to build the structural matrices K, C, and M. This choice controls the final output of parameter estimation and, consequently, its generality and applicability. In this section, we discuss some of the possibilities for parameter selection.

The simplest way to parameterized a structural matrix is to use its n_d^2 members as independent parameters. While, this representation does not need any knowledge other than the size of the model, the parameters do not have a physical basis and the model possesses an inordinately large parameter set. Symmetry of the structural matrices can be used to reduce the number of parameters. The weak assumption that the topology of the model, defining the pattern of connectivity among the elements, is known can be used to impose a skyline structure on the structural matrices; elements above the skyline can be constrained to zero. The main disadvantage of selecting the members of the structural matrices to be the unknown parameters is that the number of parameters changes as the finite element model changes, for example through mesh refinement. The use of symmetry and topology cannot ameliorate this drawback.

One can gain deeper insight into the physical structure of the model by considering that the topology and geometry of the model are known and the parameters are selected from the constitutive (stiffness, mass, and damping) equations at the element level of the model. As an example, for a plane stress element, Young's modulus, Poisson's ratio, and mass density might be suitable parameters to describe the model. These parameters have a physical basis and through standard assembly procedures lead naturally to structural matrices with proper symmetry and profile. However, if one considers each finite element to possesses its own independent parameters, then, again, the number of parameters increases as the finite element model is refined.

This feature represents a clear disadvantage since parameter estimation becomes increasingly difficult as the number of parameters increases, due to sparsity of observations.

In this work we use a simple grouping scheme to cure the problem of burgeoning of the parameter set with mesh refinement. The grouping scheme also reduces the total number of parameters in the model and thereby increases the robustness of the estimations. Elements in a group are associated with the same set of parameters and groups of parameters are disjoint from one another. The grouping schemes for the stiffness, mass, and damping parameters need not be the same, for example, the group that an element shares stiffness properties with may be different from the group that it shares mass properties with. The grouping scheme might be based on prior knowledge of the structure. For example, the columns of a story in a building might be known to have the same stiffness; plane stress elements in a layer of a multilayer halfspace might be known to have the same Young's modulus. If such knowledge is not available an appropriate grouping might be determined by a search over a discrete set of groupings to minimize the loss function with respect to grouping (as opposed to simply minimizing over the parameters themselves). The grouping scheme can be made more flexible by recognizing that the value of the parameters within a group (*e.g.* Young's modulus) need not have the same nominal value, but can simply be scaled by a common multiplicative parameter. Only the relative values of parameters within a group need to be specified in advance.

In many practical cases it may be of interest to estimate a part of the parameters with the rest taken as known. For example, the mass parameters of a structure might be known while the stiffness parameters are completely undetermined. Or, we may want to estimate parameters of nonstructural members knowing the structural parameters. Or, in a soil-structure interaction problem, the properties of the soil medium might be unknown while the properties of the superstructure are known. The predetermination of some constitutive parameters reduces the number of unknown parameters of the model and increases the robustness of the parameter estimator.

2.6. Simulation Environment

The behavior of a parameter estimation procedure depends on two main factors: the mathematical model and the richness of the data. The selection of an appropriate model is difficult and often requires the intuition and judgement of an expert in modeling. In the chapter on modal estimation we make a modest exploration of the question of model selection. For the static and transient dynamic problems we avoid the subjective step of model selection completely by simulation so that we can focus on the more tractable problem of evaluating the issue of the richness of the data. To neutralize model selection as a source of error we generate the "real" data by simulation with the model we will use as the basis of the parameter estimation scheme. Thus, the assumed mathematical model is an exact representation of the "real" structure and is, by construction, precisely valid. The only factor affecting the behavior of the proposed parameter estimation algorithm, then, is the richness of the measurements.

We use the term *richness* as a descriptor for the information content in the data. It is related not only to the quantity of measurements but also to the quality of those measurements. One compromise to the quality of the data comes from the noise (*e.g.* from experimental errors) in the measurements. Experimental errors are developed from a variety of sources. Some of the errors are systematic and some are random. We expect

certain errors to be present in any experiment. The behavior of any parameter estimation algorithm should be studied in the context of noisy measurements, whether gathered from real field tests or generated by simulation in a computer.

Another indicator of quality of data is related to the spatial distribution of the measurement locations and the spatial distributions of various excitation cases. For example, consider two load cases that excite a structure in two distinctly different modes and two other load cases that excite the same structure in two rather similar modes. One would expect the response from the former pair to contain more information about the structure than the latter pair. Consequently, these data would lead to better estimates of the parameters. Also, if one load case excites the structure only locally, one would expect the parameter estimates to be very good for those parameters associated with that local region and poor for those parameters not associated with that local region. Further, an excitation mode that involves the entire structure, as the fundamental mode of vibration often is, would lead to good qualitative estimates of most parameters, but those estimates might not be as sharp as those from local excitation.

Whenever some aspect of a given problem has a random nature, the solution to that problem is a random variable. In a parameter estimation problem, the measurements can be considered to have a random error component, therefore the estimated parameters are random variables. The essential problem is to discover the statistical properties of the solution, in our case the statistics of the estimated parameters. Determination of the statistics of the solution is particularly difficult when the problem is nonlinear or complex (or both). Monte Carlo simulation provides a useful tool for these problems.

Monte Carlo simulation uses a random sequence of numbers to change the values of the particular random aspects of the problem to construct a sample of the solution population. The statistics of the sample population are easily computed and provide an estimate of the statistical properties of the random solution. As the size of the sample population increases, so increases the reliability of the estimated statistics. Monte Carlo simulation is used in the studies presented here to assess the behavior of the proposed parameter estimation algorithms with respect to the amount of measurements, the spatial distribution of loading cases, the initial values of the parameters, and the noise in the measured responses.

In our study, we wish to estimate the parameters of a finite element model, a constrained nonlinear optimization problem expressed by Eqn. (2.4). For a given finite element model, set of load cases, bounding constraints, and initial values, the solution $\boldsymbol{x}$ is a function only of the response $\boldsymbol{u}$ measured at certain locations. These response values will, of course, be polluted with noise. In the simulation environment the noisy response $\boldsymbol{u}$ is generated by adding a noise vector $\boldsymbol{n}$ to the computed response of the given finite element model $\boldsymbol{u_o}$ as follows

$$\boldsymbol{u} = \boldsymbol{u_o} + \boldsymbol{n} \tag{2.14}$$

where $\boldsymbol{n}$ is a random vector with zero expected value and finite known variance. As schematically shown in Fig. 2.1, we model the experimental errors as a random noise vector $\boldsymbol{n}$ with an assumed distribution function. The response $\boldsymbol{u}$, computed in accord with Fig. 2.1, is taken to be the measured response of the real structure.

The estimated parameters x are functions of the noisy response u which is a random vector. Therefore, the solution x becomes a random vector whose distribution directly depends on the distribution of the noise vector n and the mathematical characteristics of the proposed estimation problem (2.4). Through Monte Carlo simulation we generate a population of random solutions x from noisy data whose statistics are completely known to us. Each individual member of the solution population corresponds to a certain noise vector. If the functional relation between x and n were explicitly known, then the distribution of solutions could be computed analytically. However, the present constrained, nonlinear optimization problem admits no such solution. In fact, it must be solved iteratively. Hence, x is a complex, nonlinear function of the noisy response, and hence we will compute its statistics by Monte Carlo simulation.

For a given mathematical model, bounding constraints, initial values, and load cases, Monte Carlo simulation uses a random number generator to produce a sequence of noisy responses as follows

$$u^t = u_o + n^t \qquad t = 1,\ldots,T \tag{2.15}$$

where n^t is the tth noise vector computed using the random number generator as explained in the next section and T is the *sample size*. For each individual noisy response u^t, the proposed parameter estimation algorithm computes an estimate of the parameters x^t of the mathematical model. Hence, the simulation develops a sample $\{x^t, t=1,\ldots,T\}$ of estimates (*i.e.* the solution population). Based on the law of large numbers, by increasing the sample size T, the statistical indices of the sample (*e.g.* the mean and standard deviation) converge to the actual statistics of the population. Monte Carlo simulation does not need the explicit form of the relationship among inputs and outputs of the algorithm and approximates the distribution of the estimated parameters by executing the algorithm repeatedly, each time altering only the values of the imposed noise. An individual execution of the estimator is referred to as a *trial* in the subsequent sections. The sample size T (number of trials) should be large enough to establish statistical significance of the estimates. The variation of the statistical indices of the sample with respect to the sample size becomes steady when the number of trials is large enough.

Noise Modeling. In our simulation study, we do not have real measurements and we simulate noisy response by adding random noise to the computed response. There are many types of errors that can be introduced into a mathematical model to simulate noisy measurements. Due to the complexity of the measurement process, any single type of random error would fall short of modeling the actual error experienced in the field. On the other hand, we need to simulate noise in measurements in order to study the behavior of our developed algorithms. Therefore, two simple types of random noise (error) are used to bound the problem

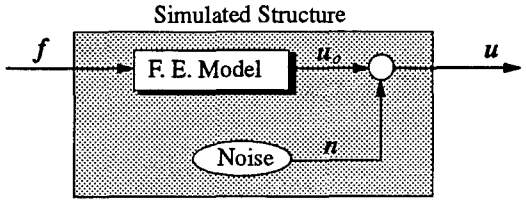

Fig. 2.1 Simulation of actual response of the structure

of noise modeling. The first type is an *absolute error* of amplitude λ multiplying a uniform random variable ξ that takes values between plus and minus one. The error is added to the computed response u_o to simulate noisy measurements. Thus, the simulated absolute measurement error is modeled as

$$u_i^t = u_{o_i} + \lambda \xi_i^t \qquad i = 1,\ldots,\hat{n}_d \quad , \quad t = 1,\ldots,T \tag{2.16}$$

where $\hat{n}_d$ is the number of measured degrees of freedom for a load case, and T is the sample size for the simulation. The random variable ξ is constructed using a pseudo-random number generator and has a zero expected value and variance equal to 1/3. Equation (2.16) shows that errors added at each measured degree of freedom for each trial ξ_i^t are independent from one another.

Absolute errors model actual experimental errors well when all instruments have the same sensitivity and are used to measure responses of the same type and order of magnitude. If some of the measurements are small, the absolute errors tend to overwhelm the actual responses. The smaller deformations may be unfairly penalized, because in practice, when the deformations are suspected to be small, the sensors would be set to a greater sensitivity. Also, if the same error amplitude is applied to measurements of different types (such as displacements and rotations) the errors can completely dominate the smaller response.

We introduce a second type of error to take these issues into account. The *proportional error* is a fraction of the computed response multiplying a uniform random variable ξ defined in Eqn. (2.16). The simulated proportional measurement error is given by

$$u_i^t = u_{o_i}(1 + \bar{\lambda}\xi_i^t) \qquad i = 1,\ldots,\hat{n}_d \quad , \quad t = 1,\ldots,T \tag{2.17}$$

where $\bar{\lambda}$ is a fraction of the computed deformation u_o which controls the magnitude of error. Proportional errors are representative of actual measurement errors when all instruments are set to optimal sensitivity. True experimental errors lie somewhere between the bounds of absolute and proportional errors. These two extreme models of noise should provide effective bounds on measurement errors for use in assessing a parameter estimation algorithm. The amplitude of absolute error λ and the fraction parameter of proportional error $\bar{\lambda}$ are referred to as the magnitude of noise in the rest of this manuscript.

Statistical Indices. In a noisy environment, the parameters we are estimating behave as random variables. To study our proposed estimation algorithms and to find trends in the behavior of these estimators we will use statistical indices to characterize our results. In this section we introduce a few appropriate statistical indices for use in probing the behavior of the proposed algorithms by simulation.

The *mean average* $\bar{x}$ of the estimation sample $\{x^t, t=1,\ldots,T\}$ approximates the expected value of the estimated parameters $E[x]$ and is computed as

$$\bar{x} = \frac{1}{T}\sum_{t=1}^{T} x^t \tag{2.18}$$

where x^t is the vector of estimates for the tth trial. We refer to $\bar{x}$ as the vector of estimated parameters for a complete ensemble of trials. (We will also refer to a complete ensemble of trials as *an experiment* in the

sequel.) The mean average indicates the centroid of the distribution of the estimates in the space of parameters for a given experiment.

The quadratic bias $\| E[x] - \hat{x} \|^2$ is a measure of the distance between the centroid (expected value) of the estimates and the actual parameters $\hat{x}$ (which we know because we are doing simulation). The *average root quadratic bias* (*RQB*) is defined as

$$RQB = \frac{\| \bar{x} - \hat{x} \|}{n_p \| \hat{x} \|} \tag{2.19}$$

where n_p is the number of parameters and $\| \bar{x} - \hat{x} \|$ is the root quadratic bias of the sample. The *RQB* is normalized with respect to the norm of actual parameters.

The *average standard deviation* (*SD*) of the estimates, normalized with respect to $\| \hat{x} \|$, is given by

$$SD = \frac{\left[\frac{1}{T-1} \sum_{t=1}^{T} \sum_{i=1}^{n_p} (x_i^t - \bar{x}_i)^2 \right]^{\frac{1}{2}}}{n_p \| \hat{x} \|} \tag{2.20}$$

The *SD* indicates the standard deviation, an approximation of the square root of the variance $E[(x - E[x])^2]$ of the estimates, and is a measure of scatter of the distribution of the estimates around the expected value. Bias and standard deviation are quantitative measures of accuracy and precision of an estimator, respectively. The smaller bias and standard deviation are, the more accurate and precise an estimator is.

To measure the scatter of the estimates with respect to the actual parameters $\hat{x}$, two indices: *average root mean square error* (*RMS*) and *average identification error* (*AIE*) are defined as follows

$$RMS = \frac{\left[\frac{1}{T} \sum_{t=1}^{T} \sum_{i=1}^{n_p} (x_i^t - \hat{x}_i)^2 \right]^{\frac{1}{2}}}{n_p \| \hat{x} \|} \tag{2.21}$$

$$AIE = \frac{\frac{1}{T} \sum_{t=1}^{T} \sum_{i=1}^{n_p} |x_i^t - \hat{x}_i|}{n_p \| \hat{x} \|} \tag{2.22}$$

Both have been normalized with respect to $\| \hat{x} \|$. The *RMS* and *AIE* compute the scatter of the sample based on L_2 and L_1 norms, respectively. The *AIE* quantity has the same property as *RMS*. Combining Eqns. (2.19) to (2.21) leads to

$$(RMS)^2 = (SD)^2 + (RQB)^2 \tag{2.23}$$

which shows that variation of the mean square error depends on variations of both bias and standard deviation. Therefore, a decrease in the scatter of the estimates around the actual parameters (*RMS*) can be generated by decreasing the distance between the centroid of the sample and the actual parameters or by reducing the scatter of the estimates around the centroid of the sample.

When the set of parameters contains different types of quantities, such as axial, shear, or flexural stiffnesses, the statistical indices are computed by weighted averaging. For example, if there are three different types of parameters, then the average root quadratic bias is calculated as follows

$$RQB = \frac{1}{n_p^2}\sum_{i=1}^{3} n_{p_i}^2 RQB_i \tag{2.24}$$

where n_{p_i} is the number of ith type parameters and RQB_i is computed based on relation (2.19) whose variables are calculated for the set of estimates and actual values for the ith type of parameters. In Eqn. (2.24) the quantity RQB can be replaced by indices SD, RMS, and AIE.

2.7. Comparison of Estimators

In the following chapters, we propose two different estimators for the parameters of a finite element model. To study the behavior of the proposed estimators and compare them, we need some criteria to measure goodness of fit. Bias indicates the distance between the estimated parameters and the actual parameters and thus provides a suitable measure of goodness of fit. An *unbiased* estimation is, practically speaking, more desirable than a *biased* estimation. The expected value $E[\boldsymbol{x}]$ for an unbiased estimator is equal to the actual parameters $\hat{\boldsymbol{x}}$. An estimator with a small bias and a small standard deviation, called a *desirable* estimator, might be preferred to one which is unbiased but has a large standard deviation. Furthermore, an estimator with a large bias and small variance is not a desirable estimator.

An unbiased estimator is more *efficient* than another unbiased estimator if it has a smaller standard deviation. Standard deviation is a measure of scatter of estimates and thus indicates the efficiency of an estimator. An estimator is *consistent* if its bias and its standard deviation converge to zero by providing more measurements. Unbiasedness, efficiency, and consistency are all criteria that are important in comparing the quality of different estimators.

2.8. Chapter Summary

We have proposed a unified approach toward the parameter estimation of a mathematical model of a structural system using measured input-output pairs of the real structure. The input-output pairs can be measured from either static, or undamped free vibration, or damped, transient, forced dynamic tests on the real structure. For these three cases, we have presented the governing equations of a mathematical model of a structure and have defined the unknown constitutive parameters and the type of the input-output pairs. Then, we have cast the problem of parameter estimation of a mathematical model into a constrained nonlinear optimization problem. We have determined the unknown constitutive parameters of a model by minimizing a scalar loss function subject to a set of constraints. Where, the loss function is the weighted summation of squared norms of discrepancies between the real structure and the model for different observation sets and the constraints impose upper and lower bounds on the unknown constitutive parameters.

We have discussed the parameterization of the mathematical model and have stressed that it controls the required amount of data, the output of the parameter estimation algorithm, its generality and applicability.

In this work, we have assumed the topology and the geometry of the model are known and we have selected the parameters from the constitutive equations in the element level of the model.

Grouping of the members of the structure with the same constitutive parameters is an implemented feature of the proposed algorithm which reduces both the number of unknown parameters and the required amount of information, especially for large and complex structural systems. Another feature of the the proposed algorithm is to implement *a priori* knowledge about some of the constitutive parameters which reduces the number of parameters to be estimated.

To compute the constitutive parameters of the model, we have to solve the constructed optimization problem. We have presented a recursive quadratic programming method to solve the constructed optimization problem. The recursive quadratic programming method requires the gradient and the Hessian of the loss function which we have derived for a general constrained nonlinear optimization problem.

To study the behavior of the proposed algorithm, we have presented a simulation environment. In this environment we have simulated the measured response of a structure by imposing independent random noises on the computed responses from the mathematical model. We have explained two ways for modeling the noise. We have also defined some statistical indices to evaluate the statistical properties of the proposed parameter estimation algorithm and to compare different parameter estimators built using different definitions for the discrepancy between the real structure and the modal.

CHAPTER THREE

Estimation of Constitutive Parameters from Static Response

The literature on parameter estimation of structural systems based on static response is limited to a few papers. Sheena and Zalmanovich (1982) presented a method for improving the analytical stiffness matrix from noise free static measurements. Their method required measurements at certain degrees of freedom, and used spline functions to predict the remaining unmeasured degrees of freedom. All elements of the stiffness matrix were adjusted to minimize the difference between the actual and analytical stiffness matrices (deviation approach) subject to measured displacements constraints. Sanayei and Nelson (1986), and Sanayei and Scamboli (1991) estimated structural stiffnesses at the element level by minimizing the difference between the applied and internal forces (equation error approach). Their method required deformations to be measured at the same degrees of freedom that the external loads were applied. This drawback was lifted in Sanayei and Onipede (1991) by using a condensation procedure. Hjelmstad, *et al.* (1990, 1992) described an approach to parameter estimation of complex linear structures based on the principle of virtual work for static and modal experiments. A condensation procedure was used to deal with the incompletely measured systems. They studied the behavior of the method in a noisy environment using numerical simulation. Hajela and Soeiro (1989, 1990) classified the parameter estimation techniques into the equation error, output error, and minimum deviation approaches. They assumed that the mass matrix did not change and lumped all elemental parameters into a single parameter. They used both measured static and modal responses to assess stiffness change on element-by-element basis in structural systems. For parameter estimation of large structures, they proposed some substructuring and order reduction techniques.

From a practical point of view, estimation of parameters from static response is less appealing than estimation of parameters from modal or transient dynamic response. It is much easier to excite a large structure dynamically, particularly with resonant harmonic loading, than it is to excite it statically. Furthermore, it is easier to measure accelerations than displacements because of simplicity of establishing an inertial reference frame for measuring accelerations. From a theoretical point of view, the distinction between static, modal, and dynamic parameter estimation is less clear. We show that the estimation problem for all three cases can be cast in a unified format as a constrained optimization problem having the form of Eqn. (2.4). The similarities between the three basic cases will become clear through our discussion of them. We present the static problem first because it is the simplest, and will help us set the stage for the remaining cases.

In this chapter, we develop two algorithms for estimating constitutive (member stiffness) parameters of a finite element model of a structural system from measured static response to a given set of loads. From a mathematical model with known geometry and topology and measured applied loads and nodal deformations

at some degrees of freedom of the model, parameter estimation problems are proposed which, when solved, determine the unknown constitutive parameters. The proposed algorithms are based on the concept of minimizing the index of discrepancy between the model and the structure, as explained in the previous chapter. The recursive quadratic programming method is used to solve the nonlinear constrained estimation problem. Both proposed estimators can handle the incompletely measured models, have robust convergence, and are amenable to modeling of complex structures.

In the following sections, first for each estimator the estimation problem is proposed and the necessary formulation to compute the sensitivity of the loss function is derived. Then, strategies for setting the initial values and scaling the unknown variables of the nonlinear estimation problem are explained. An identifiability criterion for the amount of measurements is derived. At the end, a numerical simulation is used to study the behavior of the proposed estimators with respect to the amount of measurements, loading patterns, initial values of parameters, and noise in the measured response.

3.1. The Model Equation

The matrix form of the equilibrium equations of the finite element model with n_d degrees of freedom subjected to *nlc* static load cases is

$$\boldsymbol{K}(\boldsymbol{x})\boldsymbol{u}_i = \boldsymbol{f}_i \qquad i = 1,\ldots,nlc \tag{3.1}$$

where $\boldsymbol{K}(n_d \times n_d)$ is the secant stiffness matrix, $\boldsymbol{x}$ is the vector of unknown constitutive parameters, $\boldsymbol{u}_i(n_d \times 1)$ is the response of the finite element model for the ith load case, and $\boldsymbol{f}_i(n_d \times 1)$ is the vector of equivalent nodal forces for the ith load case. From now on we will refer to Eqn. (3.1) as the model equation for the parameter estimation problem of the finite element model based on static response.

Generally, the response of the structure cannot be measured at all degrees of freedom of the finite element model. Measuring the complete response of a structure is either impractical (*e.g.* measuring rotational motion) or impossible, (*e.g.* when part of the structure is inaccessible). To resolve this inherent problem, we partition the vector of degrees of freedom $\boldsymbol{u}_i$ into two parts as follows:

$$\boldsymbol{u}_i = \begin{bmatrix} \hat{\boldsymbol{u}}_i \\ \overline{\boldsymbol{u}}_i \end{bmatrix} \tag{3.2}$$

where $\hat{\boldsymbol{u}}_i(\hat{n}_d \times 1)$ and $\overline{\boldsymbol{u}}_i(\overline{n}_d \times 1)$ are the vectors of measured and unmeasured response of the structure, respectively. We shall assume that this partitioning is fixed for all load cases. In accord with this partitioning of displacements, we shall also partition the stiffness matrix into two parts: a matrix corresponding to the measured response $\hat{\boldsymbol{K}}(\boldsymbol{x})$, with dimension $(n_d \times \hat{n}_d)$, and a matrix corresponding to the unmeasured response $\overline{\boldsymbol{K}}(\boldsymbol{x})$, with dimension $(n_d \times \overline{n}_d)$, such that

$$\boldsymbol{K}(\boldsymbol{x})\boldsymbol{u}_i = \hat{\boldsymbol{K}}(\boldsymbol{x})\hat{\boldsymbol{u}}_i + \overline{\boldsymbol{K}}(\boldsymbol{x})\overline{\boldsymbol{u}}_i \tag{3.3}$$

3.2. The Equation Error Estimator

For the proposed equation error estimator, the error function is a measure of equivalence between the mathematical model and the real structure, and represents the residual force in the model caused by failure to meet equilibrium. Substituting Eqn. (3.2) into Eqn. (3.1), the error function takes the form

$$e_i(x,\bar{u}_i) = \hat{K}(x)\hat{u}_i + \bar{K}(x)\bar{u}_i - f_i \qquad i = 1,\ldots,nlc \tag{3.4}$$

where the unknowns comprise both constitutive parameters x and unmeasured displacements $\bar{u}_i$. We will generally refer to the unmeasured displacements for all load cases by grouping them in the vector $\bar{u}=(\bar{u}_1, \bar{u}_2, \ldots, \bar{u}_{nlc})$. The error function e has the nature of a residual force and indicates how close the vector of applied forces f is to the generated internal forces in the model Ku. Figure 3.1 shows the error function schematically.

In accord with Eqn. (2.4), the constrained nonlinear optimization problem for the proposed equation error estimator is

$$\begin{aligned} &\underset{(x,\bar{u})}{\textit{minimize}} \quad J(x,\bar{u}) = \tfrac{1}{2}\sum_{i=1}^{nlc} a_i \left\| \hat{K}(x)\hat{u}_i + \bar{K}(x)\bar{u}_i - f_i \right\|^2 \\ &\textit{subject to} \quad \underline{x} \le x \le \bar{x} \end{aligned} \tag{3.5}$$

where $\underline{x}$ and $\bar{x}$ are the prescribed lower and upper bounds of the unknown constitutive parameters, respectively, and a_i is the weight associated to the ith load case. The proposed estimator simultaneously estimates the unknown constitutive parameters and the response at the unmeasured degrees of freedom for all load cases. By adding simple bounding constraints on the unknown constitutive parameters we eliminate the possibility of converging to unreasonable solutions. As explained in Chapter Two, we employ the recursive quadratic programming method (RQP) to solve optimization problem (3.5). The RQP algorithm needs the gradient and the Hessian of the loss function J with respect to unknown variables $(x, \bar{u})$. These sensitivities are computed in the following section.

Sensitivity of the Loss Function

The gradient of the loss function with respect to the variables $(x, \bar{u})$ can be computed using Eqn. (2.10), replacing N with nlc. For notational clarity, we partition the gradient of the error function with respect to the unknown variables $(x, \bar{u})$ as follows

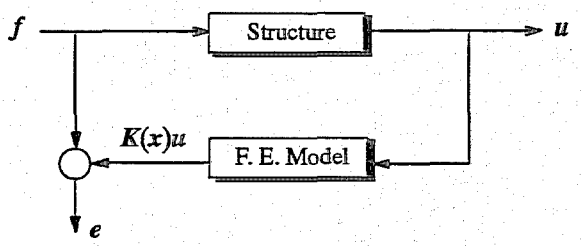

Fig. 3.1 Error function for the equation error estimator (EEE)

$$\nabla e_i(x, \bar{u}_i) = \left[\nabla_x e_i(x, \bar{u}_i) \quad \nabla_{\bar{u}} e_i(x, \bar{u}_i) \right] \tag{3.6}$$

For the sake of notational convenience, $\nabla_x e_i(x, \bar{u}_i)$ will be designated as $U(x, u_i)$ and is computed from Eqn. (3.4) as

$$\nabla_x e_i(x, \bar{u}_i) = \frac{\partial}{\partial x}[K(x)u_i] \equiv U(x, u_i) \tag{3.7}$$

The sensitivity matrix U can be computed by assembling the element sensitivity matrices U^e in the same manner as the stiffness matrix is assembled from element stiffness matrices in the finite element method. To wit,

$$U(x, u_i) = \sum_e U^e(x^e, u_i^e) \tag{3.8}$$

where x^e is the vector of unknown parameters of the eth element, u_i^e is the vector of nodal displacements associated with the eth element for the ith load case, and the element sensitivity matrix U^e is defined as

$$U^e(x^e, u_i^e) = \frac{\partial}{\partial x^e}[K^e(x^e)u_i^e] \tag{3.9}$$

where K^e is the element stiffness matrix. In Appendix B we explain how the matrix U^e can be built for finite elements whose stiffness matrices are computed by numerical quadrature. Equation (3.8) is possible because the assembly process is linear. In general, the stiffness matrix $K(x)$ might be nonlinear with respect to the unknown parameters x (such is the case for the stiffness matrix of the Timoshenko beam element). Equation (3.4) then suggests that the derivative of the error function with respect to x is still a function of x. In some instances, the stiffness matrix will be linear in x, whereby the gradient would be independent of x.

The gradient of the error function e_i with respect to the unmeasured response $\bar{u}_i$ using Eqn. (3.3) takes the form as

$$\nabla_{\bar{u}_i} e_i(x, \bar{u}_i) = \bar{K}(x) \tag{3.10}$$

We assume that the finite element model is linear, therefore the secant stiffness matrix K is not a function of deformations. Consequently, the matrix $\nabla_{\bar{u}_i} e_i$ is a fixed matrix $\bar{K}$ for all load cases. Knowing $\bar{u}_i$ is a subvector of the vector $\bar{u}$ containing the unmeasured degrees of freedom for all load cases makes the gradient of the error function e_i with respect to $\bar{u}$ a sparse matrix G_i shown as follows

$$\nabla_{\bar{u}} e_i(x, \bar{u}_i) = \begin{bmatrix} \overset{1}{0} & \overset{2}{0} & \cdots & \overset{i-1}{0} & \overset{i}{\bar{K}(x)} & \overset{i+1}{0} & \cdots & \overset{nlc}{0} \end{bmatrix} \equiv G_i(x) \tag{3.11}$$

The $\bar{K}$ matrix is a part of the stiffness matrix, therefore it can be generated by assembling $\bar{K}^e$ matrices computed from the elemental stiffness matrices K^e.

The computer program for the proposed estimators should have two libraries of element matrices: *(1)* a library of elemental matrices such as stiffness, mass and damping matrices to build the finite element model

and the sensitivity matrices $\nabla_{\bar{u}} e$, and *(2)* a library of the elemental sensitivity matrices U^e to compute the sensitivity matrices $\nabla_x e$. With this observation one can see that the structure of a program for parameter estimation can be organized very much like a program for finite element analysis. In Appendix B we show that, for elements that are linear in their parameters, the matrices U^e can be generated from elemental strain-displacement matrices and they do not need a separate library for their sensitivity matrices.

By substituting equations (3.8) and (3.11) into Eqn. (3.6), the total gradient of the error function with respect to the unknown variables $(x,\ \bar{u})$ can be written as

$$\nabla e_i(x,\bar{u}_i) = \begin{bmatrix} U(x,u_i) & G_i(x) \end{bmatrix} \tag{3.12}$$

Now, by substituting Eqns. (3.4) and (3.12) into Eqn. (2.10), the gradient of the loss function J with respect to the unknown variables $(x,\ \bar{u})$ for the proposed estimator in Eqn. (3.5) can be computed as follows

$$\nabla J(x,\bar{u}) = \sum_{i=1}^{nlc} a_i \begin{bmatrix} U(x,u_i) & G_i(x) \end{bmatrix}^T e_i(x,\bar{u}_i) \tag{3.13}$$

The recursive quadratic programming requires an estimate of the Hessian of the loss function. Often this estimate is made with a rank-two update formula (such as modified BFGS in the Han-Powell method), however, several interesting alternatives are available for the present problem, namely the exact Hessian and the Gauss-Newton approximation of the Hessian. For the proposed equation error estimator the second term in Eqn. (2.12) is simply formed from Eqn. (3.12) as

$$\nabla^T e_i(x,\bar{u}_i)\,\nabla e_i(x,\bar{u}_i) = \begin{bmatrix} U^T(x,u_i)U(x,u_i) & U^T(x,u_i)G_i(x) \\ G_i^T(x)U(x,u_i) & G_i^T(x)G_i(x) \end{bmatrix} \equiv H_i^{GN}(x,\bar{u}_i) \tag{3.14}$$

Using the definitions in Eqn. (2.9), the first term in Eqn. (2.12) can be expressed in the following form

$$\nabla^2 e_i(x,\bar{u}_i)\,e_i(x,\bar{u}_i) = \begin{bmatrix} \nabla_x U(x,u_i) & \nabla_x G_i(x) \\ \nabla_{\bar{u}} U(x,u_i) & 0 \end{bmatrix} e_i(x,\bar{u}_i) \equiv H_i^{SD}(x,\bar{u}_i) \tag{3.15}$$

Now by substituting equations (3.14) and (3.15), the explicit form of the Hessian matrix for the loss function of the parameter estimation problem in Eqn. (3.5) can be written as

$$H(x,\bar{u}) = \nabla^2 J(x,\bar{u}) = \sum_{i=1}^{nlc} a_i [H_i^{SD}(x,\bar{u}_i) + H_i^{GN}(x,\bar{u}_i)] \tag{3.16}$$

Remark. A Hessian matrix is symmetric, therefore the matrix given in Eqn. (3.16) should be symmetric. This matrix is a summation of the matrices in Eqns. (3.14) and (3.15). Because the matrix in Eqn. (3.14) is symmetric by construction, one need only check the symmetry property of the matrix in Eqn. (3.15) to prove the symmetry of the above Hessian matrix. The matrix $H_i^{SD}(x,\bar{u}_i)$ is formed by four matrices. One of its two diagonal matrices is a symmetric zero matrix and the other one $\nabla_x U(x,u_i)e_i$ is symmetric because, based on Eqn. (3.7), its *jk*th component can be expressed as

$$[\nabla_x U(x,u_i)e_i]_{jk} = \sum_l \frac{\partial^2 [Ku_i]_l}{\partial x_j \partial x_k} [e_i]_l \tag{3.17}$$

which is obviously equal to its kjth component since the order of differentiation is immaterial. The off-diagonal matrix $\nabla_{\overline{u}} U(x,u_i)e_i$ is the transposed matrix for the off-diagonal matrix $\nabla_x G_i(x)e_i$ because its jkth component, given by

$$[\nabla_{\overline{u}} U(x,u_i)e_i]_{jk} = \sum_l \frac{\partial}{\partial \overline{u}_j}\left[\frac{\partial [Ku_i]_l}{\partial x_k}\right][e_i]_l \ , \tag{3.18}$$

is equal to the kjth component of the matrix $\nabla_x G_i(x)e_i$, given by

$$[\nabla_x G_i(x)e_i]_{kj} = \sum_l \frac{\partial}{\partial x_k}\left[\frac{\partial [Ku_i]_l}{\partial \overline{u}_j}\right][e_i]_l \ , \tag{3.19}$$

again because order of differentiation is immaterial. Therefore the matrix $H_i^{SD}(x,\overline{u}_i)$ is symmetric and consequently, the derived Hessian matrix in Eqn. (3.16) is symmetric. □

Equations (3.18) and (3.19) show that the components of the third-order tensors $\nabla_x G_i(x)$ and $\nabla_{\overline{u}} U(x,u_i)$ have the following symmetry properties

$$[\nabla_x G_i(x)]_{lkj} = [\nabla_{\overline{u}} U(x,u_i)]_{ljk} \tag{3.20}$$

Hence, one can be generated from the other. Knowing the sensitivity matrix $U(x,u_i)$ is a function of only the displacements for the ith load case makes the third-order tensor $\nabla_{\overline{u}} U(x,u_i)$ sparse:

$$\nabla_{\overline{u}} U^T(x,u_i) = \begin{bmatrix} \overset{1}{0} & \overset{2}{0} & \cdots & \overset{i-1}{0} & \overset{i}{\nabla_{\overline{u}_i} U(x,u_i)} & \overset{i+1}{0} & \cdots & \overset{nlc}{0} \end{bmatrix}^T \tag{3.21}$$

The tensors $\nabla_{\overline{u}_i} U(x,u_i)$ and $\nabla_x U(x,u_i)$ can be computed by assembling element matrices as follows

$$\begin{aligned} \nabla_{\overline{u}_i} U(x,u_i) &= \sum_e \nabla_{\overline{u}_i^e} U^e(x^e,u_i^e) \\ \nabla_x U(x,u_i) &= \sum_e \nabla_{x^e} U^e(x^e,u_i^e) \end{aligned} \tag{3.22}$$

where the superscript e indicates the eth element in the finite element model. The computer program for the structural parameter estimation should have a library of the elemental tensors $\nabla_{\overline{u}^e} U^e$ and $\nabla_{x^e} U^e$ for different types of elements. However, if the element stiffness K^e is linear with respect to its constitutive parameters x^e then U^e is not a function of x^e, therefore the tensor $\nabla_{x^e} U^e$ is zero. Also, if an element is linear then its U^e matrix is linear with respect to the nodal displacements u_i^e. So, for this element the elemental sensitivity tensor $\nabla_{\overline{u}_i^e} U^e$ can simply be generated from the following relation

$$\frac{\partial [U^e(x^e,u_i^e)]}{\partial \overline{u}_{il}^e} = U^e(x^e,b_l) \tag{3.23}$$

where $\bar{u}_{il}^e$ is the lth unmeasured degree of freedom of the eth element for the ith load case, b_l is a $(n_d^e \times 1)$ unit vector $\{0 \ldots 0 \ \ 1 \ \ 0 \ldots 0\}$ whose nonzero component is at the position corresponding to the lth unmeasured degree of freedom and n_d^e is the number of degrees of freedom of the eth element. Eqn. (3.23) indicates that for the linear finite element models, there is no need for a library of elemental tensor $\nabla_{u^e} U^e$ and these tensors can be computed using the elemental matrices U^e.

The Gauss-Newton approximation of the Hessian matrix H^{GN} is constructed by substituting Eqn. (3.14) into Eqn. (2.13) and takes the form

$$H^{GN}(x, \bar{u}) = \sum_{i=1}^{nlc} a_i H_i^{GN}(x, \bar{u}_i) \tag{3.24}$$

The approximated Hessian in Eqn. (3.24) does not need the second-order derivatives of the error function nor the third-order tensors to store them. The Hessian matrix generated by the Gauss-Newton approximation is computationally simpler than the exact Hessian matrix in Eqn. (3.16) and contains enough information about the second derivative of the loss function to be computed reliably when the residual is small. The Hessian matrix used in the Gauss-Newton approach is positive semi-definite, while the Newton algorithm must be modified to restore positive definiteness of the Hessian.

3.3. The Output Error Estimator

For the proposed output error estimator, the error function e is defined to be the difference between the measured response of the structure u and the computed response of the finite element model $K^{-1}f$. The error is accrued only at the locations where measurements have been made. Figure 3.2 shows the error function schematically. For the sake of clarity, we define a Boolean matrix Q that extracts the vector of the measured response $\hat{u}_i$ from the complete displacement vector of u_i, that is, $\hat{u}_i = Qu_i$. To simplify the discussion, we assume that Q is the same for all load cases. (As a practical consideration, such an assumption would be a useful idea in setting up the experiment in the first place.)

The error function for the proposed output error estimator is given by the following expression

$$e_i(x) = QK^{-1}(x)f_i - \hat{u}_i \qquad i = 1, \ldots, nlc \tag{3.25}$$

For the output error estimator, the unknown variables comprise only the unknown constitutive parameters x. In accord with the general estimation problem (2.4), the constrained nonlinear optimization problem for the proposed output error estimator is

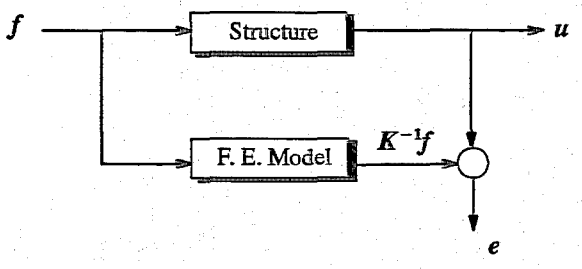

Fig. 3.2 Error function for the output error estimator (OEE)

$$\begin{aligned} &\underset{x}{\text{minimize}} \quad J(x) = \frac{1}{2}\sum_{i=1}^{nlc} a_i \| QK^{-1}(x)f_i - \hat{u}_i \|^2 \\ &\text{subject to} \quad \underline{x} \le x \le \bar{x} \end{aligned} \tag{3.26}$$

where the bound vectors $\underline{x}$ and $\bar{x}$ and the weights a_i have the same definitions as they did in Eqn. (3.5) of the previous section. The number of unknown variables for the proposed output error estimator is smaller than the number of unknown variables for the proposed equation error estimator. Thus, the optimization problem described by Eqn. (3.26) can be solved in a lower dimensional space than the optimization problem described by Eqn. (3.5). On the other hand, the loss function of the output error estimator is intrinsically more nonlinear than the loss function of the equation error estimator by virtue of the inversion of the matrix $K(x)$. In the following section, the gradient and the Hessian matrix for the loss function J in Eqn. (3.26) will be computed.

Sensitivity of the Loss Function

The gradient of the loss function with respect to the unknown parameters x can be computed using Eqn. (2.10). From Eqn. (3.25), the gradient of the error function with respect to x takes the form

$$\nabla e_i(x) = - QK^{-1}(x)\frac{\partial}{\partial x}[K(x)]K^{-1}(x)f_i \tag{3.27}$$

where we have made use of the formula for the derivative of the inverse of a matrix. Using Eqn. (3.7) and substituting $K^{-1}(x)f_i$ in place of u_i, the derivative on the right-hand side of Eqn. (3.27) can be expressed in the notation defined previously as

$$\frac{\partial}{\partial x}[K(x)]K^{-1}f_i = U(x, K^{-1}f_i) \tag{3.28}$$

By combining Eqns. (3.25), (3.27), (3.28), and (2.10) the gradient of the loss function with respect to the unknown parameters x is

$$\nabla J(x) = \sum_{i=1}^{nlc} a_i \left[- QK^{-1}(x)U(x, K^{-1}f_i) \right]^T e_i(x) \tag{3.29}$$

where the U matrix is generated for the computed displacement vector $K^{-1}f$ by assembling element sensitivity matrices U^e. The vector $K^{-1}f$ and the matrix $K^{-1}U$ are computed by a backsubstitution procedure on the vector f and columns of the U matrix, respectively, using the triangularized form of the same K matrix.

The second derivative of the loss function with respect to the unknown parameters can be computed exactly or approximately either by the rank-two update formula using the gradient of the loss function or with the Gauss-Newton method. The rank-two update methods are discussed in Appendix A. The Gauss-Newton approximation of the Hessian matrix H^{GN} is computed by substituting Eqns. (3.27) and (3.28) into Eqn. (2.13) and takes the final form as follows

$$H^{GN}(x) = \sum_{i=1}^{nlc} a_i \left[QK^{-1}(x)U(x,K^{-1}f_i) \right]^T \left[QK^{-1}(x)U(x,K^{-1}f_i) \right] \tag{3.30}$$

The simple approximate Hessian matrix generated by the Gauss-Newton approximation in Eqn (3.30) is symmetric, positive semi-definite, and contains enough information about the second derivative of the loss function to be computed reliably if the residual error is small. The exact Hessian is tedious to compute, and experience shows that it is not worth the effort.

The most important aspect of the formulation for both proposed estimators is the computation of the sensitivity matrix U. In section 3.2, we showed how to construct the U matrix by assembling the element sensitivity matrices U^e. To compute the element sensitivity matrices U^e, we have developed a general procedure discussed in Appendix B. We have shown that the sensitivity of the element stiffness matrix with respect to the unknown parameters, the primary concern for the proposed parameter estimation methods, can be generated in an elegant and straightforward procedure. The derived formulation is capable of handling an element whose stiffness matrix is numerically integrated because the explicit form is too complex to compute. The procedure can consider elements with kinematic or material nonlinearity and covers a wide range of finite element models using one dimensional to three (or higher) dimensional elements. Besides, the same approach can be used to compute the sensitivity of mass and damping matrices with respect to their parameters for dynamic case (see Chapter Seven). Also, in Appendix B, we have derived the sensitivity matrices for a planar truss element, which is a linear function of its axial stiffness parameter EA, and a planar Timoshenko beam element, which is nonlinear with respect to its parameters (EA, EI, and GA).

3.4. Initial Values for the Unknown Variables

We cast both the output error estimator and the equation error estimator as constrained nonlinear optimization problems, which are solved iteratively. Like any iterative algorithm, these estimators need initial values for the unknown variables to start the iteration. The choice of the starting point controls the convergence of the algorithm and dictates the computational effort required to achieve a solution. The farther the starting point is from the local minimum, the more computation is needed to converge. The initial guess for the unknown variables is a critical factor for the rate of convergence of estimations. The user should use all of *a priori* knowledge to improve the choice of the starting point.

While the bounding constraints on the parameters prevent convergence to solutions in the infeasible region, one still faces the possibility that either multiple distinct minima or a ravine exist within the feasible domain if the data contain insufficient information. If either one of these two conditions exists, the position of the starting point dictates to which point the algorithm will converge. If the solution point is close to the actual parameters then the estimated parameters will appear to have a small bias; if the solution point is far from the actual parameters then it will appear to have a large bias. Therefore, the choice of the initial values will appear to affect the accuracy (by apparently reducing the bias) of the estimator, particularly in a simulation environment.

The output error and the equation error estimators both need initial values for the unknown parameters x^o. If they are available, the nominal (or as-built) design values are a reasonable choice for these parameters.

One can also use auxiliary engineering methods to improve nominal guesses of the initial values for the unknown parameters. For example, the moment of inertia of a cracked cross section of a reinforced concrete member can be used if cracking is suspected. If some of the parameters are known, then the known parameters x_o can be used to guess initial values for the unknown parameters x^o having the same nature. If the initial values are selected such that their ratios are approximately correct, convergence will be enhanced. Since the algorithm scales all values automatically, the relative order of magnitude of the parameters is not as important. The user should use all *a priori* knowledge and engineering intuition available to select and improve initial values x^o and bounding values $\bar{x}$ and $\underline{x}$ in Eqn. (3.5) and (3.26) in order to reduce the computational effort required to find a solution. However, the algorithm is robust with respect to starting values. If one has complete ignorance of the properties, one might select all parameters to have unit value. The effect of initial values x^o on the behavior of the proposed estimators will be studied in Chapter Four through a numerical simulation.

The equation error estimator needs initial values not only for unknown parameters x^o but also for the response at the unmeasured degrees of freedom $\bar{u}^o$. One could provide the starting values $\bar{u}^o$ explicitly, but for large finite element models with multiple load cases this option is usually impractical. In such a case, the parameter estimation algorithm should automatically generate reasonable initial values for the unmeasured degrees of freedom. For the implementation discussed herein one has the option of specifying the initial values of the unmeasured responses explicitly. We also provide three ways to build $\bar{u}^o$ automatically. In the first approach, the average μ of the absolute values of the measured degrees of freedom $\hat{u}$ for a particular load case is computed

$$\mu = \frac{1}{\hat{n}_d} \sum_{i=1}^{\hat{n}_d} |\hat{u}_i| \tag{3.31}$$

and assigned as the initial values for all of the unmeasured deformations $\bar{u}^o$ associated with that load case

$$\bar{u}_i^o = \mu \qquad i = 1,\ldots,\bar{n}_d \tag{3.32}$$

where $\hat{n}_d$ and $\bar{n}_d$ are the number of measured and unmeasured degrees of freedom, respectively ($n_d = \hat{n}_d + \bar{n}_d$). Here, *a priori* knowledge about the order of magnitude of measurements for a load case is used to calculate a constant initial value for unmeasured response under that load case and this starting point is better than another constant value like zero for all deformations at unmeasured degrees of freedom under all load cases.

In the second approach, each component of the vector $\bar{u}^o$ is set equal to the average value μ multiplied by a random number with uniform distribution on the interval [-1,1], as follows

$$\bar{u}_i^o = \mu R_i[-1, 1] \qquad i = 1,\ldots,\bar{n}_d \tag{3.33}$$

Here, the vector of initial values $\bar{u}^o$ does not have constant components for a particular load case. Using the random number generator gives the flexibility of starting the optimization procedure from different points

in the space of unmeasured degrees of freedom and searching for the potential local minima with a given set of initial values for the unknown parameters.

The third way to generate initial values for unmeasured response $\bar{u}^o$ is to compute the response of the finite element model based on the values of the known parameters x_o and initial values of the unknown parameters x^o for a particular load case and use the computed deformations at the location of the unmeasured degrees of freedom as their initial values. This approach can be expressed as follows

$$\begin{bmatrix} \hat{u}_i^o \\ \bar{u}_i^o \end{bmatrix} = K^{-1}(x_o, x^o) f_i \qquad i = 1,\ldots,nlc \tag{3.34}$$

where $\hat{u}_i^o$ and $\bar{u}_i^o$ are the computed deformations at the locations of the measured and unmeasured degrees of freedom, respectively for the ith load case. In this approach, *a priori* knowledge about the topology and geometry of the finite element model is considered, so the vector of computed initial values of unmeasured response is closer to the nature of the model equation than the first and second approaches (Eqns. (3.32) and (3.33)), even though x^o might not be a good initial vector. The closer the initial values for the unknown parameters x^o are to the actual parameters, the better the initial values for the unmeasured response are. In order to modify the order of magnitude of the starting values for the unmeasured deformations to be close to their actual values, it is better to multiply the initial vector $\bar{u}_i^o$ by the scalar $\| \hat{u}_i \| / \| \hat{u}_i^o \|$. This scalar multiplication adjust the magnitude of $\bar{u}_i^o$ whenever the order of magnitude of the initial parameters x^o is far from the order of magnitude of the actual parameters. We have found the third approach generates better initial vector $\bar{u}^o$ than the other approaches with respect to the rate of convergence.

3.5. Scaling Unknown Variables

Both proposed estimators use the recursive quadratic programming (RQP) algorithm to minimize the loss function. The RQP algorithm is an iterative gradient search strategy that uses the local information about the gradient and curvature of the loss function at the current point in the space of optimization variables and computes a direction vector and a step length to reach the next point.

The performance of the RQP strategy depends on the local geometry of the graph of the loss function around a local minimum. Like all gradient-based search methods, if the basin of attraction around the local minimum is a ravine with steep slopes for some of the variables and shallow slopes for the rest of the variables, then the RQP algorithm minimizes the loss function along the dimensions of the optimization space with the steep slopes and exhibits a reluctance to follow the shallow slopes along the other dimensions. Consequently, RQP will have difficulty reaching the bottom of such a ravine (local minimum). This type of geometric feature will affect the convergence rate of the RQP algorithm and might sometimes lead to oscillation or divergence because of the poor conditioning of the Hessian.

One of the factors contributing to steep, narrow valleys on the graph of the loss function, is a large discrepancy in the orders of magnitude of the different variables (scaling problem). In parameter estimation of structures, we have a potential scaling problem because the parameters x can have different units, and hence radically different values depending upon the system of measurement chosen. For example, physical properties

such as axial, shear, or bending stiffnesses often have values with different orders of magnitude in the customary systems of measurement. The scaling problem becomes even more acute for the equation error estimator because the unknowns include unmeasured responses which, in customary units, can have values with orders quite different from the unknown constitutive parameters x (not to mention each other).

Some identification problems will be intrinsically ill-conditioned. For example, a structure may have two masses, which we hope to identify, that have wildly different sizes. We presume that the data have captured enough information to distinguish these two parameters. The loss function, in this case, might exhibit a ravine that no change in units will cure. The scaling problem caused by presence of the ravine will, as with the scaling problem caused by units, create difficulties in convergence for the RQP algorithm.

To ameliorate the numerical difficulties caused by the scaling problem, we propose that all of the unknown variables s be scaled to have the same order of magnitude. We generate a positive definite diagonal matrix A, based on the initial values of the unknown variables (x^o, $\bar{u}^o$), to scale the unknown variables (x, $\bar{u}$) to have a value equal to χ, which can be any positive real number. For the unknown parameters x, the scale factors are simply computed as

$$A_i = \frac{\chi}{x_i^o} \qquad i = 1,\ldots,n_p \tag{3.35}$$

where A_i is the ith diagonal member of the scaling matrix A, x_i^o is the initial value for the ith unknown parameter, and n_p is the number of unknown parameters.

For the unmeasured degrees of freedom, a single scaling factor is calculated for all of the unmeasured displacements which have the same character (*e.g.* translation as opposed to rotation) and correspond to the same load case. For simplicity, but at no loss of generality, we consider the number of different categories (types) of displacements to be equal to the number of degrees of freedom at each node n_d^n. (Thus horizontal translations would be considered different from vertical translations, which in turn are considered different from rotations). To compute the scaling factors one must first determine the average value μ for each displacement type from the values of measured displacements and the initial values of the unmeasured displacement of the same type. Consider the general case in which we have *nlc* load cases and *ndt* displacement types. Let the index set G_k contain the global degree-of-freedom numbers for the m_k displacements of type k. The absolute average of the displacements of type k for load case j are then

$$\mu_k^j = \frac{1}{m_k} \sum_{i \in G_k} |u_i^{oj}| \tag{3.36}$$

where the vector u^{oj} is the complete displacement vector, including $\hat{u}_j$ and $\bar{u}_j^o$ for the jth load case. In the special case where *ndt* is equal to the number of degrees of freedom per node n_d^n (*e.g.* for a planar frame n_d^n is equal to three), and the degrees of freedom are numbered in the same order for each node, then m_k is equal to the number of nodes. In this case the values of the index set can be computed as $G_k(i) = k + (i - 1)n_d^n$.

Using the absolute average displacements, the scaling factor for each unmeasured degree of freedom can be defined as

$$A_{l(i,j)} = \frac{\chi}{\mu^{j}_{k(i)}} \tag{3.37}$$

where index $l(i,j)$ depends upon the indices i and j and is calculated as

$$l(i,j) = n_p + (j-1)\bar{n}_d + i \qquad j = 1,\ldots,nlc \quad , \quad i = 1,\ldots,\bar{n}_d \tag{3.38}$$

and the index $k(i)$ in Eqn. (3.37) indicates that the type k is inherited from the degree of freedom number i. The equation for the index $l(i, j)$ in Eqn. (3.38) assumes that the vector of unmeasured displacements $\{\bar{u}_1, \bar{u}_2, \ldots, \bar{u}_{nlc}\}$ is placed after the vector of unknown parameters x in the vector of unknown variables s. Thus, the scaling matrix A has n_p diagonal terms for the output error estimator, and $(n_p + nlc \times \bar{n}_d)$ terms for the equation error estimator. Since A is diagonal, it is stored as a vector.

After computing all scale factors, the scaled unknown variables S are defined as

$$S = As \tag{3.39}$$

Now, the loss function J for the parameter estimation problem (2.4) is minimized with respect to the new optimization variables S. The recursive quadratic programming requires the gradient vector and the Hessian matrix for the scaled variables. Because the transformation in Eqn. (3.39) is simple and linear, the sensitivity of the loss function J with respect to S can be simply computed as follows

$$\nabla_S J(S) = A^{-1}\nabla_s J(s) \tag{3.40}$$

$$\nabla^2_S J(S) = A^{-1}\nabla^2_s J(s) A^{-1} \tag{3.41}$$

Since Eqn. (3.41) is a congruent transformation it preserves the symmetry of $\nabla^2_s J(s)$. Since A is positive definite, the new Hessian matrix $\nabla^2_S J(S)$ remains positive semi-definite if $\nabla^2_s J(s)$ is positive semi-definite. The convergence rate of the optimization algorithm is governed by the eigenvalues of the Hessian matrix $\nabla^2_S J(S)$. Therefore, the scaling process can improve the convergence rate and also the condition number of the Hessian matrix. The implemented scaling process is efficient because the computational effort required to construct and invert the scaling matrix is trivial relative to the cost of a step of RQP. Also, it needs only an additional one dimensional array to store the diagonal terms of the scale matrix A. Based on the numerical simulation, we have observed that scaling the variables significantly improves the convergence characteristics and increases the robustness of the developed estimators whenever the parameter estimation problem is plagued with a scaling problem.

Other scaling procedures are possible. For example, one might use the same procedure as proposed, but updates the scale matrix during the optimization process based on the current values of the unknown variables rather than using the initial values.

3.6. Identifiability Criterion

Both of the proposed parameter estimators are members of the class of least-square estimators, a subclass of maximum-likelihood estimators. Maximum-likelihood estimators treat the parameters as deterministic, unlike Bayesian estimators which treat the parameters as random variables. The assumption of determinism of the parameters introduces a lower bound on the amount of data that maximum-likelihood estimators need in order to have any degree of confidence in the parameter estimates. If the amount of data is less than the minimum amount required by the estimator, then the confidence interval is essentially infinite, that is, the estimated parameters are completely unreliable. As the amount of data increases above the minimum level, the confidence in the parameter estimates increases (*i.e.* the confidence interval shrinks).

The amount of information contained in the loss function of a least-square estimator is equal to the number of independent squared terms. This number is often referred to as the dimension of the observation space. An estimator is based on a model of the system and is composed of n input-output equations relating the parameters. Whatever experiment we are doing, we run it m times; that is, we provide m different sets of inputs to the model and observe the corresponding outputs. Thus, the number of squared terms in the loss function will be $n \times m$; this number represents the amount of information, regardless of what specific data have been sampled. On the other hand, the amount of information is clearly equal to the number of data samples taken, regardless of what specific loss function one uses to estimate parameters.

For the linear, least-square estimators, the amount of information available must exceed the number p of unknowns we are trying to estimate, that is $n \times m \geq p$. This restriction, which we call the *identifiability criterion*, can also be used for nonlinear estimators (like the ones considered here) by recognizing that they are approximately linear in the neighborhood of the estimated parameters. On physical grounds one can also argue that the identifiability criterion should be equivalent to saying that the total number of (independent) data samples must exceed the number of essential parameters in the model (*i.e.* the number of parameters required to simulate or predict with the model; constitutive parameters in the present context). This intrinsic definition would suggest that one cannot create information simply by modifying the loss function which is chosen at the convenience of the data analyst.

For the output error estimator based on Eqn. (3.26), the identifiability criterion can be expressed as follows

$$(nlc \times \hat{n}_d) \geq n_p \tag{3.42}$$

where nlc is the number of repetitions of the experiment (load cases), $\hat{n}_d$ is the number of equations in the model $\boldsymbol{u}(\boldsymbol{x}) = \hat{\boldsymbol{u}}$, and n_p is the number of constitutive parameters. Clearly, $\hat{n}_d$ is also the number of spatial sampling points so that $nlc \times \hat{n}_d$ represents the total number of data samples.

For the equation error estimator based on Eqn. (3.5), the identifiability criterion is

$$(nlc \times n_d) \geq n_p + (nlc \times \overline{n}_d) \tag{3.43}$$

where again *nlc* is the number of repetitions of the experiment (load cases), n_d is the number of equations in the model $K(x)u = f$, n_p is the number of constitutive parameters, and $\bar{n}_d$ is the number of unmeasured responses. In inequality (3.43) the left-hand-side is the amount of data or dimension of the observation space and the right-hand-side is the number of optimization variables. The unmeasured responses are unknowns in the optimization problem but are not essential to the model in a simulation or prediction context. The total number of data samples is $nlc \times \hat{n}_d$ and the number of essential parameters is n_p. Noting that $n_d = \hat{n}_d + \bar{n}_d$, inequality (3.43) reduces to inequality (3.42), corroborating the intrinsic lower limit on information.

Certainly if the identifiability criterion is not satisfied then the parameter estimates are not reliable; however the converse is not true. Satisfaction of the identifiability criterion does not imply that the estimated parameters are reliable. The identifiability criterion (3.42) is a lower bound on data required to estimate parameters and one might use it to index the richness of the available information. One should always check the reliability of the estimation by determining how sensitive the estimation is with respect to noise in the measurements, the amount of data, the bounding constraints, and other *a priori* knowledge that has been used in the estimating process (*e.g.* structure geometry and topology).

The reliability of the estimates (as indexed by their confidence intervals) generally improve as the ratio of information to unknown parameters increases above unity, if the estimator is consistent. According to the identifiability criterion, such an improvement can be achieved either by increasing the number of tests (*nlc*), by increasing the number of measurement locations ($\hat{n}_d$), or by decreasing the number of parameters (n_p). The number of unknown parameters can be reduced by grouping the parameters or by using a different mathematical model with fewer unknown parameters. One might also try to improve the knowledge of certain parameters by subsidiary testing. However, even if the estimator is consistent there is no guarantee that an individual parameter estimate will improve by increasing the aggregate amount of information; the data must contain sufficient information on that parameter. In some instances, the available load cases cannot sufficiently excite certain members of a structure, and thus do not generate adequate information about the parameters associated with those members. Sensitivity analysis will expose any parameter that is not adequately represented by the data, and engineering judgement should confirm such an observation.

3.7. Chapter Summary

We have presented two algorithms for estimating the constitutive parameters of a finite element model that corresponds to a real structural system from measured static response to a given set of loads. The parameter estimation algorithms are based on *a priori* knowledge of the geometry and topology of the finite element model, the applied static forces, and the response of the structure at certain locations. The proposed algorithms solve a nonlinear constrained optimization problem whose objective function is the norm of either the error in nodal force equilibrium (equation error estimator) or the error in output response at the measurement locations (output error estimator). The unknown parameters are constrained to lie between lower and upper bounds. Each algorithm locates the minimum of its respective loss function by the method of recursive quadratic programming. The optimization algorithm exhibits global convergence that is generally robust (*i.e.*

convergence in a few iterations). We have derived the sensitivity matrices necessary for executing recursive quadratic programming, we have developed strategies to scale the unknown variables to improve numerical conditioning, and we have developed strategies for starting the iteration. Both proposed algorithms can estimate constitutive parameters from spatially sparse measurements. They can both be applied to large-scale, complex structural systems. While we assume that the response of the system is linear with respect to excitation, the parameterization of the structure can be nonlinear.

The combination of the finite element method and the recursive quadratic programming algorithm constitute the kernels of two general purpose parameter estimation programs. Like a finite element analysis system, the parameter estimation programs can treat structures with different types of elements. The differences between different structure types have been isolated at the element level. If one can implement an element in a general purpose finite element system, then one can also implement that element in the parameter estimation environment presented here. The parameter estimation algorithms are embedded in an environment capable of executing Monte Carlo simulations, useful both for studying the behavior of the proposed estimators, for example with respect to noise in the data, and for studying the identifiability of specific structural systems.

CHAPTER FOUR

Numerical Simulation Studies: Static Case

The behavior of an algorithm generally depends on the particular problem to which it is applied. While one can sometimes derive theoretical estimates of algorithm performance, such estimates are rare, particularly when the problem involves random variables. In lieu of such formulae one must either assess algorithm performance by observation on specific cases or remain ignorant of the performance. Often, some aspects of the qualitative performance of an algorithm are clearly demonstrated through a well chosen example. Usually, quantitative estimates cannot be gathered from the study of a single case. In any case, one must know which aspects of the problem are worthy of study, and one must be aware that if too many problem aspects are considered important, then the chance of illuminating any of them through a single case study is quite low.

The most important factors governing the performance of any parameter estimation algorithm are the quality and quantity of measured data. To assess the performance of the equation error estimator and the output error estimator, we examine their behavior with respect to the amount of noise in the measurements, the spatial distribution of measurements, the number of spatial measurements, the number of load cases, and the character of the load cases (specifically, loading patterns). In addition to the extensive study of the effects of the physical character of the data and the experiment, we examine the effects of different starting values of the unknown parameters used to initiate the iteration.

The present work focuses mainly on the behavior of the proposed estimators in the face of noisy data; all of the simulations use noisy data. The simulation environment introduced in Section 2.6 is used to control the statistical properties of the noise in the measurements and to determine the statistics of the estimations for both estimators. Based on quantitative measures of the confidence in the estimates, the general behaviors of the algorithms are presented and compared with each other.

The geometry, topology, and node numbering of a planar bowstring truss are shown in Fig. 4.1. The truss model (*i.e.* the actual structure) consists of 25 elements with four different cross sectional areas. The actual

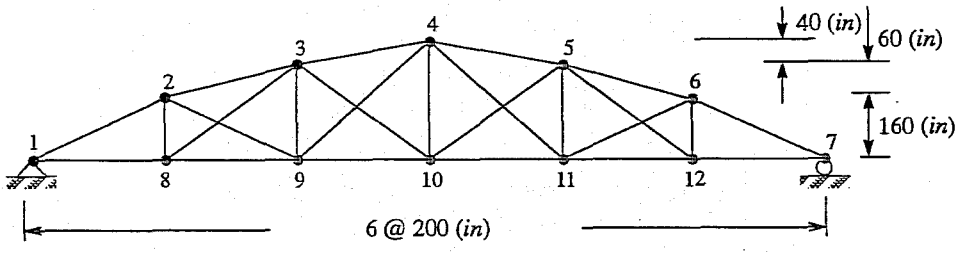

Fig. 4.1 Geometric configuration of the bowstring truss

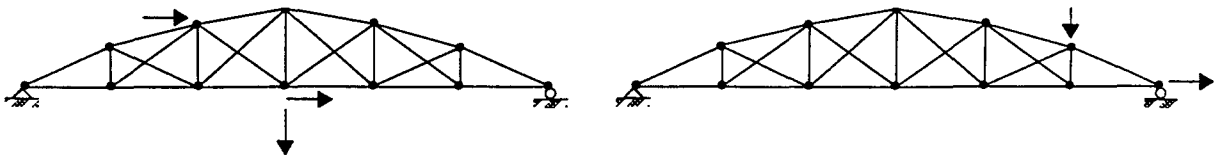

Fig. 4.2 Two typical load cases for the bowstring truss

values of the cross sectional areas are, 18 (in^2) top elements, 15 (in^2) bottom elements, 12 (in^2) cross elements, and 10 (in^2) vertical elements. The response of the structure is measured under several different static load cases. We wish to estimate the constitutive parameters of the structure. We will assume that we know in advance that the elements can be grouped into four groups of elements, the elements in each group having the same constitutive properties. A truss element has a single parameter. Assuming that Young's modulus is fixed for all elements, the parameter to be estimated is the cross sectional area of the members in the group. The number of unknown parameters for this problem is four, corresponding to the number of groups.

In this study we use a pool of 16 different (independent) load cases. Each load set in the study is taken randomly from this pool (no load set exceeds 7 load cases). Each load case has non-zero force components applied to, at most, three degrees of freedom. Figure 4.2 illustrates two typical load cases. The magnitude of nodal loads are chosen so that the maximum nodal displacement is less than 4.5 inches for all load cases. For this study, the lower bounds of unknown parameters are assumed to be zero and the upper bounds are five times the actual values, unless otherwise is mentioned. The bounding constraints ensure that the parameters will not become negative or too large.

The accuracy of Monte Carlo simulation depends on the sample size (number of trials), which should be large enough to establish statistically significant estimates. The statistical indices of the sample population converge to the actual statistics of the estimates as the sample size increases. Because a large number of trials requires great computational effort, a compromise between accuracy and computational effort is essential. A sample is sufficiently large when the sample statistics do not change with additional trials. Figure 4.3 shows the typical trend of the loss function (normalized with respect to the norm of measurements for the output error estimator and the norm of applied forces for the equation error estimator), average root quadratic bias,

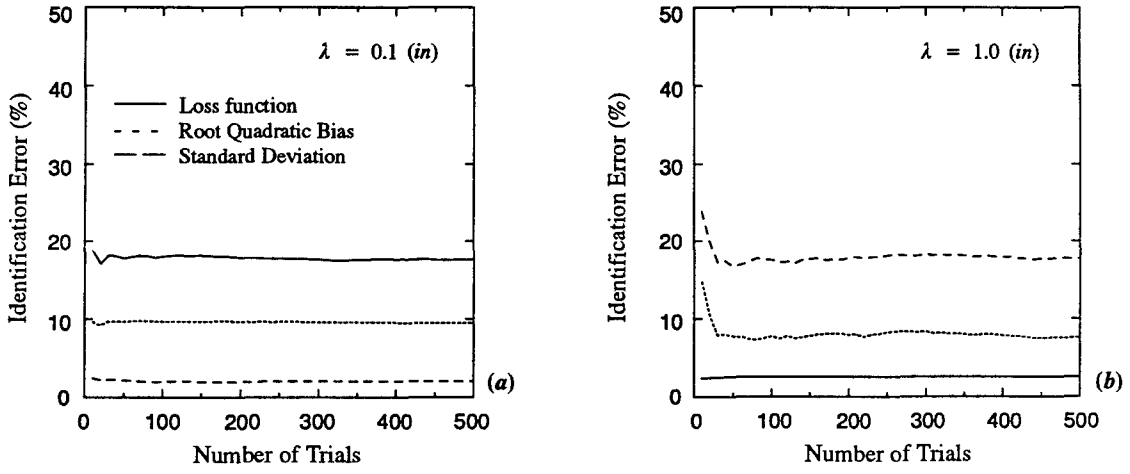

Fig. 4.3 Variations of sample statistical indices with number of trials
(*a*) Equation Error Estimator. (*b*) Output Error Estimator

and average standard deviation with the number of trials for both estimators. The statistical indices shown in Fig. 4.3, computed based on complete measurements for three load cases with absolute noise with the amplitude λ, are essentially steady after 100 trials, a conservative value for all experiments done to establish this number. In the following, all the statistical indices defined in Section 2.6 are based on a sample of 100 trials.

4.1. Initial Values for the Unknown Parameters

The outcome of the recursive quadratic programming algorithm, like any gradient-based method, depends on the topography of the loss function. Since we do not generally know where to start the iteration, the sensitivity of the algorithm to starting values is important to the general application of the method. Because the recursive quadratic programming method is a local minimization procedure, it will converge to the nearest local minimum. If the loss function has multiple local minima, then the starting point will determine to which of those minima the algorithm will converge. While we cannot, on mathematical grounds, rule out the possibility that the loss function of the present problem has multiple minima, we can examine the issue by studying the dependence of the outcome of the iteration on the starting point.

To investigate the sensitivity of the proposed estimators with respect to the initial values for the unknown parameters, we define a closeness index *CI* as follows

$$CI = 1 - \frac{\| x_{in} - \hat{x} \|}{\| \hat{x} \|} \tag{4.1}$$

where x_{in} and $\hat{x}$ are the vectors of initial and actual values of parameters, respectively. The closeness index *CI* measures the distance of the starting point from the actual point, is equal to unity when the initial values are equal to the actual values, and takes values less than one for all other starting points. Starting points x_{in} on a hypersphere whose center is at $\hat{x}$, have the same value of the closeness index. For example, a closeness index of zero includes all points on the hypershpere centered at $\hat{x}$ and having radius equal to the length of the vector $\hat{x}$ (and thus includes the origin). Clearly, the scalar measure *CI* does not distinguish among points on these hyperspheres. Similarly, the scalar measure of bias does not distinguish among estimates on a hypershpere centered at $\hat{x}$ and having a radius equal to the bias. Points with different values of bias must be distinct, but if the bias of two estimates is the same, one cannot dismiss the possibility that these points are distinct. Similarly, points with different closeness indices are distinct, but if the closeness index of two points is the same, one cannot dismiss the possibility that these points are distinct.

Figure 4.4 compares the behavior of the equation error estimator and the output error estimator as the closeness index varies. For this study, we use complete measurements from three load cases (selected from the pool of 16) having absolute noise of amplitude λ. We examine 7 different closeness indices in the range [0,1], and for each of those values of the closeness index we consider four distinct starting points x_{in}. In the figure we present the average root quadratic bias *RQB* and standard deviation *SD* for the estimates.

One can observe that the bias and standard deviation are the same for all values of the closeness index for both estimators. (Note that the replicated closeness indices plot right on top of each other). Furthermore, we observed that all cases converged to the same point (a stronger observation than convergence to different points of equal bias). For complete measurements the loss function for the equation error estimator is quadrat-

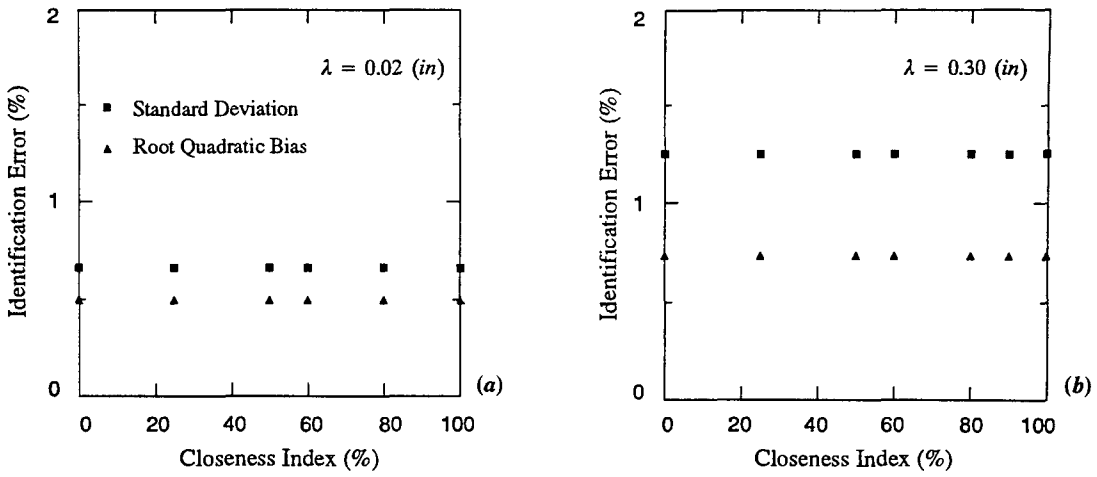

Fig. 4.4 Variations of the *RQB* and *SD* with initial values for complete measurements (*a*) Equation error estimator, (*b*) Output error estimator

ic. Hence, uniqueness of the solution point is expected. The loss function of the output error estimator is not quadratic, even for complete measurements, so uniqueness of the solution point is not guaranteed. However uniqueness did occur for this particular problem, and one might speculate that uniqueness is not exceptional.

One might expect that the probability that the minimum is unique would diminish for both estimators as the amount of information decreases. Multiple minima are certainly possible for sparse measurements from few load cases. We examine this possibility by considering the same starting values as before, but using only one load case and 5 (out of 21 possible) measurement locations. Figure 4.5 shows that the bias and standard deviation remain constant with varying closeness index for both estimators, even with scant information. The slight deviation from this constancy notable in the output error estimator is within the tolerance expected for the simulation. Again, while one case does not prove uniqueness, it suggests that it may not be exceptional.

In general, we expect the probability of multiple minima to increase as the amount of available information (*nlc*, $\hat{n}_d$) decreases. This probability should be greater for the equation error estimator because its optimization space has higher dimensions because the unknowns are augmented by unmeasured displacements.

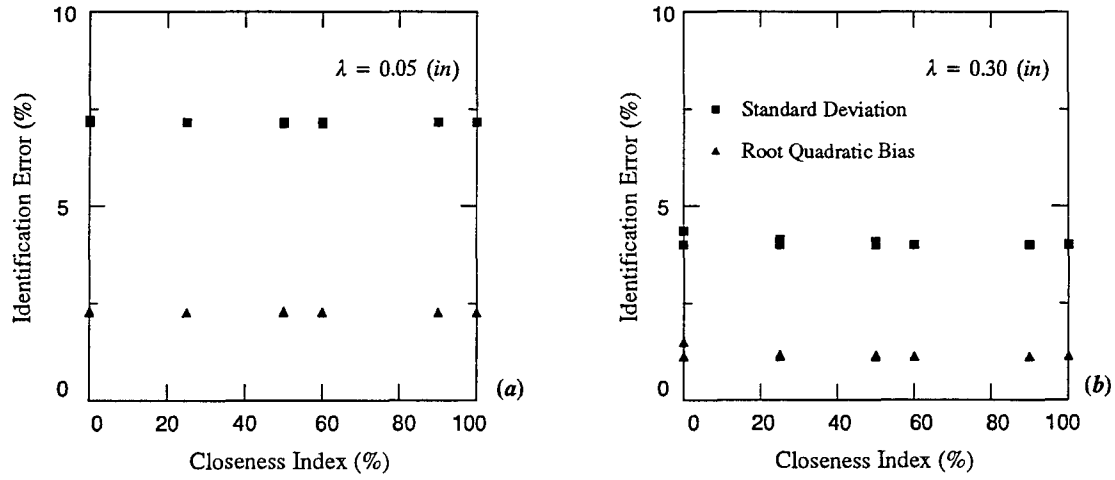

Fig. 4.5 Variations of the *RQB* and *SD* with initial values for incomplete measurements (*a*) Equation error estimator, (*b*) Output error estimator

The closeness of a starting point in the space of unknown variables $(x, \bar{u})$ for the equation error estimator depends strongly on the initial values of parameters, and has a different meaning than closeness in the space of parameters because it computes the initial values for the unmeasured deformations $\bar{u}$ using the initial values for the unknown parameters x_{in}. However, since we observed no dependence on starting values for the example at hand, we simply choose all initial values of the parameters equal to one for the remaining simulations in this chapter.

4.2. Effect of Quality and Quantity of Information

As mentioned in Chapter Two, the quality of information depends on the amount of random noise in the measurements, the spatial distribution of the measurements, and the spatial distribution of the excitation. The quantity of information is simply the number of measurements times the number of load cases. In this section we examine influence of quality and quantity of information on the bowstring truss structure. First, we consider the effect of noise amplitude (both proportional and absolute). Next, we examine the effect of the number of load cases and their spatial distribution. Finally, we study the effect of the number of measurement locations and their spatial distribution.

According to Eqns. (2.16) and (2.17), we model noise as a uniformly distributed random variate having amplitude λ and having absolute or proportional character, respectively. The amplitude of noise is the primary object of study here, however we also consider the effect of noise character throughout, presenting results for both absolute and proportional noise.

The effect of noise on the equation error estimator. For each specific pattern of noise the topography of the loss function is deterministic and the RQP algorithm is able to locate a single minimum. Since the noise is a random variable the location of the minimum in the space of parameters is also a random variable. Although we generally do not know the specific probability distribution function for the location of the minimum, the distribution can be determined numerically through simulation, and we can observe some qualitative features of this distribution.

The probability density function of the estimated parameters is a delta function at the actual parameters for zero noise amplitude. For all amplitudes of noise, the minimum is distributed within a closed region which we bound from below. As the noise increases, the region containing the local minima initially grows, reaches a maximum size, and then shrinks to a point (the lower bound point) in the limit. The peak of the probability density function shifts toward the origin as the noise amplitude increases. Thus, the probability that some of the parameters are less than a fixed number increases as the amplitude of the noise increases. Physically, the tendency to estimate small values for the parameters at large noise amplitudes indicates that in the face of great uncertainty the equation error estimator will generate a flexible structure.

Figure 4.6 shows the variations of average root quadratic bias (*RQB*), standard deviation (*SD*), root mean squared error (*RMS*), and identification error (*AIE*) with the amplitude of noise for the equation error estimator. For the equation error estimator, the root quadratic bias is a nondecreasing function of noise amplitude which saturates for large amplitudes of noise. As the amount of noise increases, the standard deviation initially increases, then becomes stationary, and finally decays. To help explain these trends we plot values of the esti-

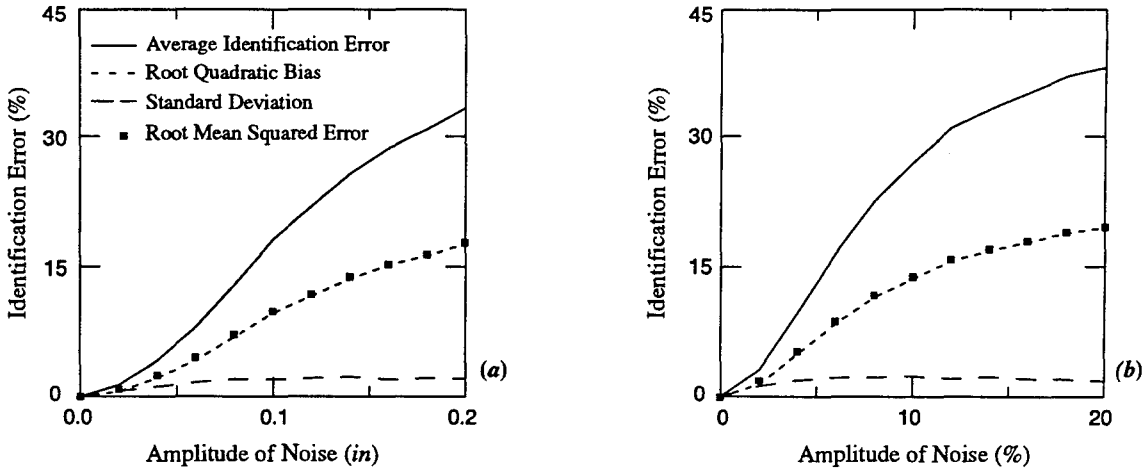

Fig. 4.6 Variations of the statistical indices with noise amplitude for EEE (*a*) absolute noise, (*b*) proportional noise

mated cross section areas against the amplitude of absolute noise in Fig. 4.7. One can observe that the estimates computed by the equation error estimator decay to small values as the amplitude of noise increases. Based on Eqn. (2.19), when the vector of estimated parameters $\bar{x}$ converges to zero, the *RQB* value saturates near $1/n_p$ which for the four parameter bowstring truss is 0.25. As the estimates converge to the region in the neighborhood of the lower bound constraints, the scatter of the estimates is confined by the bounds and the standard deviation of the estimates becomes small. According to Eqn. (2.23), if *SD* is small then *RMS* follows the trend of *RQB* and is almost equal to it. The *AIE*, by definition, behaves in a manner similar to *RMS*.

One can observe from Fig. 4.6 that for the equation error estimator, when the amplitude of noise is less than 0.03 inches for the absolute noise and 2% for the proportional error, the root quadratic bias is smaller than the standard deviation. For greater values of noise the opposite is true. It is desirable for an estimator to have smaller bias than standard deviation because it avoids the unfortunate possibility of making a precise (small standard deviation) estimate of low accuracy (large bias). In such a case, the standard deviation gives the wrong impression of the quality of the estimate. For sufficiently small amounts of noise, the equation error estimator is desirable. The closeness of the bias and standard deviation of the estimates indicates that the clus-

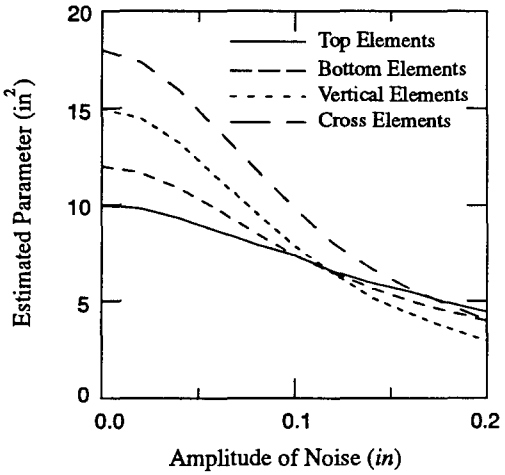

Fig. 4.7 Variations of the estimated parameters with noise amplitude for Equation Error estimator

ter of estimates contains the point corresponding to the actual parameters and that the computed estimates are in the neighborhood of that point. Let us introduce an index for the amplitude of noise, called the *desirability bound* λ_d. When the noise amplitude is less than λ_d, the bias of the estimates is less than their standard deviation and the estimator has a desirable behavior. Thus, for complete measurements, the equation error estimator has a desirability bound about 0.03 inches for the absolute noise and 2% for the proportional noise for the bowstring truss.

The effect of noise on the output error estimator. Like the equation error estimator, for noise-free data the probability that the minimum is equal to the actual parameters is unity and the problem collapses to a deterministic one for the output error estimator. For sufficiently small amplitudes of noise, the minimum is distributed within a closed region in the neighborhood of the actual parameters. As the noise increases, the measure (size) of the region grows. For sufficiently large amplitudes of the noise, the region becomes open. Specifically, it becomes unbounded in the direction of at least one of the parameters. Because we bound the parameters from below, the region containing the minimum is a cone. When the region passes from closed to open, the tail of the probability density function of the estimated parameters extends to infinite positive values. As the noise amplitude increases the mass under the tail of the probability density function, which indicates the probability that at least one of the estimated parameters is large, increases and becomes steady. The probability that at least one of the parameters is smaller than a fixed small number also increases and becomes steady as the amplitude of the noise increases. Thus, for large amplitudes of noise, local minima tend to occur at the boundaries of the feasible region, and not inside. Physically, the tendency to estimate either large or small values for the parameters at large noise amplitudes indicates that, in the face of great uncertainty the output error estimator will generate either a very stiff or a very flexible structure; the probability of a moderately stiff structure tends to zero.

The probability density function of the estimated parameters is a delta function at the actual parameters for zero noise amplitude. In the limit as noise becomes large, the probability density concentrates near the boundaries of the feasible region. These properties of the probability density function are important to understanding many of the asymptotic trends observable in the present study.

While it is most instructive to consider the topography of the loss function as random, some insight can be gained by considering the deterministic topography of the loss function developed by considering a single, fixed noise vector. For small amounts of noise the basin of attraction is similar to a well conditioned quadratic function. The RQP algorithm, like most gradient-based algorithms, has no difficulty locating the minimum in a few iterations. As the noise amplitude increases the probability of occurrence of a distorted basin of attraction increases. For certain noise vectors, the minimum will be located at large values of some of the parameters. The topography of the loss function for these cases is invariably characterized by a long, narrow ravine. Physically, the presence of the ravine represents insensitivity of the loss function to the parameters on the major axes of the ravine. This insensitivity is caused by a dearth of information or, equivalently, because the noise has swamped out the true information. For large enough noise amplitudes all good information will be lost and the estimated parameters will be totally unreliable, but not all measurements are equally sensitive and thus some data are swamped earlier than others. For partially swamped data some of the parameters can still

be reliably estimated while others cannot. Most of the statistics reported here do not try to make that distinction. We note that the RQP algorithm does not have difficulty locating minima that occur at the remote end of a narrow ravine.

Figure 4.8 presents the variations of the root quadratic bias and standard deviation of parameters estimated based on complete measurements from three different load cases with respect to the amplitude of the noise for different upper bounds. One can observe that by increasing the noise, root quadratic bias and standard deviation gradually increase and finally saturate. The kinks in the graph specially for the standard deviation are due to the limited size of the Monte Carlo simulation. Since the region containing local minima is closed for small amounts of noise, the root quadratic bias and standard deviation are not affected by the values of the upper bounds at these noise levels. The saturation level for the root quadratic bias and the standard deviation is a function of the specified upper bounds. While the proportion of bound cases remains essentially fixed for large amplitudes of noise, their mean average increases as the upper bound grows thereby increasing the saturation level. Since the saturation level increases as the upper bounds on the parameters increase, one would expect that the statistical indices of the parameters estimated by the output error estimator without upper bound constraints do not saturate.

Figures 4.9 (*a,b*) show the behavior of the output error estimator for absolute noise, and (*c,d*) for proportional noise when the upper bound is five times the actual values. Figure 4.9 (*b*) shows the same thing as (*a*), but for a larger range of noise; likewise (*d*) shows the same thing as (*c*), but for a larger range of noise. Observe that the *AIE* and *RMS* show the same trend as bias and standard deviation. By increasing the amount of noise, *RMS* initially follows the trend of *SD* and then follows the trend of *RQB*. Like the equation error estimator, the root quadratic bias is less than the standard deviation for a certain range of noise amplitude, the so-called *desirability range*. However, the desirability range is much larger for the output error estimator than it is for the equation error estimator. Unlike the equation error estimator, the standard deviation of the output error estimator does not decay for larger noise amplitudes. Scatteredness fails to persist in the equation error estimator because all the estimated parameters tend to small values at large noise amplitudes. In the output error estimator scatteredness persists because the estimated parameters distribute between large and small values.

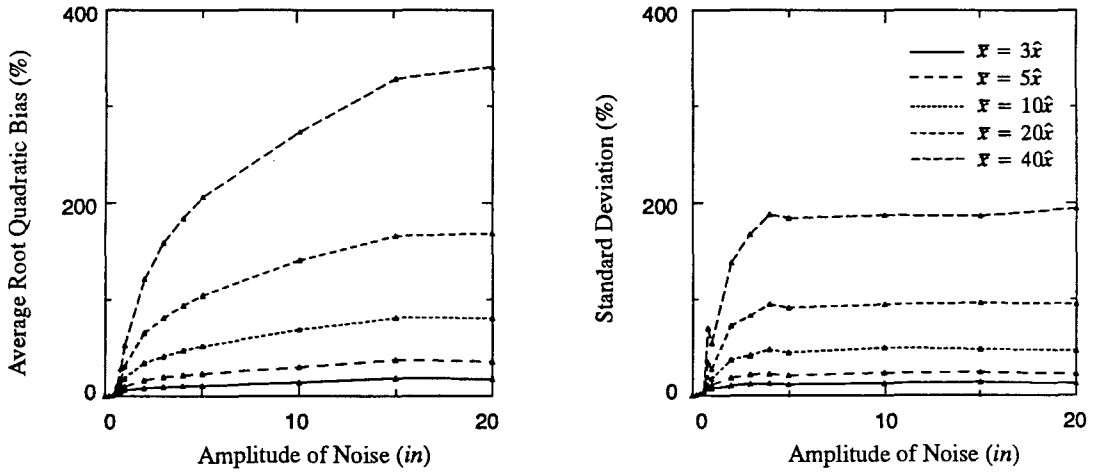

Fig. 4.8 Variations of the *RQB* and *SD* with respect to the noise amplitude for different upper bounds for OEE

The parameters (cross-sectional areas) estimated by OEE for different upper bounds are plotted against the amplitude of absolute noise in Fig. 4.10. One can observe that as noise amplitude increases the values of the estimated parameters increase and saturate, unlike the parameters estimated by the equation error estimator which converge to small values (as shown in Fig. 4.7). Figure 4.10 shows the variation of the mean average of the sample of estimates for each parameter with respect to noise amplitude. Therefore, the trends observed in Fig. 4.10 reflect the variations of the distributions of the estimated parameters with respect to the amplitude of noise. To illustrate how the distributions of the estimated parameters change with noise amplitude, we present in Fig. 4.11 the probabilities that the estimate of each parameter x becomes equal to its upper bound $P(x = \bar{x})$, is less than its upper bound and is greater than the 30% of its actual value $P(0.3\hat{x} < x < \bar{x})$, and is smaller than the 30% of its actual value $P(x \leq 0.3\hat{x})$, for different amounts of noise when the upper bounds are five times the actual values. The probability of an event is taken to be the ratio of trials associated with that event. One can observe that for small amounts of noise, $P(0.3\hat{x} < x < \bar{x})$ is equal to one for all parameters, indicating that the region containing the estimates is closed and is inside the feasible region in the neighborhood of the actual parameters. As the noise increases, $P(0.3\hat{x} < x < \bar{x})$ decreases to small values and simul-

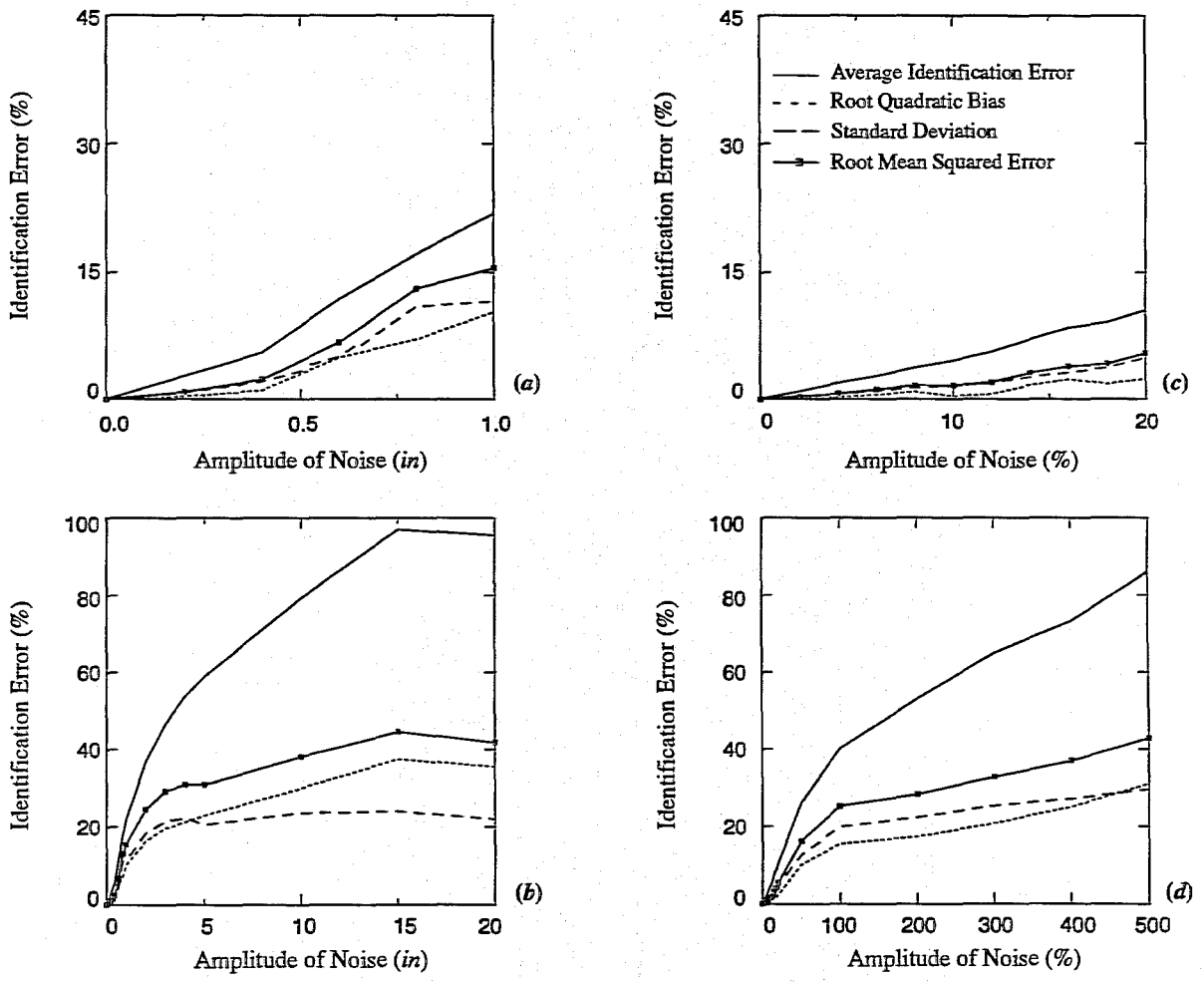

Fig. 4.9 Variations of the statistical indices with noise amplitude for OEE
(*a, b*) absolute noise, (*c, d*) proportional noise

taneously $P(x = \bar{x})$ and $P(x \leq 0.3\hat{x})$ increase and become steady. The trends in Fig. 4.11 indicate that for large amounts of noise, the estimated parameters are distributed near the boundaries of the feasible region. Therefore, if the lower bounds are set to zero, the mean average of each estimated parameter converges to a saturation limit equal to a ratio of its upper bound, and this ratio is equal to the probability that a parameter becomes equal to its upper bound. For a well posed parameter estimation problem, $P(x = \bar{x})$ is the same value for all parameters and is about 0.5. If one does not prescribe upper bounds for the parameters, equivalent to setting $\bar{x}$ to infinity, one will not observe the saturation phenomena for the trends in Fig. 4.10 and consequently, in Fig. 4.8. Also, in Fig. 4.11 one can observe that the event of converging to the upper bound starts at smaller amounts of noise than the event of converging to the lower bounds.

A parameter estimate starts to grow when the noise swamps out the information needed to estimate that parameter. The rate of growth of the saturating parameters can be fast for the parameters most poorly represented in the data (*i.e.* the loss function is insensitive to those parameters). In the present case, as shown in Fig. 4.10, estimated cross-sectional areas of the vertical elements are most prone to saturation because they are the

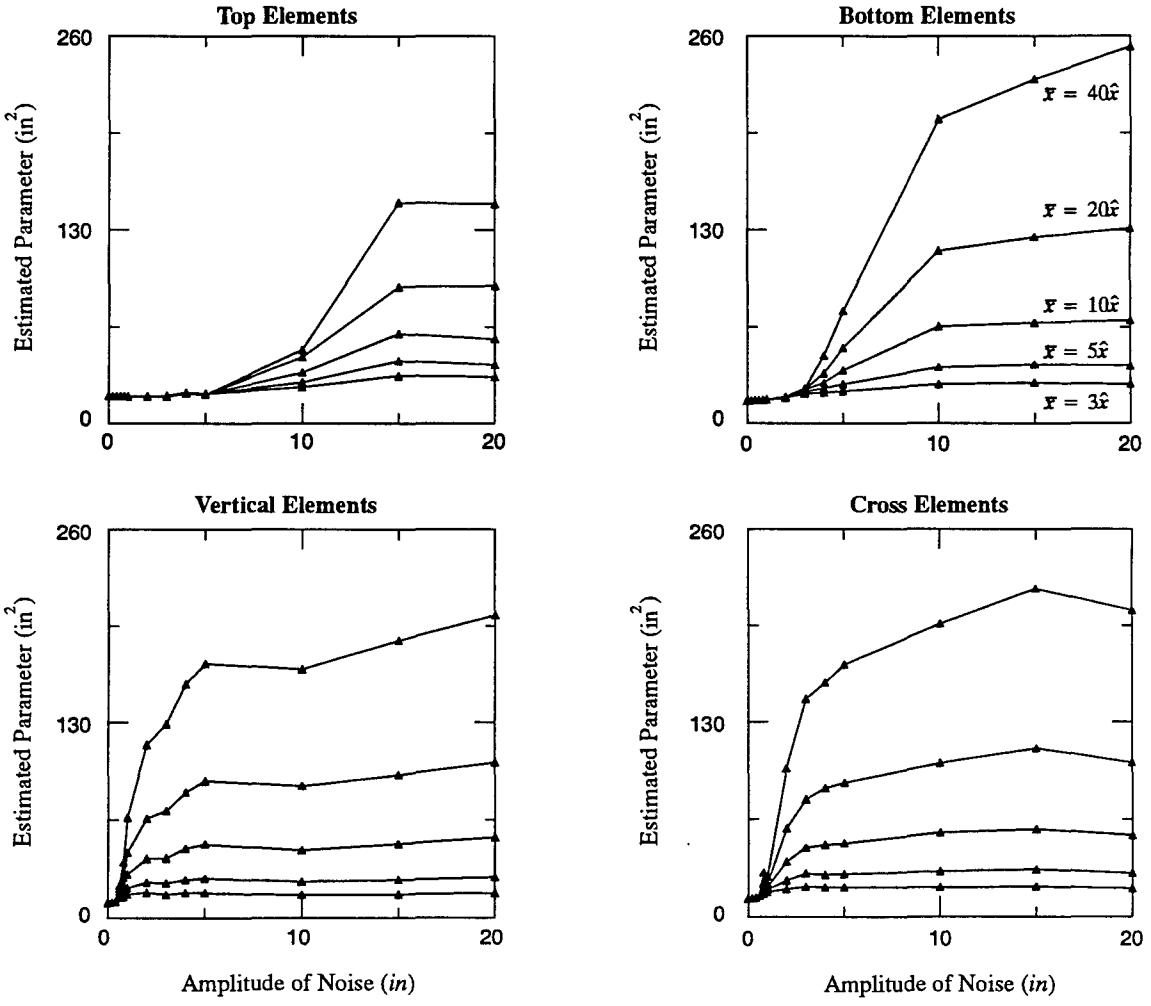

Fig. 4.10 Variations of the parameters estimated by OEE with noise amplitude for different upper bounds

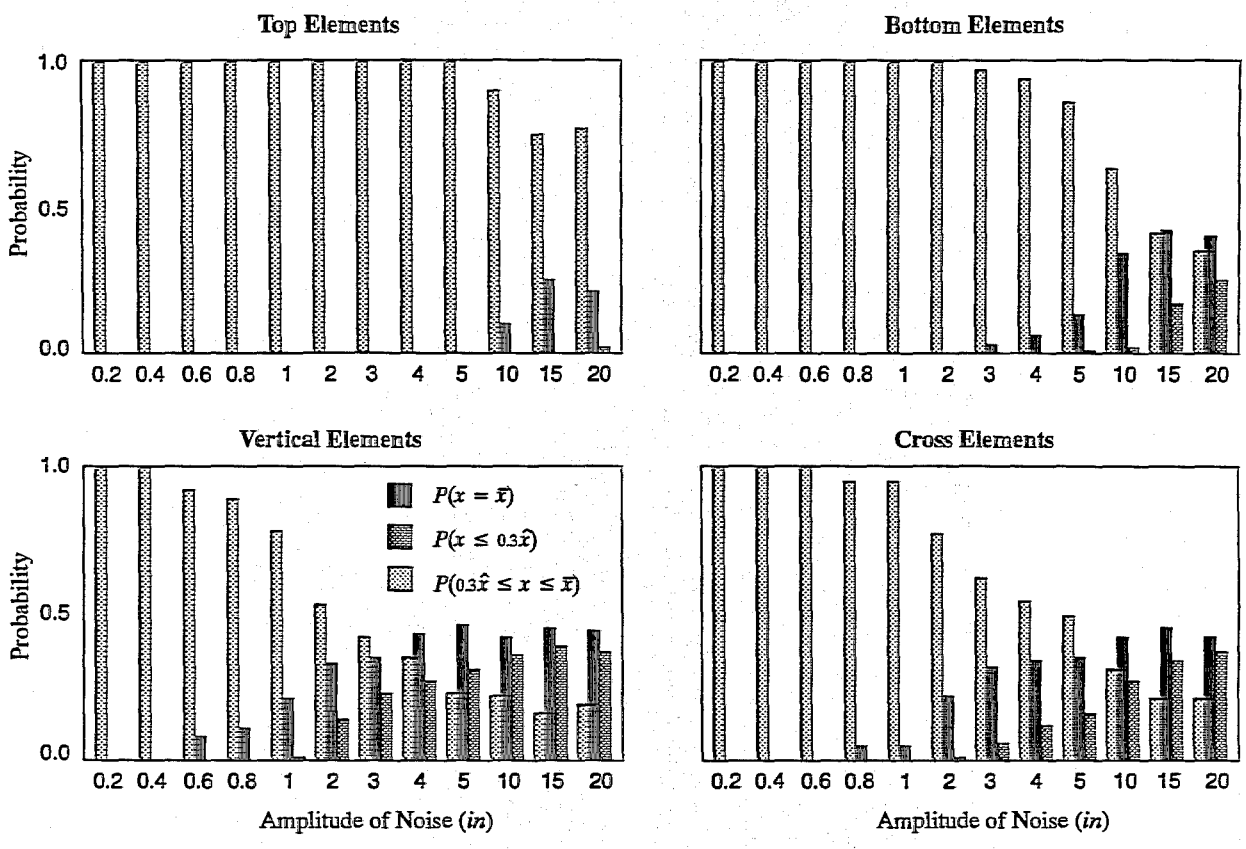

Fig. 4.11 Distributions of the estimated parameters by OEE

least excited by the loadings. Also, the phenomenon of converging to upper bounds for the group of vertical elements starts at the smaller amounts of noise than other groups of elements, as shown in Fig. 4.11

Figure 4.12 shows the variation of the probability that all of the estimated parameters are less than their upper bounds $P(x < \bar{x})$ with respect to the noise amplitude for different values of upper bounds. When the noise is small, $P(x < \bar{x})$ is unity, indicating that all the local minima are located in the interior of the feasible region. As noise amplitude increases, $P(x < \bar{x})$ decreases. We have previously observed (Figs. 4.8 through 4.11) that as noise increases, the estimates converge in probability to the boundaries of the feasible region. For large amplitudes of noise, cases with $x \leq \bar{x}$ correspond to cases in which all of the parameters are small because the probability of there being an intermediate point is small. Thus, the probability of estimating all small parameters asymptotically approaches zero as the noise amplitude increases. Figure 4.12 also suggests that, for a fixed amount of noise, $P(x < \bar{x})$ increases as the upper bounds increase, indicating that some of the estimated parameters and their corresponding local minima which are on the boundaries or outside the feasible region, come inside the feasible region by increasing the size of the feasible region.

Both estimators behave similarly for both absolute and proportional noise. Both estimators are biased and their *RQB* values increase as the amplitude of noise increases. Although the bowstring truss responds linearly with excitation and the parameterization of the stiffness matrix is linear, the bias of the estimates varies nonlinearly with noise amplitude, even for complete measurements. For the equation error estimator the nonlinearity with respect to noise is due to the presence of products of parameters and noise in the loss function. For

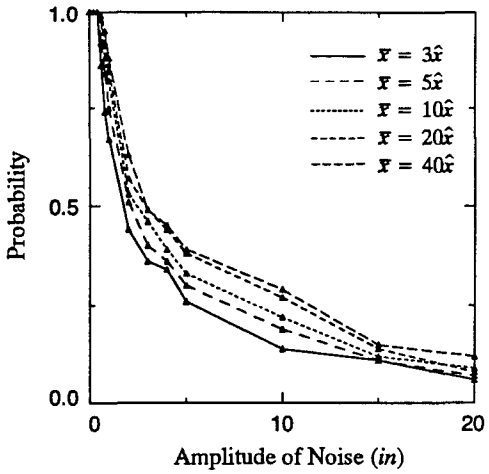

Fig. 4.12 Probability of all parameters are smaller than their upper bounds

the output error estimator the nonlinearity is due to the nonlinearity of the loss function with respect to the parameters. Incompleteness of measurements adds yet another source of nonlinearity of estimates with respect to noise.

The output error estimator has an acceptable amount of bias for a wider range of noise amplitude than does the equation error estimator. For average root quadratic bias not exceeding 15%, the OEE can deal with noise amplitude about 2.0 inches, while EEE requires measurements with the amplitude of noise about 0.15 inches for the bowstring truss with complete measurements. The main reason for the low biasedness of OEE is that the error function for OEE has an additive noise vector which is independent from the parameters. The equation error estimator has a noise vector which is multiplied by the stiffness matrix and is not independent from the parameters. Consequently, the output error estimator satisfies the main assumption for the unbiased least squares estimators, that is, the independence of the noise vector from the parameters (Trenkler 1981 and Goodwin 1984). The equation error estimator becomes a low bias estimator when noise is added to the vector of applied forces because, in this case, noise is independent from the parameters.

Effect of number of measurements. Confidence in the estimated parameters depends strongly on the amount of data. The identifiability criterion (3.42) gives a lower bound for the amount of information for the proposed estimators. For both estimation algorithms, the amount of information is the product of the number of load cases and the number of measured degrees of freedom, $(nlc \times \hat{n}_d)$. In this section, we study the behavior of the proposed estimators as *nlc* and $\hat{n}_d$ vary.

Figures 4.13 and 4.14 show the variation of the root quadratic bias and standard deviation with the number of load cases. In these figures, displacements were measured at all degrees of freedom and an absolute noise of 0.02 inches for EEE and 0.1 inches for OEE were applied to the displacements. For each value of *nlc*, we examine four different sets of load cases, taken from the pool of sixteen, to assess the influence of loading pattern. The number of load cases *nlc* provides a quantitative measure of the richness of loading. Considering four different loading patterns adds a qualitative measure for the information content of loading. The statistics corresponding to each load set are shown as triangles in Figs. 4.13 and 4.14. Note that these load cases were chosen at random; no attempt was made to select loading patterns having better statistics.

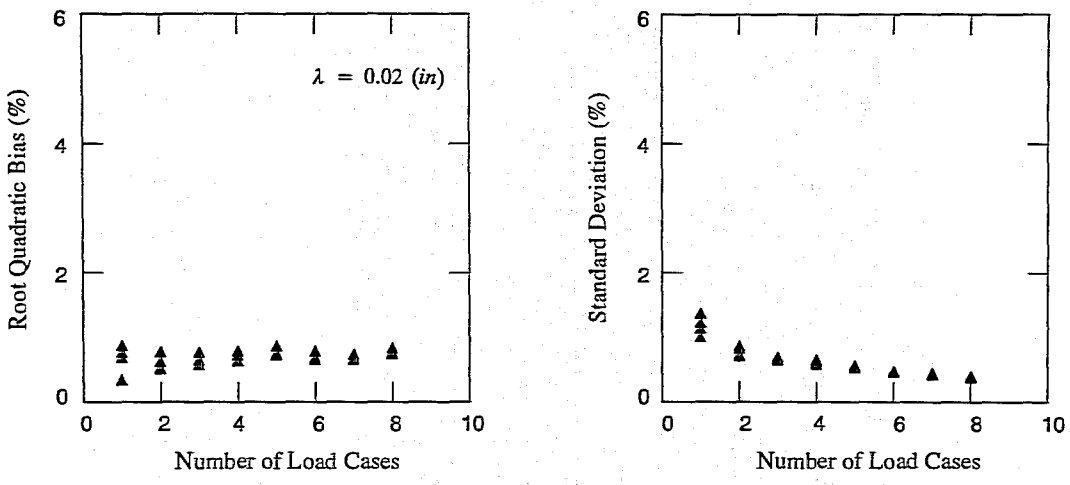

Fig. 4.13 Variations of the *RQB* and *SD* with number of load cases for EEE

The bowstring truss has 21 degrees of freedom and four unknown parameters. Therefore, for complete measurements, one load case is adequate to satisfy identifiability criterion (3.42). As long as load cases are added to the load set, the standard deviation of the estimates decreases. The decrement of the scatter of the estimates with the increment in the number of load cases is a general trend for both equation error and output error estimators. However, as the number of load cases increases, the *RQB* value remains constant for the equation error estimator, as shown in Fig. 4.13, and decreases for the output error estimator, as shown in Fig. 4.14. Also, one can observe from Figs. 4.13 and 4.14 that for small *nlc* values, the statistics of the estimates depend on the pattern of loading, especially for the output error estimator; for large *nlc* values, the statistical indices are independent of the loading patterns.

Figures 4.15 and 4.16 compare the behavior of the proposed estimators as the number of load cases and amplitude of noise vary. In these figures, the *RQB* values are plotted for the loading patterns which have the least bias for a given *nlc* and noise amplitude and the *SD* values are plotted for the loading patterns with the largest standard deviation. The root quadratic bias remains smaller than the standard deviation for OEE. One

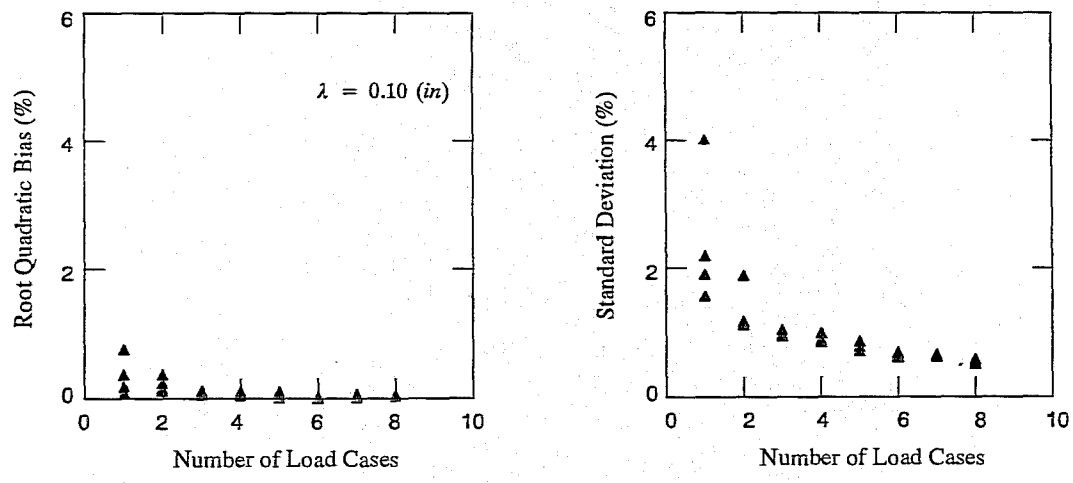

Fig. 4.14 Variations of the *RQB* and *SD* with number of load cases for OEE

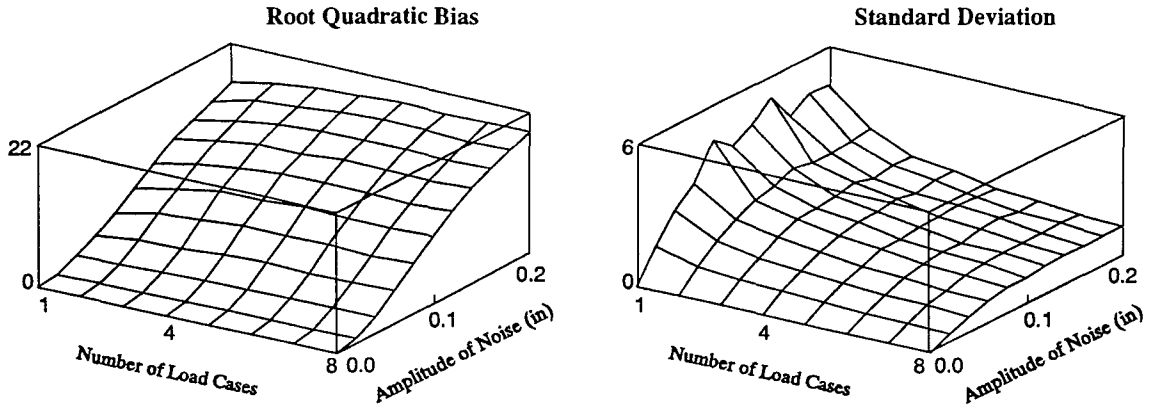

Fig. 4.15 Variations of the *RQB* and *SD* with number of load cases and amplitude of noise for EEE

can observe the same tendency in the EEE when the amplitude of the noise is adequately small. As the noise amplitude increases, the bias value becomes greater than the *SD* value for EEE. It is evident that the scatter of the estimates decreases as the number of load cases increases. Figure 4.15 indicates that the bias of the estimates does not change with increasing *nlc* for the equation error estimator. For the output error estimator, the bias decreases as the number of load cases increases. In other words, as *nlc* increases the accuracy and precision of the estimates computed by OEE increase and the precision of the estimates computed by EEE increases, but their accuracy does not change. Therefore, the output error estimator is a consistent estimator but the equation error estimator is not. For the same number of load cases and the same amplitude of noise, the output error estimator has smaller bias than the equation error estimator. Also, one can infer from Eqn. (2.23) and the trends in Figs. 4.15 and 4.16 that for both estimators, the root mean squared error *RMS* and similarly average identification error *AIE* decrease as the number of load cases increases. However, *RMS* and *AIE* are not pure indicators for the accuracy of the estimates.

Another way to increase the amount of information for the proposed estimators is to increase the number of measured degrees of freedom $\hat{n}_d$. Both estimation algorithms are applicable to problems with sparse mea-

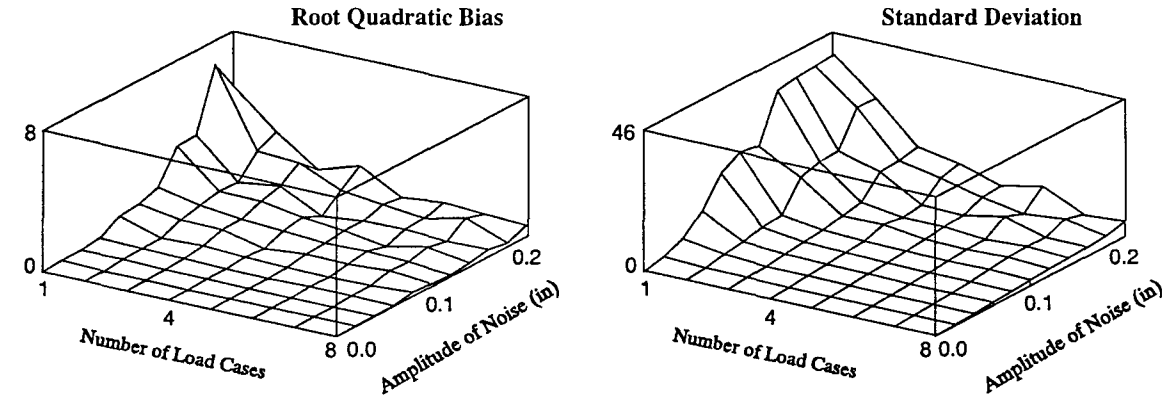

Fig. 4.16 Variations of the *RQB* and *SD* with number of load cases and amplitude of noise for OEE

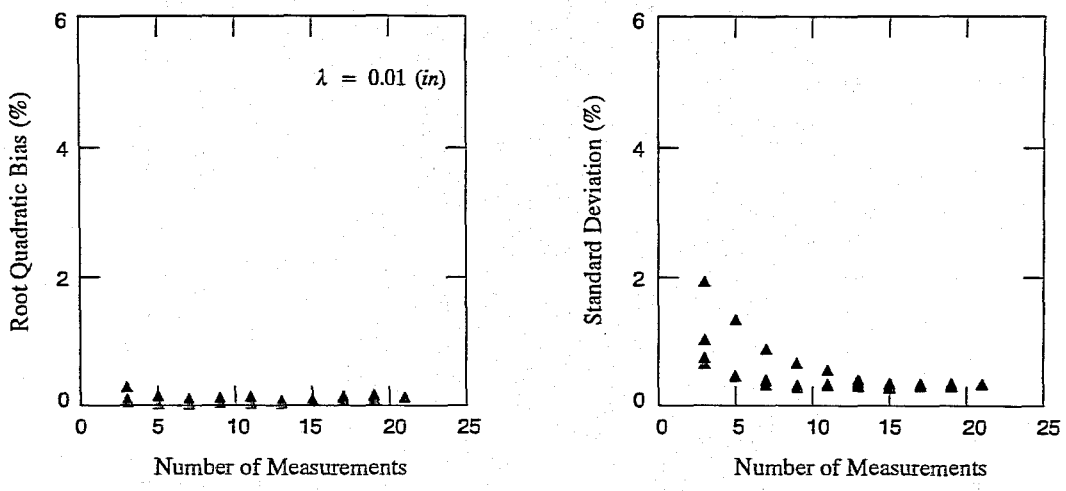

Fig. 4.17 Variations of the *RQB* and *SD* with number of measurements for a small amplitude of noise (EEE)

surements. The maximum value of $\hat{n}_d$ for the bowstring truss is 21. Figures 4.17 to 4.20 show the variations of the root quadratic bias and standard deviation with the number of measured displacements $\hat{n}_d$ for different amplitudes of noise λ. In these figures, the estimates are computed for three load cases. Based on the identifiability criterion, the minimum value of $\hat{n}_d$ is 2 to have $(nlc \times \hat{n}_d)$ greater than n_p, which is equal to 4. The abscissa values for Figs. 4.17 to 4.20 range from 2 to 21. To study the effect of the spatial distribution of the measurement locations on the estimation errors, we consider four different patterns of measurement for each specific value of $\hat{n}_d$.

It is evident from Figs. 4.17 through 4.20 that the standard deviation of the estimates decreases as the number of measurements increases. This trend is observed for both estimators and is independent from the amount of noise. One can also observe that, for both estimators, the sensitivity of the estimation errors to the pattern of measurements reduces as the amplitude of noise decreases or as the number of measured displacements increases. The bias and scatter of the estimates computed by both estimators increase as the number of

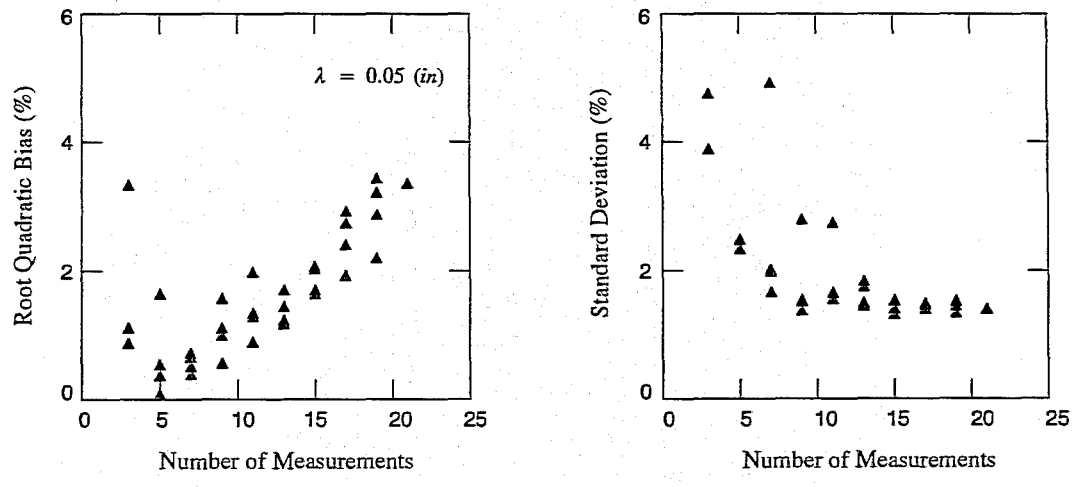

Fig. 4.18 Variations of the *RQB* and *SD* with number of measurements for a large amplitude of noise (EEE)

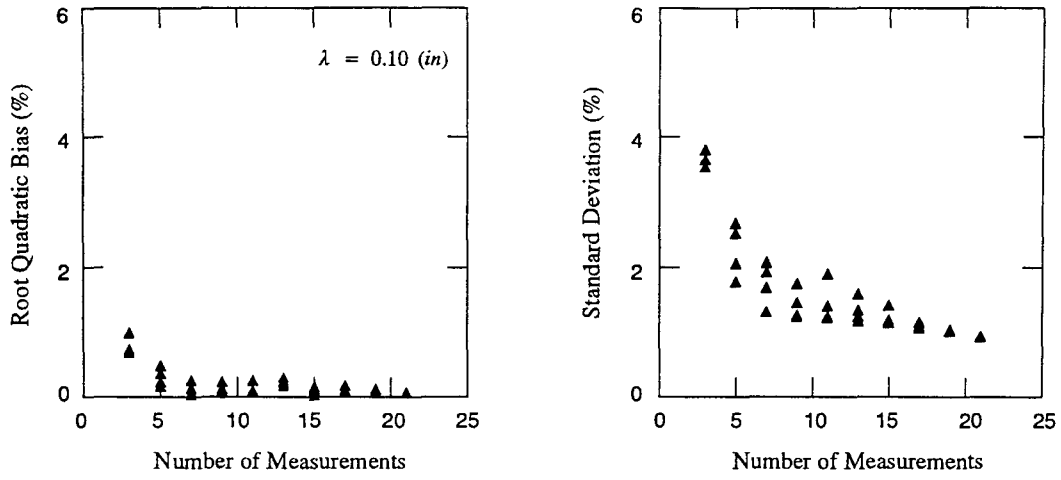

Fig. 4.19 Variations of the *RQB* and *SD* with number of measurements for a small amplitude of noise (OEE)

measurements approaches its minimum value. This increase is more significant when the amplitude of noise is large. In general, for equation error estimator, the root quadratic bias does not decrease as $\hat{n}_d$ increases. As shown in Fig. 4.17, by increasing the number of measurements, the bias of estimates does not change when the noise amplitude is small compared to the desirability bound, λ_d equal to 0.03 inches, for EEE (for complete measurements). However, as shown in Fig. 4.18, the root quadratic bias increases as $\hat{n}_d$ increases for larger amplitudes of noise. This trend indicates that for the equation error estimator, the estimates based on a few noisy measurements may have better accuracy than the estimates computed for complete measurements. The bias of estimates computed by the output error estimator decreases as the number of measured degrees of freedom increases and this trend is independent of the amount of noise, as shown in Figs. 4.19 and 4.20. Also, standard deviation of the estimates computed by OEE is larger than their bias for different numbers of measurements. For the same number of measurements and amplitude of noise, the output error estimator has smaller bias than the equation error estimator.

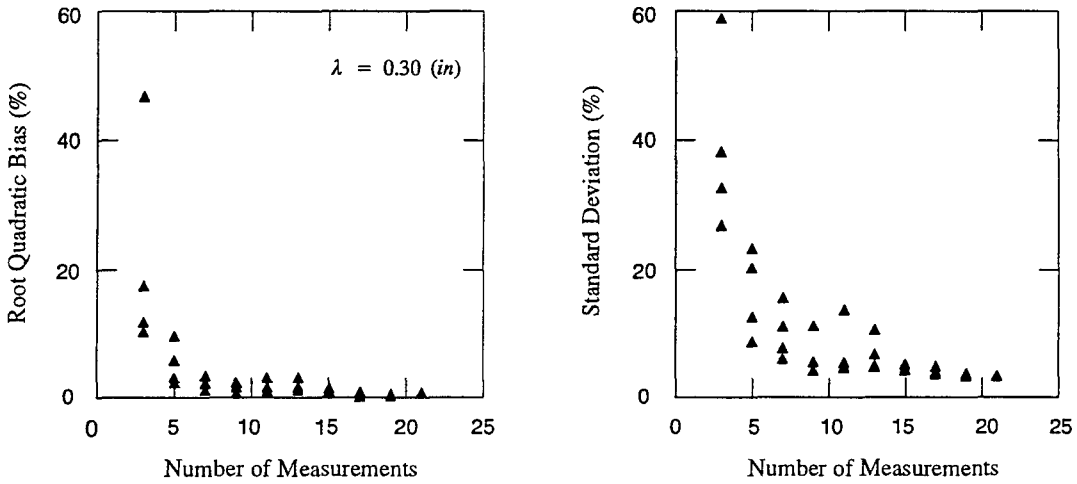

Fig. 4.20 Variations of the *RQB* and *SD* with number of measurements for a large amplitude of noise (OEE)

We have observed in this section that the precision of the estimates and the effectiveness of the estimators increases as the number of measurements $(nlc \times \hat{n}_d)$ increases. For the output error estimator, the bias and scatter of its estimates decrease (or in other words, their accuracy and precision increase) as the amount of information increases. Besides, the estimates computed by OEE have standard deviation less than bias. Therefore, the output error estimator is a desirable, consistent estimator. Since the bias of the equation error estimator does not decrease as the amount of measurements increases, EEE is not a consistent estimator. However, for small amounts of noise, EEE is a desirable estimator. In general, for a fixed amount of information the output error estimator has less bias than the equation error estimator. We should mention that all characteristics of the proposed estimators are observed for the estimation problems in which noise is added to the response of the structure. When the applied forces are noisy, the EEE should exhibit characteristics similar to those of the OEE with noisy response, and vice versa. The equation error estimator would be a desirable, low bias, consistent estimator when there is no noise in measurements and random noise is added to the applied forces.

4.3. Chapter Summary

We have used Monte Carlo simulation to study the behavior of the proposed estimators using a bowstring truss as the model problem. We have observed from the numerical simulation studies that the recursive quadratic programming algorithms based on Gauss-Newton and Han-Powell approximations of the Hessian are robust and globally convergent. Also, we observed that bounding the unknown parameters significantly increases the reliability of the proposed estimators and reduces the sensitivity of the algorithms to the initial values for the unknown parameters.

In the presence of noise in the measurements, both equation error and output error estimators are biased and their biases increase with the amplitude of noise and eventually saturate. For practical amounts of noise, the output error estimator exhibits smaller bias than the equation error estimator. The output error estimator has a standard deviation larger than bias for a greater range of noise than the equation error estimator, but both estimators have this desirable feature for suitably small amounts of noise. For large amounts of noise the equation error estimator suggests high precision (small standard deviation) but has low accuracy (large bias). The output error estimator predicts low precision when the accuracy is low for a large range of noise. By increasing the amount of information, both estimators become more effective, that is, the standard deviations of their estimates decrease. The precision and accuracy of the estimates computed by the output error estimator increase as the amount of information increases. However, the bias of the equation error estimator does not decrease as more data become available.

The output error estimator is a low bias, desirable, consistent estimator. The equation error estimator is not consistent, but is desirable for sufficiently small noise levels. In the simulations presented here we have added noise to the response measurements and not to the excitation. When noise is added to the applied forces but not to the measurements, one would expect the equation error estimator to behave consistently with low bias.

CHAPTER FIVE

Estimation of Constitutive Parameters from Modal Data

System identification and parameter estimation from modal data have received considerable attention in structural engineering and structural mechanics over the last three decades. Identification techniques using modal data are particularly popular due to the existence of well-established experimental methods for measuring mode shapes and natural frequencies of structural systems (Klosterman 1971, Ibrahim and Mikulcik 1977, Ewins 1984).

In parameter estimation one endeavors to find the values of the parameters of a mathematical model such that the model accurately represents the measured modes of the real structure. Methods for parameter estimation with modal data generally fall into one of three main categories that reflect the criterion used to establish equivalence between the model and the structure: *(1)* methods that attempt to satisfy the eigenvalue equation directly, *(2)* methods that minimize the difference between computed and measured eigenpairs, and *(3)* methods that attempt to satisfy the modal orthogonality relationships. Each method is further distinguished by the parameterization used to construct the model. There are two main approaches to structure parameterization: *(1)* use of the system stiffness and mass coefficients as parameters, and *(2)* use of parameterized constitutive models. In the former parameterization the parameters are related to nodal quantities whereas in the latter the parameters are related to element quantities. Some of the earliest parameter estimation techniques required a complete set of modes sampled at all degrees of freedom of the model. These methods gave way to techniques that could make estimates based on an incomplete set of modes with complete spatial sampling. A modern view of the problem is that one must be able to obtain estimates from an incomplete mode set that is sparsely sampled in the spatial domain. We give a brief summary of the main contributions to modal identification in structural mechanics in the following paragraphs.

One of the earliest methods for model improvement using modal data was introduced by Gravitz (1958) and modified by Rodden (1967) and McGrew (1969). They first assumed that the model mass matrix was known and computed a flexibility matrix based on a complete set of measured modes. The measured mode shapes were then modified to satisfy orthogonality relations with respect to the given mass and computed flexibility matrices. Chen and Wada (1975) used a matrix perturbation technique to establish a criterion for structural-test correlation. They used analytical and test measured eigenpairs and external forcing function to compute the modified displacement vector and based on that a criterion for verifying the analytical model. Beliveau (1976) used eigenpair perturbations within a Bayesian framework to determine members of the structural matrices. Baruch and Bar-Itzhack (1978) presented a method to find the stiffness matrix by minimizing the error in the eigenvalue equation subjected to the orthogonality condition. They also assumed the

model mass matrix was known and altered the measured mode shapes to be orthogonal to the model mass matrix. From 1978 to 1982 Baruch published several works to improve his method by using a weighted norm of the error, adjusting the flexibility matrix instead of the stiffness matrix, using the given mass matrix only to correct rigid body modes to be orthogonal, and allowing adjustments in the mass matrix to minimize error in the eigenvalue equation. Wei (1980) also improved the method of Baruch (1978) and found a closed-form solution for the stiffness matrix by allowing alteration of either the mass matrix, the mode shapes, or both. In 1978 Berman and Flannelly published a method which considered the measured mode shapes to be correct and modified the mass and stiffness matrices to satisfy orthogonality in a least squares sense. This method could operate with a truncated set of modes but still required mode vectors to be completely sampled in space. Berman (1979) improved his method by minimizing the error in the eigenvalue equation subject to orthogonality constraints, like Baruch (1978). Berman and Nagy (1983) presented a method for improving the model mass and stiffness matrices from natural frequencies and sparsely sampled mode shapes. They assumed that the finite element model adequately represented the structure and used the initial structural matrices to compute modal displacements at the unmeasured degrees of freedom from the measured ones in the mode vectors. The adjusted mass and stiffness matrices did not necessarily have the same profiles as the original matrices.

Chen and Garba (1980) proposed a matrix perturbation technique to estimate the parameters of a finite element model of a mechanical system. They modified the eigenpairs by assuming the changes in the parameters were small. Further, they assumed the difference between the correct and the analytical mass and stiffness matrices were small. The method required the sensitivity of the eigenvalues and eigenvectors with respect to the unknown parameters. They approximately computed the derivatives of the eigenpairs with respect to the unknown parameters using matrix perturbation technique. Chen *et al.* (1983) improved the method of Berman (1979) using a matrix perturbation technique. They used the measured eigenpairs and assumed that the differences between the actual and initial mass and stiffness matrices were small. Luck and Mitchel (1983) and Chen and Fuh (1984) used the pseudoinverse of the measured mode shape matrix to compute mass and stiffness matrices from a truncated set of measured modes. They assumed the measured eigenpairs were exact. Zak (1983) proposed an eigenvector updating method which used to modified mass and stiffness matrices of a finite element model of a structure. He assumed that the difference between the structural matrices of the initial finite element model and the modified matrices were small and some eigenpairs were available. He further assumed that the number of measured degrees of freedom for each mode shape was equal to the number of mode shapes (a square matrix of mode shapes).

In 1985 Kabe published a method which preserved the connectivity condition; zero members of the mass and stiffness matrices were forced to remain zero during the modification process. Because of the need to solve eigenvalue problems, the method was not suitable for complex structures with many parameters. Zimoch (1987) computed the sensitivity matrices of the spectral matrix and eigenvectors of a linear mechanical system with respect to small changes in the members of the structural matrices of a finite element model of the system. The method required the complete, noise free set of eigenpairs of the original system. Kammer (1988) improved Kabe's method and presented a stiffness matrix modification method based on projec-

tion matrix theory. Baruh and Khatri (1988) presented a method based on unitary transformations of the postulated modal coordinates for identification of eigenpairs of vibrating systems. They estimated stiffness properties by assuming that the mass properties were known. Torkamani and Ahmadi (1988) studied the effects of non-structural elements on the natural frequencies, mode shapes and stiffness of a tall building using ambient response. The method required modal data and assumed that the stiffness matrix of a finite element model of the structure comprised of two matrices. A known stiffness matrix of structural elements and an unknown matrix of non-structural elements which were estimated. Kabe (1990) introduced a method to improve the measured modes. He assumed the mass matrix was known and minimized the difference between the measured and computed mode shapes subject to the orthogonality condition.

The idea of using element constitutive parameters to reduce the number of unknowns in model building techniques has been used by several researchers (Wang and Chu 1983, Sanayei and Nelson 1986, Flanigan 1988, Lim 1990, and Hjelmstad, *et al.* 1990). Lim (1990) used submatrix techniques and measured modal data to correct a stiffness matrix. He assumed the mass matrix was known, and grouped the elements with the same stiffness properties. To overcome the problem of sparsely measured mode shapes he suggested to use either computed modal responses from the initial finite element model or to reduce the model size by static condensation. Hjelmstad, *et al.* (1990) and Alcoe (1992) presented methods to estimate elemental mass and stiffness parameters by satisfying orthogonality in a least squares sense. They condensed out the modal displacements at the unmeasured degrees of freedom.

A study by Janter and Sas (1990) on model-updating techniques showed that the mass and stiffness matrices should be updated simultaneously and that increasing the identification accuracy within a specific band may decreases the accuracy elsewhere. They also recommend that the modal mass changes should be carefully evaluated. Weaver, Smith and Beatti (1991) showed that the stiffness adjustment techniques based on measured modal data were related to quasi-Newton methods in nonlinear optimization. Baruh and Boka (1992) discussed issues related to implementation of modal parameter identification methods to real-time problems. They investigated the accuracy level of using the discrete models for continuous systems. Glaser, *et al.* (1992) used the generalized least squares method to revise mass and stiffness matrices and proposed three techniques to construct the covariance matrix for the generalized least squares method.

In this chapter we propose two parameter estimation methods to determine elemental constitutive parameters of a finite element model of a real structure using measured modal data. We assume that the topology, and geometry of the finite element model are known and that the elemental constitutive parameters are grouped together. First, we assume that the mass matrix is known and develop the equation error estimator and the output error estimator. Although this assumption is rather restrictive, it has considerable practical importance because engineers generally have more confidence in their knowledge of the inertia of a structure than its constitutive properties. Then, we consider the general case, where both mass and stiffness parameters are unknown, and propose an equation error estimator.

When the mass matrix is known, our approach to estimate the stiffness parameters is simple. First, we modify the eigenvalue equation to have a form similar to the static equilibrium equation. Then, we apply the same nonlinear constrained optimization technique used to solve the static problem. Both proposed meth-

ods can deal with a set of truncated modes whose mode shapes are sparsely sampled, both are robustly convergent, and both are amenable to large complex structures.

5.1. Model Equation for Free Vibration

In undamped free vibration a structure responds in modes governed by the following discrete eigenvalue problem

$$\boldsymbol{K}(\boldsymbol{x})\boldsymbol{u}_i = \lambda_i \boldsymbol{M}\boldsymbol{u}_i \qquad i = 1,\ldots,nmd \tag{5.1}$$

where nmd is the number of measured modes, the eigenvalue λ_i is the square of the ith angular frequency, $\boldsymbol{u}_i(n_d \times 1)$ is the ith mode shape (eigenvector), $\boldsymbol{K}(n_d \times n_d)$ is the stiffness matrix, $\boldsymbol{x}$ is the vector of unknown constitutive parameters with dimension n_p, matrix $\boldsymbol{M}(n_d \times n_d)$ is the mass matrix, and n_d is the number of degrees of freedom. The eigenvalue problem has n_d eigenpairs $(\lambda, \boldsymbol{u})$ for a positive definite $\boldsymbol{M}$ and a positive semi-definite $\boldsymbol{K}$ matrix. One will generally not have a complete set of measured eigenpairs $(\lambda_i, \boldsymbol{u}_i)$, but rather a subset of them numbering $nmd<n_d$, which might not contain all the modes between the largest and the smallest measured frequencies. We have assumed that the mass matrix is completely known and only the stiffness parameters of the structure need to be estimated.

One of the main difficulties in estimating the unknown parameters from modal data is that the mode shapes $\boldsymbol{u}_i$ are often sparsely sampled in space. There are several reasons why sparsity of measurement locations is not exceptional. First, there may be regions of the structure that are inaccessible because they lie on the interior of a solid domain. Second, certain types of measurements may be impractical to make because of technological limitations, *e.g.* nodal rotations. Third, the number of sensors may be limited due to their cost. Even if one measures displacements at all of the degrees of freedom of a model, these measurements become sparse if we subdivide the mesh of the model. Hence, completeness of measurements is, at best, an illusion.

To overcome the problem of incomplete measurements, we partition the mode shape vector into two parts as follows

$$\boldsymbol{u}_i = \begin{bmatrix} \hat{\boldsymbol{u}}_i \\ \bar{\boldsymbol{u}}_i \end{bmatrix} \equiv \boldsymbol{u}_i(\bar{\boldsymbol{u}}_i) \tag{5.2}$$

where $\hat{\boldsymbol{u}}_i(\hat{n}_d \times 1)$ and $\bar{\boldsymbol{u}}_i(\bar{n}_d \times 1)$ are the vectors of measured and unmeasured modal displacements, respectively and $\hat{n}_d$ and $\bar{n}_d$ are the number of measured and unmeasured degrees of freedom, respectively. The notation indicates that the total displacement vector $\boldsymbol{u}$ is a function of the unknown displacements. For practical purposes we assume that this partitioning is fixed for all measured modes.

The discrete governing equation of the finite element model of a structure for undamped free vibration is given in Eqn. (5.1) which we refer to as the model equation. Now, we partition the known mass matrix of the model into two matrices: a matrix corresponding to the measured displacements $\hat{\boldsymbol{M}}(n_d \times \hat{n}_d)$ and a matrix corresponding to the unmeasured displacements $\bar{\boldsymbol{M}}(n_d \times \bar{n}_d)$ and rewrite Eqn. (5.1) based on the partition in Eqn. (5.2) as follows

$$K(x)u_i = \lambda_i[\hat{M}\ \ 0]u_i + \lambda_i[0\ \ \overline{M}]u_i \qquad i = 1,\ldots,nmd \tag{5.3}$$

In the right hand side of Eqn. (5.3) the first term is a completely known vector and the second term contains the unknown vector $\overline{u}_i$. Now, we rearrange Eqn. (5.3) as follows

$$\left[K(x) - \lambda_i[0\ \ \overline{M}]\right]u_i = \lambda_i[\hat{M}\ \ 0]u_i \tag{5.4}$$

and define a modified stiffness matrix $K_i^*(x)$ and a force vector f_i^* as follows

$$\begin{aligned} K_i^*(x) &= K(x) - \lambda_i[0\ \ \overline{M}] \\ f_i^* &= \lambda_i[\hat{M}\ \ 0]u_i \end{aligned} \tag{5.5}$$

By substituting definitions (5.5) into Eqn. (5.4) the modified model equation becomes

$$K_i^*(x)u_i = f_i^* \qquad i = 1,\ldots,nmd \tag{5.6}$$

which is almost the same as the governing equation of a structure under *nmd* static load cases Eqn. (3.1). The only difference between the modified model equation and static equilibrium equation is in definition of the stiffness matrix. In Eqn. (5.6) the modified stiffness matrix is a function of the eigenvalues, changing for each mode. The stiffness matrix for the static problem is fixed for all load cases. All the operations used to derive Eqn. (5.6) from Eqn. (5.1) are reversible. If one finds a set of parameters x that satisfies the modified model equation (5.6), these parameters also satisfy the eigenvalue problem (5.1). From now on we refer to Eqn. (5.6) as the model equation for an undamped free-vibration experiment.

In the following sections, we develop two methods for estimating the constitutive parameters of a finite element model of a real structure from measured modal response. One method minimizes the error in modal force equilibrium (equation error estimator), while the other minimizes the differences in modal displacements (output error estimator). We first establish appropriate error measures with which we construct the loss functions. We then establish the estimation algorithms by minimizing the loss function for the model equation (5.6) subject to bounding constraints on the parameters. We explicitly formulate the gradients and Hessians required by the RQP algorithm.

5.2. The Equation Error Estimator (EEE)

For the proposed equation error estimator, we define the error function e_i based on the residual force vector for mode i as follows

$$e_i(x, \overline{u}_i) = K_i^*(x)u_i(\overline{u}_i) - f_i^* \qquad i = 1,\ldots,nmd \tag{5.7}$$

where x is the vector of unknown elemental constitutive parameters. The error function represents the amount of residual developed by failure to satisfy the model equation. Let $\overline{u} = (\overline{u}_1, \overline{u}_2, \ldots, \overline{u}_{nmd})$ be the

vector of unmeasured modal degrees of freedom for all measured modes. Based on the general form of the estimation problem (2.4), the nonlinear constrained optimization problem for the proposed equation error estimator for modal parameter estimation can be stated as

$$\begin{aligned} &\underset{(x,\bar{u})}{\textit{minimize}} \quad J(x,\bar{u}) = \frac{1}{2}\sum_{i=1}^{nmd} \alpha_i \| K_i^*(x)u_i(\bar{u}_i) - f_i^* \|^2 \\ &\textit{subject to} \quad \underline{x} \le x \le \bar{x} \end{aligned} \tag{5.8}$$

where $\underline{x}$ and $\bar{x}$ are the prescribed vectors of lower and upper bounds of the unknown constitutive parameters, respectively and α_i is the weight associated to the ith mode which reflects the degree of confidence to the ith measured mode. The proposed estimation problem (5.8) tries to satisfy the model equation in a least-squares sense. The proposed equation error estimator simultaneously estimates the unknown constitutive parameters and the unmeasured displacements for all measured modes. By adding simple bounding constraints on the unknown constitutive parameters we eliminate the possibility of converging to infeasible solutions. The recursive quadratic programming RQP, explained in Chapter Two and in more detail in Appendix A, is employed to solve the optimization problem (5.8). The RQP algorithm requires the gradient vector and the Hessian matrix of the loss function J with respect to unknown variables $(x, \bar{u})$. These sensitivities are computed in the following section.

Sensitivity of the Loss Function

The loss function of the proposed modal parameter estimation problem (5.8) is similar to the loss function of the equation error estimator for the static problem, given by Eqn. (3.5). Consequently, the sensitivities of both loss functions with respect to the unknown variables $(x, \bar{u})$ are similar. The gradient of the loss function J in problem (5.8), with respect to unknown variables $(x, \bar{u})$, can be computed using Eqn. (2.10), replacing N with *nmd*. The gradient matrix of the error function with respect to unknown variables $(x, \bar{u})$ can be partitioned as

$$\nabla e_i(x,\bar{u}_i) = \left[\nabla_x e_i(x,\bar{u}_i) \quad \nabla_{\bar{u}} e_i(x,\bar{u}_i)\right] \tag{5.9}$$

In many cases the stiffness matrix $K(x)$ and consequently the modified stiffness matrix $K_i^*(x)$ are linear with respect to the unknown constitutive parameters x. However, there are important cases, such as the stiffness matrix of a Timoshenko beam element, in which the parameterization is nonlinear. To maintain the requisite generality, we will assume that the error function is nonlinear with respect to the unknown constitutive parameters, and thus the gradient, $\nabla_x e_i(x,\bar{u}_i)$, is also a nonlinear function of those parameters. For the sake of clarity, the gradient matrix $\nabla_x e_i(x,\bar{u}_i)$ is represented by the matrix $U(x,u_i)$ and is computed as

$$\nabla_x e_i(x,\bar{u}_i) = \frac{\partial}{\partial x}[K_i^* u_i - f_i^*] \equiv U(x,u_i) \tag{5.10}$$

Since the mass matrix is completely known, the vector f_i^* as defined in Eqn. (5.5) is not a function of x and the derivative of the modified stiffness matrix K^* with respect to x is equal to the derivative of the stiffness matrix K with respect to x. Thus, the gradient matrix U simplifies to

$$U(x,u_i) = \frac{\partial}{\partial x}[K(x)u_i] \tag{5.11}$$

which is exactly the same as Eqn. (3.7) for computing the derivative of the error function for the static parameter estimation problem. As before, the structural sensitivity matrix U of the model can be computed by assembling the element sensitivity matrices U^e as follows

$$U(x,u_i) = \sum_e U^e(x^e,u_i^e) \tag{5.12}$$

where x^e is the vector of unknown parameters associated with the eth element and u_i^e is the vector of nodal displacements associated with the eth element for the ith mode. The element sensitivity matrix U^e is computed by the procedure explained in Appendix B.

In order to compute the gradient of the error function with respect to the unmeasured displacements $\overline{u}$, we partition the modified stiffness matrix $K_i^*(x)$ into two parts: a matrix corresponding to the measured response $\hat{K}_i^*(x)$ and a matrix corresponding to the unmeasured response $\overline{K}_i^*(x)$. Therefore, Eqn. (5.7) can be recast as

$$e_i(x,\overline{u}_i) = \hat{K}_i^*(x)\hat{u}_i + \overline{K}_i^*(x)\overline{u}_i - f_i^* \tag{5.13}$$

Based on Eqn. (5.5) the gradient of the error function with respect to the unmeasured modal response $\overline{u}_i$ takes the form

$$\nabla_{\overline{u}_i} e_i(x,\overline{u}_i) = \overline{K}_i^*(x) = \overline{K}(x) - \lambda_i \overline{M} \tag{5.14}$$

where $\overline{K}(x)$ is the stiffness matrix corresponding to the unmeasured displacements. Matrices $\overline{M}$ and $\overline{K}$ are fixed matrices for all modes and are computed by assembling element stiffness and mass matrices. Knowing that $\overline{u}_i$ is a subvector of the vector $\overline{u}$, the gradient of the error function e_i with respect to $\overline{u}$ can be represented by a sparse matrix $G_i(n_d \times (n_m \cdot \overline{n}_d))$ as follows

$$\nabla_{\overline{u}} e_i(x,\overline{u}_i) = \begin{bmatrix} \overset{1}{0} & \overset{2}{0} & \cdots & \overset{i-1}{0} & \overset{i}{\overline{K}_i^*(x)} & \overset{i+1}{0} & \cdots & \overset{nmd}{0} \end{bmatrix} \equiv G_i(x,\lambda_i) \tag{5.15}$$

Observe that Eqn. (5.15) and Eqn. (3.11) are constructed in the same way, except that for the free vibration experiment $K_i^*(x)$ is a function of frequency and is thus not constant for all modes. By substituting equations (5.10) and (5.15) into Eqn. (5.9), the total gradient matrix of the error function with respect to the unknown variables (x, $\overline{u}$) can be written as

$$\nabla e_i(x, \bar{u}_i) = \begin{bmatrix} U(x, u_i) & G_i(x, \lambda_i) \end{bmatrix} \tag{5.16}$$

Further, by substituting Eqns. (5.7) and (5.16) into Eqn. (2.10), the gradient of the loss function J with respect to the unknown variables $(x, \bar{u})$ for the proposed equation error estimator can be computed as follows

$$\nabla J(x, \bar{u}) = \sum_{i=1}^{nmd} a_i \begin{bmatrix} U(x, u_i) & G_i(x, \lambda_i) \end{bmatrix}^T e_i(x, \bar{u}_i) \tag{5.17}$$

The exact Hessian matrix for the loss function J can be computed from Eqn. (2.12) in the same way as the static case and can be expressed in a form analogous to Eqn. (3.16) as follows

$$H(x, \bar{u}) = \sum_{i=1}^{nmd} a_i \begin{bmatrix} U^T(x, u_i)U(x, u_i) + \nabla_x U(x, u_i)e_i & U^T(x, u_i)G_i(x) + \nabla_x G_i(x)e_i \\ G_i^T(x)U(x, u_i) + \nabla_{\bar{u}} U(x, u_i)e_i & G_i^T(x)G_i(x) \end{bmatrix} \tag{5.18}$$

where the third-order tensors $\nabla_x G_i$, $\nabla_{\bar{u}} U$, and $\nabla_x U$ are computed as described in Section 3.2. Accordingly, the Gauss-Newton approximation of the Hessian matrix H^{GN} takes the form

$$H^{GN}(x, \bar{u}) = \sum_{i=1}^{nmd} a_i \begin{bmatrix} U^T(x, u_i)U(x, u_i) & U^T(x, u_i)G_i(x) \\ G_i^T(x)U(x, u_i) & G_i^T(x)G_i(x) \end{bmatrix} \tag{5.19}$$

The Gauss-Newton approximation of the Hessian has the advantages that it does not depend on the second derivatives of the error function, making it easier to compute than the exact Hessian, and it is guaranteed to be positive semi-definite. The Hessian can also be approximated with a rank-two update formula like the modified BFGS (Han-Powell) method. Numerical studies show that the recursive quadratic programming method using the Gauss-Newton approximation converges in fewer iterations than the Han-Powell method.

5.3. The Output Error Estimator (OEE)

For the proposed output error estimator, we define an error function e to be the difference between the measured and computed mode shapes at the locations where the physical measurements are taken. Let us define a Boolean matrix Q such that $\hat{u}_i = Qu_i$. In other words, Q extracts the measured modal deformation $\hat{u}_i$ from the complete vector of modal degrees of freedom u_i. We assume that Q is the same for all modes. The error function for the proposed output error estimator is given by the following expression

$$e_i(x) = QK_i^{*-1}(x)f_i^* - \hat{u}_i \tag{5.20}$$

In contrast with the equation error estimator, the vector of unknown variables contains only the unknown constitutive parameters x for the output error estimator. Thus, the nonlinear constrained optimization problem for the proposed output error estimator can be stated as

$$\begin{aligned} &\underset{x}{\text{minimize}} \quad J(x) = \frac{1}{2}\sum_{i=1}^{nmd} a_i \| QK_i^{*-1}(x) f_i^* - \hat{u}_i \|^2 \\ &\text{subject to} \quad \underline{x} \le x \le \bar{x} \end{aligned} \tag{5.21}$$

where the bound vectors $\underline{x}$ and $\bar{x}$ and the weights a_i are the same as those defined in Eqn. (5.8). Like the equation error estimator, the output error estimator tries to satisfy the model equation in a least-squares sense. The number of unknowns for the output error estimator is smaller than the number of unknowns for the equation error estimator. Consequently, the solution of the former is carried out in a space of smaller dimensional than the latter. On the other hand, the loss function of the output error estimator has a higher degree of nonlinearity than the loss function of the equation error estimator. In the following section, we derive the gradient and the Hessian matrix for the loss function J for the output error estimator.

Sensitivity of the Loss Function

The the loss function of the proposed output error estimator for modal data is similar to the loss function of the output error estimator for static data (*cf.* Eqn. (3.26)). Thus, one would expect the gradient and Hessian to be formed in an analogous way. The gradient of the loss function J in the optimization problem (5.21) with respect to the unknown constitutive parameters x can be computed by replacing $K(x)$ and f_i in Eqn. (3.29) with $K_i^*(x)$ and f_i^* as follows

$$\nabla J(x) = \sum_{i=1}^{nmd} a_i \left[- QK_i^{*-1}(x) U(x, K_i^{*-1} f_i^*) \right]^T e_i(x) \tag{5.22}$$

where the structural sensitivity matrix U is computed by assembling element sensitivity matrices U^e as described in Appendix B.

The second derivative of the loss function with respect to unknown parameters can be computed exactly, it can be constructed with a rank-two update formula using the gradient of the loss function (*e.g.* the Han-Powell method explained in Appendix A), or it can be approximated with the Gauss-Newton method. The Gauss-Newton approximation, H^{GN}, can be computed as in Eqn. (3.30) by replacing $K(x)$ and f_i with $K_i^*(x)$ and f_i^* as follows

$$H^{GN}(x) = \sum_{i=1}^{nmd} a_i \left[QK_i^{*-1}(x) U(x, K_i^{*-1} f_i^*) \right]^T \left[QK_i^{*-1}(x) U(x, K_i^{*-1} f_i^*) \right] \tag{5.23}$$

The Hessian matrix generated by the Gauss-Newton approximation in Eqn (5.23) is symmetric and positive semi-definite, and contains enough information about the second derivative of the loss function to be computed reliably for this general class of problems if the residual error is small.

The loss function, gradient vector, and Hessian matrix in the output error estimator all require the computation of the inverse of the matrix K^*. Thus we must examine the conditions that would cause this matrix to be singular. Recall that the modified stiffness matrix K_i^* is simply a shift λ_i of the stiffness matrix K by a

positive semi-definite matrix $[0 \ \ \overline{M}]$. Assume that there exists a set of critical shifts $\{\mu_j\}$ that cause the modified stiffness matrix K_j^* to be singular. It follows that

$$K\phi_j = \mu_j[0 \ \ \overline{M}]\phi_j \qquad j = 1,\ldots,n_d \tag{5.24}$$

where ϕ_j is the jth eigenvector and n_d is the number of degrees of freedom of the finite element model. When a computed eigenvalue λ_i of the model equation (5.1) is equal to one of the eigenvalues of Eqn. (5.24), the modified stiffness matrix will be singular. Since, $\hat{n}_d$ columns of the matrix $[0 \ \ \overline{M}]$ are zero, the eigenvalue problem (5.24) has $\hat{n}_d$ eigenvalues equal to infinity. Therefore, the number of real value shifts which cause singularity is equal to the number of unmeasured modal degrees of freedom $\overline{n}_d$. The eigenvalues $\{\mu_j\}$ of the truncated mass system are larger than the eigenvalues $\{\lambda_i\}$ of the original system, roughly by the ratio of total modal mass to modal mass associated with the unmeasured degrees of freedom. The probability of having a singular K^* matrix increases by measuring more modes or increasing the number of critical shifts. Thus, the eigenvalues μ_j in Eqn. (5.24) depend on the stiffness matrix K which changes during the iterations of the optimization process as a consequence of changes in the unknown constitutive parameters. The theoretical number of critical shifts is equal to $\overline{n}_d$ multiplied by the number of optimization iterations and therefore the probability that one of the critical shifts is equal to one of the measured eigenvalues of the free vibration problem theoretically increases as the number of optimization iterations increases. Coincidence of eigenvalues of the two systems can only occur if an eigenvalue of the truncated system matches an eigenvalue of the original system with a different ordinal value. Clearly, such a random occurrence is possible. By increasing more measured degrees of freedom or reducing the number of optimization iterations, which is controlled by the criteria of convergence, one can reduce the number of critical shifts and consequently, the possibility of developing a singular K^* matrix. If the matrix is singular, the inverse can be computed using the singular value decomposition.

In the previous sections, we developed two estimators to determine stiffness parameters of a finite element model of a structure using measured modal data in conjunction with the known mass matrix. In the following section, we propose an equation error algorithm to estimate both the mass and the stiffness parameters.

5.4. Equation Error Estimator: The General Case

The governing equation for undamped free vibration is given in Eqn. (5.1). Since the mode shapes are often sparsely measured in the space, we use the partitioning given in Eqn. (5.2). Further, we partition the mass and the stiffness matrices of the model each into two matrices: a matrix corresponding to the measured displacements, respectively shown by $\hat{M}(n_d \times \hat{n}_d)$ and $\hat{K}(n_d \times \hat{n}_d)$ and a matrix corresponding to the unmeasured displacements, respectively shown by $\overline{M}(n_d \times \overline{n}_d)$ and $\overline{K}(n_d \times \overline{n}_d)$ and rewrite Eqn. (5.1) based on the partition in Eqn. (5.2) as follows

$$[\hat{K}(x) - \lambda_i\hat{M}(x)]\hat{u}_i + [\overline{K}(x) - \lambda_i\overline{M}(x)]\overline{u}_i = 0 \tag{5.25}$$

where x is the vector of unknown constitutive parameters and consists of both the mass, x_M, and the stiffness, x_K, parameters. Now, we define an error function e_i based on the residual force vector for mode i as follows

$$e_i(x, \overline{u}_i) = [\hat{K}(x) - \lambda_i \hat{M}(x)]\hat{u}_i + [\overline{K}(x) - \lambda_i \overline{M}(x)]\overline{u}_i \tag{5.26}$$

where $\overline{u} = (\overline{u}_1, \overline{u}_2, ..., \overline{u}_{nmd})$ is the vector of unmeasured modal degrees of freedom for all measured modes. In accord with the general form of the estimation problem (2.4), the constrained nonlinear optimization problem for the proposed equation error is

$$\begin{aligned} &\underset{(x,\,\overline{u})}{\textit{minimize}} \quad J(x_M, x_K, \overline{u}_1, ..., \overline{u}_{nmd}) = \tfrac{1}{2}\sum_{i=1}^{nmd} a_i \| e_i(x, \overline{u}_i) \|^2 \\ &\textit{subject to} \quad \underline{x} \le x \le \overline{x} \end{aligned} \tag{5.27}$$

where *nmd* is the number of measured modes. The loss function J must be augmented by a constraint relating the constitutive parameters. For example, the total mass might be known *a priori* or some of the individual parameters might be known. Now we compute the gradient of the loss function J with respect to the unknown variables $(x, \overline{u})$ using Eqn. (2.10) as

$$\nabla J(x, \overline{u}) = \sum_{i=1}^{nmd} a_i \nabla^T e_i(x, \overline{u}_i)\, e_i(x, \overline{u}_i) \tag{5.28}$$

The gradient of the error function with respect to $(x, \overline{u})$ can be partitioned as follows

$$\nabla e_i(x, \overline{u}_i) = \left[\nabla_{x_M} e_i \quad \nabla_{x_K} e_i \quad \nabla_{\overline{u}_1} e_i \quad \cdots \quad \nabla_{\overline{u}_{nmd}} e_i \right] \tag{5.29}$$

The gradients with respect to the constitutive parameters are easily computed using Eqn. (5.1) as

$$\nabla_{x_M} e_i(x, \overline{u}_i) = \frac{\partial}{\partial x_M}[\lambda_i M(x) u_i] \equiv U_M(x, u_i) \tag{5.30}$$

$$\nabla_{x_K} e_i(x, \overline{u}_i) = \frac{\partial}{\partial x_K}[K(x) u_i] \equiv U_K(x, u_i) \tag{5.31}$$

where U_M and U_K are structural sensitivity matrices computed by assembling element sensitivity matrices U_M^e and U_K^e derived in Appendix B.

We must also compute the gradient of the error function $e_i(x, \overline{u}_i)$ with respect to the unmeasured displacements $\overline{u}_i$. Using Eqn. (5.26) the gradient of the error function with respect to the unmeasured displacements of the ith modal vector is given by

$$\nabla_{\overline{u}_i} e_i(x, \overline{u}_i) = \overline{K}(x) - \lambda_i \overline{M}(x) \tag{5.32}$$

We assume that the finite element model is linear, therefore the structural matrices M, C, and K do not depend on the response. Consequently, for a particular finite difference method based on displacement vectors, the matrix $\nabla_{\bar{u}_i} e_i(x, \bar{u})$ is constant for all modes.

The total gradient of the error function with respect to the unknown variables, defined in Eqn. (7.23) can now be explicitly written as

$$\nabla e_i(x, \bar{u}_i) = \begin{bmatrix} U_M & U_K & \overset{1}{0} \cdots \overset{i-1}{0} & \overset{i}{\bar{K}(x) - \lambda_i \bar{M}(x)} & \overset{i+1}{0} \cdots \overset{nmd}{0} \end{bmatrix} \equiv \begin{bmatrix} U & G_i \end{bmatrix} \tag{5.33}$$

where the matrix U is the concatenation of the individual gradients with respect to the variables x and the matrix G_i is the concatenation of the gradients with respect to the unknown responses, and is quite sparse. The gradient of the loss function J with respect to the unknown variables for the proposed estimator in Eqn. (5.27) takes the following form

$$\nabla J(x, \bar{u}) = \sum_{i=1}^{nmd} a_i \begin{bmatrix} U(x, \bar{u}_i) & G_i(x) \end{bmatrix}^T e_i(x, \bar{u}_i) \tag{5.34}$$

With the notation used here, the Hessian approximations are identical to those developed earlier.

5.5. Initial Values, Scaling, and Identifiability

The proposed equation error estimator and the output error estimator are based on nonlinear constrained optimization problems. The recursive quadratic programming method, like any iterative process, needs initial values for the unknown variables. The choice of starting point is one of the important factors which control the speed of convergence of the algorithm, and one should employ any prior knowledge about the parameters.

Both of the developed estimators need initial values for the unknown constitutive parameters. One could use design values as a reasonable choice for the initial values of the unknown parameters. One could also use analytical methods and engineering modeling to generate initial values. In the absence of any a *priori* knowledge, one must guess the initial values for the unknown constitutive parameters x. If for some parts of the structure parameters are known, then the known parameters x_o can be used to guess initial values x^o for the unknown parameters with the same nature.

The equation error estimator also needs initial values for the unmeasured modal displacements $\bar{u}^o$. We have found that the best way to generate $\bar{u}^o$ is to compute the modal response from the model equation (5.6), with the modified stiffness matrix K^* constructed analytically from the known parameters x_o and initial values of the unknown parameters x^o. To wit,

$$\bar{u}_i^o = {K_i^*}^{-1}(x_o, x^o) f_i^* \qquad i = 1, \ldots, nmd \tag{5.35}$$

where the matrix P is a Boolean matrix that picks the unmeasured displacements $\bar{u}_i^o$ from the total computed displacements $\bar{u}_i^o$.

The estimation algorithms suffer from the same scaling problems as their static counterparts. To solve the scaling problem, we scale the optimization variables to have the same order of magnitude. The scale matrix is constructed based on the initial values of the optimization variables using the procedure explained in Section 3.5. Based on numerical studies, we have observed that the scaling process improves the convergence rate and robustness of the proposed estimators for modal experiments by changing the shape of attraction basin around the local minima to be more suitable for a gradient search strategy whenever the estimators confront with the nonhomogeneous optimization variables.

The proposed estimators for modal problems are in the class of least-squares estimators, and thus cannot reliably make an estimation if less that a certain minimum amount of data are available. Confidence in the estimates increases with the amount of information above this minimum level. Since the algorithms for the modal problem are analogous to those of the static problem, the basic identifiability criterion is the same. Hence, we must have

$$(nmd \times \hat{n}_d) \geq n_p \tag{5.36}$$

where $(nmd \times \hat{n}_d)$ is the number of independent measurements and n_p is the number of unknown constitutive parameters. The identifiability criterion (5.36) is a quantitative index for the richness of the available information. If this criterion is not satisfied, then the estimates are totally unreliable. However, satisfaction of the identifiability criterion does not guarantee reliable estimates. If the estimator is consistent, the confidence in the estimation can be improved by increasing the amount of available data $(nmd \times \hat{n}_d)$ and/or reducing the number of unknown parameters n_p. One can increase the amount of information by measuring more modes or more degrees of freedom of the finite element model. Grouping the parameters, using a simpler model with less number of parameters, or increasing the number of known parameters using *a priori* knowledge reduces the number of unknown parameters. The introduction of bounding constraints eliminates the possibility of converging to infeasible solutions. For example, for a structural system, the unknown constitutive parameters must be positive and are probably not much larger than their nominal values. The bounding constraints can be used to enforce these limits. One should always check the reliability of the estimates with a sensitivity analysis.

Remark. The shape of the surface of the loss function inside the feasible region controls the output of the developed parameter estimation methods. It is desirable to find a unique set of parameters, however there always exists the possibility of multiple local minima and narrow ravines. One can use a global optimization scheme to converge to the the smallest of the feasible local minima to find the most desirable solution. But even a global minimum may not be unique. The existence of desirable minima increases the estimation range of parameters. On the other hand, when the attraction basin of a minimum is a narrow ravine with steep slopes for some of the parameters and shallow slopes for the rest of parameters, the loss function is sensitive with respect to the parameters corresponding to steep slopes (*sensitive* parameters) and insensitive with respect to the rest of them (*insensitive* parameters). Therefore, the insensitive parameters can have large estimation ranges without changing the value of the loss function significantly. The number of local minima

and the shape of attraction basin depend on the shape of the loss function which is a function of available information and the shape of feasible region. One can expect that the estimation ranges of parameters are reduced by shrinking the feasible region, increasing the amount of measurements if the estimator is consistent, and decreasing the number of unknown parameters.

One should not be deceived by satisfying the identifiability criterion and should always check the reliability of the estimates by a sensitivity analysis. One should find out how sensitive the estimation is for the given amount of measurements, bounding constraints, starting point, topology, geometry, and other *a priori* knowledge. □

5.6. Chapter Summary

We have developed the equation error estimator and the output error estimator to determine elemental constitutive parameters of a finite element model of a real structure using measured modal data. We have assumed that the topology, and geometry of the finite element model are known and an incomplete set of spatially sparse measured modal data are available. We have considered two cases: when the mass parameters are known and when both mass and stiffness parameters are unknown.

For the case with known mass matrix, we have simply modified the eigenvalue problem to a form similar to the static equilibrium equation. We have partitioned the mass matrix and the response vector into two parts: a part corresponding to the measured degrees of freedom and a part corresponding to the unmeasured degrees of freedom. Then, we have defined a modified stiffness matrix and a modified load vector and derived the governing equation. Following the procedure explained in Chapters Two and Three we have developed the equation error estimator and the output error estimator using modal data. We have derived the sensitivity of loss functions for these two estimators with respect to their corresponding unknown variables.

When both mass and stiffness parameters are unknown, we have proposed an equation error estimator. We have derived the sensitivity of the loss function with respect to the mass and stiffness parameters.

We have also provided a grouping scheme to group the elemental constitutive parameters of similar members of the finite element model together. Elements with similar mass parameters can be grouped together regardless their stiffness parameters and vis versa. In other word, an element might belong to two different groups solely based on its mass parameter or its stiffness parameter.

We have briefly explained strategies, described in Chapter Three, for generating the initial values for unknown constitutive parameters and unmeasured responses at the locations of the unknown degrees of freedom. We have also discussed a strategy to scale the unknown variables to improve numerical conditioning. We have derived the identifiability criterion to reliably estimate the unknown constitutive parameters and have stressed the need for sensitivity analyses with respect to the shape of the loss function, bounding constraints, and initial values.

CHAPTER SIX

Oakland City Hall Building: A Real Case Study

In this chapter we use the developed modal estimator to build a mathematical model for an existing building, Oakland City Hall, using measured modal data. The Oakland City Hall building is a 19 story structure with setbacks along the elevation, as shown in Fig. 6.1. The rectangular plan is fairly regular. The structure suffered some damage during the 1989 Loma Prieta earthquake and was the focus of engineering studies into its repair and retrofit. Decisions regarding repair and retrofit of earthquake resistant structures can be facilitated by knowledge of the actual dynamic properties of the structure. A solid understanding of the linear properties of the structure generally provides a good foundation for launching further studies into the behavior of the extant structure or modifications to it.

One of the most reliable methods of assessing the modal properties of a structure is to monitor its behavior through forced vibration tests in the field. The resonant frequencies are first established by sweeping through the frequencies and noting the frequencies of maximum amplification. The mode shapes are then established

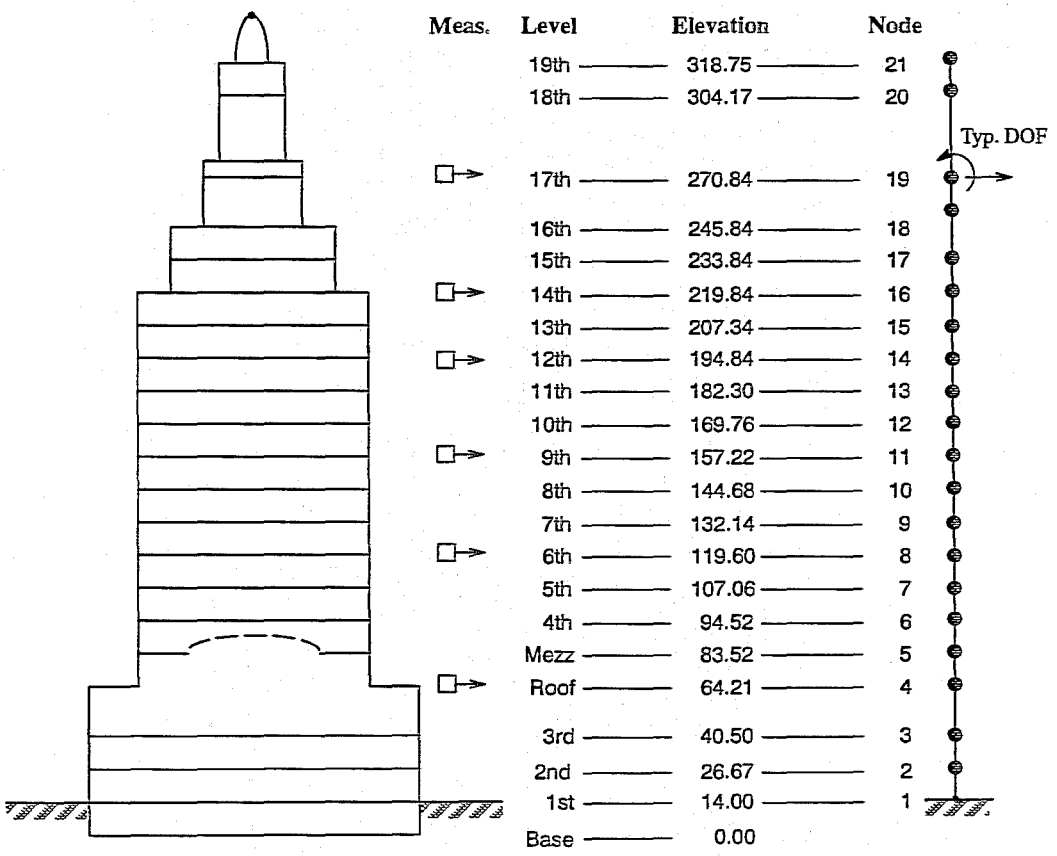

Fig. 6.1 Oakland City Hall building and the beam model

by measuring the steady-state response of certain locations of the structure during a dwell test with sinusoidal motion at the natural frequency.

In order to investigate the effects of modifying a structural system, the modal data must be expressed in terms of parameters which can be identified with physical properties of the structure. The physically based properties can then be perturbed from their basic values analytically. The post processing of modal data can be achieved by postulating a model of the structure and then estimating the parameters of that model. The estimated parameters are simply an alternative way of looking at the modal data. The parameters cannot be better than the underlying model, but insight can often be gained with a rather simple representation of the structure topology.

The present study documents efforts to identify the constitutive properties of a beam model of the Oakland City Hall building from modal measurements taken during forced vibration tests performed in 1990. The results of the forced vibration tests are summarized first. Then, two models of the building are identified: *(1)* a structure comprising beams with rotations constrained to be zero at the ends (*i.e.* a shear building) and *(2)* a structure comprising beam elements with shear and flexural deformations. The identified models are analyzed and compared with the measured modal properties. Finally, the identified models are compared with a model obtained by an engineering approach which does not directly use the modal data.

For the purposes of the present study the building will be modeled as a beam with masses lumped at the story levels. The north-south and east-west directions will be treated independently as planar structures. The idealized model comprises twenty elements connected to twenty one nodes as shown in Fig. 6.1. Element number i is connected to the nodes numbered i and i+1. The mathematical model is completely fixed at node

Table 6.1. General properties of the beam models

Node	Elevation *(ft)*	Mass *(k-sec^2/ft)*	Measured displacement
1	14.00	0.0	
2	26.67	155.1	
3	40.50	193.9	
4	64.21	175.2	*(measured)*
5	83.52	132.0	
6	94.52	66.9	
7	107.06	51.8	
8	119.60	50.0	*(measured)*
9	132.14	49.9	
10	144.68	49.8	
11	157.22	49.3	*(measured)*
12	169.76	48.8	
13	182.30	50.0	
14	194.84	57.8	*(measured)*
15	207.34	52.3	
16	219.84	81.1	*(measured)*
17	233.84	24.7	
18	245.84	40.4	
19	270.84	39.8	*(measured)*
20	304.17	20.2	
21	318.75	7.2	

one. The translational masses used in this study are presented in Table 6.1. Rotational masses are taken as zero for all analyses.

6.1. Summary of the Forced Vibration Tests

The dynamic properties of the Oakland City Hall building were measured by forced vibration tests by ANCO Engineers, Inc. for the City of Oakland Office of Public Works, Division of Architectural Services. These tests are documented in the report by ANCO (1990). The data obtained from these tests comprise the mode shapes and natural frequencies of the lower several modes of the structure, which are summarized in Table 6.2. The lateral motion was measured at levels *Roof*, 6th, 9th, *12*th, *14*th, and *17*th (corresponding to nodes 4, 8, 11, 14, 16, and 19 of the stick model).

According to the reports on the forced vibration tests, there was some confusion concerning the coupling among the east-west and torsional modes of vibration. Both ambient and forced vibration tests indicated that both east-west and torsional motions were sensed at the resonant frequencies of 1.36 *Hz* and 3.62 *Hz*. Since the building has two axes of symmetry, translation and torsional modes were expected to be uncoupled. Consequently, closely spaced modes were suspected as the cause of the torsional-translational coupling.

The presence of closely spaced modes would seem to be important to the proper modeling of the three dimensional response of the structure, and should be scrutinized more carefully. Even if the natural frequencies of two modes are close, the mode shapes are different. During a dwell test it is highly likely that there would be a continual exchange of energy between these two modes (Lu and Hall, 1990). If the instruments measuring the mode shapes did not exhibit a beating phenomenon, then the possibility of closely spaced modes should be dismissed in favor of a simple, but torsionally coupled, mode (indicating that the apparent symmetry is not realized).

Unfortunately, the instrumentation deployed during the forced vibration tests would appear to be insufficient to assess the degree of coupling of translation and torsion. At least three instruments would be required to monitor the motion of a rigid body in a plane. Most of the story levels had only two instruments.

If certain of the east-west and torsional modes are simple and coupled, the identified models will not reflect it. However, for the sake of comparison, the east-west modes have been labeled *1(ew)*, *3(ew)*, and *5(ew)*; suggesting that modes *2(ew)* and *4(ew)* are missing. In the comparisons of measured and estimated mode shapes, we will use *1(t)* in place of the missing *2(ew)* and *2(t)* in place of the missing *4(ew)*.

Table 6.2. Measured modal properties of Oakland City Hall

Direction		North-South				East-West			Torsional	
Mode number		*1(ns)*	*2(ns)*	*3(ns)*	*4(ns)*	*1(ew)*	*3(ew)*	*5(ew)*	*1(t)*	*2(t)*
Frequency *(Hz)*		0.76	1.68	2.64	4.38	0.64	2.28	4.65	1.36	3.62
Level	*Roof*	0.10	0.34	-1.27	-1.28	0.08	-0.59	0.40	0.10	-1.77
	6th	0.48	0.79	-1.59	0.92	0.28	-0.73	-0.79	0.40	-1.06
	9th	0.91	1.04	-0.48	3.27	0.71	0.71	-0.91	0.86	1.38
	12th	1.00	1.00	1.00	1.00	1.00	1.00	1.00	1.00	1.00
	14th	1.04	0.95	1.29	0.50	1.06	1.33	1.17	1.14	1.23
	17th	1.40	-2.48	0.23	-2.37	1.55	0.33	-3.17	-0.32	-2.05

6.2. Results of Parameter Estimation

Three different models of the structure are discussed in this section: *(1)* The structure identified as a shear building (*i.e.* the rotational degrees of freedom are held fixed). The only parameter associated with this model is the flexural modulus of the beam, *EI*. *(2)* The structure identified as a Timoshenko beam, the parameters identified are the flexural stiffnesses *EI* and shear stiffnesses *GA* of the elements. *(3)* A model of the structure obtained by an "engineering approach" which does not use the modal data.

Since the number of measured degrees of freedom is small, elements are grouped together to reduce the number of unknown constitutive parameters and satisfy the identifiability criterion. The properties of the model were lumped into 9 different element types, giving 9 total parameters to estimate for the shear buildings and 18 total parameters to estimate for the shear-flexure models. The elements were lumped as follows, using the convention ***group****(elements)*: ***1****(1,2,3)*; ***2****(4,5)*; ***3****(6,7)*; ***4****(8,9,10)*; ***5****(11,12,13)*; ***6****(14,15)*; ***7****(16,17)*; ***8****(18)*; ***9****(19,20)*. The assumed grouping of elements with the same parameters is shown schematically in Fig. 6.2.

Matching of the natural frequencies is implicit in the loss function through the specification of the error function, but is not otherwise enforced. Since natural frequencies are easy to measure reliably, one should place a premium on their accurate representation in the model. The only mechanism available for controlling the frequencies of the identified model is the adjustment of the weighting factors α_i in the loss function. Making one of these weighting factors greater emphasizes the importance of that mode in the loss function with the result that both the frequency and the mode shape of that mode will more closely match the measured data. With a typical engineer's bias toward lower modes, we generally made an effort to match the frequencies in the lower modes the best, with some sacrifice in the higher modes.

The identification of the north-south properties used the four modes indicated ***ns*** in Table 6.2. As mentioned earlier, we suspect that the torsional modes, indicated as ***t*** in Table 6.2, are actually the missing east-

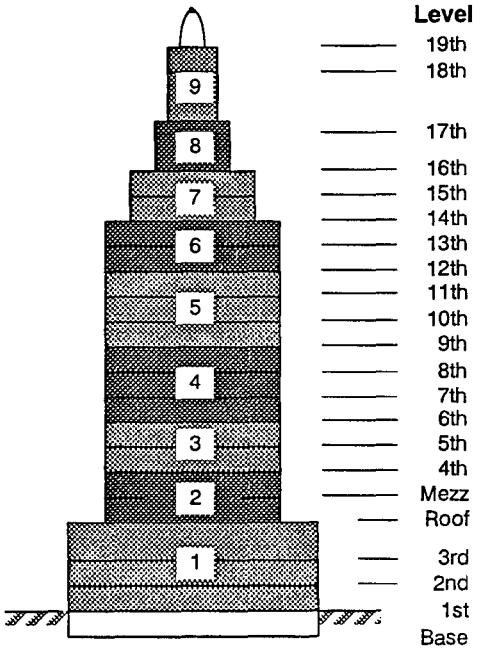

Fig. 6.2 Element parameter groupings

west modes with coupled torsional motion. We identified the east-west model using only the three modes labeled *ew* in Table 6.2. As expected, the identified models had modes between the measured frequencies with frequencies corresponding to the so-called torsional modes. Because the missing modes corresponded well with the torsional modes, we tried to make the frequencies of the missing modes match the measured "torsional" frequencies by adjusting the weighting factors of the measured modes, without using the torsional mode shape data. Throughout the presentation of results, we compare the missing modes with the torsional modes, even though we did not use those data to make the estimations.

The natural frequencies of the models identified by both estimators and those of the engineering model are listed in Table 6.3 along with the measured values. It should be evident that the natural frequencies of the identified models represent the dynamic characteristics of the building well, particularly for the lower modes. For the identified models the spectral distribution is consistently good and the missing modes are properly identified.

We normalize the mode shapes presented in the following sections by setting the norm of the six displacement components at the measurement locations to unity. This scaling will allow us to compare measured and computed modes. For all estimations in the following sections, the lower bounds for the parameters x were taken to be zero. The influence of the upper bounds are examined through the sensitivity analyses.

6.3. Shear Building Model

For the shear building model, the flexural moduli of the beam elements are the only constitutive parameters that need to be estimated. With the grouping scheme shown in Fig. 6.2, the number of unknown parameters, n_p, is 9. The number of measured modal displacements, $\hat{n}_d$, is equal to 6 and the number of measured modes, *nmd*, is equal to 4 for the north-south model and 3 for the east-west model. Therefore, there are $nmd \times \hat{n}_d = 24$ measurements for the north-south model and 18 for the east-west model. The ratio of measurements to the unknown parameters is marginal but acceptable in both directions.

North-South. The shear building models identified by the output error estimator (OEE) and equation error estimator (EEE) for the north-south direction are shown in Table 6.4. The computed natural frequencies for these models are presented in Table 6.3 and their first four computed mode shapes are plotted along with the measurements in Figs. 6.3 and 6.4. The weighting factors for the first through the fourth measured modes, found by trial and error to produce models with acceptable spectral distributions, were 100, 5, 1, and 10, re-

Table 6.3. Natural frequencies (*Hz*) of the identified models and the measured frequencies

Mode (direction)	*1(ns)*	*2(ns)*	*3(ns)*	*4(ns)*	*1(ew)*	*2(ew)*†	*3(ew)*	*4(ew)*†	*5(ew)*
Measured	0.76	1.68	2.64	4.38	0.64	1.36	2.28	3.62	4.65
Engineering Model	0.76	2.13	3.21	4.93	0.64	1.74	2.75	4.10	5.27
Shear Building (EEE)	0.76	1.64	2.48	4.15	0.65	1.34	2.25	3.17	4.16
Shear Building (OEE)	0.76	1.69	2.80	4.38	0.64	1.32	2.17	3.48	4.65
Shear-Flexure (EEE)	0.77	1.72	2.37	4.21	0.65	1.34	2.47	3.40	4.08
Shear-Flexure (OEE)	0.76	1.68	2.68	4.36	0.64	1.50	2.32	3.66	4.65

† Mode not used in estimation procedure

spectively. One can observe that for both identified models the first computed frequency and mode shape are represented almost exactly, indicating a near zero error vector in the modified eigenvalue problem. The higher modes are also quite well represented and show the important effects induced by the presence of the tower. Since the first and fourth modes are weighted more heavily than the second and third modes, their corresponding computed mode shapes follow the measured values better, as shown in Figs. 6.3 and 6.4. For the OEE the first and fourth computed frequencies exactly match the measured values.

The overall quality of the computed mode shapes is quite good, indicating that the assumption of shear dominated behavior is in harmony with the data. The shear building identified by the output error estimator has closer natural frequencies to the measured values than does the model built by the equation error estimator. We can attribute the better accuracy to the fact that we used the OEE to perform a sensitivity analysis, and hence the investigation of the influence of the upper bound values was more thorough than it was for the EEE. The values given in Table 6.3 and Fig. 6.4 are for the best model found.

The models identified by the output error estimator shows a rather large value for the stiffness of group 6. The equation error estimate does not show this feature. Since both identified models have similar natural frequencies, one would expect that there exist other models with plausible spectra close to these identified models. To examine the issue of the inherent variability of a parameter, one must perform an analysis of the sensitivity of the loss function around the solutions in question. Such an analysis will produce a picture of the topography of the basin of attraction of the loss function. Since the number of optimization variables for the output error estimator is smaller than the number for the equation error estimator, we performed the sensitivity analysis for the identified model only for the OEE.

To check the sensitivity of the loss function numerically, we altered the size of the feasible region by changing the upper bound constraints and started the optimization process from different initial points. Using this numerical technique, one can study the topology of the attraction basin around the solution, search for other plausible points at the bottom of the attraction basin, and determine the influence of parameters that are bound at their constrains. We accepted only solutions computed during the sensitivity analysis that had natural frequencies close to the model given in Table 6.4. Since matching the frequencies is not explicitly enforced

Table 6.4. Identified shear building models for the north-south direction

Parameter group	*EI (ns)* (10^8 *k–ft*^{2})	
	EEE	OEE
1	2.378	4.442
2	0.503	0.757
3	0.278	0.220
4	0.141	0.110
5	0.513	0.756
6	0.518	3.330
7	0.139	0.114
8	0.108	0.111
9	0.378	0.503

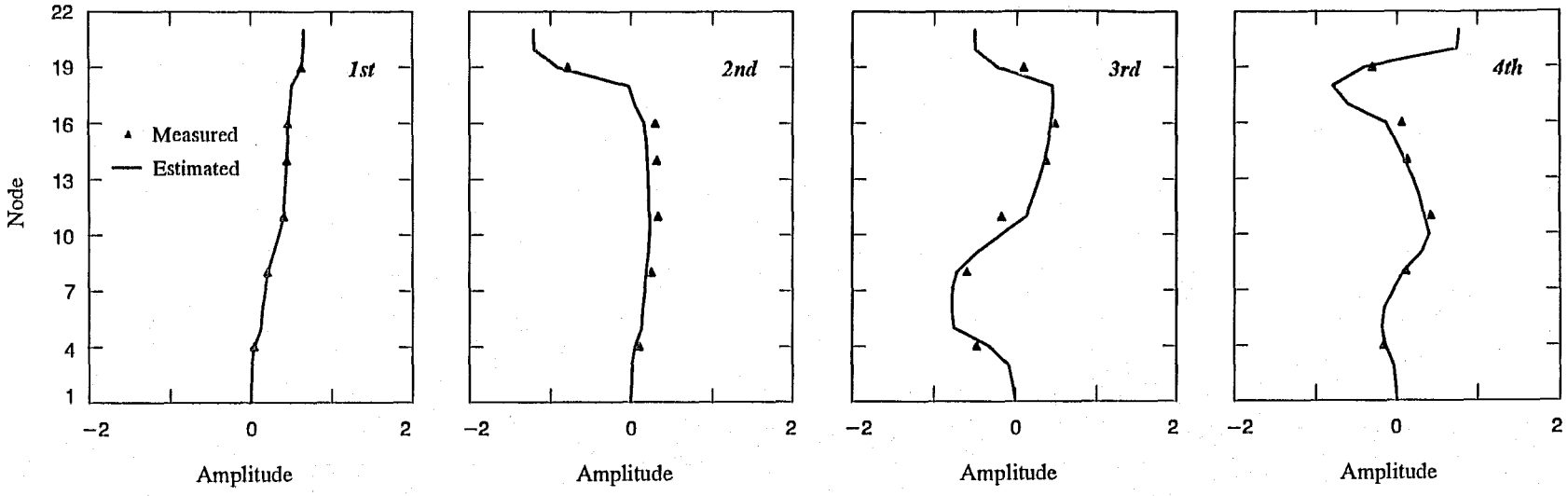

Fig. 6.3 North-south, shear building model (EEE)

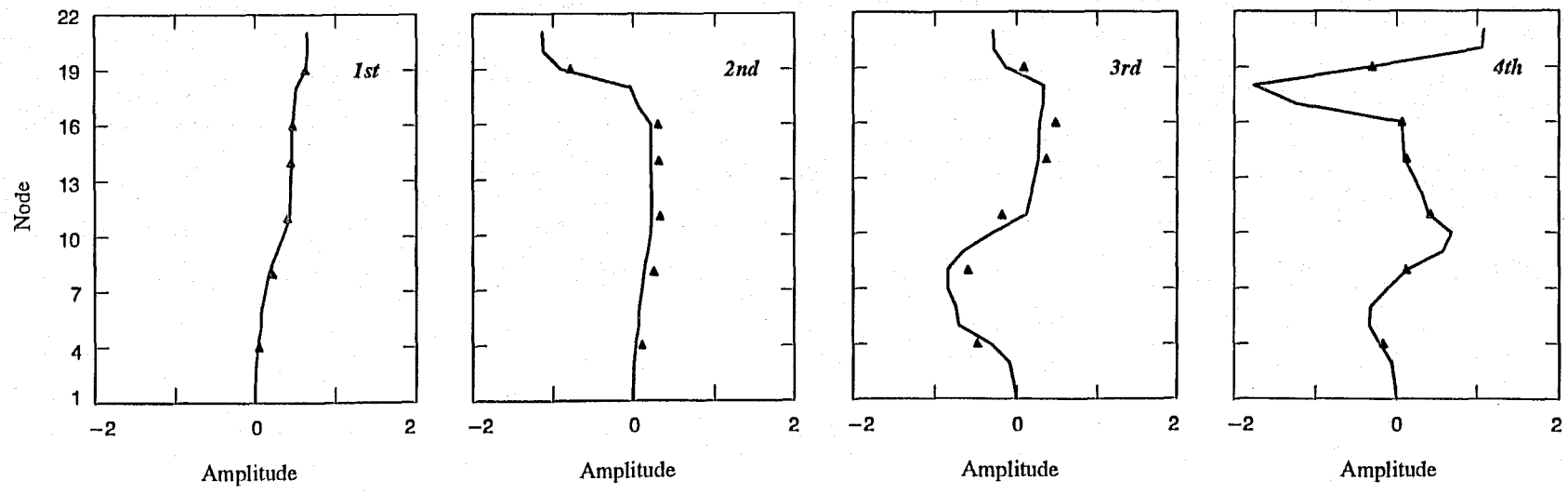

Fig. 6.4 North-south, shear building model (OEE)

Table 6.5. Bounds of element properties for the north-south, shear building model

Parameter group	*EI (ns)* (10^8 *k-ft*^{2})	
	Max.	Min.
1	4.866	3.000
2	0.812	0.232
3	0.404	0.204
4	0.540	0.110
5	0.750	0.281
6	3.453	0.520
7	0.117	0.112
8	0.141	0.119
9	0.508	0.465

by the loss function, we searched for alternative models whose loss function values were close to the value of the loss function for the identified model shown in Table 6.4 and then determined their natural frequencies by eigenvalue analysis. If the frequencies were close to the measured frequencies, we took the models to be reasonable.

In Table 6.5, the maximum and minimum values of the estimated flexural moduli are listed for the alternative models found during the sensitivity analysis. The ranges of natural frequencies and values of the loss function for these alternative models are shown in Table 6.6. The value of the loss function has units of length squared. The estimation ranges given in Tables 6.5 and 6.6 include the identified model shown in Table 6.4, which has the smallest value of the loss function among the plausible alternative models. All estimated alternative models have natural frequencies close to the measured values. It is evident from Table 6.5 that the estimation ranges for parameter groups 1 and 6 are larger than those for the other groups, indicating that the loss function is less sensitive to these parameters than other parameters. Based on the given measurements, we have less confidence in the estimated stiffnesses for elements in groups 1 and 6 than in the other groups. Table 6.5 does not indicate that any shear building model represented by a point inside the hypercube defined by the bounds given in this table is a plausible model. All plausible models satisfy the optimality criteria. Table 6.5 simply shows the extreme values of parameters found within the plausible set of models.

East-West. The east-west shear building models were identified using the three modes indicated as *ew* in Table 6.2. The ratio of measurements to unknowns is less favorable than it was for the north-south direction. The models identified by both estimators for the east-west direction are given in Table 6.7. Table 6.3 contains the computed natural frequencies for these models and Figs. 6.5 and 6.6 show their first five computed mode

Table 6.6. Bounds of the loss function and the natural frequencies for the north-south shear, building model

Value	Frequency (*Hz*)				
	Loss function	*1*st	*2*nd	*3*rd	*4*th
Minimum	8.06	0.76	1.69	2.69	4.37
Maximum	17.15	0.76	1.72	2.88	4.38

Table 6.7. Identified shear building models for the east-west direction

Parameter group	*EI (ew)* (10^8 *k-ft*^{2})	
	EEE	OEE
1	1.910	5.382
2	1.962	0.710
3	0.190	0.194
4	0.101	0.123
5	0.121	0.074
6	0.269	6464.700
7	0.095	0.126
8	0.062	0.056
9	0.402	0.446

shapes along with the measured values. The computed second and fourth east-west translation modes are compared with the first and second measured torsional modes in Table 6.2 even though those measured values were not used in estimation process. By trial and error, the suitable weighting factors for the first, third, and fifth measured modes were chosen to be 100, 1, and 20, respectively.

Both identified models reproduce the first measured natural frequency and mode shape, indicating a near zero error vector in the modified eigenvalue problem. The computed frequencies of the missing second and fourth modes are close to the measured torsional frequencies. The model identified by the EEE has the second and third frequencies closer to the measured values than the model built by the OEE, however the OEE model represents the fourth and fifth natural frequencies better than the EEE shear building model. The computed higher mode shapes follow the general trends of the measured modes, but not as well as the north-south direction. One should recall that the second and fourth modes were not used in the estimation scheme. Since the first and fifth modes are weighted more heavily than the third mode, their corresponding computed natural frequencies and mode shapes represent the measured values better than the other modes, as shown in Figs. 6.5 and 6.6. The fifth mode of the OEE model exactly reproduces the measured values. The third computed mode does not follow the measured values quite as well, probably because of the presence of outliers in the measured data or because of inadequacy of the topological representation of the structure.

The shear building model identified by the output error estimator reveals a large value for the stiffness in group 6, indicating that the loss function may not be sensitive to this parameter. A sensitivity analysis for the output error estimator, similar to the north-south direction, was done to examine the expected variability of the estimated parameters. By changing the upper bound constraints and starting points, we identified several other models with loss function values close to the value of the loss function of the OEE model shown in Table 6.7. From among these solutions, those which had plausible frequency spectra were chosen as alternative models. In Table 6.8, the maximum and minimum values of the estimated flexural moduli are listed for the computed alternative models. The range of natural frequencies and values of the loss function for these models are shown in Table 6.9. The shear building model presented in Table 6.7 has the smallest value of the loss function among the plausible identified models. One can see from Table 6.8 that, except for the parameter group 6, all of the estimation ranges are small, indicating good confidence in the estimated parameters. The

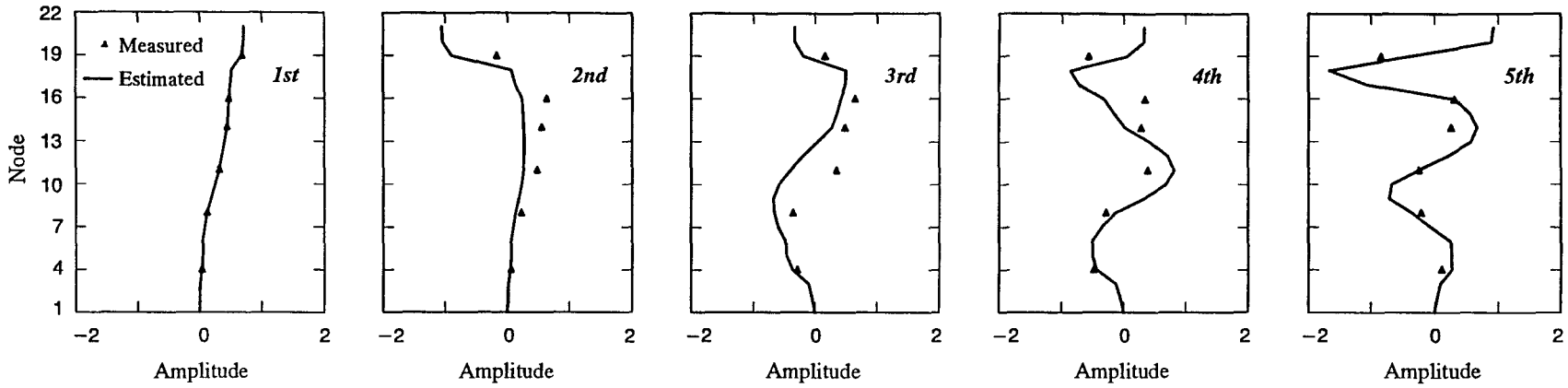

Fig. 6.5 East-west, shear building model (EEE)

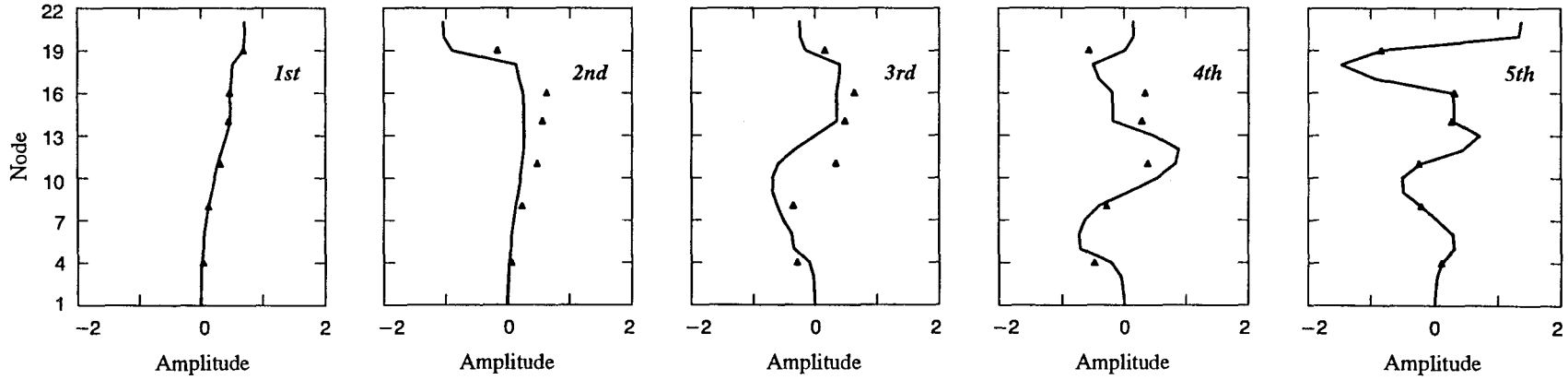

Fig. 6.6 East-west, shear building model (OEE)

Table 6.8. Bounds of element properties for the east-west, shear building model

Parameter group	EI (ew) (10^8 k-ft^2)	
	Max.	Min.
1	5.400	5.382
2	0.710	0.659
3	0.205	0.194
4	0.123	0.121
5	0.079	0.074
6	6464.700	1.000
7	0.131	0.126
8	0.056	0.054
9	0.446	0.444

large estimation range for the constitutive parameters of elements in group 6 represents the insensitivity of the loss function with respect to this parameter and consequently, low confidence in its estimated value.

6.4. Shear-Flexure Model

For the shear-flexure model, the flexural stiffnesses and shear stiffnesses of the Timoshenko beam elements are the constitutive parameters that we need to estimate. Since we have 9 parameter groups, the number of unknown parameters, n_p, is 18. Therefore, for the shear-flexure model, the excess of measurements over unknowns is 6 for the north-south model and zero for the east-west model. The ratio of measurements to unknowns is less favorable than it was for the shear building model, actually hitting the limit of identifiability for the east-west direction. One would expect to have less confidence in the estimates and greater variability with respect to the bounding constraints for the shear-flexure model as compared to the shear building model.

North-South. Table 6.10 gives the properties of the shear-flexure models identified by the output error and equation error estimators. The computed natural frequencies for these models are presented in Table 6.3 and their first four computed mode shapes are plotted along with the measurements in Figs. 6.7 and 6.8. All four measured modes were weighted equally. The computed frequencies and mode shapes are closer to the measured values than the shear building models, especially for the OEE model. Because all modes had equal weight in the loss function, all the computed modes show approximately the same level of error, except the first mode of the EEE model which exactly reproduces the first measured mode. The OEE model has frequencies closer to the measured values than the EEE model since the OEE model is the best model among the plausible models found during the sensitivity analysis.

Table 6.9. Bounds of the loss function and the natural frequencies for the east-west, shear building model

Value	Frequency (Hz)					
	Loss function	1st	2nd	3rd	4th	5th
Minimum	5.60	0.64	1.30	2.17	3.46	4.65
Maximum	7.10	0.64	1.32	2.17	3.49	4.65

Table 6.10. Identified shear-flexure models for the north-south direction

Parameter group	EEE		OEE	
	GA (10^6 *k*)	*EI* (10^9 *k–ft*^{2})	*GA* (10^6 *k*)	*EI* (10^9 *k–ft*^{2})
1	5.023	3255.000	6.449	48.188
2	4.756	820.190	107.760	21156.000
3	2.188	206.960	4.173	46864.000
4	1.067	141.940	3.117	17756.000
5	4.835	182.470	1.692	80199.000
6	3.954	116.880	12.907	22464.000
7	1.588	53.541	0.747	1.056
8	0.228	7.964	0.757	0.793
9	0.768	8.267	1007.401	487.851

The shear-flexure model identified by the output error estimator shows large values for the flexural stiffnesses of all groups except groups 1 and 8 and shear stiffness of groups 2, 6, 7, and 9 indicating that the loss function may not be sensitive to these parameters. We did a sensitivity analysis similar to the shear building models to find other plausible models for the output error estimator. Table 6.11 summarizes the estimation ranges for the computed plausible models. The ranges of natural frequencies and values of the loss function for these models are shown in Table 6.12. The loss function values for the shear-flexure models are much smaller than the corresponding values for the shear building models listed in Table 6.6, explaining the better computed natural frequencies. The OEE model listed in Table 6.10 has the smallest value of the loss function among the plausible models found in the sensitivity study. One can observe from Table 6.11 that the estimation ranges for flexural stiffness of parameter groups 2, 3, 4, 5, 6, 7, and 9 and shear stiffness of parameter groups 2, 6, 7, and 9 are large and better confidence exists for the other parameters. A large estimation range for a parameter indicates the insensitivity of the loss function with respect to that parameter. The number of insensitive parameters for the shear-flexure model is greater than the number for the shear building model. This tendency was expected because the difference between the number of measurements and unknowns for the shear-flexure model is less than that for the shear building model.

Table 6.11. Bounds of element properties for the north-south, shear-flexure model

Parameter group	*GA (ns)* (10^6 *k*)		*EI (ns)* (10^9 *k–ft*^{2})	
	Max.	Min.	Max.	Min.
1	7.020	5.678	195.880	48.171
2	111.610	4.198	2865600.000	200.000
3	4.673	3.894	1314600.000	200.000
4	3.565	2.973	1032800.000	9.229
5	3.896	1.686	643020.000	16.105
6	192.190	10.000	221580.000	4.803
7	17080.000	0.747	1434.400	1.048
8	0.951	0.490	1.175	0.316
9	1007.400	0.458	1979.900	26.163

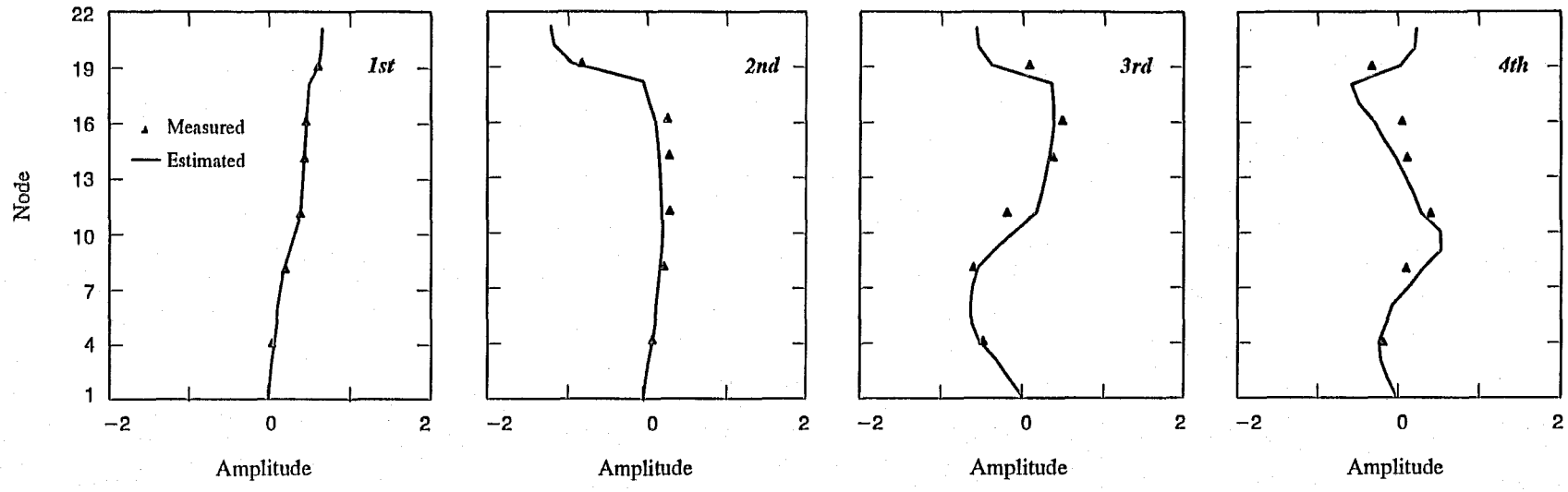

Fig. 6.7 North-south, shear-flexure model (EEE)

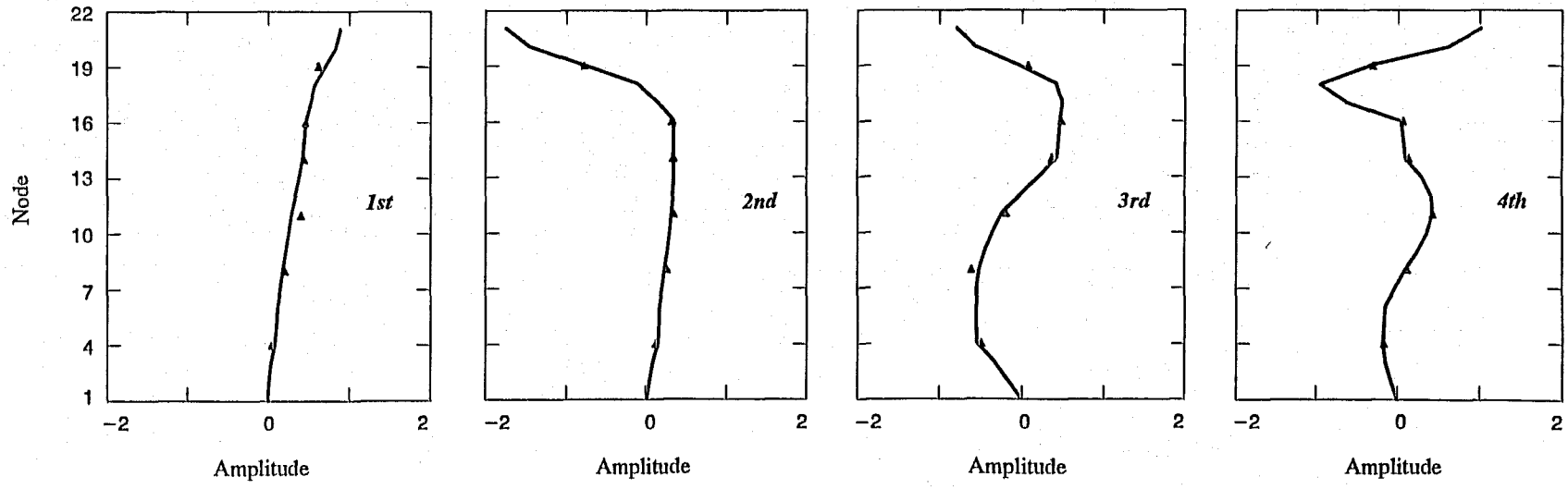

Fig. 6.8 North-south, shear-flexure model (OEE)

Table 6.12. Bounds of the loss function and the natural frequencies for the north-south, shear-flexure building model

Value	Frequency (*Hz*)				
	Loss function	*1*st	*2*nd	*3*rd	*4*th
Minimum	0.056	0.76	1.66	2.68	4.37
Maximum	0.530	0.76	1.68	2.68	4.36

East-West. The number of measurements is equal to the number of unknown parameters for the east-west direction, making the ratio of measurements to unknowns poorest among all identified models. The models identified by both estimators are shown in Table 6.13. The computed frequencies for these models are listed in Table 6.3 and their first five computed mode shapes are plotted along with the measurements in Figs. 6.9 and 6.10. Suitable weighting factors for the first, third, and fifth measured modes were found to be 100, 1, and 10, respectively. For the EEE model, no significant improvements can be observed in the frequencies and mode shapes compared with the shear building model identified by EEE. However, the OEE model, which is the best model found during the sensitivity analysis, has closer frequencies to the measured values and its computed mode shapes follow the measured modes better than other identified models for the east-west direction. Since the first and fifth modes were weighted more heavily than the third mode, their corresponding mode shapes follow the measurements more accurately than the other modes, especially for the OEE model as shown in Fig. 6.10.

Because the identifiability criterion was just satisfied, we performed a sensitivity analysis to assess our confidence in the estimates. By changing upper bound constraints and starting points of the optimization problem for the output error estimator, we found several plausible models which have low values of the loss function and natural frequencies close to the measured values. In Table 6.14, the maximum and minimum values of the estimated parameters are listed for the plausible models found. The ranges of frequencies and values of the loss function for these plausible models are shown in Table 6.15. Like the north-south direction, the identified shear-flexure models have values of the loss function that are much smaller than the corresponding values for the shear building models. One might recall that the value of the loss function is a measure of

Table 6.13. Identified shear-flexure models for the east-west direction

Parameter group	EEE		OEE	
	GA (10^6 *k*)	*EI* (10^9 *k–ft*^{2})	*GA* (10^6 *k*)	*EI* (10^9 *k–ft*^{2})
1	11.495	1314.700	3.123	45566000.000
2	15.381	602.430	5.243	1008800.000
3	1.511	149.020	10.056	11.346
4	0.766	192.300	1.339	8.093
5	0.922	229.550	2.400	471990.000
6	1.653	29.800	2626.400	7487.400
7	0.544	28.080	1.603	3932.200
8	0.120	5.110	0.686	4618.650
9	3.148	176.800	0.193	4283.600

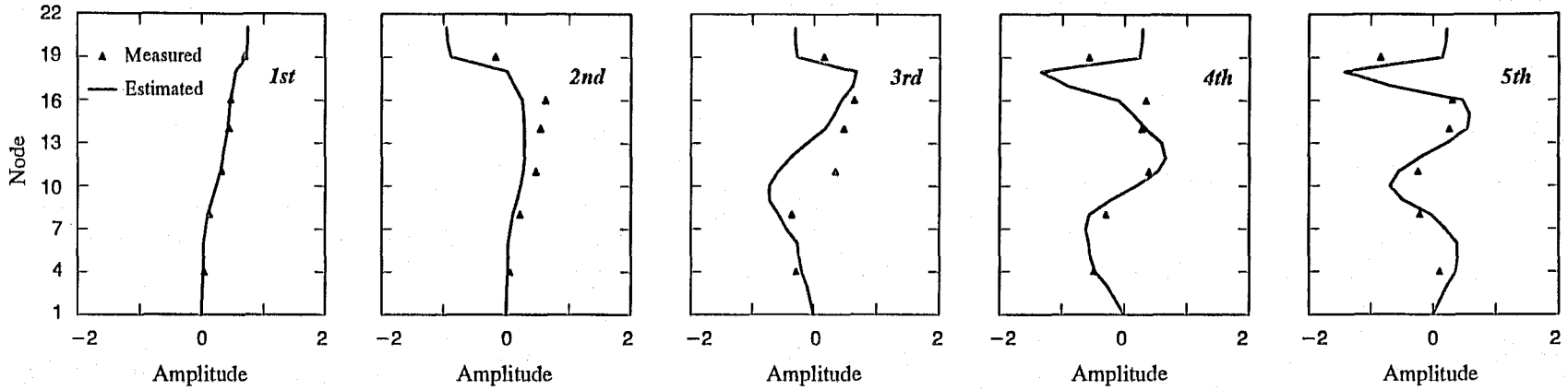

Fig. 6.9 East-west, shear-flexure model (EEE)

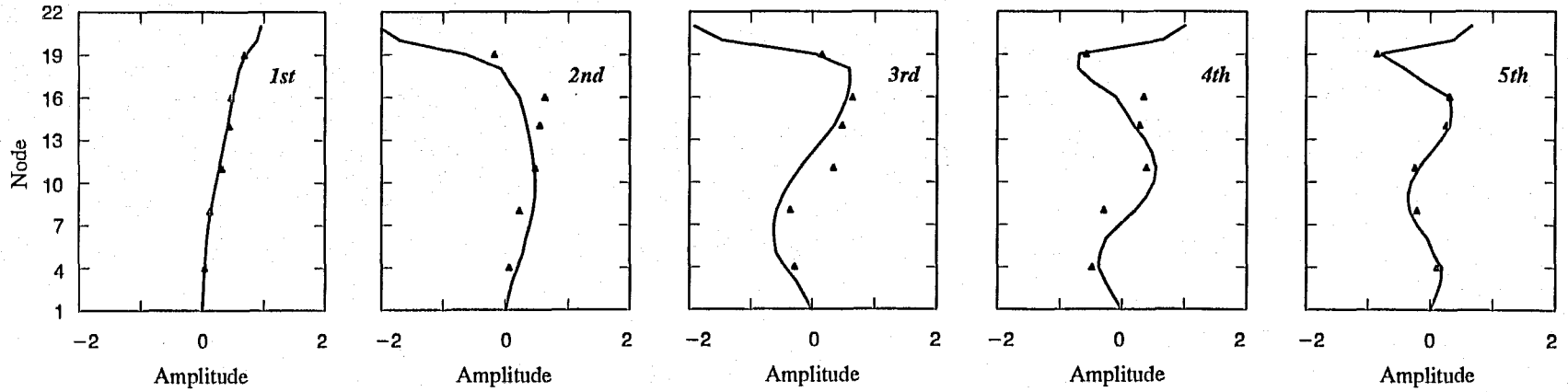

Fig. 6.10 East-west, shear-flexure model (OEE)

Table 6.14. Bounds of element properties for the east-west, shear-flexure model

Parameter group	*GA (ns)* (10^6 *k*)		*EI (ns)* (10^9 *k–ft*^{2})	
	Max.	Min.	Max.	Min.
1	7.720	3.030	45566000.000	99.977
2	5.710	1.478	1008800.000	99.948
3	1025.900	2.131	932.320	9.074
4	3.832	1.258	9.580	5.967
5	2.556	1.837	1336100.000	8.245
6	640790.000	2.013	1085900.000	10.057
7	1.721	1.113	48649.000	0.736
8	1.031	0.674	13677.000	0.399
9	0.433	0.189	4283.600	6.913

model validation and between two models, the one with the smallest loss function is the most valid. The smallness of loss function values explains why the OEE shear-flexure model has the best computed modes among all identified models for the east-west direction. The OEE model presented in table 6.13 has the smallest value of the loss function among all plausible models found during the sensitivity analysis. It is evident from Table 6.14 that except for parameter group 4 the estimation ranges of flexural stiffnesses are large and for the shear stiffnesses, the third and sixth parameter groups have large estimation ranges.

6.5. Engineering Model

An independent beam model (including shear and flexural) was developed based on an engineering approach using nominal building properties and simple mechanical assumptions to get story stiffnesses. The estimates were made by an independent practicing engineer in California. The initial stiffnesses of the engineering model, obtained from nominal properties, were scaled linearly such that the fundamental ***ns*** and ***ew*** frequencies matched the measured values (a one variable parameter estimation procedure). The final properties of the engineering model are given in Table 6.16. The computed natural frequencies are shown in Table 6.3 and the computed mode shapes are plotted along with the measured modes in Figs. 6.11 and 6.12.

The frequency distribution of the structure, which is the most reliable measurement available, is much better represented by the identified models, even the shear building models, than by the engineering model. For both directions, the engineering model has higher frequencies than the measured values, indicating that the engineering model is stiffer than the actual building. In order to improve the engineering model's spectrum the stiffness distribution would have to become more like the OEE shear-flexure model. Consequently,

Table 6.15. Bounds of the loss function and the natural frequencies for the east-west, shear-flexure building model

Value	Frequency (*Hz*)					
	Loss function	*1*st	*2*nd	*3*rd	*4*th	*5*th
Minimum	0.26	0.64	1.52	2.23	3.61	4.65
Maximum	1.52	0.64	1.54	2.31	3.61	4.65

the identified model provides a guide for critical assessment of the engineering procedure. The computed mode shapes in both directions are smooth and quite similar to the mode shapes of the OEE shear-flexure model shown in Figs. 6.8 and 6.10.

In Figs. 6.13 and 6.14 we plot element properties of engineering model and plausible shear-flexure models identified by the output error estimator and their estimation ranges shown in Tables 6.11 and 6.14. We show parameters in a practical range about the properties of the engineering model. Several observations can be made in comparing the shear-flexure models obtained by parameter estimation and the stiffer model built by the engineering procedure. The shear stiffnesses of both models have the same order of magnitude and have the same distribution, however in general, the engineering model has higher shear stiffnesses in both directions. The identified models tend to have higher flexural stiffnesses than the engineering model for bottom elements 1 through 7. Both models show a reduction in the flexural stiffnesses in elements 8 through 10 and have close parameters. The identified models show a dramatic increase in flexural stiffnesses in element 11 through 13 for the north-south direction and in elements 11 through 15 for the east-west direction with higher flexural stiffnesses than the engineering model. For top elements 14 through 18 in north-south models and elements 16 through 18 in east-west models, both engineering and identified models have close flexural stiffnesses. The identified models for both directions show tower elements 19 and 20 to be considerably stiffer in flexure than the engineering model indicates. The over all distributions of shear and flexural stiffnesses in the engineering model follow the mass distribution of the building given in Table 6.1. The identified models try

Table 6.16. Element properties of engineering model

Parameter group	Element	North-South		East-West	
		GA (10^6 *k*)	*EI* (10^9 *k–ft*^{2})	*GA* (10^6 *k*)	*EI* (10^9 *k–ft*^{2})
1	1	9.149	119.911	8.611	95.979
	2	9.149	119.953	8.611	96.123
	3	10.130	121.753	9.181	122.020
2	4	6.308	42.703	7.303	89.586
	5	5.588	29.218	3.308	21.540
3	6	4.983	26.456	3.779	13.814
	7	4.179	26.456	2.512	13.814
4	8	4.035	26.456	2.734	13.814
	9	4.145	26.456	2.638	13.814
	10	4.275	26.456	2.512	13.814
5	11	3.940	26.456	2.973	13.814
	12	3.940	26.456	2.600	13.814
	13	3.906	26.456	2.672	13.814
6	14	9.166	41.501	7.183	21.893
	15	9.542	46.524	7.377	24.058
7	16	3.373	6.997	1.459	4.395
	17	3.055	6.997	1.572	4.395
8	18	1.914	1.788	1.148	0.825
9	19	1.340	0.783	1.148	0.621
	20	0.957	0.317	0.957	0.317

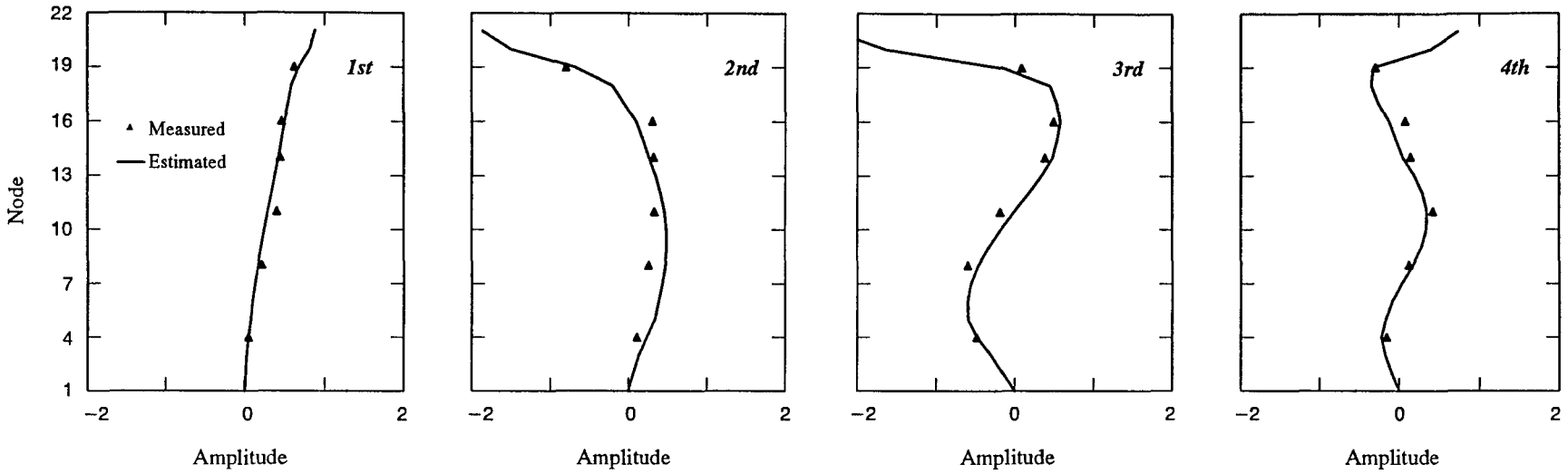

Fig. 6.11 North-south, engineering model

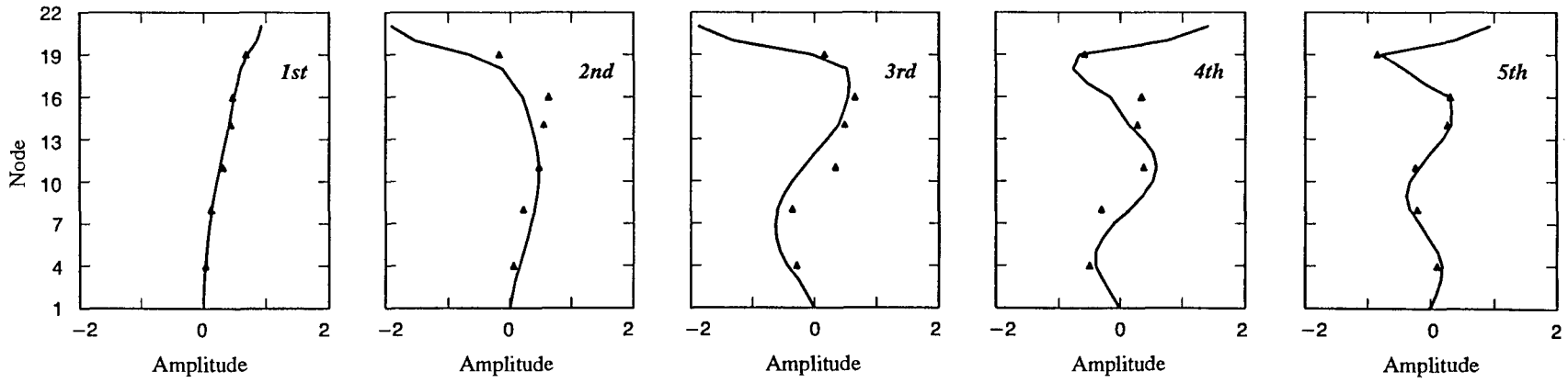

Fig. 6.12 East-west, engineering model

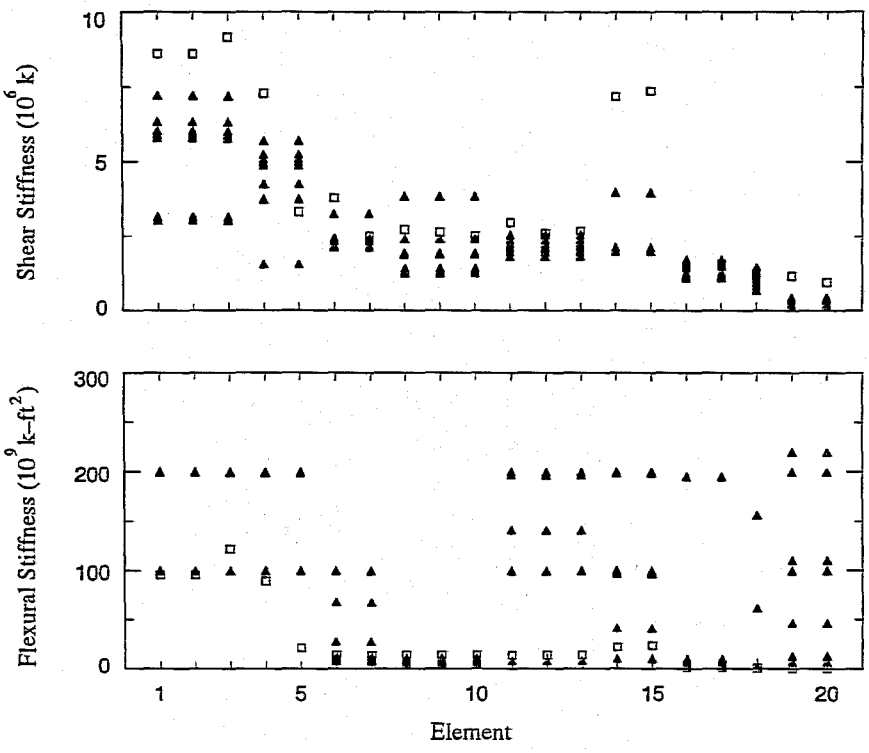

Fig. 6.14 Element properties of east-west, shear-flexure and engineering models

forced vibration tests. With proper data, a three dimensional beam model could be identified with additional parameters associated with the eccentricity of center of mass of a floor with respect to center of rigidity.

Finally, the building was modeled as a beam (with or without shear deformation). Such a model ignores the actual topology of the structure with the concomitant risk of obliterating important modes of response. The correspondence between measurements and computation obtained with the beam model would indicate that the beam model is a reasonably valid assumption in the present case.

The above caveats notwithstanding, the approach followed here would appear to be superior to generating a model of the structure based on ordinary engineering calculations without benefit of the modal data. The measurements, if reliable, carry the truth about the behavior of the structure. If used properly, the measurements can be a valuable aid to the assessment of structural performance. The engineering model can assist the parameter estimation approach to find reasonable bounding constraints and initial values for the unknown parameters. On the other hand, the parameter estimation procedure can be used to adjust some of the parameters of an engineering model in order to represent the measurements better and have a better and more valid model for the structure.

to follow the same distribution for shear stiffnesses with smaller estimated values and make elements, especially bottom and top elements, flexurally much stiffer than the engineering model in order to build mathematical models whose modes are spectrally close to the measured modes.

6.6. Chapter Summary

The parameter estimation procedure produced beam models with excellent dynamic properties; the frequency spectra of the identified models accurately matched the measured values and the mode shapes appeared to represent the measured modes well, both qualitatively and quantitatively. Accomplishment of such estimations would be virtually impossible by trial and error procedures.

While the computed results are excellent, there are several inherent limitations which should be emphasized. First of all the mass distribution was computed by an "engineering" procedure, and was considered known *a priori*. In general, one might expect that the mass distribution is known better than the stiffness distribution. However, the mass assumption may not accurately represent the actual mass distribution of the structure during the experiment that is implicit in the data. The mass parameters could also be estimated to improve the correspondence between measured and estimated properties, but the sparsity of measurement would seem to preclude such an estimate in the present case.

Secondly, the planar response was assumed *a priori*. Indeed, the planar response was even assumed in the selection of instrumentation for the forced vibration tests. At least three measurements per floor are required to track the motion of a floor in its own plane. The assumption of planar response was not borne out by the

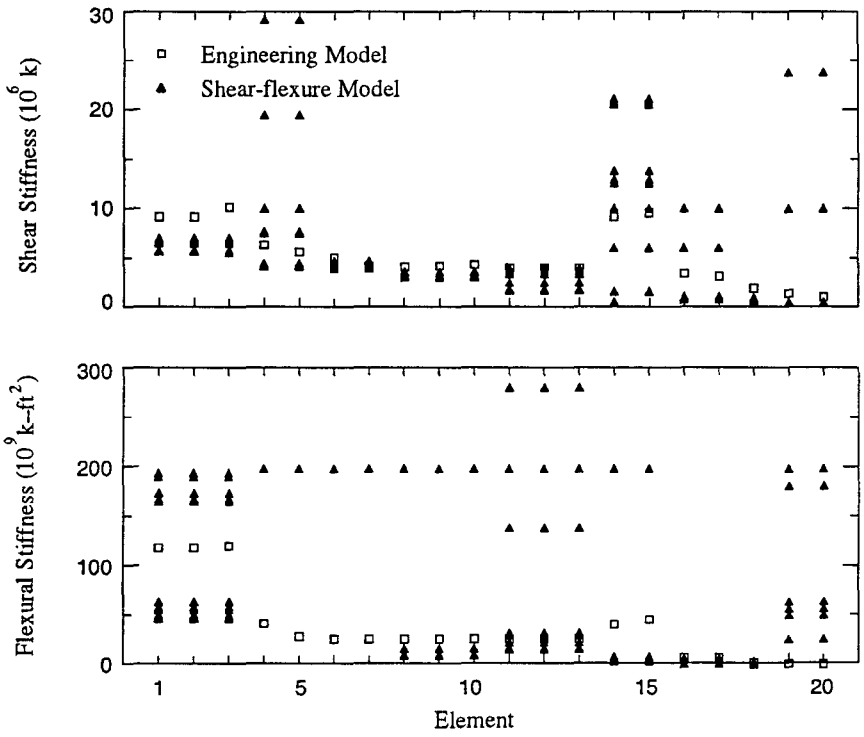

Fig. 6.13 Element properties of north-south, shear-flexure and engineering models

CHAPTER SEVEN

Parameter Estimation in Structures from Transient Dynamic Response

Estimating the unknown constitutive parameters of a finite element model of a structural system from the measured transient dynamic response of the real structure is more complicated than estimating them from static or modal response because the measured response is incomplete in both space and time. Since we generally measure only one of the state vectors (usually acceleration or displacement), the measurements are also incomplete in state. Furthermore, the parameterization of the model is more complicated because there are unknown stiffness, mass, and damping parameters, and numerical difficulties accrue from the fact that these parameters scale differently.

Transient dynamic parameter estimation is attractive, on the other hand, because of the wealth of data available and the ease of testing. Data collected at each point in time is analogous to a load case in the static problem or a mode in the modal dynamic problem. While the data at adjacent time points does not possess the same level of information content as different static load cases or different modes, the time points are plentiful, generally assuring adequate redundancy in the data sample.

In this study, we use the response of the structure and a history of the dynamic loads in the time domain to compute the unknown constitutive parameters of a finite element model of a structure. The proposed estimator is an equation error estimator and can accommodate measured displacements or measured accelerations. From a mathematical model with known geometry, topology, load history, and responses at certain locations, we pose a parameter estimation problem that, when solved, determines the unknown constitutive parameters of that (finite element) model. The proposed algorithm is based on the concept of minimizing the difference between the force applied to the structure and the residual force predicted by the model, as explained in Chapter Two.

The proposed parameter estimation algorithm has two main steps. In the first step, we compute the unmeasured state vectors using numerical differentiation and/or numerical integration methods. We treat the evolution of each measurement as an independent time series. Thus, the responses at different locations do not interact with each other. In the second step, we estimate the unknown constitutive parameters by solving a constrained nonlinear optimization problem. We use the recursive quadratic programming method (RQP) to solve the estimation problem. In the second phase, the measurements interact with each other through the objective function, which measures equilibrium error between the structure and the model. The proposed estimator can handle incompletely measured response in time, state, and space. It exhibits robust convergence, and is amenable to modeling of complex structural systems.

In the following sections, we define the model equation in time domain and present methods for computing the state vectors from measured displacements or accelerations. Next, we pose the estimation problem

and derive the necessary formulas to compute the sensitivity of the loss function with respect to the unknown variables. We also briefly explain a procedure for generating initial values of the unknown variables and a scaling strategy, followed by comments about the estimation time step and time windows. We demonstrate how the algorithm for the transient dynamic estimator can be used through analogy to solve the problem of modal identification when both mass and stiffness parameters are unknown. Finally, we mention the relationship of the method advocated here with some of the other methods available in the literature.

7.1. The Model Equation

Let us assume that we can adequately represent our structure with a linear finite element model with n_d degrees of freedom. The equations of dynamic equilibrium of the model can be expressed as an initial value problem as follows

$$\begin{aligned} \boldsymbol{M}(\boldsymbol{x})\ddot{\boldsymbol{u}}(t) + \boldsymbol{C}(\boldsymbol{x})\dot{\boldsymbol{u}}(t) + \boldsymbol{K}(\boldsymbol{x})\boldsymbol{u}(t) &= \boldsymbol{f}(t) \\ \boldsymbol{u}(0) &= \boldsymbol{u}_o \\ \dot{\boldsymbol{u}}(0) &= \boldsymbol{v}_o \end{aligned} \tag{7.1}$$

where $\boldsymbol{M}$, $\boldsymbol{C}$, and $\boldsymbol{K}$ are the usual (time-invariant) mass, damping, and stiffness matrices, respectively. The vector $\boldsymbol{f}(t)$ represents the applied nodal force. The nodal displacements are a function of time and are represented by the vector $\boldsymbol{u}(t)$. The first and second derivatives of $\boldsymbol{u}(t)$ are the velocity, $\dot{\boldsymbol{u}}(t)$, and acceleration, $\ddot{\boldsymbol{u}}(t)$, respectively. These three vectors, each having dimension n_d, characterize the state of the system at any time, and hence are referred to as *state vectors*. The initial displacement, $\boldsymbol{u}_o$, and velocity, $\boldsymbol{v}_o$, complete the specification of the initial value problem.

As we have done for the static and modal estimation problems, we assume that the system matrices depend on n_p unknown constitutive parameters $\boldsymbol{x}$. While the parameterization depends upon the specific model, the parameters include mass parameters, $\boldsymbol{x}_M$, damping parameters, $\boldsymbol{x}_C$, and stiffness parameters, $\boldsymbol{x}_K$. The mass parameters might comprise element mass densities or nodal masses; the damping parameters might comprise viscosity coefficients or modal damping ratios; the stiffness parameters might comprise material constitutive parameters such as Young's modulus (or for beams generalized moduli like *EA* and *EI*). For the present development we need not concern ourselves with a specific parameterization, only that the model is parametric.

In general, we will sample the dynamic response of our structures incompletely in both time and space. The measured response is incomplete in time because we sample our responses at discrete intervals, separated by a constant time interval Δt. The measured response is incomplete in space for the reasons described in the chapters on static and modal estimation: One generally would not attempt to measure the response at all points that correspond to degrees of freedom of the model simply because the economics of deploying that much instrumentation is not favorable. Furthermore, some responses might be difficult to make reliably (*e.g.* nodal rotations). Other measurements may be impossible to make because the point is inaccessible (*e.g.* points in the interior of a solid domain). The principle difficulties in parameter estimation accrue from incompleteness of the sampled response.

Acceleration, velocity, and displacement are related to each other through differential relations involving the continuous time variable t. As such they do not represent independent descriptors of the state of motion, but rather non-holonomic constraints among them. The discrete temporal sampling process prevents us from exactly enforcing these differential relations. It is thus profitable to view the acceleration $\boldsymbol{a}_k \approx \ddot{\boldsymbol{u}}(t_k)$, the velocity $\boldsymbol{v}_k \approx \dot{\boldsymbol{u}}(t_k)$, and the displacement $\boldsymbol{d}_k \approx \boldsymbol{u}(t_k)$ as independent state vectors. In general, one would not measure all of $\boldsymbol{a}_k$, $\boldsymbol{v}_k$, and $\boldsymbol{d}_k$, so that in addition to temporal and spatial incompleteness we also have incompleteness of state. For the sake of clarity, we will assume that we have measured either displacement $\boldsymbol{u}(t)$ or acceleration $\ddot{\boldsymbol{u}}(t)$, but not both. With the current state of measurement technology this assumption is practical. One rarely measures velocity directly, however it should be clear how to formulate the problem with such measurements from the succeeding derivations.

To deal with the temporal incompleteness of the data caused by discrete sampling we will enforce equilibrium of our model only at the sampled time points. Consequently, the equations of dynamic equilibrium at time t_k for our model problem take the form

$$M(x)a_k + C(x)v_k + K(x)d_k = g_k \tag{7.2}$$

where g_k approximates the applied force vector $f(t_k)$. These discrete equations will form the basis of our parameter estimation algorithm. For static and modal data we demonstrated two basic approaches to the parameter estimation problem: the equation error method and the output error method. Recall that, while the output error method for static and modal data did not require the estimation of the state at the unsampled degrees of freedom, the equation error method did require such an estimate. For the transient dynamic case, we shall formulate the parameter estimation problem using an equation error method. Hence, it will be necessary to estimate the state at the unsampled degrees of freedom. In contrast with the static and modal cases, the dynamic case will require the estimation of the displacement, velocity, and acceleration at the unmeasured degrees of freedom. The performance of the parameter estimation algorithm depends crucially upon the estimates of the unmeasured states, particularly when the data are polluted with noise. To encourage good performance of our algorithm, we will insist that it be consistent with the model problem (7.1) in some sense. In particular, we will require that the discrete state vectors and the discrete load vectors exactly satisfy a discrete version of the governing equations of the dynamic model problem for noise free data.

7.2. Estimation of the State Vectors

In our tests there are certain points in space that we monitor (the so-called measured degrees of freedom). At these points we record a discrete time series representing either displacement or acceleration according to the type of instrument we have deployed there. The determination of the remaining two state vectors (*e.g.* velocity and acceleration if we have measured displacements) is a straightforward exercise in univariate signal processing. That is, the state variables at a point are related only through time differentiation, not through physical laws like momentum balance. There are many algorithms for integrating or differentiating time series. In addition to the various numerical integration and differentiation schemes used, most of these methods include filtering procedures and baseline correction procedures. Here, we will assume that the measured sig-

nal has been suitably filtered to reduce the amount of noise from the measurements. No baseline adjustments will be considered. We will use numerical differentiation to compute velocity and acceleration when displacements are available and numerical integration to compute velocity and displacement when accelerations are available.

In the following sections we present two methods for computing the discrete load vector g_k and the discrete state vectors $\{d_k, v_k, a_k\}$. The first approach, called *EEEA*, assumes that the given data are accelerations while the second approach, called *EEED*, assumes that the given data are displacements. Both methods are aimed at preparing us for parameter estimation using the equation error approach.

Estimating state vectors from accelerations. When the history of acceleration is known at a certain location one can estimate the state variables at discrete times from the measured acceleration $\ddot{u}(t)$ by direct quadrature as follows

$$a_k = \ddot{u}(t_k) \tag{7.3}$$

$$v_k = v_o + \int_0^{t_k} \ddot{u}(t)dt \approx v_o + \Delta t \sum_{i=0}^{k} c_i a_i \tag{7.4}$$

$$d_k = u_o + v_o t_k + \int_0^{t_k} (t_k - t)\ddot{u}(t)dt \approx u_o + \Delta t \sum_{i=0}^{k} c_i v_i \tag{7.5}$$

where the coefficients c_i are particular to the specific numerical integration scheme chosen. One can use any numerical integration technique to compute the discrete state $\{d_k, v_k, a_k\}$ at that point. For example, the trapezoidal rule approximates the velocity and displacement at time t_k according to the following expressions

$$\begin{aligned} v_k &= v_o + \Delta t(\tfrac{1}{2}a_o + a_1 + \ldots + a_{k-1} + \tfrac{1}{2}a_k) \\ d_k &= u_o + \Delta t(\tfrac{1}{2}v_o + v_1 + \ldots + v_{k-1} + \tfrac{1}{2}v_k) \end{aligned} \tag{7.6}$$

Estimating state vectors from displacements. When the history of displacement is known at a certain location one can estimate the state variables at discrete times from the measured displacement $u(t)$ using a finite difference method as follows

$$d_k = \sum_{i \in D} \xi_i^d \, u(t_{k+i}) \tag{7.7}$$

$$v_k = \sum_{i \in D} \xi_i^v \, u(t_{k+i}) \tag{7.8}$$

$$a_k = \sum_{i \in D} \xi_i^a \, u(t_{k+i}) \tag{7.9}$$

where the coefficients ξ_i^d, ξ_i^v, and ξ_i^a define the numerical differentiation scheme. We define the summation to be over the index set $D = \{-n_o, -n_o+1, ..., 0, ... n_f-1, n_f\}$, where n_o is the number of points from the past

and n_f is the number of points from the future used in the approximation of the present state variable. A numerical differentiation rule is often classified according to the number of points covered. Here, the rule covers n_o+n_f+1 points, and is not necessarily centered in the interval. A centered three-point method, like Newmark or Houbolt, has the index set $\boldsymbol{D}=\{-1, 0, 1\}$. Most numerical schemes used to integrate second order ordinary differential equations do not look more than one point into the future (because of problems with numerical stability), but may look into the past to increase accuracy. These operators would have $n_f=1$. The best known methods for integrating the model problem fall into this category, and include the Newmark method, the Houbolt method, and the four-step scheme derived by Zienkiewicz (1987). As will become clear soon, there is no reason to avoid methods that reach into the future for the parameter estimation problem.

A differencing scheme consistent with the Newmark method for solving Eqn. (7.1) uses the displacements at three time points, with index set $\boldsymbol{D} = \{-1, 0, 1\}$. The coefficients for the Newmark method can be observed in the following equations

$$d_k = (\tfrac{1}{2} + \beta - \gamma)u_{k-1} + (\tfrac{1}{2} - 2\beta + \gamma)u_k + \beta u_{k+1} \tag{7.10}$$

$$v_k = \tfrac{1}{\Delta t}(\gamma - 1)u_{k-1} - \tfrac{1}{\Delta t}(2\gamma - 1)u_k + \tfrac{1}{\Delta t}\gamma u_{k+1} \tag{7.11}$$

$$a_k = \tfrac{1}{\Delta t^2}u_{k-1} - \tfrac{2}{\Delta t^2}u_k + \tfrac{1}{\Delta t^2}u_{k+1} \tag{7.12}$$

where β and γ are the Newmark integration constants, Δt is the time step, and u_{k-1}, u_k, and u_{k+1} are displacements at a certain location at times t_{k-1}, t_k, and t_{k+1}, respectively. For the values $\beta = \frac{1}{4}$ and $\gamma = \frac{1}{2}$ the Newmark equations are identical to the classical central difference method, except that the displacement at time t_k is computed as the moving average of displacements at the three time points. In particular, $d_k = \frac{1}{4}(u_{k-1} + 2u_k + u_{k+1})$. In essence, the Newmark estimator adds a simple filter to the central difference estimator.

Integrating accelerations to get velocities and displacements is much more stable with respect to noise in the sample than is differentiating displacements to get velocities and accelerations. One might expect that a parameter estimation scheme based on measured displacements would not perform as well as one based on acceleration measurements. Fortunately, it is far more practical to measure accelerations because of the simplicity of establishing an inertial frame of reference. Establishing a frame of reference for displacements is difficult, except possibly in a laboratory environment.

In the sequel we shall assume that the state vectors corresponding to the points of measurement have been processed. Accordingly, for the remaining developments, the entire state is available at those locations.

Estimation of the state vectors at unmeasured points. In accord with our standard notation, we partition the displacement vector $u(t)$ into two parts: one part corresponding to the measured degrees of freedom $\hat{u}(\hat{n}_d \times 1)$ and the other part corresponding to the unmeasured degrees of freedom $\bar{u}(\bar{n}_d \times 1)$ as follows

$$u(t) = \begin{bmatrix} \hat{u}(t) \\ \bar{u}(t) \end{bmatrix} \tag{7.13}$$

Clearly the number of measured and unmeasured degrees of freedom must sum to the total number of degrees of freedom of the model, $\hat{n}_d + \bar{n}_d = n_d$. This partition will be helpful in our treatment of the spatial incompleteness of the data. The partition can, by inference, be applied to accelerations and velocities. Let us also partition the discrete state vectors $\{d_k, v_k, a_k\}$ into two parts: one part corresponding to the measured degrees of freedom $\{\hat{d}_k, \hat{v}_k, \hat{a}_k\}$, each vector having dimension $\hat{n}_d$, and the other part corresponding to the unmeasured degrees of freedom $\{\bar{d}_k, \bar{v}_k, \bar{a}_k\}$, each vector having dimension $\bar{n}_d$, as follows

$$d_k = \begin{bmatrix} \hat{d}_k \\ \bar{d}_k \end{bmatrix} \qquad v_k = \begin{bmatrix} \hat{v}_k \\ \bar{v}_k \end{bmatrix} \qquad a_k = \begin{bmatrix} \hat{a}_k \\ \bar{a}_k \end{bmatrix} \tag{7.14}$$

For simplicity let us assume that this partitioning is fixed for all time points k=0, ..., *ntp*, where *ntp* is the number of time points in the sample. Each component of the measured state vectors $\{\hat{d}_k, \hat{v}_k, \hat{a}_k\}$ can be estimated from Eqns. (7.3), (7.4), and (7.5) or from Eqns. (7.7) (7.8), and (7.9), according to whether accelerations or displacements were measured. We must still estimate the discrete state vectors at the unmeasured degrees of freedom, $\{\bar{d}_k, \bar{v}_k, \bar{a}_k\}$.

The main concern in the formulation of a parameter estimation scheme is the influence of noise in the measurements. We have described two experiments, one where the displacements are measured and the velocities and accelerations are estimated by numerical differentiation, and the other where the accelerations are measured and the velocities and displacements are estimated by numerical integration. In both experiments we expect the measured data to be polluted with noise. Numerical difference methods tend to amplify noise while numerical integration methods tend to filter it. As a consequence we prefer measured accelerations to measured displacements. The estimation of the unmeasured state is a different story. There is no reason to view the unmeasured displacements $\bar{u}(t)$ as being polluted with noise.

We shall estimate the unmeasured state by numerically differentiating the unmeasured (and as yet unknown) displacements using the finite difference operators described previously as follows

$$\bar{d}_k = \sum_{i \in D} \xi_i^d \, \bar{u}(t_{k+i}) \tag{7.15}$$

$$\bar{v}_k = \sum_{i \in D} \xi_i^v \, \bar{u}(t_{k+i}) \tag{7.16}$$

$$\bar{a}_k = \sum_{i \in D} \xi_i^a \, \bar{u}(t_{k+i}) \tag{7.17}$$

If we view the state vectors at the measured locations as known, and estimate the state vectors at the unmeasured locations using the above finite difference scheme, then the discrete dynamic equations, given by Eqn. (7.2), are a function of unknown parameters x and unmeasured displacements $\bar{u} = \{\bar{u}_o, ..., \bar{u}_{ntp}\}$.

Discrete load vector. Zienkiewicz (1977) showed that some well known single-step numerical integration methods for the model problem could be cast as multi-time-step methods involving only the displacement state. The Newmark method, for example, can be expressed as a three-time-step method using the finite difference equations (7.10), (7.11), and (7.12). If the force vector is also suitably discretized, then the discrete version of the dynamic equations of motion is exactly consistent with the original model problem. The discrete force vector g_k can be approximated in a manner that guarantees it to be consistent with the discrete state vectors. For example, the consistent force vector at time t_k for the Newmark method, has the following form

$$g_k = (\tfrac{1}{2} + \beta - \gamma)f_{k-1} + (\tfrac{1}{2} - 2\beta + \gamma)f_k + \beta f_{k+1} \tag{7.18}$$

where f_{k-1}, f_k, and f_{k+1} are the load vectors at times t_{k-1}, t_k, and t_{k+1}, respectively. For the specific values of $\beta = 1/4$ and $\gamma = 1/2$ the expression reduces to $g_k = 1/4(f_{k-1} + 2f_k + f_{k+1})$.

The estimator based on measured displacements, *EEED*, estimates the velocities and accelerations for both the measured and unmeasured locations by numerical differentiation. The force vector given by Eqn. (7.18) is consistent with the numerical differentiation scheme. The estimator based on measured accelerations, *EEEA*, estimates the velocities and displacements for the measured locations by numerical integration, but expresses the velocity and acceleration for the unmeasured locations in terms of the unmeasured displacements by numerical differentiation. There is no known expression for the discrete force vectors that is consistent with the discrete state vectors computed by a numerical integration. In this case there is not any way to exactly satisfy the discrete dynamic equations of motion, Eqn. (7.2). In the absence of a consistent formula, we estimate the discrete force vector for *EEEA* at time t_k as follows

$$g_k = f(t_k) \tag{7.19}$$

Using finite-element interpolation functions in the temporal dimension, Zienkiewicz (1977) and Ghaboussi (1987) also showed how to compute the multi-step versions of other known methods, *e.g.* the Houbolt and Wilson-θ methods. For a noise free, complete displacement vector $u(t)$, the discrete state vectors and the discrete load vector g_k computed from any of these direct integration methods provides the required consistency among the coefficients of the discrete state vectors and coefficients of the discrete load vector, thereby exactly satisfying the discrete dynamic equations of motion, Eqn. (7.2).

7.3. The Equation Error Estimator

Our goal in parameter estimation is to find a set of parameters x that best represent the model problem. The model is defined up to the unknown constitutive parameters. In accord with the previous developments, the discrete form of the governing equations, Eqn. (7.2), are a function of the unknown constitutive parameters x and the unknown displacements corresponding to the unmeasured degrees of freedom at ntp+1 time points $\{\overline{u}_i\ , i=0, ..., ntp\}$. We shall use a least-squares estimator that endeavors to minimize the difference between the known applied force and the internal resistance estimated from the measured data. In essence,

our estimator tries to minimize the residual forces in the model caused by failure to meet equilibrium. To wit, we define the error function for time point t_k as follows

$$e_k(x, \bar{u}) = M(x)a_k(\bar{u}) + C(x)v_k(\bar{u}) + K(x)d_k(\bar{u}) - g_k \tag{7.20}$$

where the unknowns comprise both the unknown constitutive parameters $x = \{x_M, x_C, x_K\}$ and the displacements at the unmeasured degrees of freedom for all time points $\bar{u} = \{\bar{u}_o, ..., \bar{u}_{ntp}\}$. The acceleration, velocity, and displacement are explicit functions of the unknown displacements through the numerical differentiation of the unmeasured responses. In general, the dependence of these state vectors on $\{\bar{u}_o, ..., \bar{u}_{ntp}\}$ is sparse because the state at time point k depends only on the state at adjacent time points. The error at time point k for a three-step method like Newmark, for example, depends only on $\bar{u}_{k-1}$, $\bar{u}_k$, and $\bar{u}_{k+1}$.

The structural property matrices, mass matrix M, damping matrix C, and stiffness matrix K, depend upon their respective constitutive parameters $x = \{x_M, x_C, x_K\}$. The columns of these system matrices can be partitioned along the same lines as the state vectors, that is, with respect to measured versus unmeasured degrees of freedom. To wit, we define the matrices corresponding to the measured degrees of freedom to be $\hat{M}(x)$, $\hat{C}(x)$, and $\hat{K}(x)$, each having dimension $(n_d \times \hat{n}_d)$, and the matrices corresponding to the unmeasured degrees of freedom $\overline{M}(x)$, $\overline{C}(x)$, and $\overline{K}(x)$, each having dimension $(n_d \times \bar{n}_d)$. With this notation, the error function at time point k can be explicitly written as

$$e_k(x, \bar{u}) = \hat{M}(x)\hat{a}_k + \hat{C}(x)\hat{v}_k + \hat{K}(x)\hat{d}_k - g_k + \sum_{i \in D}\left[\xi_i^a \overline{M}(x) + \xi_i^v \overline{C}(x) + \xi_i^d \overline{K}(x)\right]\bar{u}_{k+i} \tag{7.21}$$

In accord with the general form of the estimation problem (2.4), the constrained nonlinear optimization problem for the proposed equation error is

$$\begin{aligned} &\underset{(x, \bar{u})}{\textit{minimize}} \quad J(x_M, x_C, x_K, \bar{u}_o, ..., \bar{u}_{ntp}) = \frac{1}{2}\sum_{k=n_o}^{ntp-n_f} \alpha_k \| e_k(x, \bar{u}) \|^2 \\ &\textit{subject to} \quad \underline{x} \le x \le \bar{x} \end{aligned} \tag{7.22}$$

where $\underline{x}$ and $\bar{x}$ are the prescribed vectors of lower and upper bounds on the unknown constitutive parameters, respectively and α_k is the weight associated with the kth time point. The most convenient norm to use in the loss function is the Euclidean norm $\| e \|^2 = e^T e$. The summation of error terms in the loss function starts with time point n_o and ends with time point $ntp - n_f$ because of the scheme used to estimate accelerations and velocities from displacements for the unmeasured locations. If the loss function involves the error in equilibrium from time points n_o to $ntp - n_f$, then it is a function only of the unmeasured displacements $\{\bar{u}_o, ..., \bar{u}_{ntp}\}$.

The proposed estimator simultaneously estimates the unknown constitutive parameters and the displacements at the unmeasured degrees of freedom for all time points in the sample. By adding bounding constraints on the unknown constitutive parameters we eliminate the possibility of converging to infeasible solutions. As explained in Chapter Two, we employ the recursive quadratic programming (RQP) to solve optimization

problem (7.22). The RQP algorithm needs the gradient vector and the Hessian matrix of the loss function $J(\boldsymbol{x}_M, \boldsymbol{x}_C, \boldsymbol{x}_K, \bar{\boldsymbol{u}}_o, ..., \bar{\boldsymbol{u}}_{ntp})$ with respect to the unknown variables $\{\boldsymbol{x}_M, \boldsymbol{x}_C, \boldsymbol{x}_K, \bar{\boldsymbol{u}}_o, ..., \bar{\boldsymbol{u}}_{ntp}\}$. These sensitivities are computed in the following section.

7.4. Sensitivity of the Loss Function

The minimization algorithm requires the gradient of the loss function with respect to the unknown variables $\{\boldsymbol{x}_M, \boldsymbol{x}_C, \boldsymbol{x}_K, \bar{\boldsymbol{u}}_o, ..., \bar{\boldsymbol{u}}_{ntp}\}$. We compute this gradient according to the following partition

$$\nabla e_k(\boldsymbol{x}, \bar{\boldsymbol{u}}) = \left[\nabla_{\boldsymbol{x}_M} e_k \quad \nabla_{\boldsymbol{x}_C} e_k \quad \nabla_{\boldsymbol{x}_K} e_k \quad \nabla_{\bar{\boldsymbol{u}}_o} e_k \quad \cdots \quad \nabla_{\bar{\boldsymbol{u}}_{ntp}} e_k \right] \tag{7.23}$$

The gradients with respect to the constitutive parameters are easily computed as

$$\nabla_{\boldsymbol{x}_M} e_k(\boldsymbol{x}, \bar{\boldsymbol{u}}) = \frac{\partial}{\partial \boldsymbol{x}_M}[\boldsymbol{M}(\boldsymbol{x}) a_k(\bar{\boldsymbol{u}})] \equiv \boldsymbol{U}_M(\boldsymbol{x}, \boldsymbol{u}) \tag{7.24}$$

$$\nabla_{\boldsymbol{x}_C} e_k(\boldsymbol{x}, \bar{\boldsymbol{u}}) = \frac{\partial}{\partial \boldsymbol{x}_C}[\boldsymbol{C}(\boldsymbol{x}) v_k(\bar{\boldsymbol{u}})] \equiv \boldsymbol{U}_C(\boldsymbol{x}, \boldsymbol{u}) \tag{7.25}$$

$$\nabla_{\boldsymbol{x}_K} e_k(\boldsymbol{x}, \bar{\boldsymbol{u}}) = \frac{\partial}{\partial \boldsymbol{x}_K}[\boldsymbol{K}(\boldsymbol{x}) d_k(\bar{\boldsymbol{u}})] \equiv \boldsymbol{U}_K(\boldsymbol{x}, \boldsymbol{u}) \tag{7.26}$$

Further simplification of these expressions is possible if one recognizes that the global coefficient matrices $\boldsymbol{M}$, $\boldsymbol{C}$, and $\boldsymbol{K}$ of a finite element model are assembled from element contributions as follows

$$\boldsymbol{M}(\boldsymbol{x}) = \sum_{e=1}^{N_m} \boldsymbol{M}^e(\boldsymbol{x}_M^e) \qquad \boldsymbol{C}(\boldsymbol{x}) = \sum_{e=1}^{N_m} \boldsymbol{C}^e(\boldsymbol{x}_C^e) \qquad \boldsymbol{K}(\boldsymbol{x}) = \sum_{e=1}^{N_m} \boldsymbol{K}^e(\boldsymbol{x}_K^e) \tag{7.27}$$

where $\boldsymbol{M}^e$, $\boldsymbol{C}^e$, and $\boldsymbol{K}^e$ are element mass, damping, and stiffness matrices, each with size of $(n_d^e \times n_d^e)$, where n_d^e is number of degrees of freedom associated with each element. A superscript e indicates association with element e and N_m is the number of elements in the structure. For example, $\boldsymbol{x}_M^e$, $\boldsymbol{x}_C^e$, and $\boldsymbol{x}_K^e$ are the vectors of unknown mass, damping, and stiffness parameters, respectively, associated with the eth element. The number of parameters per element is n_p^e. The assembly process is linear, and hence the gradient matrices $\boldsymbol{U}$ are sparse with respect to the constitutive parameters. The element sensitivity matrix $\boldsymbol{U}^e$ consists of element sensitivity matrices with respect to $\boldsymbol{x}_M^e$, $\boldsymbol{x}_C^e$, and $\boldsymbol{x}_K^e$, respectively shown by $\boldsymbol{U}_M^e$, $\boldsymbol{U}_C^e$, and $\boldsymbol{U}_K^e$, and computed as follows

$$\begin{aligned}
\boldsymbol{U}_M^e(\boldsymbol{x}_M^e, a_k^e) &= \frac{\partial}{\partial \boldsymbol{x}_M^e}[\boldsymbol{M}^e(\boldsymbol{x}_M^e) a_k^e] \\
\boldsymbol{U}_C^e(\boldsymbol{x}_C^e, v_k^e) &= \frac{\partial}{\partial \boldsymbol{x}_C^e}[\boldsymbol{C}^e(\boldsymbol{x}_C^e) v_k^e] \\
\boldsymbol{U}_K^e(\boldsymbol{x}_K^e, d_k^e) &= \frac{\partial}{\partial \boldsymbol{x}_K^e}[\boldsymbol{K}^e(\boldsymbol{x}_K^e) d_k^e]
\end{aligned} \tag{7.28}$$

where a_k^e, v_k^e, and d_k^e are discrete acceleration, velocity, and displacement vectors at the kth time point associated with the eth element. (Localization of the state variables is a basic operation in a general purpose finite element program. Clearly, it is useful here too.) All of these local vectors have the size $(n_d^e \times 1)$. Often, the element matrices M^e, C^e, and K^e are linear with respect to their parameters x_M^e, x_C^e, and x_K^e (as they are, for example, in a truss bar or a Bernoulli-Euler beam). In these cases, the sensitivity matrix U is independent of the unknown parameters x. In Appendix B we have explained how the element sensitivity matrices U_M^e, U_C^e, and U_K^e can be built from the fundamental relations of the finite element method.

Since displacements at the locations of the unmeasured degrees of freedom for ntp time points are also unknown, we must compute the gradient of the error function $e_k(x, \bar{u})$ with respect to $\bar{u}_i$ where index i takes values i=0, ..., ntp. To help describe the computation of this gradient let us define the matrix Z_j as

$$Z_j(x) \equiv \begin{cases} \xi_j^a \overline{M}(x) + \xi_j^v \overline{C}(x) + \xi_j^d \overline{K}(x) & j \in D \\ 0 & j \notin D \end{cases} \tag{7.29}$$

The matrix Z_j is a function of the constitutive parameters x because of its dependence on the matrices $\overline{M}$, $\overline{C}$, and $\overline{K}$. It also depends upon the specific operator used for time differentiation of the unknown state vectors at the locations of the unmeasured degrees of freedom. The matrices $\overline{M}$, $\overline{C}$, and $\overline{K}$ are fixed for all time points and are computed with standard assembly procedures. For the (three-point) Newmark method, the matrices Z_{-1}, Z_0, and Z_1 take the following form

$$\begin{aligned} Z_{-1} &= \tfrac{1}{\Delta t^2}\overline{M} + \tfrac{1}{\Delta t}(\gamma - 1)\overline{C} + (\tfrac{1}{2} + \beta - \gamma)\overline{K} \\ Z_0 &= -\tfrac{2}{\Delta t^2}\overline{M} - \tfrac{1}{\Delta t}(2\gamma - 1)\overline{C} + (\tfrac{1}{2} - 2\beta + \gamma)\overline{K} \\ Z_1 &= \tfrac{1}{\Delta t^2}\overline{M} + \tfrac{1}{\Delta t}\gamma\overline{C} + \beta\overline{K} \end{aligned} \tag{7.30}$$

The value of Z for any index other that $\{-1, 0, 1\}$ is zero for this case. Using the preceding notation the gradient of the error function at the kth time point is given by

$$\nabla_{\bar{u}_i} e_k(x, \bar{u}) = Z_{i-k} \tag{7.31}$$

where the index k takes values k=n_o, ..., $ntp-n_f$, and the index i takes values i=0, ..., ntp. We assume that the finite element model is linear, therefore the structural matrices M, C, and K do not depend on the response. Consequently, for a particular finite difference method based on displacement vectors at n_o+n_f+1 time points, the matrix $\nabla_{\bar{u}_i} e_k(x, \bar{u})$ is constant for all time points.

The total gradient of the error function with respect to the unknown variables, defined in Eqn. (7.23) can now be explicitly written as

$$\nabla e_k(x, \bar{u}) = \begin{bmatrix} U_M & U_C & U_K & Z_{n_o-k} & Z_{n_o+1-k} & \cdots & Z_{ntp-n_f-k} \end{bmatrix} \equiv \begin{bmatrix} U & G_k \end{bmatrix} \tag{7.32}$$

where the matrix $\boldsymbol{U}$ is the concatenation of the individual gradients with respect to the variables $\boldsymbol{x}$ and the matrix $\boldsymbol{G}_k$ is the concatenation of the gradients with respect to the unknown responses, and is typically quite sparse. Now, the gradient of the loss function $\nabla J(\boldsymbol{x}, \bar{\boldsymbol{u}})$ with respect to the unknown variables for the proposed estimator in Eqn. (7.22) takes the following form

$$\nabla J(\boldsymbol{x}, \bar{\boldsymbol{u}}) = \sum_{k=n_o}^{ntp-n_f} a_k \nabla^T e_k(\boldsymbol{x}, \bar{\boldsymbol{u}}) e_k(\boldsymbol{x}, \bar{\boldsymbol{u}}) = \sum_{k=n_o}^{ntp-n_f} a_k \left[\boldsymbol{U}(\boldsymbol{x}, \boldsymbol{u}) \quad \boldsymbol{G}_k(\boldsymbol{x})\right]^T e_k(\boldsymbol{x}, \bar{\boldsymbol{u}}) \tag{7.33}$$

The recursive quadratic programming algorithm requires an estimate of the Hessian of the loss function. This estimate can be made with a rank-two update formula (such as the modified BFGS update used in the Han-Powell method), however, two interesting alternatives are available for the present problem. In particular, one can compute the exact Hessian and the Gauss-Newton approximation of the Hessian of the loss function $J(\boldsymbol{x}, \bar{\boldsymbol{u}})$.

The Gauss-Newton approximation of the Hessian matrix $\boldsymbol{H}^{GN}$ is the part of the Hessian involving only first derivative terms and can be computed as $\boldsymbol{H}^{GN} = \sum_k a_k \nabla^T e_k \nabla e_k$. Accordingly it takes the form

$$\boldsymbol{H}^{GN}(\boldsymbol{x}, \bar{\boldsymbol{u}}) = \sum_{k=n_o}^{ntp-n_f} a_k \begin{bmatrix} \boldsymbol{U}^T(\boldsymbol{x}, \boldsymbol{u}) \boldsymbol{U}(\boldsymbol{x}, \boldsymbol{u}) & \boldsymbol{U}^T(\boldsymbol{x}, \boldsymbol{u}) \boldsymbol{G}_k(\boldsymbol{x}) \\ \boldsymbol{G}_k^T(\boldsymbol{x}) \boldsymbol{U}(\boldsymbol{x}, \boldsymbol{u}) & \boldsymbol{G}_k^T(\boldsymbol{x}) \boldsymbol{G}_k(\boldsymbol{x}) \end{bmatrix} \tag{7.34}$$

The exact Hessian matrix $\boldsymbol{H} = \nabla^2 J(\boldsymbol{x}, \bar{\boldsymbol{u}}) = \boldsymbol{H}^{GN} + \sum_k a_k \nabla^2 e_k(\boldsymbol{x}, \bar{\boldsymbol{u}}) e_k(\boldsymbol{x}, \bar{\boldsymbol{u}})$ has the following expression

$$\boldsymbol{H}(\boldsymbol{x}, \bar{\boldsymbol{u}}) = \boldsymbol{H}^{GN}(\boldsymbol{x}, \bar{\boldsymbol{u}}) + \sum_{k=n_o}^{ntp-n_f} a_k \begin{bmatrix} \nabla_{\boldsymbol{x}}^T \boldsymbol{U}(\boldsymbol{x}, \boldsymbol{u}) & \nabla_{\bar{\boldsymbol{u}}}^T \boldsymbol{U}(\boldsymbol{x}, \boldsymbol{u}) \\ \nabla_{\boldsymbol{x}}^T \boldsymbol{G}_k(\boldsymbol{x}) & \boldsymbol{0} \end{bmatrix} e_k(\boldsymbol{x}, \bar{\boldsymbol{u}}) \tag{7.35}$$

where the third order tensors $\nabla_{\boldsymbol{x}} \boldsymbol{G}_k$, $\nabla_{\boldsymbol{x}} \boldsymbol{U}$, and $\nabla_{\bar{\boldsymbol{u}}} \boldsymbol{U}$ represent the second derivatives of the loss function, and can be computed according to the procedures outlined in Section 3.2.

The Gauss-Newton approximation of the Hessian requires considerably less computation and storage than the exact Hessian, and generally constitutes an adequate representation of the exact Hessian when the residual is small. Further, $\boldsymbol{H}^{GN}(\boldsymbol{x}, \bar{\boldsymbol{u}})$ is positive semi-definite for all values of the parameters, while $\boldsymbol{H}(\boldsymbol{x}, \bar{\boldsymbol{u}})$ may not be.

Our experience with Newton methods (using either the exact or approximate Hessian) and quasi-Newton suggests that RQP converges in fewer iterations using a Gauss-Newton method than it does using the Han-Powell method. This observation is consistent with observations made by other researchers solving least-squares problems.

7.5. Initial Values, Scaling, and Identifiability

The proposed equation error estimator is based on solving a nonlinear constrained optimization problem. Like any iterative process, the recursive quadratic programming method needs initial values for the unknown variables in order to start the iteration. In Section 3.4, we discussed in detail different alternatives that one can use to generate initial values for the unknown constitutive parameters and the unmeasured displacements.

The recursive quadratic programming (RQP) method is used to minimize the loss function of the proposed estimator. The RQP algorithm is an iterative gradient search strategy. Therefore, the performance of the RQP method depends on the local properties of the surface of the loss function around a local minimum. A large difference between the order of magnitudes of the optimization variables (scaling problem) can manifest as large narrow ravines in the topography of the loss function. These ravines can affect the convergence rate of the RQP algorithm and occasionally cause the algorithm to oscillate. If the bottom of the ravine has directions in which the curvature is negligible (*i.e.* flat spots), the Hessian may become singular (or nearly singular), causing additional problems with convergence. The scaling problem exists for parameter estimation since the unknown constitutive parameters $\boldsymbol{x}$ may represent different classes of physical properties and thus may have different orders of magnitude. Further, the displacements at the locations of the unmeasured degrees of freedom $\bar{\boldsymbol{u}}$ have magnitudes quite different from the unknown parameters $\boldsymbol{x}$.

To solve the scaling problem, we scale the optimization variables to have the same order of magnitude. The scale matrix is constructed based on the initial values of the optimization variables using the procedure explained in Section 3.5.

The estimations are reliable if a certain minimum amount of data are available. Confidence in the estimates increases with the amount of information above this minimum level. Since the algorithm for the transient dynamic is analogous to those of the static and modal problems, the basic identifiability criterion is the same. Hence, we must have

$$(ntp - n_f - n_o + 1) \times \hat{n}_d \geq n_p \tag{7.36}$$

where the left-hand side of Eqn. (7.36) is the number of independent measurements and n_p is the number of unknown constitutive parameters. The identifiability criterion (7.36) is a quantitative index for the richness of the available information. If this criterion is not satisfied, then the estimates are totally unreliable. However, satisfaction of the identifiability criterion does not guarantee reliable estimates.

7.6. Time Windowing

In a forced vibration experiment, we measure histories of displacements $\boldsymbol{u}(t)$ or accelerations $\ddot{\boldsymbol{u}}(t)$ for a period of time which begins at time T_o and ends at time T_f, (see Fig. 7.1). The measured response of the structure is recorded digitally at time points equally spaced by the time step ΔT. One can determine the number of recorded time points *NTP* as follows

$$NTP = \frac{T_f - T_o}{\Delta T} + 1 \tag{7.37}$$

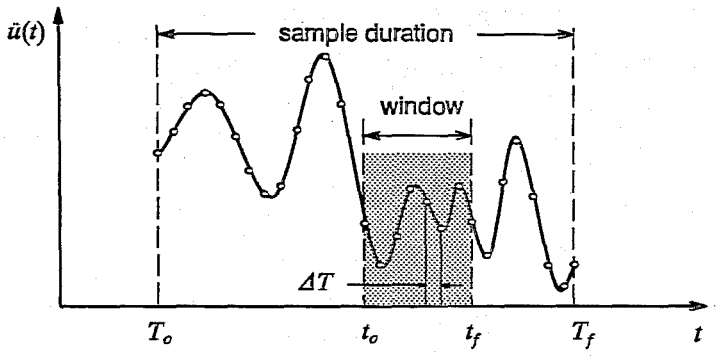

Fig. 7.1 Schematic representation of location and size of a window

One can use the entire history of measurements to estimate the unknown parameters. However, this strategy is neither necessary nor computationally efficient, particularly for complex structures. For a fixed number of measured degrees of freedom $\hat{n}_d$ and a fixed number of unknown parameters n_p one must provide data at a sufficient number of time points to reliably estimate the unknown parameters. Therefore, we theoretically need only a portion of the measured response. We call this portion of the measured response, which begins at time t_o and ends at time t_f and contains *ntp* time points, a *time window* or simply a *window* and we refer to *ntp* as the *window size*.

Since the forced transient dynamic response is incomplete in time and space, numerically approximation of the discrete state vectors adds error to the parameter estimation problem. One can minimize the effect of this error if one takes the time step to be reasonably small. But, the distance between two consecutive time points in a window controls not only the numerical errors but also one of the estimation error sources. If time points are relatively far from each other, numerical errors in integration and/or differentiation will accrue. On the other hand, if time points are close to each other, data at adjacent time points do not provide distinguishing new information for the estimator. As a consequent one must generally have a sample frequent enough to control numerical errors. From that sample we use intermittent points to estimate parameters. The estimation time step Δt might be a multiple of the recording time step ΔT as follows

$$\Delta t = JUMP \times \Delta T \tag{7.38}$$

One can adjust Δt by changing *JUMP* to find a suitable time step that keeps estimation errors reasonably low. Figure 7.1 schematically shows a window, window size, and window time step ΔT along a history of accelerations.

7.7. Averaging Estimates for Multiple Time Windows

After computing the discrete state vectors at the measured locations and the discrete load vector, we estimate the unknown constitutive parameters of the model and the unmeasured state vectors by solving a constrained nonlinear optimization problem. Each of these estimates necessarily corresponds to a specific time window. A small time window might have sufficient data to make these estimates, but they would tend to be sensitive to the location of the window, particularly for large amplitudes of noise. However, many such

windows would be available to make independent estimates. To improve the reliability of the estimated values we compute the average over a sample of N windows located sequentially or randomly along the measured history of response. Consequently, we will solve N different constrained nonlinear optimization problems corresponding to N different windows which generate N different vectors of parameters $\boldsymbol{x}$. We compute the average of estimates $\boldsymbol{x}$ for all the windows as the estimates parameters $\boldsymbol{x}^*$ as follows

$$\boldsymbol{x}^* = \frac{1}{N}\sum_{i=1}^{N} \boldsymbol{x}_i \tag{7.39}$$

As an alternative, one could take comparatively few time windows each having a large number of time points. Again, one can average the results, but there would be fewer members in the sample. The optimal strategy is not obvious, but will be explored in the next chapter.

7.8. Modal Identification: A Special Case

In Chapter Five, we developed two estimators to determine stiffness parameters of a finite element model of a structure using measured modal data in conjunction with the known mass matrix. Also, we proposed an equation error estimator when both mass and stiffness parameters are unknown. If both the mass and the stiffness matrices are unknown and the modal data are available then modal identification can be viewed as a special case of the parameter estimation problem based on forced, transient response.

The governing equation for undamped free vibration has the following form

$$\boldsymbol{M}(\boldsymbol{x})\lambda_k \boldsymbol{u}_k - \boldsymbol{K}(\boldsymbol{x})\boldsymbol{u}_k = \boldsymbol{0} \tag{7.40}$$

where λ_k is the square of the kth natural frequency and $\boldsymbol{u}_k$ is the kth mode shape and k takes values from one to the number of measured modes *nmd*. If we let $\boldsymbol{a}_k = \lambda_k \boldsymbol{u}_k$ and $\boldsymbol{d}_k = -\boldsymbol{u}_k$, and assume our usual partitioning of measured and unmeasured modal displacements, then an error function corresponding to Eqn. (7.40) can be expressed in a manner similar to Eqn. (7.21) as follows

$$\boldsymbol{e}_k(\boldsymbol{x}, \overline{\boldsymbol{u}}) = \hat{\boldsymbol{M}}(\boldsymbol{x})\hat{\boldsymbol{a}}_k + \hat{\boldsymbol{K}}(\boldsymbol{x})\hat{\boldsymbol{d}}_k + [\overline{\boldsymbol{M}}(\boldsymbol{x})\lambda_k - \overline{\boldsymbol{K}}(\boldsymbol{x})]\overline{\boldsymbol{u}}_k \tag{7.41}$$

The main difference between Eqns. (7.41) and (7.21) is that, in Eqn. (7.41) the error function corresponding to the kth mode $\boldsymbol{e}_k$ is a function of the constitutive parameters $\boldsymbol{x}$ and unmeasured displacements of only the kth mode $\boldsymbol{u}_k$. While, the error function corresponding to the kth time point in Eqn. (7.21) depends on the unmeasured displacements at the locations of unmeasured degrees of freedom from the other time points too. When the modal data is available the algorithm skips the first part, computation of the discrete unmeasured state vectors and begins directly with the second step, estimation of the unknown variables.

In accord with the general form of the estimation problem (2.4), the constrained nonlinear optimization problem for the proposed equation error is

$$\underset{(x,\,\bar{u})}{\textit{minimize}} \quad J(x_M, x_K, \bar{u}_1, \ldots, \bar{u}_{nmd}) = \frac{1}{2}\sum_{k=1}^{nmd} a_k \| e_k(x,\bar{u}) \|^2 \tag{7.42}$$

$$\textit{subject to} \quad \underline{x} \le x \le \bar{x}$$

The loss function for the modal estimation problem must be augmented by a constraint relating the constitutive parameters. For example, the total mass be known *a priori* or some of the individual parameters might be known. Now we can compute the gradient of the error function as follows

$$\nabla e_k(x,\bar{u}) = \left[\nabla_{x_M} e_k \quad \nabla_{x_K} e_k \quad \nabla_{\bar{u}_1} e_k \quad \cdots \quad \nabla_{\bar{u}_{nmd}} e_k\right] \tag{7.43}$$

The gradients with respect to the constitutive parameters are easily computed as

$$\nabla_{x_M} e_k(x,\bar{u}) = \frac{\partial}{\partial x_M}[M(x)a_k(\bar{u})] \equiv U_M(x,u) \tag{7.44}$$

$$\nabla_{x_K} e_k(x,\bar{u}) = \frac{\partial}{\partial x_K}[K(x)d_k(\bar{u})] \equiv U_K(x,u) \tag{7.45}$$

We must also compute the gradient of the error function $e_k(x,\bar{u})$ with respect to $\bar{u}_i$. To help describe the computation of this gradient let us define the matrix Z_i for our present purposes to be

$$Z_i(x) \equiv \lambda_i \overline{M}(x) - \overline{K}(x) \tag{7.46}$$

Using this notation the gradient of the error function with respect to the kth modal vector is given by

$$\nabla_{\bar{u}_i} e_k(x,\bar{u}) = Z_i \delta_{ik} \tag{7.47}$$

where δ_{ik} is the Kronecker delta. In this case of the indices take values k=0, ..., nmd, and i=0, ..., nmd. We assume that the finite element model is linear, therefore the structural matrices M, C, and K do not depend on the response. Consequently, for a particular finite difference method based on displacement vectors, the matrix $\nabla_{\bar{u}_i} e_k(x,\bar{u})$ is constant for all modes.

The total gradient of the error function with respect to the unknown variables, defined in Eqn. (7.23) can now be explicitly written as

$$\nabla e_k(x,\bar{u}) = \left[U_M \quad U_K \quad 0 \ \ldots \ 0 \quad Z_k \quad 0 \ \ldots \ 0\right] \equiv \left[U \quad G_k\right] \tag{7.48}$$

where the matrix U is the concatenation of the individual gradients with respect to the variables x and the matrix G_k is the concatenation of the gradients with respect to the unknown responses, and is quite sparse. Now, the gradient of the loss function $\nabla J(x,\bar{u})$ with respect to the unknown variables for the proposed estimator in Eqn. (7.22) takes the following form

$$\nabla J(x,\bar{u}) = \sum_{k=1}^{nmd} a_k \nabla^T e_k(x,\bar{u}) e_k(x,\bar{u}) = \sum_{k=1}^{nmd} a_k \left[U(x,u) \quad G_k(x) \right]^T e_k(x,\bar{u}) \tag{7.49}$$

With the notation used here, the Hessian approximations are identical to those developed earlier.

The analogy between the modal parameter estimation problem and the transient dynamic parameter estimation problem is quite clear. Mode numbers are analogous to time point numbers and we must still estimate the unmeasured modal displacements. However, we do not need to estimate discrete state vectors at the measured degrees of freedom because both the "acceleration" and "displacement" are given in terms of the modal displacements u_k. There also is no need for a numerical differentiation scheme since the succeeding points are not related through time differentiation. The main advantage of recognizing the analogy is that the modal estimation procedure can be programmed as a direct subset of the transient dynamic procedure.

7.9. Relation to Other Methods

Parameter estimation in structures from dynamic response data has enjoyed considerable attention in recent years. The methods that have been developed span the range from linear deterministic models to nonlinear stochastic models. The applications range from improving mathematical models of systems to damage detection, from identifying the input of a system to controlling its response.

One can broadly classify a parameter estimation method using dynamic response as either a time- domain method or a frequency-domain method. The equations governing the mathematical model are generally defined in the time domain, but can be transformed to the frequency domain using either the Laplace or Fourier transform. In general, the choice between time domain and frequency domain is dictated by the prior knowledge of the system and the intended use of the model. When the system is governed by differential or difference equations, when the model is intended to predict future response or to simulate the system, or when a stochastic control is desired, a time-domain model will eventually be required. When the objective of the identification process is to determined resonances in the response of a system, to design a model for a frequency domain control system, or when the bandwidth and the frequency resolution are available as *a priori* information, then a frequency-domain model must be employed.

The theory and practice of system identification in engineering, particularly in control, were dominated by frequency-domain methods up to the 1960's. From the end of the 1960's onward, interest in time-domain methods has increased. Now, time-domain methods seem to dominate the literature on identification. Ljung and Glover (1981) compare the frequency-domain methods and time-domain methods and summarize some of the most popular methods in these two domains. They conclude that, although time-domain and frequency-domain identification methods are often viewed as competitive, they actually complement each other. In the following sections we briefly explain the problem of parameter estimation in the time and frequency domains.

Time Domain Methods. Recall the governing equations of motion of a structural system with mass M, damping C, and stiffness K, subject to a force $f(t)$:

$$M\ddot{u}(t) + C\dot{u}(t) + Ku(t) = f(t) \tag{7.50}$$

where $u(t)$, $\dot{u}(t)$, and $\ddot{u}(t)$, represent the nodal displacements, velocities, and accelerations, respectively. These equations can be recast in *state space* by defining the state vector $Y(t)$ as

$$Y(t) = \begin{Bmatrix} u(t) \\ \dot{u}(t) \end{Bmatrix} \tag{7.51}$$

and the (constant) system matrix A and system input vector $b(t)$, respectively as follows

$$A = \begin{bmatrix} 0 & I \\ -M^{-1}K & -M^{-1}C \end{bmatrix} \qquad b(t) = \begin{Bmatrix} 0 \\ -M^{-1}f(t) \end{Bmatrix} \tag{7.52}$$

With these definitions, Eqn. (7.50) takes the form

$$\dot{Y}(t) = AY(t) + b(t) \tag{7.53}$$

Most state-space methods exploit the closed-form solution of Eqn. (7.53), which is given in terms of matrix exponentials as

$$Y(t) = e^{A(t-t_o)}Y(t_o) + \int_{t_o}^{t} e^{A(t-\tau)}b(\tau)d\tau \tag{7.54}$$

Some of the earliest methods, for example those proposed by Ibrahim and Mikulcik (1973 and 1976), take advantage of the simplicity of the free vibration problem, *i.e.* $b(t)=0$. Ibrahim's method assembles two matrices of observations that lag each other by an amount $t_{i+1} - t_i \equiv \Delta t$. Let the dimension of the state space be $2n$, and the number of observation time points be $m+1$. Further, define the two observation matrices as follows

$$Y_o = [Y(t_o) \ldots Y(t_{m-1})] \qquad Y_1 = [Y(t_1) \ldots Y(t_m)] \tag{7.55}$$

By virtue of Eqn. (7.54), these two matrices satisfy

$$Y_1 = e^{A\Delta t}Y_o \tag{7.56}$$

and the exponential matrix can be estimated by least-squares as

$$e^{A\Delta t} \approx Y_1 Y_o^T [Y_o Y_o^T]^{-1} \equiv B \tag{7.57}$$

Let ϕ be an eigenvector of A and λ the corresponding eigenvalue, that is $A\phi = \lambda\phi$. One can easily show that ϕ is also an eigenvector of $e^{A\Delta t}$ with corresponding eigenvalue $\omega \equiv e^{\lambda\Delta t}$ using the definition of the matrix exponential. To wit,

$$e^{A\Delta t}\phi = [I + A\Delta t + \frac{(A\Delta t)^2}{2!} + \cdots]\phi = [1 + \lambda\Delta t + \frac{(\lambda\Delta t)^2}{2!} + \cdots]\phi = e^{\lambda\Delta t}\phi \tag{7.58}$$

The complex numbers λ are clearly the damped natural frequencies of the structure corresponding to the damped modes ϕ. Thus Ibrihim's method amounts to *(a)* assembling the observation matrices, *(b)* forming the approximation $\boldsymbol{B}$ according to Eqn. (7.57), *(c)* finding the eigenvalues and eigenvectors of $\boldsymbol{B}$, and *(d)* relating the eigenvalues of $\boldsymbol{B}$ to the frequencies and damping ratios of the system.

Tsen and Mook (1987) derived an estimation algorithm for linear, time-invariant dynamic models of structures by minimizing the difference between observations $\hat{Y}(t)$ and a linear expansion of the model in terms of the parameter p. The error function of time t then takes the form

$$e(t,\Delta p) = Y(t,p+\Delta p) - \hat{Y}(t) \approx Y(t,p) + \frac{\partial Y}{\partial p}\Delta p - \hat{Y}(t) \tag{7.59}$$

and is linear in the increment Δp. They recognized that the sensitivity of Y evolves in a manner similar to Y itself. In fact, if one defines

$$\boldsymbol{D} = \begin{bmatrix} \boldsymbol{A} & \boldsymbol{0} \\ \frac{\partial \boldsymbol{A}}{\partial p} & \boldsymbol{A} \end{bmatrix} \qquad Z(t) = \begin{Bmatrix} Y(t) \\ \frac{\partial Y(t)}{\partial p} \end{Bmatrix} \qquad Z(t_o) = \begin{Bmatrix} Y(t_o) \\ \boldsymbol{0} \end{Bmatrix} \tag{7.60}$$

Then the augmented system evolves according to

$$Z(t) = e^{\boldsymbol{D}(t-t_o)}Z(t_o) \tag{7.61}$$

Since $\boldsymbol{D}$ is completely known, one can compute both the state vector and its sensitivity for any given value of the parameter p for all times t. The error given in Eqn. (7.59) can then be minimized with respect to Δp. The method requires state-observable, free or force, discrete time domain measurements.

Hac and Spanos (1990) used state variables and the concept of Kalman filter to estimate members of the system matrix. They tried to improve the quality of data by using an adaptive Kalman filter. The implementation of the Kalman filter requires known system matrix $\boldsymbol{A}$. Therefore, they proposed an iterative procedure using Ibrahim's method. This algorithm had three steps. In the first step, the initial system matrix was estimated using Ibrahim's method. In the second step, the data were smoothed and in the third step the smooth data were given back to Ibrahim's method to compute the system matrix. They concluded that this method improved the results of Ibrahim's method, but if Ibrahim's method used least-squares to compute the state system, filtering the data would not improve the results significantly. The developed method required complete eigenvectors and assumed the covarience matrix of the measurements was known.

There are some other methods developed to estimate the forcing function or to model a structure using ARMA methods. Here, we briefly explain and list a few of these methods. Pi and Mickleborough (1989) presented a time domain method for estimating the modal parameters of a linear vibrating structure. The method was based on an ARMAX model and the modal parameters were related to the coefficient matrices. They assumed the vibrating structure was completely observable and displacements were measured. Lee and Chen (1989) proposed an approach to estimate autoregressive parameters of an AR model of a randomly excited structure. The method required displacements and velocities at all degrees of freedom and assumed an unmeasured white noise in the input sequence. Yun and Shinozuka (1990) developed a method for identification of

the coefficient matrices in the equation of motion for linear structures. They transformed the equation of motion into an ARMAX model and estimated the parameters of the ARMAX model, then they recovered the coefficient matrices of the original problem. This method requires time histories of the excitations and displacements at all degrees of freedom, assumes the system is observable with an index two and for models with order larger than two or large, complex structures has serious problem with number of parameters and recovering the members of the coefficient matrices from the estimated ARMAX model. In 1992 Yun, *et al.* modified the model to estimate the modal parameters. Hollkamp and Batill (1991) developed an algorithm for parameter estimation of an ARMA model of a structure using discrete time history of the response. The method was used for response prediction and was limited to SISO applications.

Wang (1990) proposed two methods for prediction of vibration at inaccessible points using measurable data. The first method assumed the structural matrices were known and used state variable method to estimate displacements at inaccessible locations of the system. The second method used an impulse response function to predict the unknown vibrations. Lim and Pilkey (1992) presented a procedure for lightly damped flexible structures to estimate forcing functions. They assumed the structural matrices, all state vectors at some degrees of freedom, and the locations of of loads on the structure were known. The method used the modal reduction technique to approximate the state vectors at unmeasured degrees of freedom using the known mass and stiffness matrices.

Frequency Domain Methods. One can transfer the equation of motion, Eqn. (7.50), into the frequency domain using Fourier or Laplace transformation and assuming the initial displacements and velocities are zero. For example, using the Laplace transform we have

$$[s^2M + sC + K]\tilde{u}(s) = \tilde{f}(s) \tag{7.62}$$

where $\tilde{u}(s)$ and $\tilde{f}(s)$ are the Laplace transform of the history of displacements $u(t)$ and history of excitation $f(t)$, respectively. Equation (7.62) can be inverted to yield

$$\tilde{u}(s) = H(s)\tilde{f}(s) \tag{7.63}$$

where $H(s)$ is called the frequency response function or transfer function. The inverse of the frequency response function is known as dynamic stiffness matrix or impedance matrix. In the frequency domain, the equations of motion look exactly like the static parameter estimation problem. The main difficulty lies in computing the Laplace transform of the excitation and response functions.

Caravani and Thomson (1974) formulated a method to determine members of a symmetric viscous damping matrix from frequency responses. They assumed the mass and stiffness matrices were known. Their algorithm was a recursive output error approach, wherein they processed one frequency point at a time in an effort to improve the estimated damping matrix. For the most recent frequency point they estimated the damping matrix. Then, using the updated damping matrix they computed frequency responses for all the previous frequency points and again estimated the damping matrix. This algorithm required the complete and noise free

frequency responses over some frequency range and assumed that the load vector was a known function of frequency.

Fritzen (1986) presented an iterative algorithm using both least squares and instrumental variable methods to compute members of the structural matrices. His method required displacements or frequency response function. He used an equation error function rather than an output error function because it is linear with respect to the members of the structural matrices. He considered only the elements that are linear with respect to their constitutive parameters. He assumed the complete frequency response function was available and used the method of Young (1970) to build an instrumental variable function. Young had suggested using the undisturbed output signals of the system which are unknown but can be approximated using an auxiliary model.

Wang (1988) combined a weighted frequency response function with the instrumental variable method or least squares method to identify the structural matrices. The developed method tried to estimate the members of the structural matrices such that the error between the theoretical and measured frequency response functions $\boldsymbol{H}(s)$ was minimal. He discussed a procedure for finding a relatively small number of data points from the frequency response function such that the accuracy of the estimates increased and computational cost and measurement time decreased. This method required a complete frequency response function. He concluded that using more data points increases the accuracy of estimates and the instrumental variable method computes more accurate quantities than least squares method.

Hoff (1989) proposed a model-updating method in conjunction with a model-order-reduction technique. He concluded that, to simulate the lower spectrum frequencies of a structure, a model with a large number of degrees of freedom is usually required. He introduced a transformation matrix built by computed lower eigenvectors of the undamped initial analytical model. Then, he reduce the order of the initial model by orthogonal similarity transformations of all structural matrices and input output vectors using the introduced transformation matrix. This technique was sensitive to the number of modes and the selection of modes used to construct the transformation matrix. The computed natural frequencies from the reduced-order model were sensitive to the transformation matrix. He divided each structural matrix into two submatrices: a submatrix that remained constant and a submatrices that was modified during the identification process. He defined the modified submatrix as a linear combination of some known matrices and computed the coefficients of these series using a weighted least squares method. He applied the developed algorithm for two cases: modal data and frequency domain data. When modal data were available, he used an input error approach and complete mode shapes. For incomplete mode shapes, he completed them using the members of the computed eigenvectors of the large initial model. For damped free vibration data he assumed a Rayleigh damping. When transient dynamic response was available, he transferred the data to frequency domain and considered both the input error and output error approaches. The developed method required lower eigenpairs of the undamped model and computed modified members for the structural matrices. The modified terms were very sensitive to the selected frequency band.

Foster and Mottershead (1990) estimated members of the structural matrices using frequency domain data and least squares and singular value decomposition techniques. They assumed that the initial finite element

model would be modified by a minimum amount. Further, they used static condensation to reduce the order of the model which caused serious errors into the modified finite element model and limited the application of the method. They had some problems with modifying the damping matrix and with the dimension of the structure.

Jiang, *et al.* (1990) proposed a frequency domain technique for estimating natural frequencies and damping ratios of large, complex structures subject to multiple steady sinusoidal excitation. The method used results from a conventional ground vibration test and resolved some drawbacks of the testing requirements.

7.10. Chapter Summary

We have studied the problem of parameter estimation using forced, transient, damped response of a real structure. We have developed an equation error estimator using either measured displacements or accelerations in the time. We have assumed that the geometry and topology of the model are known and have used the history of applied loads, and nodal responses at some degrees of freedom of the model.

For the proposed parameter estimation algorithm, we first compute the unmeasured state vectors at the locations of the measured degrees of freedom using a numerical differentiation method if displacements have been measured or a numerical integration method if accelerations have been measured. Then, we compute all the state vectors at the locations of the unmeasured degrees of freedom using a finite difference method. Next, we estimate the unknown constitutive parameters by solving a constrained nonlinear optimization problem. We advocate the use of the recursive quadratic programming method (RQP) to solve the optimization problems. The proposed estimator can accommodate response sampled incompletely in time, state, and space. It has robust convergence, and is amenable to identification of complex structural systems.

We have briefly explained a procedure for generating initial values of the unknown variables and a scaling strategy. The concepts of estimation time step and time windows have also been discussed.

As a special case of the transient, dynamic estimator, we have shown that this estimator can accept modal information and estimate mass and stiffness parameters of a model. We have derived the necessary equations and have also explained the way that the input should be provided.

CHAPTER EIGHT

Numerical Simulation Studies: Transient Dynamic Case

In this chapter we examine the performance of the transient dynamic estimator through a simulation study. The subject structure is the 49 element planar bridge truss shown in Fig. 8.1. We examine the behavior of the estimator with respect to noise, the location of the window, the size of the window, the size of the time step, and the number of measured degrees of freedom. In addition to our study of the effects of the physical character of the data, we study the effects of different starting values of the unknown parameters used to initiate the iteration. We investigate our parameter estimation algorithm for two cases: *(1)* when a history of displacements at some degrees of freedom is available and *(2)* when a history of accelerations at some degrees of freedom is available.

The present work focuses on the behavior of the proposed estimator in the face of noisy data. All of the simulations use noisy data. We use the simulation environment introduced in Section 2.6 to control the statistical properties of the noise in the measurements and to determine the statistical properties of the estimations.

The geometry, topology, and element numbering of the bridge truss are shown in Fig. 8.1 and in the rest of this chapter we refer to this finite element model as the real structure. This structure represents a truss of a highway bridge designed to carry a moving load of 0.8 *kpf* including impact and a uniform dead load of 2.0 *kpf*. It has 26 nodes and consists of 49 elements with four different cross sectional areas. Table 8.1 lists element numbers, type, actual mass density, and actual cross sectional area of each group of elements.

We will assume that the structure is lightly damped, and model it as consistent viscous damping, with viscosity equal to 0.01 $(kips/(ft/sec)/ft)$. Further, we assume that the dead load of the structure is uniformly distributed along all 49 elements with a mass density equal to 0.017 $(kips/(ft/sec^2)/ft)$. All elements have Young's modulus of 432×10^4 $(kips/ft^2)$. In Table 8.2 the first three and the last natural frequencies of the structure are listed and indicate that the structure is relatively stiff.

The axial stiffnesses, mass densities, and damping parameters of the elements can be taken as the unknown parameters in the simulation study. Since the program is capable of grouping the elements with the

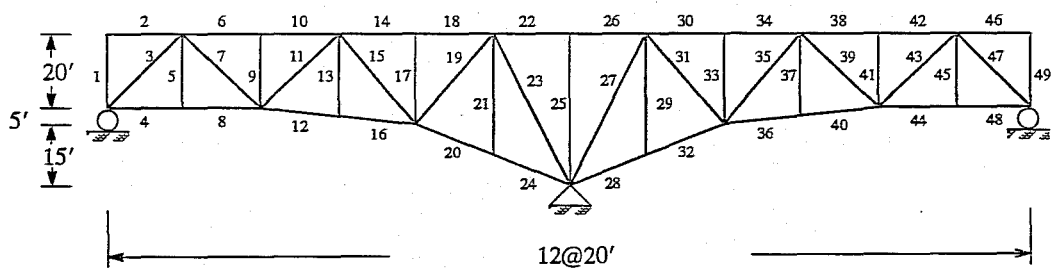

Fig. 8.1 Schematic representation of the bridge truss

Table 8.1. Nominal properties of the bridge truss

Element Group	Element Number	Element Type	Mass $lb/(fl/sec^2)/ft$	Area (in^2)
1	1–5, 45–49	W21 x 83	2.58	24.3
2	6–13, 37–44	W21 x 93	2.90	27.3
3	14–21, 29–36	W24 x 104	3.23	30.6
4	22–28	W24 x 146	4.54	43.0

same properties, the number of unknown stiffness parameters can be reduced to four, corresponding to the number of groups of elements. We shall assume that all of the elements have the same mass densities and damping. Thus, we have one group for the mass densities and one group for the damping parameters. The total number of constitutive parameters of the finite element model of the structure is six, including four stiffness parameters, one mass parameter, and one damping parameter. The program can estimate all the constitutive parameters. But since the value of mass and damping parameters are very small, noise in measurements might swamp the estimation of these parameters and mask the behavior of the estimator. So, for this simulation study we assume the mass density and viscosity are known and investigate the behavior of the estimator from the estimation of the stiffness parameters.

We use Monte Carlo simulation to investigate the statistical behavior of the estimator. Monte Carlo simulation is based on the generation of a sample of responses from which we estimate the statistical properties of the output parameters. For each random incarnation of noise which is added to the computed response the estimator processes the given information and solves a nonlinear constrained optimization problem to compute the unknown parameters. The ensemble of these estimates constitutes the Monte Carlo sample.

8.1. Simulated Response

To simulate field measurements, we add different noise vectors to the output of the finite element model of the structure under the dynamic loads. The noise vector is either absolute or proportional and is added to either displacements or accelerations, depending on which of these we assume to be measured (see Section 2.6). The simulated field measurements are given as the input to the estimator.

We will simulate a dynamic loading of the structure and measure its response. The load set consists of five dynamic loads with sinusoidal variations, simultaneously applied at five nodes of the structure shown

Table 8.2. Natural frequencies and period of vibration of the bridge truss

Mode Number	Natural frequency (rad/sec)	Period (sec)
1	22.00	0.29
2	41.23	0.15
3	55.70	0.11
48	707.99	0.01

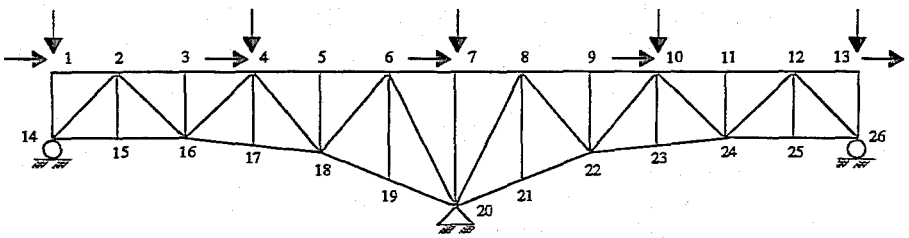

Fig. 8.2 Schematic representation of the dynamic loads

in Fig. 8.2. The duration of each test will exceed one second. Each load has amplitude of 200 (*kips*) and frequency of 20 (*rad/sec*) which is close to the first natural frequency of the structure. The magnitude of nodal loads are chosen such that the maximum nodal displacement is less than 5.0 inches. In the rest of this chapter we use either the first second of the measured displacements or the first 0.15 seconds of the measured accelerations to estimate the unknown parameters and study the statistical behavior of the proposed estimator.

As mentioned in Chapter Seven, we use the Newmark method to solve the model equation. For this class of direct integration methods, the time step ΔT should satisfy the relationship $\Delta T \leq 2/\omega_{\max}$, where $\omega_{\max}$ is the largest natural frequency of the structure. If this relation holds, the direct solution is guaranteed to be stable. By decreasing the time step the analytical solution converges to the actual solution of the governing equation. From Table 8.2, the largest natural frequency for this structure is about 708 (*rad/sec*) therefore, the time step should be less than 0.003 seconds to satisfy the stability condition. To reduce the numerical errors for the problem at hand, ΔT is taken to be 0.001 seconds.

To illustrate the analytical behavior of the structure under applied loads, the vertical responses of node 16 are plotted in Fig. 8.3. The small disturbances observable in the accelerations are due to the effects of higher modes. In the following four figures, the noisy measured response and the discrete equivalent forms of all the state vectors are plotted. If the displacements are measured at a certain degrees of freedom, the discrete displacements, velocities and accelerations at these measured degrees of freedom are approximately computed using the Newmark method with $\gamma = 1/2$ and $\beta = 1/4$, (Eqns. (7.10), (7.11), and (7.12)). When a history of accelerations at some degrees of freedom are measured, discrete state vectors are computed by the trapezoidal rule (Eqns. (7.3) and (7.6)).

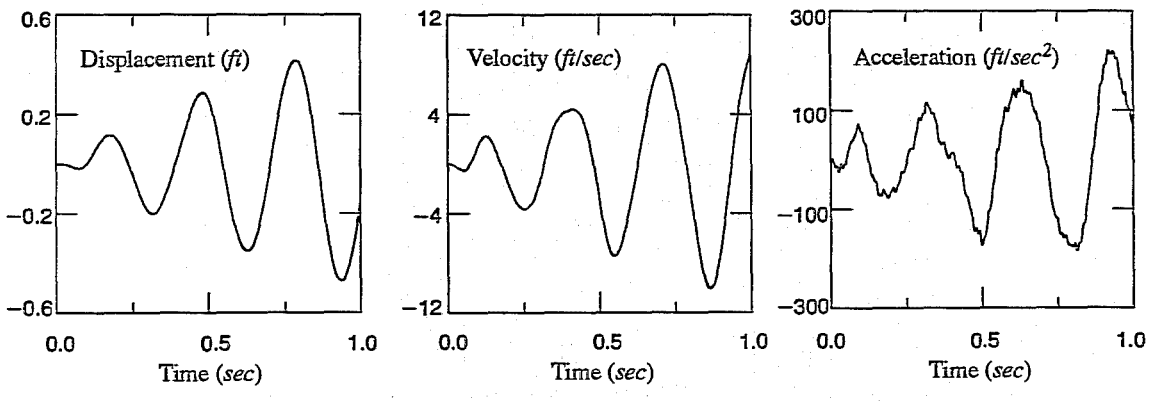

Fig. 8.3 Analytical responses of the structure at node 16

Figure 8.4 shows the noisy vertical displacement of node 16 and discrete state vectors, computed by Eqns. (7.10), (7.11), and (7.12), for amplitudes of 0.0024 inches and 0.024 inches. The same plots are presented for proportional noise in Fig. 8.5 for a small noise with the amplitude of 1% and a large noise with the amplitude of 20%. As we expect, even for a small amount of noise in displacement, large disturbances develop in the discrete velocity and acceleration vectors from numerical differentiation.

The measured vertical acceleration at node 16 and its corresponding discrete state vectors for a small absolute noise with the amplitude of 24 (in/sec^2) and a large absolute noise with the amplitude of 180 (in/sec^2) are shown in Fig. 8.6. The same plots for a small proportional noise of 2% and a large proportional noise of 20% are presented in Fig. 8.7. One can notice that by using numerical integration, the effect of noise in discrete velocity and displacement vectors is reduced.

8.2. Estimation Time Step

The estimator requires measured response at discrete time points. One must provide information about the response of the structure at a finite number of time points equally spaced from each other. Finding an appropriate time step Δt is crucial for the reliability of the estimations (see Section 7.6). One can study the measured responses of the structure to choose an appropriate estimation time step. For the problem at hand, when we have a history of displacements, we choose Δt equal to 0.01 seconds (see Figs. 8.4 and 8.5). When we use measured accelerations, the estimation time step should be very small to grasp all the information contained in the recorded response (see Figs. 8.6 and 8.7). We choose Δt equal to 0.0001 seconds. The effect of the size of the time step on the estimated parameters will be discussed later in this chapter.

8.3. Location of the Time Window and the Effect of the Sample Size

We have observed that the estimator is quite sensitive to the location of the window, especially for large amplitudes of noise. To overcome this problem we use a sample of windows which can be located specifically or randomly along the history of the measured response instead of using one window to estimate the parameters. We increase the number of windows until the statistical indices become steady. Then, we compute the average of estimates from all the windows and consider the vector of average parameters as the estimated parameters.

The reliability of the statistical behavior of the estimator also depends on the sample size (number of trials). In order to establish statistical significance of the estimates, the sample size should be sufficiently large. Increasing the size of the sample demands more computation, so a compromise between the accuracy of the estimates and computational efficiency determines a lower bound for the sample size. A sufficient sample size is one for which the statistical indices of the sample of estimated parameters do not change by increasing the number of trials.

To establish how many trials and time windows are sufficient, one must consider plots like those shown in Figs. 8.8 and 8.9 for different amplitudes of noise. In Fig. 8.8, for example, the variations of the root quadratic bias *RQB* and standard deviation *SD* of the estimated parameters from complete displacement measurements and a small absolute noise of 0.0024 inches and a large absolute noise of 0.024 inches versus number

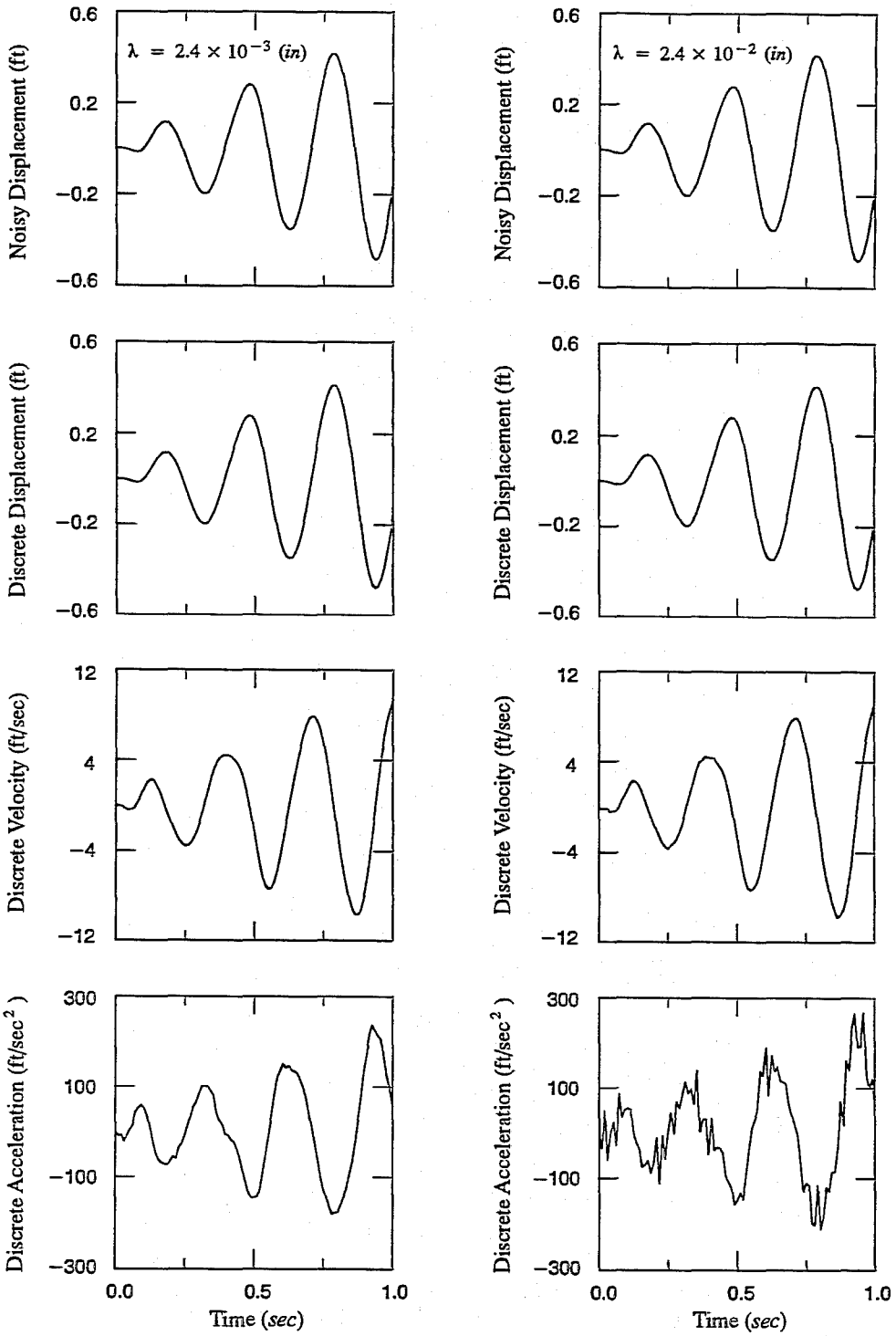

Fig. 8.4 Absolute noise: Measured vertical displacement and computed discrete states vectors at node 16

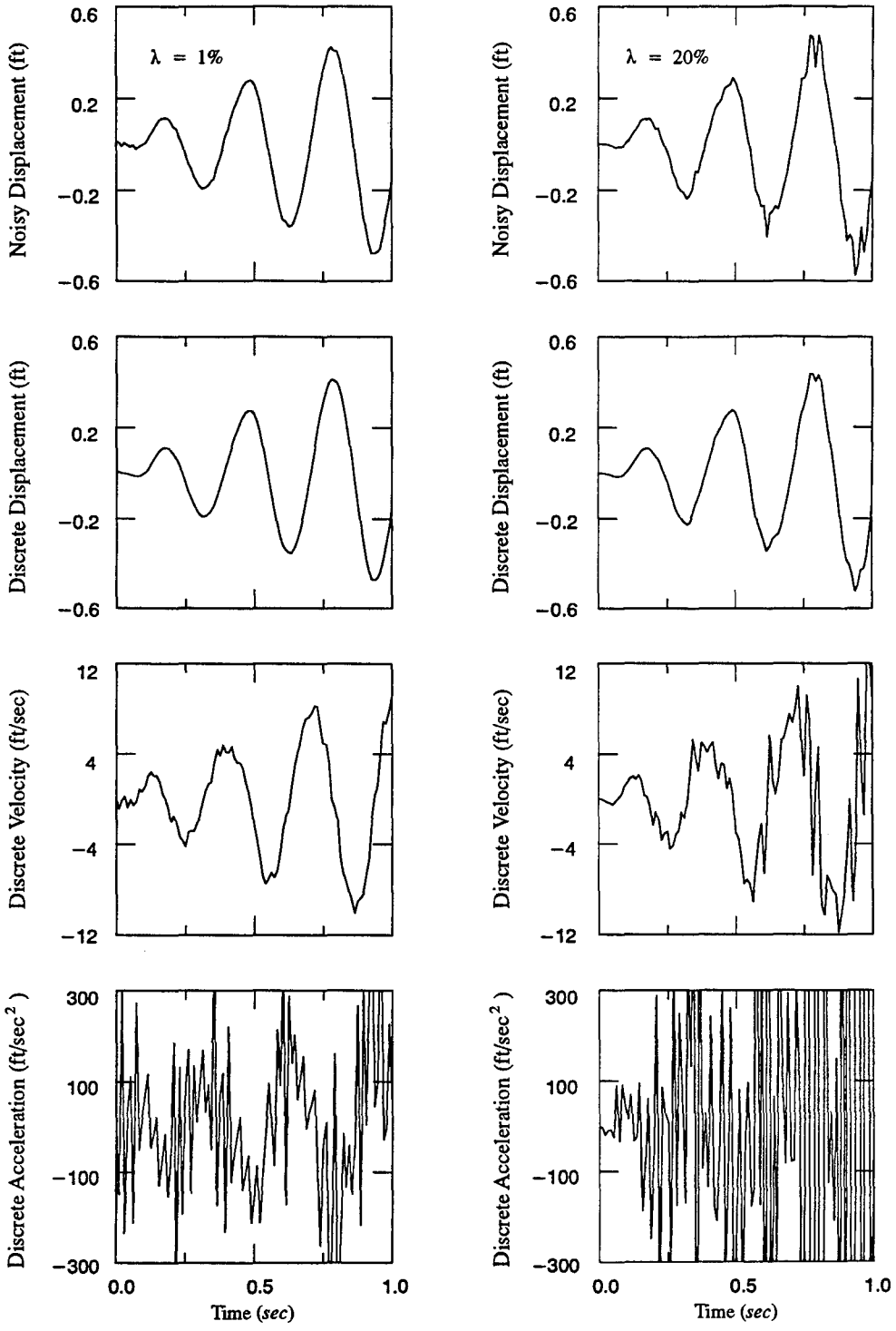

Fig. 8.5 Proportional noise: Measured vertical displacement and computed discrete state vectors at node 16

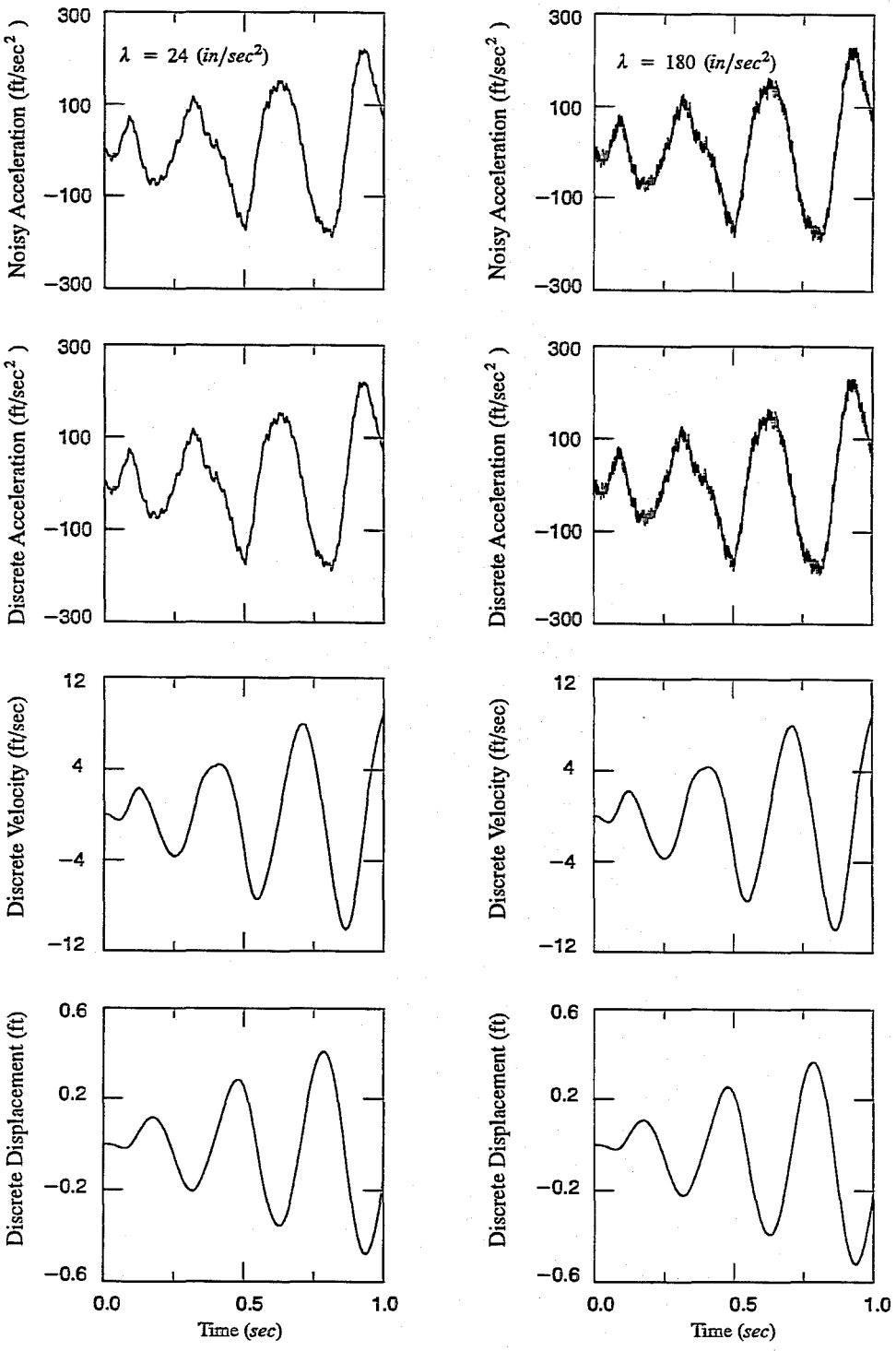

Fig. 8.6 Absolute noise: Measured vertical acceleration and computed discrete state vectors at node 16

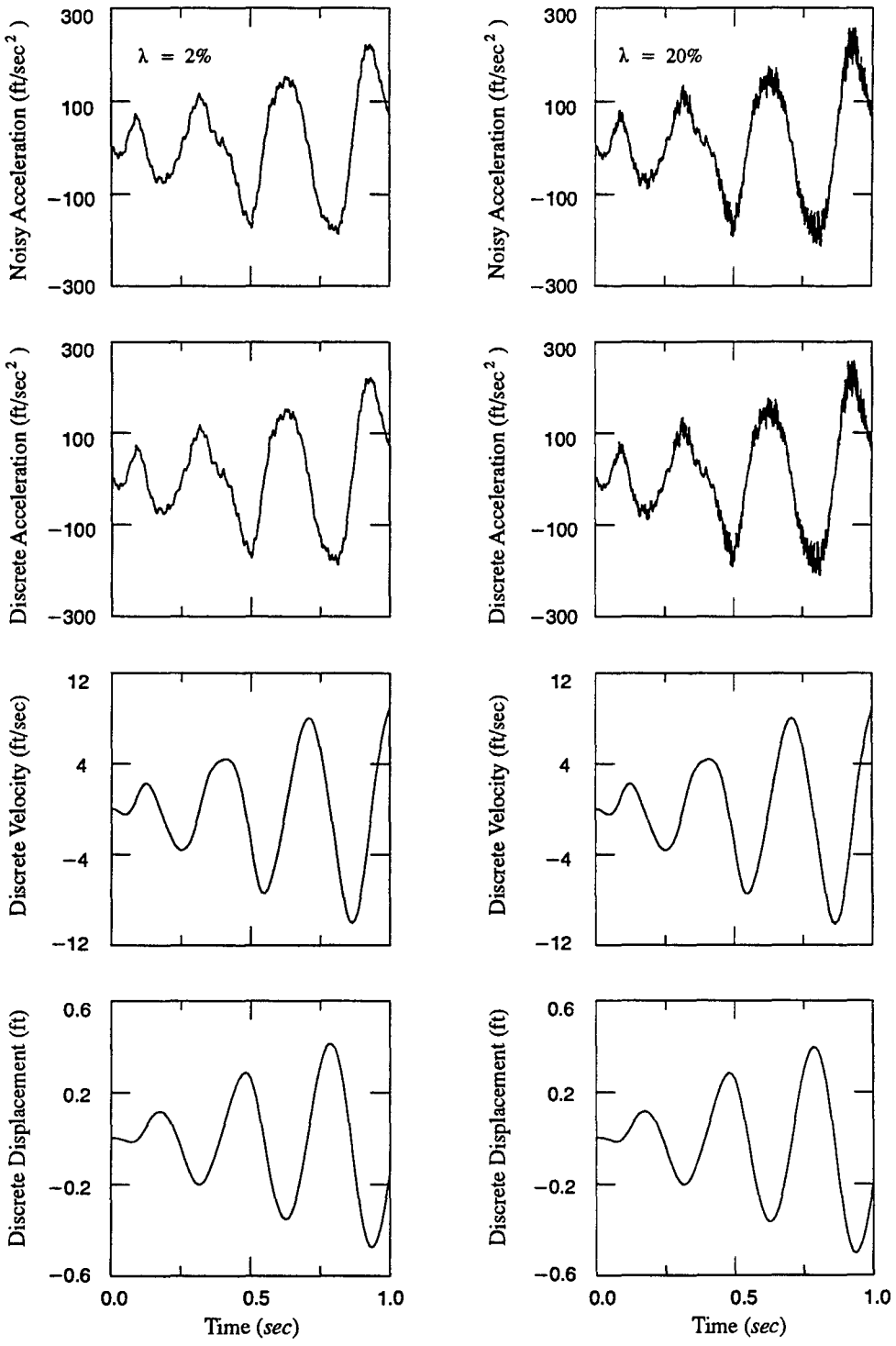

Fig. 8.7 Proportional noise: Measured vertical acceleration and computed discrete state vectors at node 16

of trials and number of time windows are plotted. The time windows are randomly located along the history of the response. As one increases the number of windows, the statistical indices become steady, leveling off at about 15 time windows. When the number of windows is small, the statistical indices are sensitive to the number of trials. When one uses more than 15 time windows the estimator is insensitive to the number of trials as well as to the location of the window.

Figure 8.9 shows variations of the root quadratic bias and standard deviation versus the number of time windows and number of trials when the acceleration vector is completely measured for a small noise amplitude of 24 (in/sec^2) and a large noise amplitude of 360 (in/sec^2). The time windows are randomly located along the history of the response. One can observe that the number of time windows influences the statistical indices. The estimator becomes steady at about 10 windows. Increasing the number of trials does not significantly change the root quadratic bias and standard deviation, even for a small number of windows. In general, based on Figs. 8.8 and 8.9 one can observe that the estimator is insensitive to the location of the window and number of trials if a sufficient number of windows are considered.

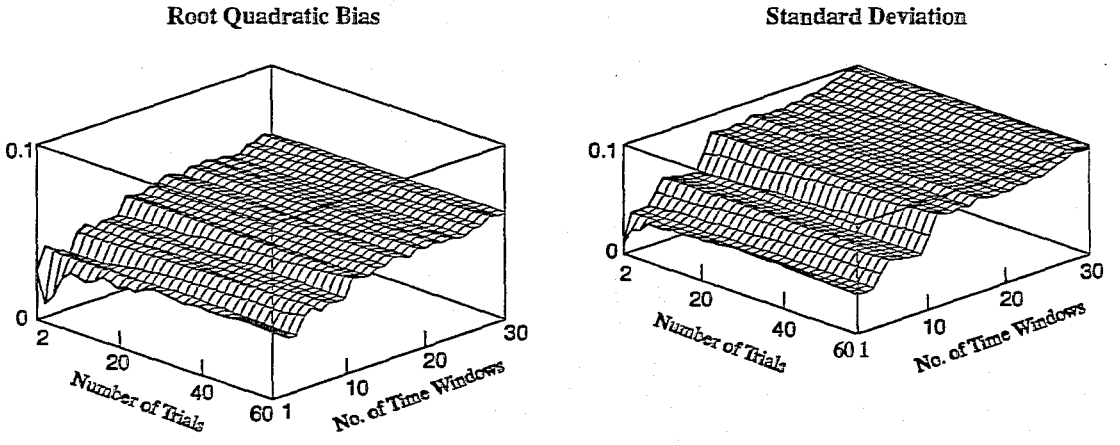

(*a*) A small amount of noise $\lambda = 2.4 \times 10^{-3}$ (in)

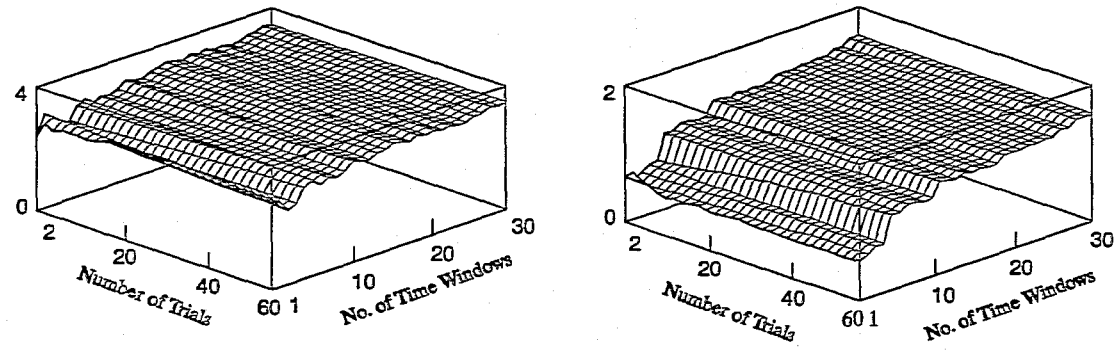

(*b*) A large amount of noise $\lambda = 2.4 \times 10^{-2}$ (in)

Fig. 8.8 Variations of the *RQB* and *SD* versus number of trials and number of time windows for a small and a large absolute noise in measured displacements

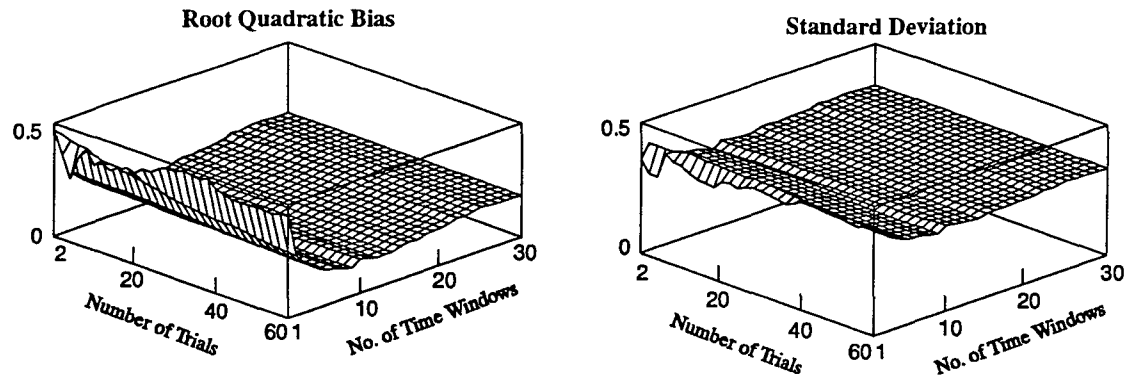

(*a*) A small amount of noise $\lambda = 24\ (in/sec^2)$

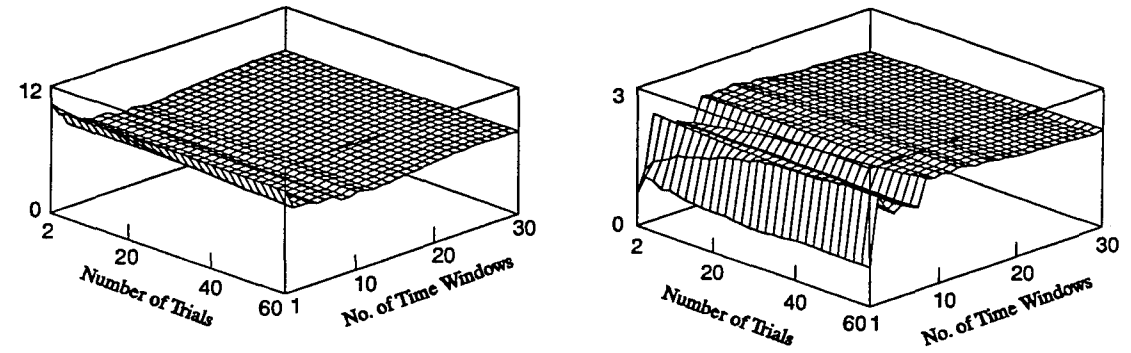

(*b*) A large amount of noise $\lambda = 360\ (in/sec^2)$

Fig. 8.9 Variations of the *RQB* and *SD* versus number of trials and number of time windows for a small and a large absolute noise in measured accelerations

8.4. Effect of the Estimation Time Step

The developed estimator solves a parameter estimation problem based on the dynamic response recorded at discrete time points equally spaced by ΔT. The quality of information provided for the estimator is controlled largely by the estimation time step Δt. In the rest of this chapter when we refer to the time step we mean the estimation time step. If the time step is too short, the data at adjacent time points are very similar and hence contain little new information about the system. On the other hand, for large time steps, numerical errors in differentiation and integration of the response for computing the discrete state vectors grow and swamp the output of the estimator. Understanding the influence of the time step on the quality of the estimates is crucial. One must find an appropriate time step that compromises between numerical errors and estimation errors. We have provided an option in the identification algorithm, called *JUMP*, that faciliates the search for an appropriate time step.

Figures 8.10 to 8.12 show variations of the root quadratic bias and standard deviation with respect to the time step for different number of windows. These figures show the statistical indices computed for random selection of windows with five time points and 20 trials per window. For a noise free history of complete

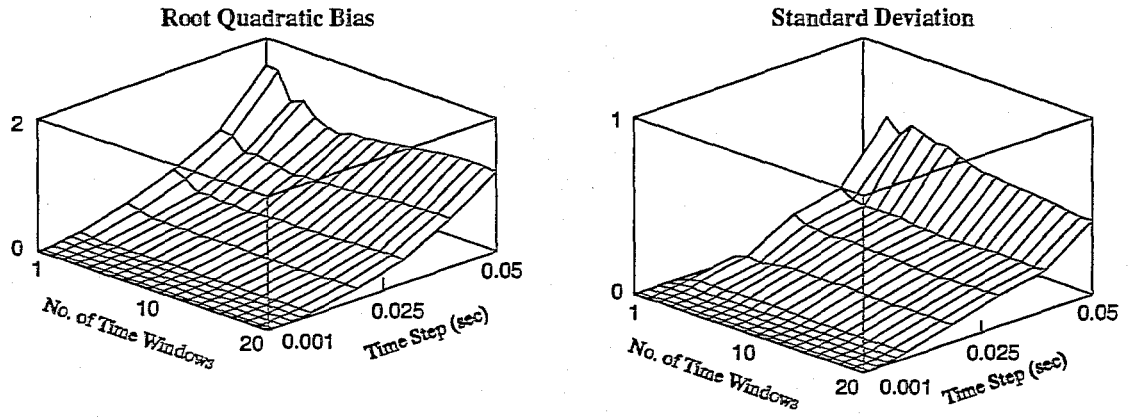

Fig. 8.10 Variations of the *RQB* and *SD* with respect to the time step and number of windows for noise free displacements

displacements, one might expect the estimator to be unbiased. However, one can observe in Fig. 8.10 that, by increasing the time step, the root quadratic bias and standard deviation increase. We attribute this behavior to errors caused by numerical differentiation. The variations of the statistical indices for noisy, complete measured displacements against the time step for a relatively small noise of 0.0024 inches and a relatively large noise of 0.012 inches are presented in Figs. 8.11 and 8.12. For time steps less than 0.003 seconds, numerical

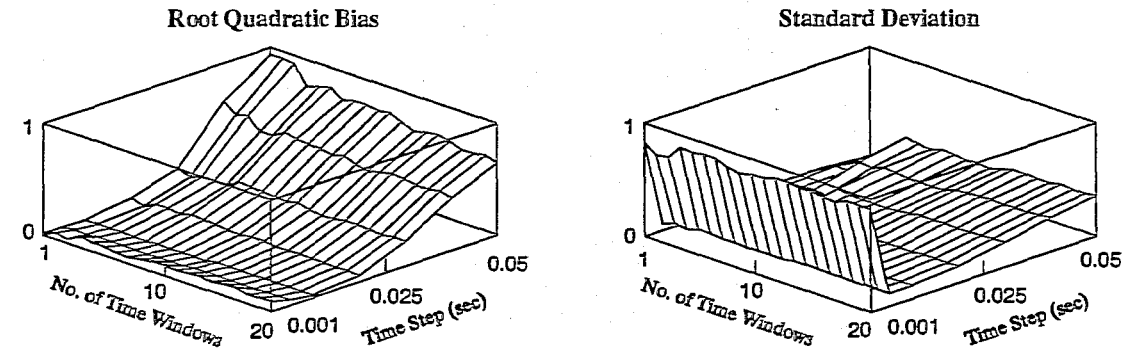

(*a*) A small amount of noise $\lambda = 2.4 \times 10^{-3}$ (*in*)

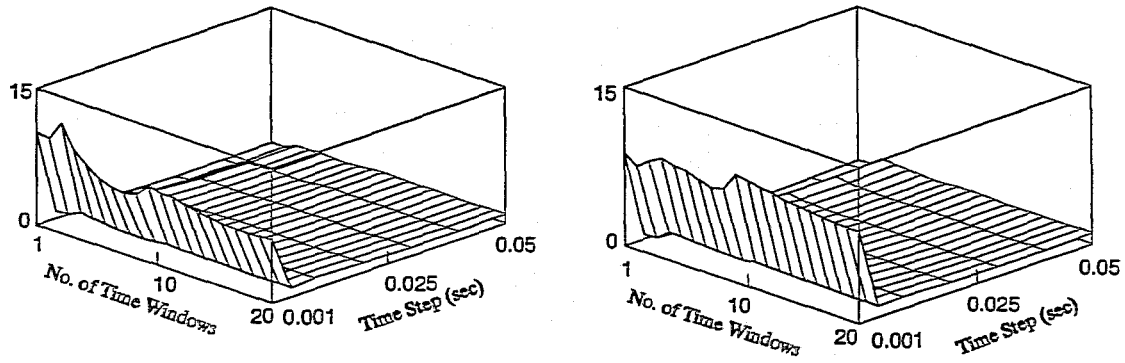

(*b*) A large amount of noise $\lambda = 1.2 \times 10^{-2}$ (*in*)

Fig. 8.11 Variations of the *RQB* and *SD* with respect to the time step and number of windows for a small and a large absolute noise in measured displacements

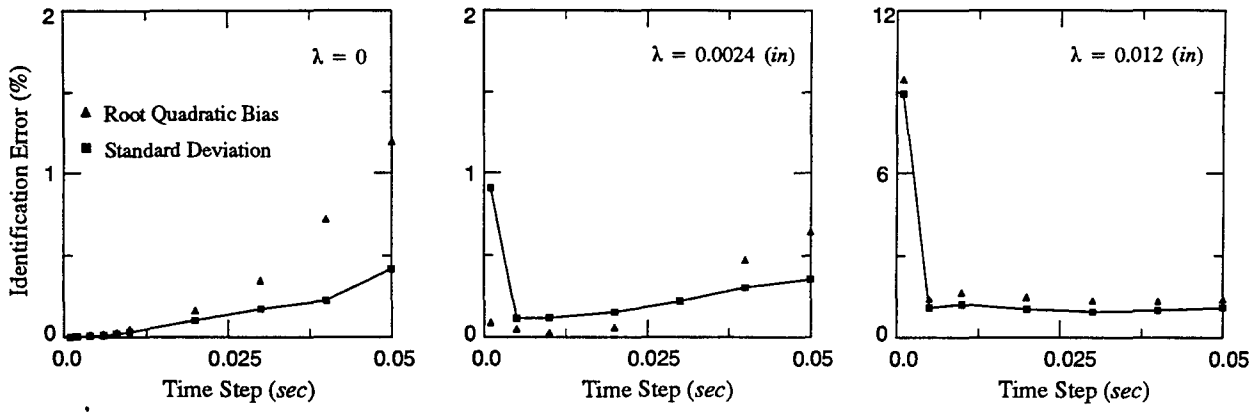

Fig. 8.12 Variations of the *RQB* and *SD* with respect to the time step for complete measured displacements after considering 20 windows

differentiation errors are small, but estimation errors influence the behavior of the algorithm and increase the root quadratic bias and standard deviation. As the time step increases, the estimation errors decrease and numerical errors take over, increasing the statistical indices for small amplitudes of noise but do not significantly changing them for large amplitudes of noise. Figure 8.12 shows the variations of the statistical indices with respect to the time step for noise free and noisy measured displacements after considering 20 time windows and suggests that the optimal time step for this simulation study is about 0.01 seconds.

Figures 8.13 to 8.15 show variations of the statistical indices with respect to the time step and different number of windows for complete measured accelerations. These figures show the statistical indices computed for random selection of windows with five time points and 20 trials per window. For noise free measurements, increasing the time step does not affect the estimation errors (they remain at zero) but it does amplify the numerical integration errors, increasing the root quadratic bias, as shown in Fig. 8.13. The rate of change of the root quadratic bias is smaller for time steps less than 0.001 seconds than it is for time steps larger than 0.001 seconds. To investigate the effect of the time step on the behavior of the estimator for noisy data, two amplitudes of noise are considered: a small noise with the amplitude of 24 (in/sec^2) and a large noise with the amplitude of 180 (in/sec^2). As shown in Figs. 8.14 and 8.15, as the time step increases, the statistical

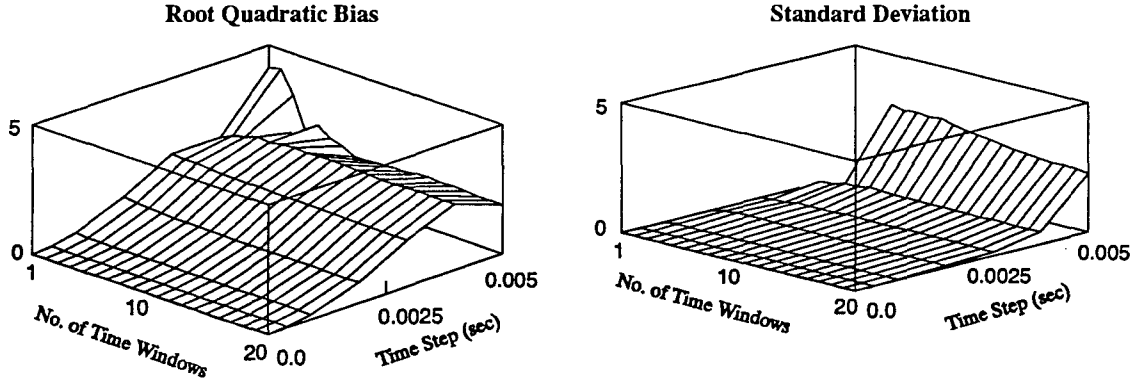

Fig. 8.13 Variations of the *RQB* and *SD* with respect to the time step and number of windows for noise free acceleration

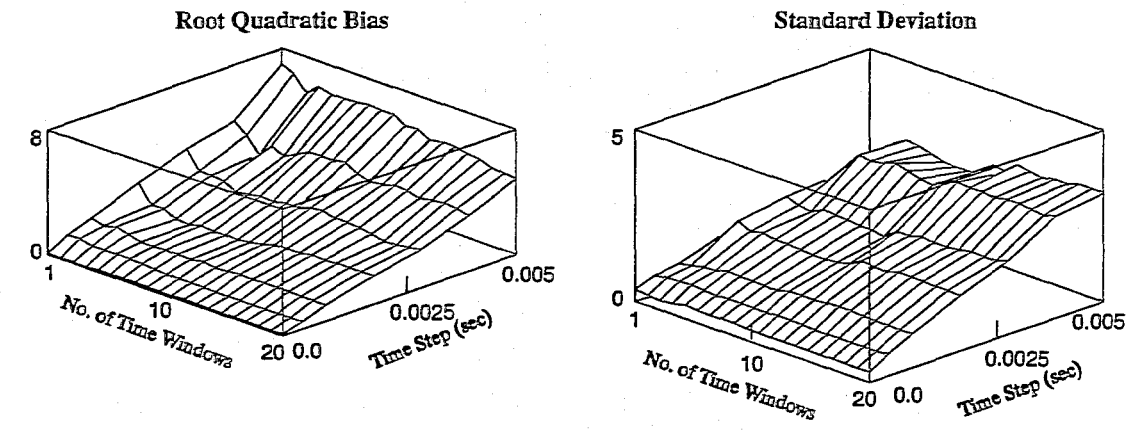

(*a*) A small amount of noise $\lambda = 24\ (in/sec^2)$

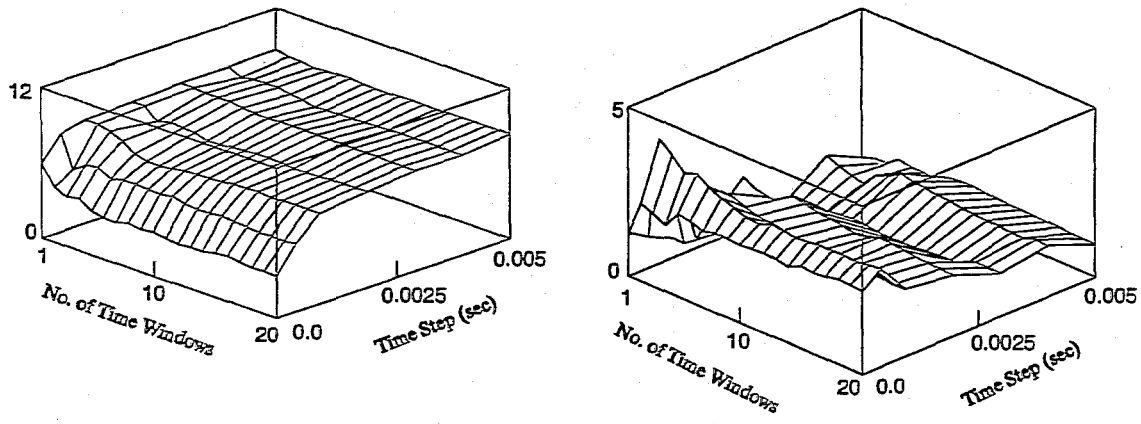

(*b*) A large amount of noise $\lambda = 180\ (in/sec^2)$

Fig. 8.14 Variations of the *RQB* and *SD* with respect to the time step and number of windows for a small and a large absolute noise in measured accelerations

indices increase and then level off. The statistical indices level off earlier for large amplitudes of noise than for small amplitudes. Figure 8.15 shows that, for a large amplitude of noise, numerical errors reach their maximum values for a time step of about 0.001 seconds and the statistical indices do not change significantly for

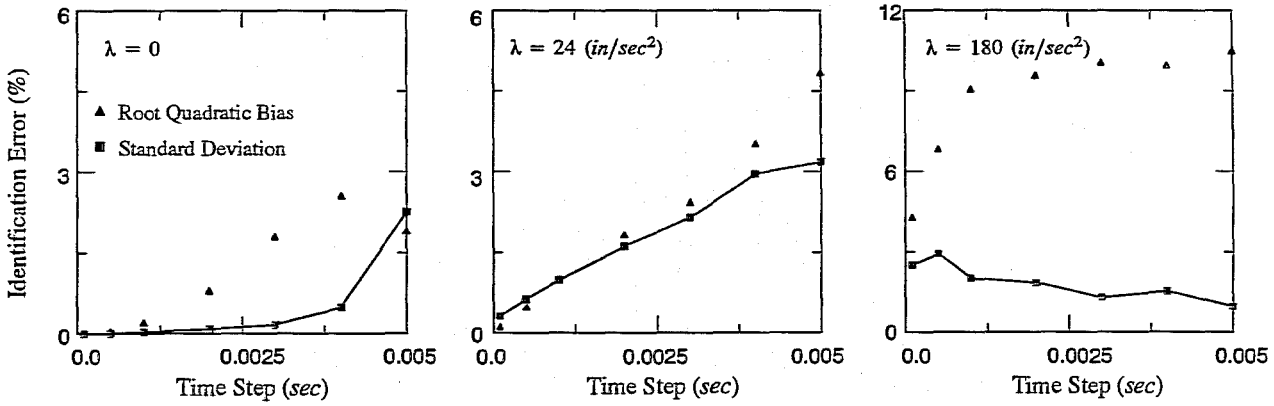

Fig. 8.15 Variations of the *RQB* and *SD* with respect to the time step for complete measured accelerations after considering 20 time windows

time steps larger than 0.001 seconds. For small amplitudes of noise, numerical errors saturate for a time step larger than 0.005 seconds. Figure 8.15 shows the variations of the root quadratic bias and standard deviation with respect to the time step for complete measured accelerations after considering 20 time windows and 20 trials per window. One can observe that, the time step should be small enough to reduce the numerical errors and consequently, the bias. For this simulation study when a history of accelerations is available the optimal time step is about 0.0001 seconds. The developed estimator is more sensitive to the time step when accelerations or displacements are incompletely measured.

8.5. Initial Values for the Unknown Parameters

The developed estimator converges to the feasible local minimum nearest to the location of the starting point. The bounding constraints ensure the feasibility of the solution, but to which local minimum the estimator converges depends on the distribution of the local minima of the loss function and the starting point of the minimization search. The proposed constraints significantly decrease the sensitivity of the estimator to the initial values of the unknown parameters and increase the reliability of the estimator. Again, we use the closeness index, Eqn. (4.1), to investigate the sensitivity of the estimator with respect to feasible initial values for the unknown parameters.

Figure 8.16 compares the behavior of the estimator using measured displacements with its behavior using measured accelerations with respect to the closeness index for absolute noise of amplitude λ. The average root quadratic bias *RQB* and standard deviation *SD* are computed for the estimates based on noisy, completely measured displacements or accelerations from one window which contains three time points with the first time point at 0.03 seconds and for 20 different trials. Both estimates based on displacements and those based on acceleration have constant root quadratic bias and standard deviation for different starting points with closeness indices between zero and one. From this typical experiment and many other ones in this simulation study, one can observe that the estimator is not sensitive to the initial values of the unknown parameters regardless the type of measured response if measurements are spatially complete.

The proposed estimation algorithm becomes more sensitive to the starting point as the amount of information decreases. The closeness of a starting point in the space of unknown variables $(\boldsymbol{x}, \overline{\boldsymbol{u}})$ for the pro-

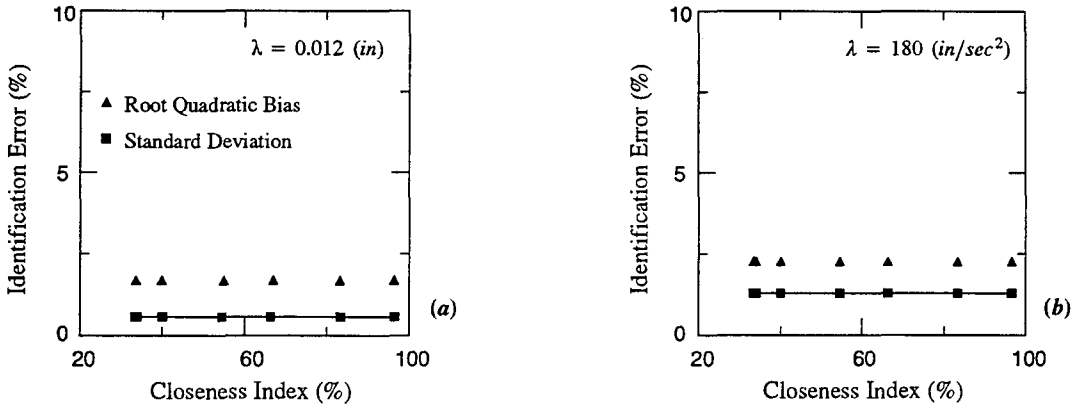

Fig. 8.16 Variations of the *RQB* and *SD* versus closeness index for complete measurements (*a*) Displacement, (*b*) Acceleration

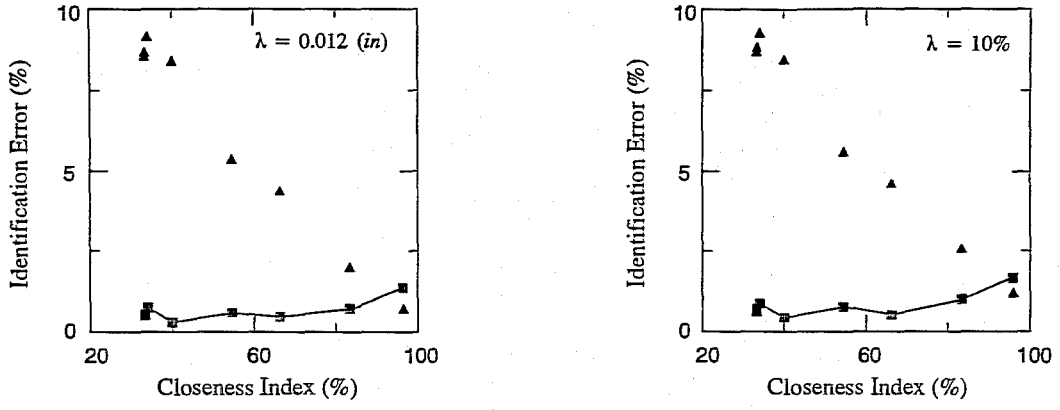

Fig. 8.17 Variations of the *RQB* and *SD* versus closeness index for incomplete measured displacements

posed estimator depends on the initial values of the parameters. The initial values of the unmeasured deformations $\bar{u}$ are computed based on the initial values for the unknown parameters. Figure 8.17 shows variations of the root quadratic bias and standard deviation with respect to closeness index for absolute and proportional noise with the amplitudes λ when displacements at 28 degrees of freedom are measured. As the initial values of the unknown parameters come closer to the actual values of the parameters, the root quadratic bias decreases and converges to a small value and the standard deviation slowly increases but remains smaller than the root quadratic bias. When the starting point is very close to the actual point, the root quadratic bias and standard deviation are both small and *RQB* value is smaller than *SD* value. The same trend can be observed for proportional noise.

The variations of the root quadratic bias and standard deviation with respect to the closeness index for estimates from measured accelerations at 28 degrees of freedom are shown in Fig. 8.18. The trend is the same as shown in Fig. 8.17. By increasing the closeness index the *RQB* value decreases and the *SD* value slightly increases. The estimator behaves in this manner, because by increasing the closeness index the distance between the starting point and the actual point decreases and the possibility to converge to the other local minima decreases. When initial values are close to the actual values of the parameters, the root quadratic bias and

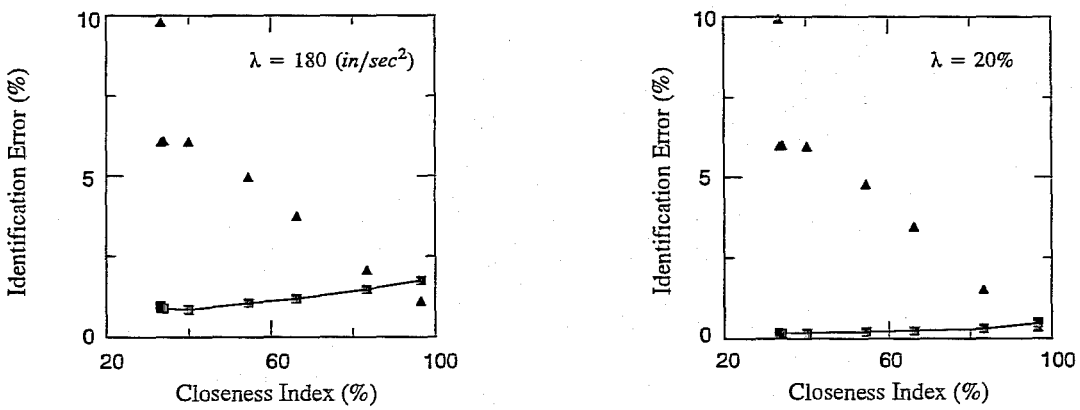

Fig. 8.18 Variations of the *RQB* and *SD* versus closeness index for incomplete measured accelerations

standard deviation are both small and the *SD* value is larger than than the *RQB* value which is a desirable feature, (see Section 4.2). Figures 8.17 and 8.18 are developed for relatively large amplitudes of noise. For small amplitudes of noise the behavior of the estimator follows the same trend observed for large amplitudes of noise except the *RQB* remains smaller than *SD* even for starting points far from the actual point regardless the type of measured response.

8.6. Effect of Quality of Information

One of the most important features of an estimator is the way it behaves in the presence of noise. One would expect that by increasing the noise, the accuracy of the estimated parameters for a fixed amount of information would decrease. Figures 8.19 and 8.20 compare the behavior of the proposed estimator for absolute and proportional noise in the measured response. The average root quadratic bias *RQB*, standard deviation *SD*, root mean square error *RMS*, and identification error *AIE* are plotted against the amplitude of noise. The estimates of axial stiffnesses are computed based on noisy, complete measurements for 20 trials and 30 time windows randomly picked from a one second history of displacements or 0.15 seconds of accelerations. The estimator behaves in a similar manner for absolute and proportional noise regardless the type of measured response. The developed estimator is biased and its *RQB* value increases as the amplitude of noise increases. Although, the bridge truss is a linear structure with elements linear in their parameters , the bias of the estimates varies nonlinearly with noise amplitude. This nonlinear relationship indicates that the solution of the proposed parameter estimation algorithm is a nonlinear function of measurements.

From Fig. 8.19 one can observe that, for measured displacements, the root quadratic bias is smaller than the standard deviation when the amplitude of noise is less than 0.002 inches for absolute noise and 1% for proportional noise. In other words, for complete measured displacements the desirability bound λ_d, (see Section 4.2), of the estimator is about 0.002 inches for absolute noise and 1% for proportional noise. By increasing the amplitude of noise, the standard deviation increases and then becomes steady. To explain these trends, we plot values of the estimated axial stiffnesses against the amplitude of noise in Fig. 8.21. The estimates converge to small values in the neighborhood of the lower bounds of parameters as the amplitude of noise

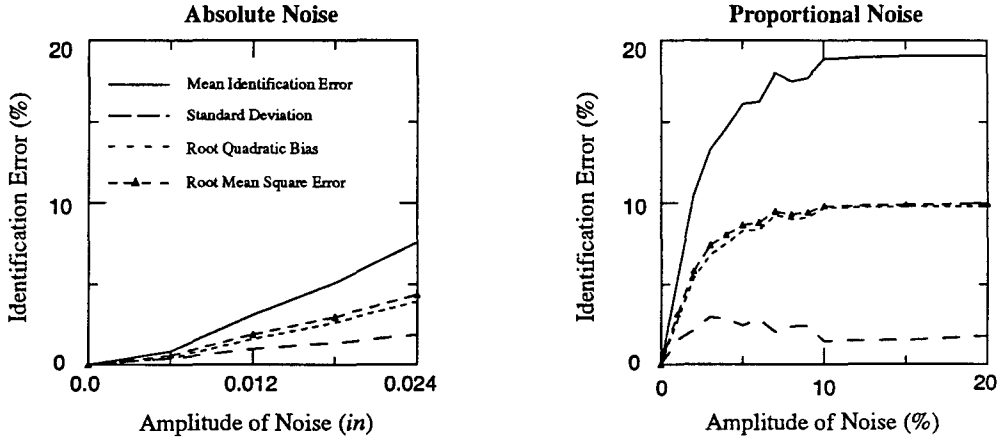

Fig. 8.19 Variations of the *RQB* and *SD* versus amplitude of noise for complete measured displacements

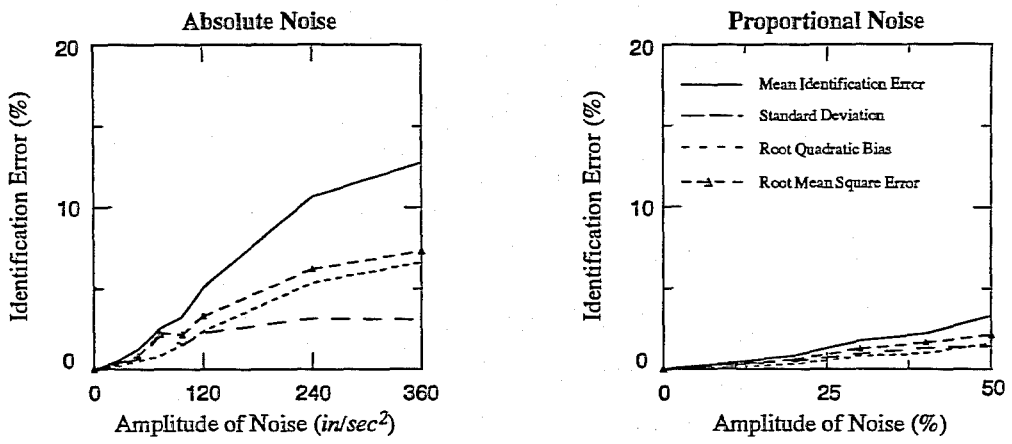

Fig. 8.20 Variations of the *RQB* and *SD* versus amplitude of noise for complete measured accelerations

increases. Based on Eqn. (2.19), when the vector of estimated parameters $\bar{x}$ converges to zero, the *RQB* value saturates near $1/n_p$ which for the bridge truss is about 25%. The scatter of the estimates is confined by the boundaries of the constraints and the standard deviation becomes small. From Eqn. (2.23), the smallness of *SD* value makes the *RMS* value follow the trend of the *RQB* value and be almost equal to it. The *AIE* value, which is a scatter index like *RMS* but based on an absolute norm, behaves in the same manner as *RMS* value behaves. The statistical indices *AIE*, *RQB*, and *RMS* of the proposed estimator based on measured displacements vary like a sigmoid function with the amplitude of noise. These statistical indices increase with a small rate as noise amplitude is small $\lambda<\lambda_d$ then rapidly increase, and finally saturate.

Figure 8.20 presents the variations of the statistical indices for the estimates computed from complete measured accelerations with respect to the amplitude of noise. The desirability bound λ_d of the estimator is about 100 (in/sec^2) for absolute noise and 45% for proportional noise. All the statistical indices vary like a sigmoid function with respect to the noise amplitude. They increase with a small rate as the amplitude of noise is small, then rapidly increase, and finally saturate. The saturation limit of *RQB*, which is 25%, occurs for a much larger amplitude of noise than what is shown in Fig. 8.20. The increment rate of the *SD* value is smaller

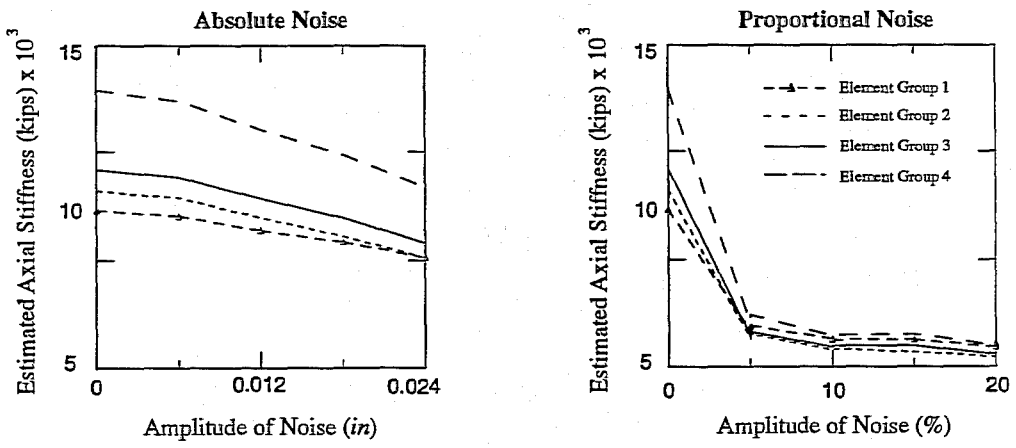

Fig. 8.21 Variations of the estimated parameters versus amplitude of noise for complete measured displacements

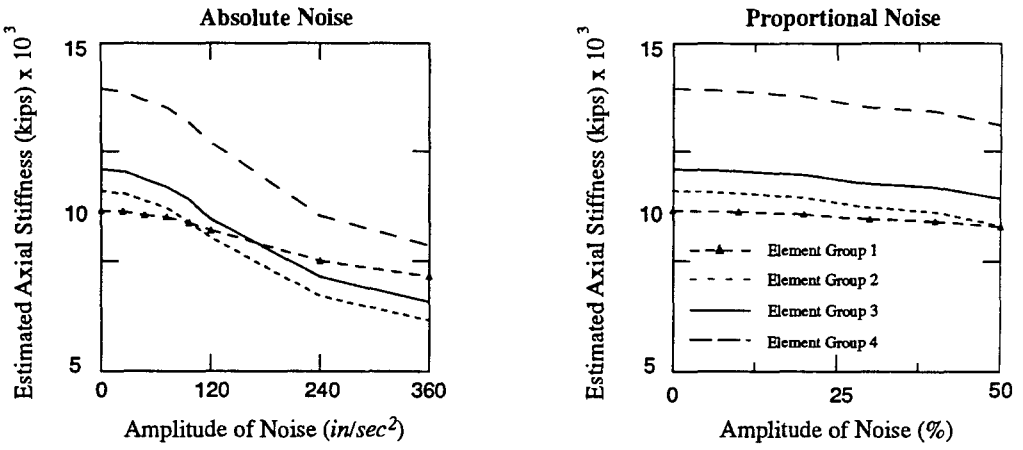

Fig. 8.22 Variations of the estimated parameters versus amplitude of noise for complete measured accelerations

than the other statistics for absolute noise. As shown in Fig. 8.20, for amplitudes of noise less than λ_d, the *RMS* and similarly *AIE* are close to the standard deviation and for large amplitudes of noise they separate and follow their own saturation paths, because the *RQB* and *SD* values become relatively large.

Figure 8.22 illustrates the variations of the estimated parameters with respect to the amplitude of noise when a history of complete accelerations is available. As the amplitude of noise increases the estimated parameters converge to regions near the lower bounds of the parameters. The rate of decrease for the axial stiffness of the elements in group 1 is smaller than the rates of decrease for the other groups. The lower limit for all parameters is zero and based on Eqn. (2.19), the root quadratic bias saturates near 25% as the noise becomes large. The value of the saturation limit of *RQB* value depends on the bounding constraints. One should anticipate this behavior, because it is an inherent characteristic of equation error estimators. The estimates based on a history of accelerations have an acceptable bias for a relatively wider range of noise than the estimates based on the measured displacements. The main reason for high biasedness of displacement-based estimates is the occurrence of numerical differentiation errors in the higher derivatives.

8.7. Effect of Quantity of Information

For the proposed estimator confidence in the estimated parameters strongly depends on the amount of information (or the number of measurements which we interchangeably use in the rest of this chapter), $ntp \times \hat{n}_d$. The identifiability criterion $ntp \times \hat{n}_d \geq n_p$ gives a lower bound for the number of measurements (or observations). In this section, we study the behavior of the proposed estimator as the number of time points, *ntp*, and the number of measured degrees of freedom, $\hat{n}_d$, increase.

Size of the window. The number of time points in a window *ntp* defines the size of a window. One would expect that, for a fixed $\hat{n}_d$ and a fixed n_p, increasing the size of the window would improve the accuracy of the estimates. Figures 8.23 and 8.25 show variations of the statistical indices with respect to the number of time points for a small amplitude of noise (0.0024 inches) and a large amplitude of noise (0.024 inches) for complete measured displacements. The number of trials per window is 20. One can observe that the estimator is not sensitive to the number of time points for this simulation study regardless the amplitude of noise. The

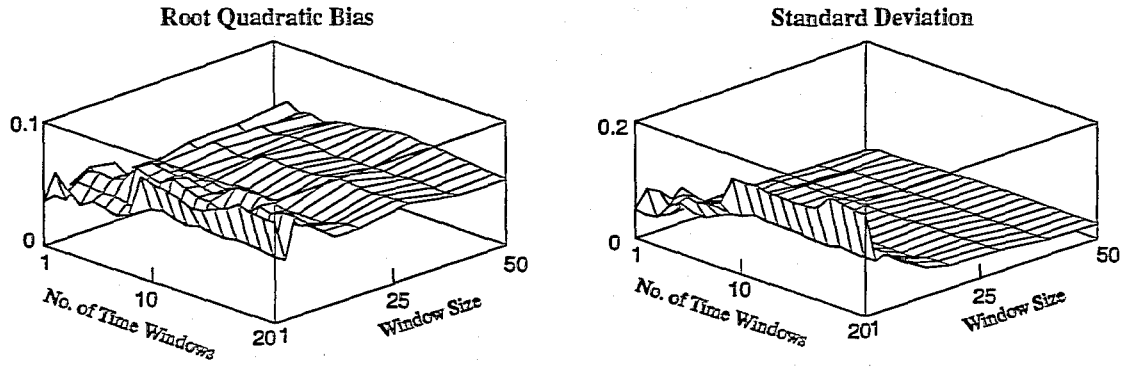

(*a*) A small amount of noise $\lambda = 2.4 \times 10^{-3}$ (*in*)

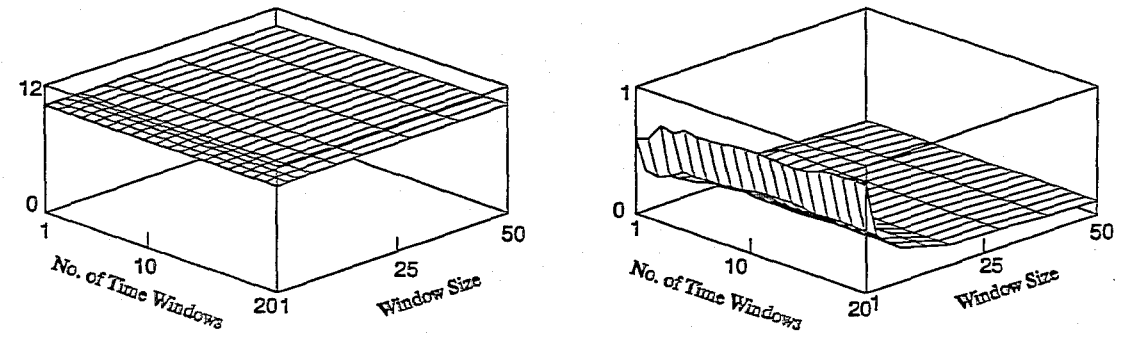

(*b*) A large amount of noise $\lambda = 2.4 \times 10^{-1}$ (*in*)

Fig. 8.23 Variations of the *RQB* and *SD* with respect to the size and number of windows for a small and a large absolute noise in measured displacements

reason is simple. For the bridge truss the number of unknown parameters is four and number of measured degrees of freedom is 48. Therefore, even for one time point the number of measurements is adequate to reliably estimate the parameters. For large amplitudes of noise, the estimation errors cannot be effectively reduced by increasing the size of the window because, when the noise is large, it dominates the behavior of the estimator. The estimator is more sensitive to the size of the window for noisy, incomplete measured displace-

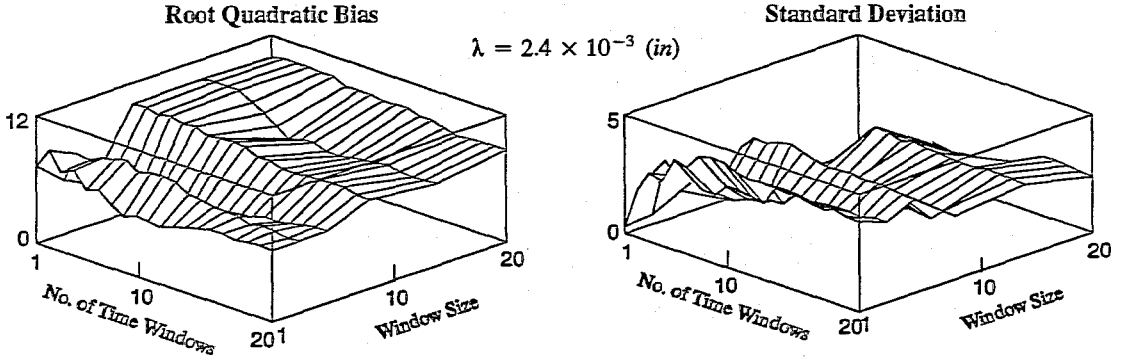

Fig. 8.24 Variations of the *RQB* and *SD* with respect to the size and number of windows for a small absolute noise and incomplete measured displacements

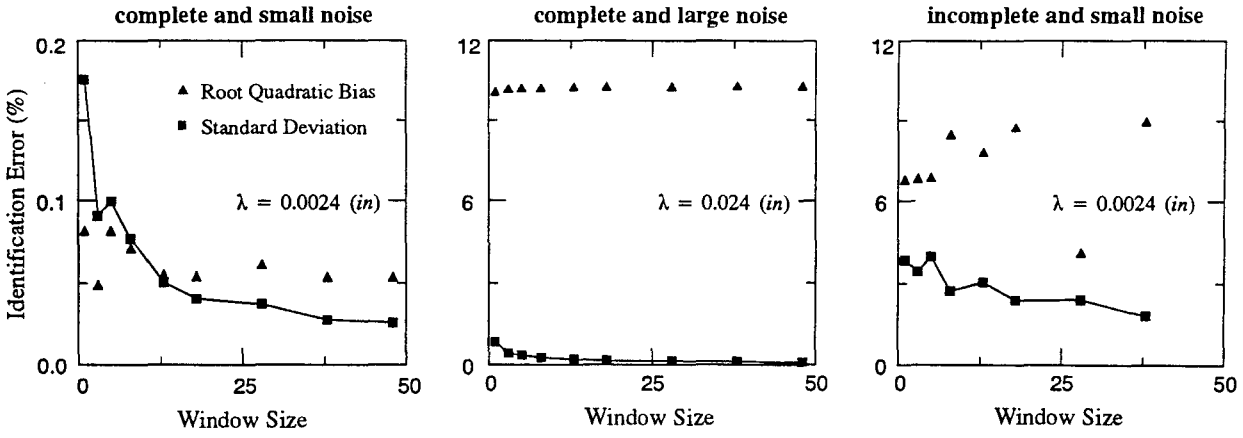

Fig. 8.25 Variations of the *RQB* and *SD* with respect to the size of windows for measured displacements

ments. Figure 8.24 shows variations of the root quadratic bias and standard deviation with respect to the number of time points in a window for a case with measured displacements at 13 degrees of freedom and an absolute noise of 0.0024 inches. By increasing the size of the window, the root quadratic bias increases and the standard deviation decreases; then both become steady. This trend suggests that less information with high

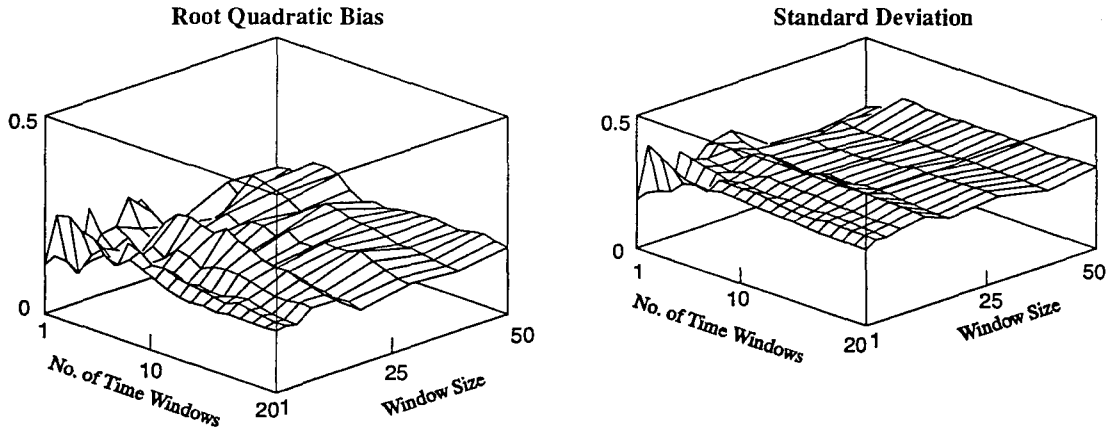

(*a*) A small amount of noise $\lambda = 24\ (in/sec^2)$

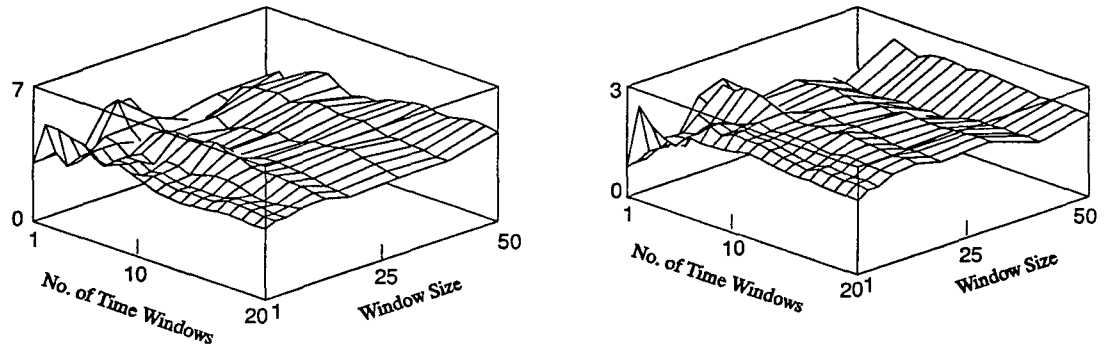

(*b*) A large amount of noise $\lambda = 180\ (in/sec^2)$

Fig. 8.26 Variations of *RQB* and *SD* with respect to the size and number of windows for a small and a large absolute noise in measured accelerations

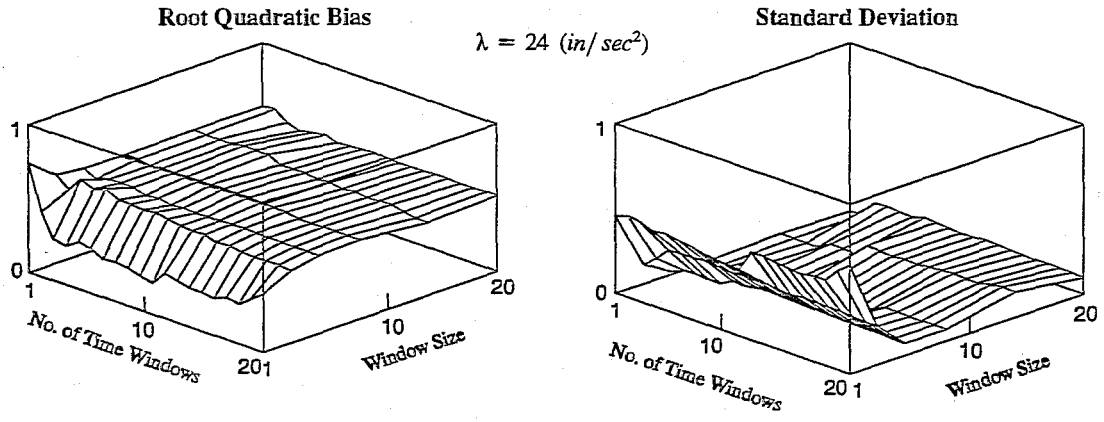

Fig. 8.27 Variations of *RQB* and *SD* with respect to the size and number of windows for a small absolute noise and incomplete measured accelerations

confidence is better than more information with low confidence. Figure 8.25 presents the statistical behavior of the estimator for complete and incomplete measured displacements with different amplitudes of noise after considering 20 windows and 20 trials per window.

Figures 8.26 and 8.28 show the statistical behavior of the proposed estimator with respect to the size of the window for noisy, complete measured accelerations. We consider two amplitudes for absolute noise: one small ($24\ in/sec^2$) and the other one relatively large ($180\ in/sec^2$). One can observe that the estimator is not sensitive to the size of the window regardless of the amplitude of noise because even one time point in a window provides 48 measurements, to estimate only four unknown stiffness parameters. The variations of the root quadratic bias and standard deviation for the case with measured accelerations at only 13 degrees of freedom and an absolute noise of 24 (in/sec^2) are presented in Fig. 8.27. For incomplete measurements, as the size of the window increases the root quadratic bias increases and the standard deviation decreases and then both become steady. Like the case with incomplete measured displacements, less information of good quality results in a better estimation than more information of less quality. Figure 8.28 presents variations of the root

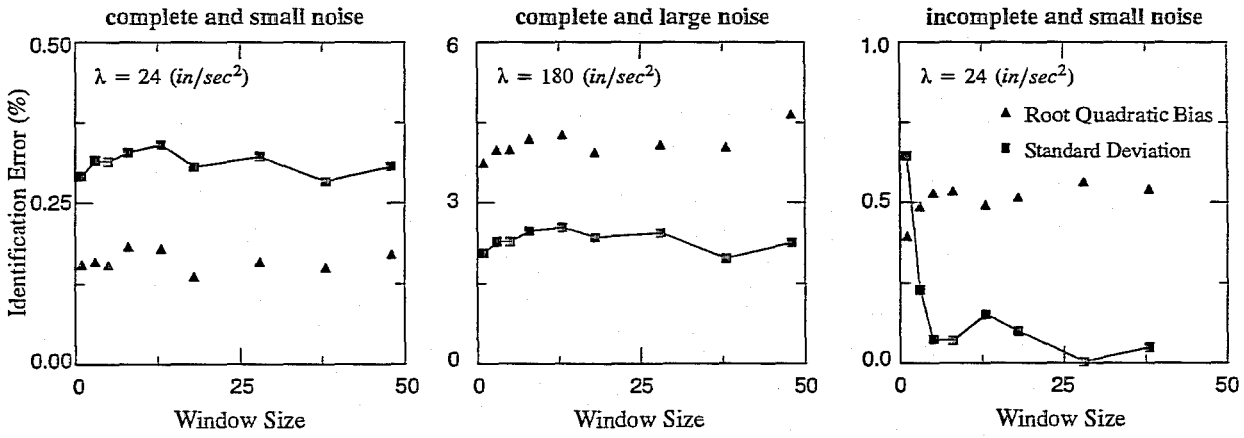

Fig. 8.28 Variations of the *RQB* and *SD* with respect to the size and number of windows for measured accelerations

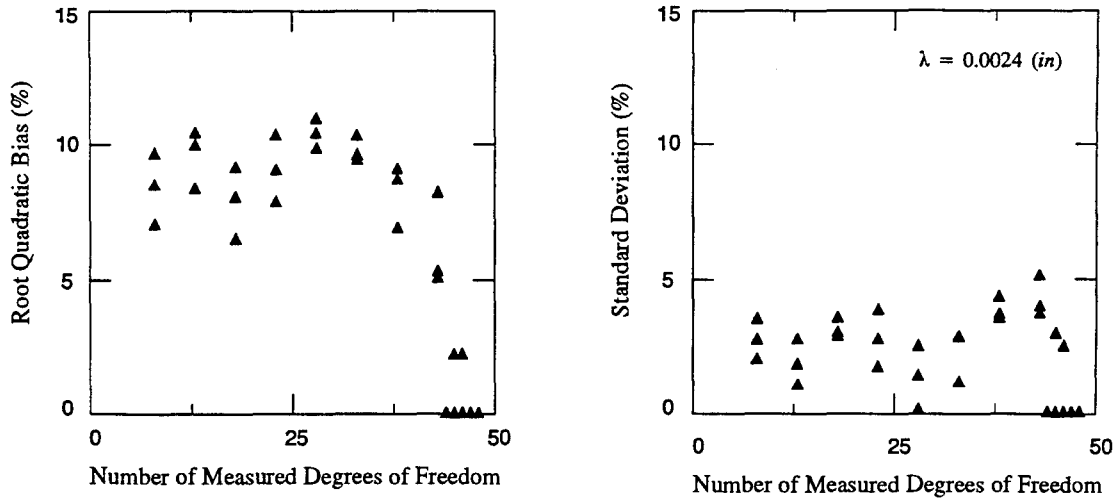

Fig. 8.29 Variations of the *RQB* and *SD* versus number of measured displacements

quadratic bias and standard deviation of the estimates from complete and incomplete measured accelerations for different amplitudes of noise after considering 20 different windows and 20 trials per window.

Number of measured degrees of freedom. The estimator is applicable to problems with sparse measurements. Thus, another way to increase the number of measurements for the estimator is to increase the number of measured degrees of freedom $\hat{n}_d$. Figures 8.29 to 8.32 show the behavior of the proposed estimator with respect to the number of measured degrees of freedom for an absolute noise with amplitude λ. In these figures the estimates are computed from 20 different windows with three time points per window. The maximum value of $\hat{n}_d$ for the bridge truss is 48 and its minimum value, based on the identifiability criterion, is two. The abscissa values for Figs. 8.29 to 8.32 range from 8 to 48. To study the effect of measurement locations on the estimation errors, we consider three different patterns of measurements for each specific value of $\hat{n}_d$. One pattern of measurements differs from another according to which degrees of freedom are measured. Figures 8.29 and 8.30 illustrate variations of the root quadratic bias and standard deviation with respect to different numbers of measured displacements for an absolute noise of 0.0024 inches. For a small number of measured displacements, the statistical indices oscillate. When the number of measured degrees of freedom exceeds

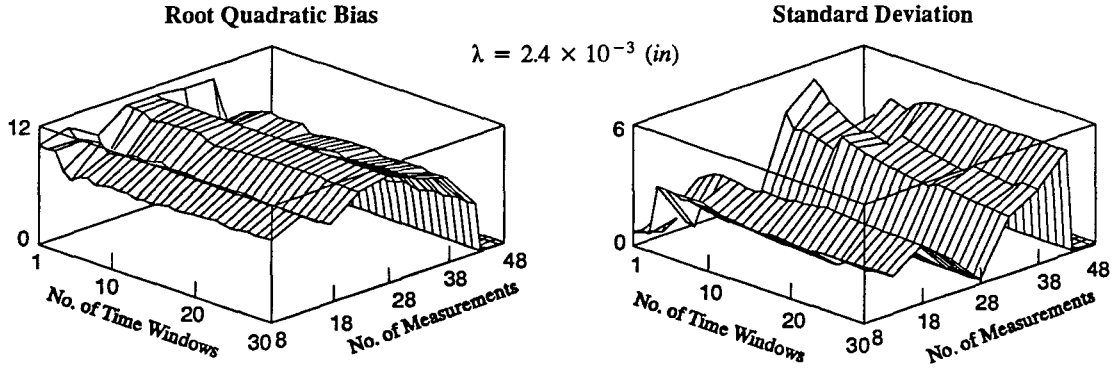

Fig. 8.30 Variations of the *RQB* and *SD* with respect to the number of measured displacements and number of windows for a small absolute noise

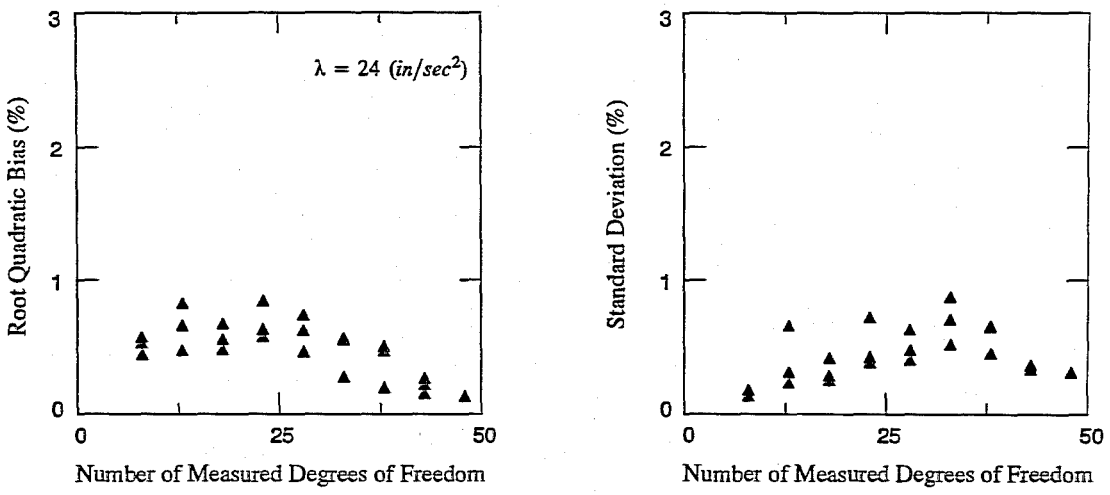

Fig. 8.31 Variations of the *RQB* and *SD* versus number of measured accelerations

28, the root quadratic bias significantly decreases, but the standard deviation continues to oscillate until $\hat{n}_d$ exceeds 43. Then it decreases. Increasing the number of measured degrees of freedom decreases the sensitivity of the estimator to the locations of measurements. If the amplitude of noise is large it dominates the behavior of the estimator, therefore increasing the number of measured displacements does not significantly change the statistical indices; they remain almost steady.

For measured accelerations and an absolute noise of 24 (in/sec^2), Figs 8.31 and 8.32 show variations of the statistical indices with respect to the number of measured degrees of freedom. When the amplitude of noise is small the standard deviation remains almost steady for different numbers of measured accelerations. But, the root quadratic bias oscillates if the number of measured degrees of freedom is less than 23. If one provides more measurements, *RQB* decreases. One can observe that, the estimator is not sensitive to the locations of measurements when the number of measured degrees of freedom is large. For large amplitudes of noise, increasing the number of measured degrees of freedom does not significantly change the root quadratic bias or standard deviation.

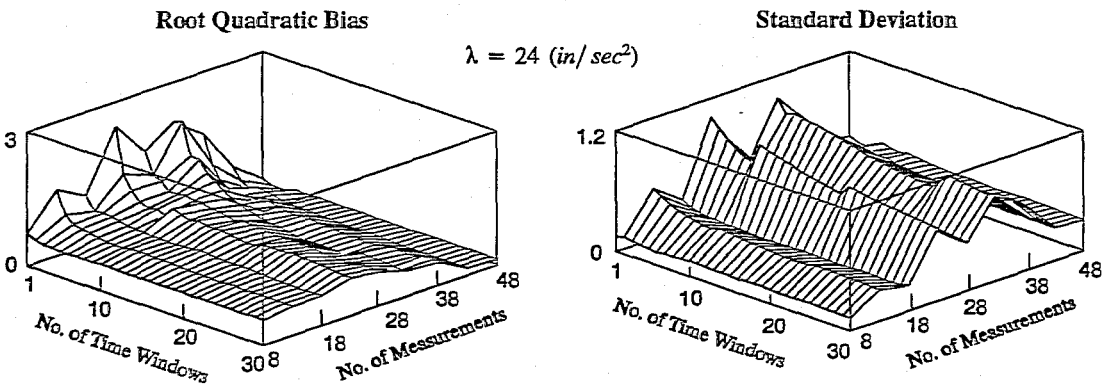

Fig. 8.32 Variations of the *RQB* and *SD* with respect to the number of measured accelerations and number of windows for a small absolute noise

8.8. Chapter Summary

We have used Monte Carlo simulation to study the statistical behavior of our estimator using a bridge truss as an example. Both displacement and acceleration data were considered. Some measurements were spatially incomplete. We observed that the recursive quadratic programming algorithm based on Gauss-Newton and Han-Powell approximations of the Hessian matrix are robust and globally convergent. We also observed that the bounding constraints on the unknown parameters significantly increase the reliability of the proposed estimator and reduce its sensitivity with respect to the initial values for the unknown parameters.

We demonstrated that the time step should be small enough to control numerical errors in differentiation and integration but should be large enough to provide new information for the estimator. In the presence of noise in the measurements, the estimator is biased. The bias saturates at large amplitudes of noise. For practical amounts of bias, the estimator can deal with relatively large amplitudes of noise if accelerations are measured. The estimator has desirable characteristics when the noise amplitude is small. For adequately small amounts of noise, the accuracy of the estimates increases as the amount of information increases. The amount of information can be increased by increasing the size of the window or increasing the number of measured degrees of freedom. When the number of unknown parameters is considerably smaller than the amount of measurements, increasing the size of the time window does not significantly improve the estimations. For small numbers of measured degrees of freedom, the bias of the estimates increases if the size of the window is increased.

The estimator is sensitive to the location of the window especially for large amplitudes of noise. We solved this sensitivity by considering a sample of windows instead of a single window and compute the average of the estimates from the sample of windows as the estimated parameters.

CHAPTER NINE

Closure

System identification and parameter estimation techniques can be used in the field of structural mechanics to improve existing analytical models, or to establish relatively reliable mathematical models for structural systems, from test data. These techniques can be used in a variety of applications, from simulation and prediction studies for design to damage detection in existing structures. While identification methods have evolved a great deal over the last thirty years, many challenging problems still remain in the field of parameter estimation. In particular, identification of complex systems suffers from the effects of sparse data and, like all physical measurements, from noise in the observations. The number of constitutive parameters of the model can also be troublesome for large structures.

In this research study we have presented an approach to the problem of parameter estimation of finite element models of complex structural systems for static, modal, and transient dynamic problems. We have endeavored to develop a unified approach to these discrete inverse problems with a particular view toward evolving methods that are amenable to large-scale computation. The proposed framework for estimating constitutive parameters for structures with known topology and geometry is a batch method using all observations in the computation scheme. We have assumed that the structure is discretized by the finite element method, that the excitation is known, and that deformations are measured at certain spatial locations on the structure. Also, we have assumed the selected finite element model is linear in its response. However, the parameter estimation problem is inherently nonlinear, and hence, the linearity of the response accrues no great advantage. Linearity of the constitutive model is not essential (the structural matrices can be nonlinear with respect to the constitutive parameters). We have assumed that our models have lumped, time independent, deterministic parameters.

9.1. Summary

In Chapter One, we introduced our subject, justified system identification as the appropriate tool for solving our inverse problems, and described the basic features of the parameter estimation problem.

In Chapter Two, we developed the general framework for parameter estimation problem as a constrained, nonlinear minimization of the difference between the response of the real structure and the prediction of a mathematical model of that structure. We advocate a least-squared error approach, using the recursive quadratic programming method as the numerical engine. This algorithm is attractive because it applies directly to problems with inequality as well as equality constraints, it is globally convergent, and it is amenable to large-scale computation. Finally, we examined the statistical framework for evaluating the performance of our identification algorithms.

In Chapter Three we considered the identification of a structure subjected to static loads. We developed two estimators: *(a)* an equation-error estimator, which measures the discrepancy between model and structure as the nodal force imbalance, *i.e.* $\boldsymbol{Ku-f}$, and *(b)* an output error estimator, which measures the discrepancy between model and structure as the difference in nodal displacements, *i.e.* $\boldsymbol{u-K^{-1}f}$. The unknowns for the equation error estimator comprise both unknown constitutive parameters and displacements at the unmeasured degrees of freedom. The unknowns for the output-error estimator comprise the unknown constitutive parameters. For both estimators, the constitutive parameters are assumed to be bounded from above and below.

In Chapter Four, we used Monte Carlo simulation to study the behavior of the proposed estimators using a bowstring truss as the model problem. We demonstrated that, in the presence of noise in the measurements, both the equation-error and the output-error estimators are biased. For practical amounts of noise, the output-error estimator exhibited a smaller bias than the equation-error estimator. Unfortunately, for large amounts of noise the equation-error estimator suggested high precision (small standard deviation) but had low accuracy (large bias). Fortunately, the output-error estimator predicted low precision when the accuracy was low for a large range of noise and high precision when the accuracy was high for practical amounts of noise. We observed that the precision and accuracy of the estimates computed by the output-error estimator increased monotonically as the amount of information increased. The bias of the equation-error estimator, on the other hand, did not decrease as more data became available. We observed from the numerical simulation studies that the recursive quadratic programming algorithms based on Gauss-Newton and Han-Powell approximations of the Hessian were robust and globally convergent. Also, we observed that bounding the unknown parameters significantly increased the reliability of the proposed estimators and reduced the sensitivity of the algorithms to the initial values for the unknown parameters.

In Chapter Five, we studied modal identification techniques. First, we assumed that the mass matrix was known and developed an equation-error estimator and an output-error estimator using modal data. Then, we considered the general case, where both mass and stiffness parameters were unknown, and proposed an equation-error estimator. When the mass matrix was known, we modified the eigenvalue equation to have a form similar to the static equilibrium equation. Then, we applied the same nonlinear constrained optimization technique used to solve the static problem. Both proposed methods could deal with a set of truncated modes whose mode shapes were sparsely sampled, both were robustly convergent, and both were amenable to large, complex structures. We applied the proposed estimators to build an analytical model for the Oakland City Hall building using measured modal data, in Chapter Six.

In Chapter Seven, we studied the problem of parameter estimation from the transient response of a structure. We developed an equation-error estimator for two cases: when histories of displacements at some degrees of freedom were available and when histories of accelerations at some degrees of freedom were available. We discussed the concepts of the estimation time step and the time window. We also showed that the developed estimator could, by analogy, use modal data to estimate the mass and stiffness parameters of a finite element model.

In Chapter Eight, we used Monte Carlo simulation to study the statistical behavior of the estimator developed in Chapter Seven using a bridge truss as an example. Both spatially incomplete displacement and acceleration data were considered. We investigated the effect of the estimation time step and the size and location of the time window along the history of response. In the presence of noise in the measurements, the estimator was biased. We concluded that for practical amounts of bias, the estimator could deal with relatively large amplitudes of noise if accelerations were measured. We also studied the effect of the amount of information on the accuracy and precision of the estimator.

In Appendix A we studied the class of recursive quadratic programming methods and described the algorithm we used in this study. We tailored the existing alternatives for each step of a recursive quadratic programming algorithm to suit our objective.

The recursive quadratic programming is a gradient-search method that requires the gradient and the Hessian of the loss function with respect to the unknowns. In Appendix B, we have proposed a straightforward method to compute the sensitivity of the loss function with respect to the unknown variables.

For the static and modal identification problems, we have proposed and implemented algorithms for the equation-error estimator as well as the output-error estimator. For transient vibration problems, we have proposed and implemented the equation-error estimator for the cases in which the history of displacements or accelerations is available. All of the proposed algorithms perform well when measurements are sparse in space and, for the dynamic case, in state and time. The proposed algorithms have all the flexibilities of the finite element method and new elements can easily be implemented.

9.2. General Features of the Proposed Approach

The finite element discretization and the recursive quadratic programming algorithm form the basis of our general purpose parameter estimation programs. Like a finite element analysis system, the parameter estimation programs can treat structures with different types of elements. The differences between structure types have been isolated at the element level. If one can implement an element in a general purpose finite element system, then one can also implement that element in the parameter estimation environment presented in this work.

Like a finite element analysis system the algorithm is organized on the basis of assembling the estimation equations from element contributions. An implementation of these algorithms should have a library of different element types. Each element in the library would provide the elemental stiffness, mass, and damping, matrices, as a finite element system does, in addition to the sensitivity of those elemental matrices with respect to the unknown constitutive parameters. We have demonstrated these features for one-dimensional elements (*i.e.* truss bar and Bernoulli and Timoshenko beams with axial stiffness) in Appendix B, where we also outline the procedure for developing the sensitivity matrices for elements computed by numerical quadrature method. To show the procedure, we have derived and implemented the stiffness and sensitivity matrices for a truss element. Currently, the algorithms support truss and beam elements as well as plane stress elements.

Both the output-error estimator and the equation-error estimator are cast as constrained nonlinear optimization problems that are solved iteratively. One should bring to bear all available knowledge in selecting

the starting point of the iteration. Both estimators require initial values for the unknown parameters. Further, the equation-error estimator needs initial values for the displacements at the unmeasured degrees of freedom. We have supplied several options to generate these initial values.

The reliability of the estimates generally improve as the ratio of information to the unknowns increases above unity, if the estimator is consistent. Such an improvement can be achieved either by increasing the number of tests (*i.e.* number of load cases for the static case, number of measured modes for the modal case, and number of time points in a window for the dynamic case), by increasing the number of measurement locations, or by decreasing the number of parameters. The number of unknown parameters can be reduced by grouping the parameters or by using a different mathematical model with fewer unknown parameters.

We have used a simple grouping scheme to keep the number of parameters small enough to be manageable. The grouping scheme can reduce the total number of parameters in the model and thereby increase the robustness of the estimations. Elements in a group are associated with the same set of parameters and groups of parameters are disjoint from one another. The grouping schemes for the stiffness, mass, and damping parameters need not be the same, that is, an element can be a member of different groups based on its stiffness, mass, or damping parameters. The grouping scheme might be based on prior knowledge of the structure. The grouping scheme can be made more flexible by recognizing that the value of the parameters within a group need not have the same nominal value, but can simply be scaled by a common multiplicative parameter. Only the relative values of parameters within a group need to be specified in advance. One might also try to improve the knowledge of certain parameters by subsidiary testing. In this case, the user can introduce the known parameters to the program.

We have embedded our algorithms in an environment capable of executing Monte Carlo simulation, useful both for studying the behavior of the proposed estimators and for studying the identifiability of specific structures. Monte Carlo simulation uses a random sequence of numbers to generate a sample of measurement sets and consequently, to construct a sample of the solution population. We have introduced a few appropriate statistical indices to probe the behavior of the proposed algorithms by simulation.

9.3. Where Do We Stand?

At last, we are left with the question of whether or not there is engineering value in our ability to identify structures. Certainly, any competent engineer would gladly accept such information, if it were free. It is not.

At the present time, one must look forward to transporting excitation and measurement devices to a structure that has no natural places for them. The cost of such devices is presently quite high. Usually, there are no baseline measurements to aid the assessment of currently acquired data. Usually, data reduction is done by someone other than the one that physically tests the structure; thus, the conditions of the test are not quite right or the data are incomplete or ambiguous. Usually, an analytical model is constructed long after the test equipment has been removed from the structure. Probably more important than all of the above obstacles to monitoring structures, the average engineer has not had a reliable, informative means of processing *in situ* test data from large, complex structures.

Let us consider a brighter future; a future where the monitoring system is planned by the engineer at the time the structure is designed; a future where the monitoring system is installed as the structure is built, just as the electrical and mechanical systems are now; a future where maintenance of the monitoring system is as simple as changing a lightbulb. This is the future where the identification of the structure is essentially free.

There remains, in our present, a tremendous void in our knowledge of the environments in which our structures must survive, of the actual performance of our structures over their lifetimes, of the consequences of many of our design decisions. Our bright future would, at the very least, provide a laboratory to examine these engineering problems. There is no limit to what we could learn from a constantly, or even intermittently, monitored structure if the monitoring system was more than haphazardly placed. But we must first decide if the knowledge is worth the price.

After a natural disaster we are always left with impossibly difficult decisions regarding the fate of our damaged infrastructure. Is a bridge crossable, a building inhabitable, a pipeline usable? Can we redirect the flow of traffic, repair a building, fill a dam? In our present we yearn for more data to help with those decisions, but acknowledge the impossibility of gathering those data in time to make a difference. In our bright future those data would be available and could be of tremendous value in making engineering decisions. The economics might be favorable, even if the investment risk is large.

Thus, while the technology is ready today, as evidenced by the fact that we have already used it, its time is probably yet to come. Whether or not its time will come at all depends upon how we view engineering in the future. What do we need to know that we do not know today? What sort of investments should we make to enhance our ability to engineer with competence in the future?

APPENDIX A

Recursive Quadratic Programming

We begin by considering a general nonlinear programming problem (NP) with both inequality and equality constraints as follows

$$\text{(NP)} \qquad \begin{array}{lll} \underset{x \in R^n}{\textit{minimize}} & F(x) & \\ \textit{subject to} & c_i(x) = 0 & i = 1,\ldots,m' \\ & c_i(x) \leq 0 & i = (m'+1),\ldots,m \end{array} \tag{A.1}$$

where the objective function F and/or some of the constrains $\boldsymbol{c}$ are nonlinear with respect to the unknown variables $\boldsymbol{x}$. For the purpose of discussion we assume that the objective function is twice differentiable, and a solution $\boldsymbol{x}^*$ exists for the nonlinear programming problem, such that the normals to the binding constraints are linearly independent. In other words, $\boldsymbol{x}^*$ is a regular point. No further properties such as convexity are assumed, and hence we shall be concerned only with local minima. We shall discuss those methods which approach the solution $\boldsymbol{x}^*$ iteratively. A typical iteration of a method for solving NP includes the following procedure. If the current iterate $\boldsymbol{x}_k$ does not satisfy the appropriate optimality conditions: (*1*) compute a *search direction* $\boldsymbol{d}_k$ by solving a subproblem, (2) determine a step length β_k such that specified properties hold at $\boldsymbol{x}_k + \beta_k \boldsymbol{d}_k$. Following these steps $\boldsymbol{x}_k + \beta_k \boldsymbol{d}_k$ becomes the new iterate $\boldsymbol{x}_{k+1}$. The second step is usually termed the *step length* procedure or *line search.*

Algorithms in which the search direction is computed by solving a quadratic programming subproblem are called *recursive quadratic programming* techniques. The search direction $\boldsymbol{d}_k$ is the solution of a minimization subproblem with the general form as follows

$$\text{(QP)} \qquad \begin{array}{lll} \underset{d_k \in R^n}{\textit{minimize}} & QF(d_k) & \\ \textit{subject to} & Lc_j(d_k) = 0 & j = 1,\ldots,m' \\ & Lc_j(d_k) \leq 0 & j = (m'+1),\ldots,l\ (\leq m) \end{array} \tag{A.2}$$

In the subproblem (A.2) QF is a quadratic function which can be viewed, for the moment, as being quadratic approximation of F about the point $\boldsymbol{x}_k$. Similarly, Lc_j is a linearization of the constraint c_j. A number of different forms have been proposed for the subproblem (A.2) and it is not entirely clear which ideas will lead to the most successful algorithm. A common form for the quadratic function in (A.2) is

$$QF(d_k) = \nabla F(x_k)d_k + \tfrac{1}{2}d_k^T B_k d_k \tag{A.3}$$

where B_k is a positive definite approximation to the Hessian matrix of the Lagrangian function associated with problem (A.1). The matrix B_k is defined in this way because the second order conditions for optimality of x^* are expressed in terms of the Hessian of the Lagrangian function.

Any algorithm for solving NP must include some procedure, usually termed an *active set strategy*, for determining which constraints are bunding at the solution. Some algorithms include a *pre-assigned* active set strategy that specifies which constraints are to be treated as equalities in the QP subproblem and solve an *equality constrained* QP (EQP) subproblem to find a search direction. Their linear constraints represent a subset of the original constraints ($l \leq m$). The term "preassigned" signifies that the decision about the active set is made before posing the QP subproblem. Others proposed (A.2) as an *inequality constrained* QP subproblem (IQP) with $l = m$, so that linearizations of all constraints in NP are included. With a pure IQP approach, a QP-*assigned* active set strategy can be used such that the set of active constraints at the solution of the QP subproblem will be taken as a prediction of the active set of the original problem NP. Algorithms employing an equality constrained subproblem (EQP) have been discussed by Biggs (1972 and 1975), Murray and Wright (1978), and Van der Hoak (1980). IQP based methods seem to have received more attention and are described by Wilson (1963), Fletcher (1973 and 1975), Han (1977), Powell (1978), and Tupia (1977). There are many variants in the formulation of QP subproblems between EQP and IQP approaches.

A.1. Motivation

Consider a nonlinear optimization problem with equality constraints as follows

$$\begin{aligned} &\underset{x \in R^n}{\text{minimize}} \quad F(x) \\ &\text{subject to} \quad c_i(x) = 0 \qquad i = 1,\ldots,l \end{aligned} \tag{A.4}$$

The Lagrange first order necessary conditions for the problem (A.4) are

$$\begin{aligned} &\nabla F(x) + \Lambda^T \nabla c(x) = 0 \\ &c(x) = 0 \end{aligned} \tag{A.5}$$

where $c(l \times 1)$ is the vector of equality constraints and $\Lambda(l \times 1)$ is the vector of Lagrange multipliers. The set of necessary conditions is a nonlinear system of $n+l$ unknowns comprising the components of x and Λ. These equations can be solved by Newton's method. The linearized form of Eqn. (A.5) about the configuration (x_k, Λ_k) is

$$\begin{aligned} &H(x_k, \Lambda_k)d_k + \nabla c(x_k)^T y_k + \nabla F(x_k)^T + \nabla c(x_k)^T \Lambda_k = 0 \\ &\nabla c(x_k)d_k + c(x_k) = 0 \end{aligned} \tag{A.6}$$

where $H(x_k, \Lambda_k)$ is the Hessian matrix for the Lagrangian function $F(x_k) + \Lambda_k^T c(x_k)$ and d_k and y_k are the increments for the vectors x_k and Λ_k at the kth iteration, respectively. The system of equations (A.6) can be simplified to the following form

$$\begin{aligned} H_k d_k + A_k^T \Lambda_{k+1} &= -\nabla F(x_k)^T \\ A_k d_k &= -c_k \end{aligned} \tag{A.7}$$

where symbols H_k, A_k, and c_k represent the matrices $H(x_k, \Lambda_k)$ and $\nabla c(x_k)$, and the vector $c(x_k)$, respectively. We note that the Eqns. (A.7) are the necessary conditions for a quadratic programming problem with the following form

$$\begin{aligned} \underset{d_k \in R^n}{\textit{minimize}} \quad & \nabla F(x_k) d_k + \tfrac{1}{2} d_k^T H_k d_k \\ \textit{subject to} \quad & A_k d_k + c_k = 0 \end{aligned} \tag{A.8}$$

where the vector Λ_{k+1} in Eqns. (A.7) corresponds to the vector of the Lagrange multipliers of problem (A.8). The analogy with the quadratic programming suggests a procedure for extending the above Lagrange optimization method to minimizing problems with inequality constraints. Similarly for the problem NP, the quadratic subproblem (A.2) takes the form

$$\begin{aligned} \underset{d_k \in R^n}{\textit{minimize}} \quad & \nabla F(x_k) d_k + \tfrac{1}{2} d_k^T H_k d_k \\ \textit{subject to} \quad & A_k^{eq} d_k + c_k^{eq} = 0 \\ & A_k^{in} d_k + c_k^{in} \leq 0 \end{aligned} \tag{A.9}$$

where the superscripts *eq* and *in* refer, in a manner similar to (A.7), to the equality and inequality constraints in problem (A.1), respectively. In problem (A.9), the constraints are linearized forms of the original constraints in Eqn. (A.1) and the objective function is a quadratic approximation of the Lagrangian for the problem NP. The Lagrange multipliers of problem (A.9) correspond to the Lagrange multipliers of the original nonlinear programming problem (A.1).

The corresponding quadratic subproblem (A.8) or (A.9) can be interpreted as an approximation to the problem of minimizing the Lagrangian over the tangent hyperplane. Since the second order sufficiency conditions of the original constrained problem require that the Hessian of the Lagrangian be positive definite on the tangent hyperplane at the solution, the quadratic subproblem is guaranteed to be well-defined near the solution. Based on this observation, the class of methods which minimize (an approximation to) the Lagrangian over the tangent hyperplane, are sometimes referred to as *projected Lagrangian* methods.

The recursive quadratic programming method extends Newton's method to solve the Lagrange first order necessary conditions for nonlinear inequality constrained problems. However, this form of the RQP method can be improved to relax the requirement of the second order derivative information and by implementing a suitable line search to guarantee global convergence, especially useful for problems with inequality constraints.

A.2. Modifications to the Quadratic Subproblem

The objective function for the quadratic subproblem is given in Eqn. (A.3). Based on the analogy with Eqns. (A.8) and (A.9), one can see that the matrix B_k in Eqn. (A.3) is an approximation to the Hessian matrix H_k of the Lagrangian function at each iteration. For the EQP approach to recursive quadratic programming, the QP subproblem takes the form

$$\text{(EQP)} \qquad \begin{aligned} &\underset{d_k \in R^n}{\text{minimize}} && \nabla F(x_k)d_k + \tfrac{1}{2}d_k^T B_k d_k \\ &\text{subject to} && A_k d_k + c_k = 0 \end{aligned} \tag{A.10}$$

and for the IQP approach, the QP subproblem is stated as follows

$$\text{(IQP)} \qquad \begin{aligned} &\underset{d_k \in R^n}{\text{minimize}} && \nabla F(x_k)d_k + \tfrac{1}{2}d_k^T B_k d_k \\ &\text{subject to} && A_k^{eq} d_k + c_k^{eq} = 0 \\ & && A_k^{in} d_k + c_k^{in} \le 0 \end{aligned} \tag{A.11}$$

To relax the requirement of computing the second derivative in the algorithm, B_k is built from first derivatives gathered along the search path. There are various ways to make the approximation matrix B_k. Here we will focus on the Gauss-Newton approximation to the Hessian and a on various rank-two update formulas.

The convergence of the recursive quadratic programming method is not necessarily impaired if we use a positive definite approximation to the Hessian matrix even when the Hessian matrix is indefinite. On the other hand, superlinear convergence can be proved if $B_k \approx H(x_k, \Lambda_k)$. Obviously, $H(x_k, \Lambda_k)$ is not always positive definite, but the computational convenience of using a positive definite approximation can be justified by the observation that the superlinear convergence result requires B_k to agree with the actual Hessian matrix only in the subspace where the Lagrangian must have positive curvature. Some authors, however, are considering how to devise stable algorithms where B_k is not forced to be positive definite.

The approximate Hessian matrix B_k can be taken to be positive definite even though H_k is not. Let us assume that this is so. Similar to the Eqn. (A.7), we can write the first order necessary conditions for subproblem (A.10) as follows

$$\begin{aligned} B_k d_k + A_k^T \Lambda_{k+1} &= -f_k \\ A_k d_k &= -c_k \end{aligned} \tag{A.12}$$

where the vector f_k is the gradient of the objective function $\nabla F^T(x_k)$ at the kth iteration. Since B_k is not singular, Eqn. (A.12) has the following explicit solution

$$d_k = -B_k^{-1}\left[I - A_k^T[A_k B_k^{-1} A_k^T]^{-1} A_k B_k^{-1}\right] f_k - B_k^{-1} A_k^T [A_k B_k^{-1} A_k^T]^{-1} c_k \tag{A.13}$$

$$\Lambda_{k+1} = [A_k B_k^{-1} A_k^T]^{-1}[c_k - A_k B_k^{-1} f_k] \tag{A.14}$$

The Lagrange multipliers can be computed using Eqn. (A.14). However, the multiplier update methods in the following section can be used to avoid computing the complete solution for Eqn. (A.12).

Update Methods for the Lagrange Multipliers

Estimates of the Lagrange multipliers are needed to compute and update matrix B_k in order to construct an approximation of the Lagrangian function and its Hessian matrix. For example, the active set strategies in the original problem and the quadratic programming subproblem need the Lagrange multiplier estimates to update the working set of active constraints. Algorithms based on the quadratic line search functions need an estimate of the Lagrange multipliers to construct constraints of the QP subproblem. The lower bound for the penalty parameters of the line search functions are also defined based on the values of the Lagrange multipliers.

The multiplier update methods reduce the computational efforts. For example, to avoid computing the complete solution for system of equations (A.12), its first equation can be written as

$$B_k d_k = -f_k - A_k^T \hat{\Lambda}_k \tag{A.15}$$

where $\hat{\Lambda}_k$ is an estimate of the vector of the Lagrange multipliers Λ_{k+1}. And the general iteration formula for the system of equations (A.12) is stated as

$$x_{k+1} = x_k - B_k^{-1}[f_k + A_k^T \hat{\Lambda}_k] \tag{A.16}$$

where the term in the brackets is the gradient of the Lagrangian with respect to x. One can use the exact form of the updated Lagrange multipliers from Eqn. (A.14), but there are several other strategies one can use to determine a suitable estimate for the updated $\hat{\Lambda}_k$ (Luenberger 1989; Murray and Wright 1982). The strategies include: *(1)* $\hat{\Lambda}_k = \Lambda_k + rc_k$ where r is a penalty parameter. This formula is used in the method of augmented Lagrangian to update the multipliers. *(2)* $\hat{\Lambda}_k = [A_k A_k^T]^{-1} A_k f_k$, a least squares approximation. *(3)* If matrix B_k in Eqn. (A.14) is set to the identity matrix an estimate for the updated Lagrange multipliers will be computed as $\hat{\Lambda}_k = [A_k A_k^T]^{-1}[c_k - A_k f_k]$. This formula is also obtained by adding vector $[A_k A_k^T]^{-1} c_k$ to the second updating formula that corrects the least squares estimate for the nonzero active constraints. *(4)* $\hat{\Lambda}_k = [\frac{1}{r} I + A_k B_k^{-1} A_k^T]^{-1}[c_k - A_k B_k^{-1} f_k]$, the same as Eqn. (A.14) except it is corrected to consider the effect of the quadratic line search function and reduces to Eqn. (A.14) as r becomes a large number (Biggs 1975).

Hessian Matrix Update Methods

The approximation matrix B for the Hessian matrix of the Lagrangian can be estimated from first derivative information using a rank-two update formulae. As such, the recursive quadratic programming extends the quasi-Newton approach to constrained optimization problems. Standard update formulae such as BFGS and DFP formulae can be implemented to update the matrix B used to approximate the Hessian of the Lagrangian $H(x_k, \Lambda_k)$. For example the BFGS formula takes the form

$$B_{k+1} = B_k - \frac{B_k d_k d_k^T B_k}{d_k^T B_k d_k} + \frac{q_k q_k^T}{d_k^T q_k} \tag{A.17}$$

where $d_k = x_{k+1} - x_k$ is the increment for x_k at the kth iteration and q_k is the difference between the gradients of the Lagrangian at two consecutive iterations computed with the same Lagrange multipliers and is stated as

$$q_k = \left[\nabla F(x_{k+1})^T + \nabla c(x_{k+1})^T \Lambda_{k+1}\right] - \left[\nabla F(x_k)^T + \nabla c(x_k)^T \Lambda_{k+1}\right] \tag{A.18}$$

One can show that quasi-Newton methods for equality constrained optimization problems converge superlinearly when initiated sufficiently close to the solution if a unit step length is used. Rank-two update formulae such as Eqn. (A.17) should be modified to preserve the positive definiteness that can be lost if the line search is not exact (Han 1977; Powell 1978). For example, Han-Powell algorithm modifies Eqn. (A.17) as follows

$$B_{k+1}^{HP} = B_k^{HP} - \frac{B_k^{HP} d_k d_k^T B_k^{HP}}{d_k^T B_k^{HP} d_k} + \frac{r_k r_k^T}{d_k^T r_k} \tag{A.19}$$

where the matrices B_k^{HP} and B_{k+1}^{HP} are the approximate Hessian matrices at iterations k and k+1, respectively and the vectors d_k and q_k are the same as in Eqn. (A.17). The vector r_k is defined as follows

$$r_k = \theta q_k + (1 - \theta) B_k^{Hp} d_k \tag{A.20}$$

where parameter θ is introduced to assure that positive definiteness of the approximate Hessian is preserved from B_k^{HP} to B_{k+1}^{HP} and is calculated as

$$\theta = \begin{cases} 1 & \text{if } p_k^T q_k \geq 0.2 p_k^T B_k^{HP} p_k \\ \dfrac{0.8 p_k^T B_k^{HP} p_k}{p_k^T B_k^{HP} p_k - p_k^T q_k} & \text{if } p_k^T q_k < 0.2 p_k^T B_k^{HP} p_k \end{cases} \tag{A.21}$$

If the constraints $c(x)$ are linear, then vector q_k is only the difference between the gradients of the loss function F at two consecutive iterations and takes the form as

$$q_k = \nabla F(x_{k+1}) - \nabla F(x_k) \tag{A.22}$$

obviating the need to compute the gradient of the Lagrangian. The Han-Powell update formula requires an initial positive definite matrix B_o^{HP}; one can use an identity matrix as the initial matrix B_o^{HP}.

In practice one needs to consider which of the many low-rank update formulae will be most suitable for building a good estimate of the Hessian, while avoiding the singularity or unboundness of the matrix B.

A.3. Global Analysis

A line search procedure is necessary to ensure global convergence of the recursive quadratic programming method (Murray 1969). The line search is important as a means for promoting convergence from bad starting points. Also, the superlinear convergence of QP methods depends upon the use of unit step length near the solution. The line search (merit) function must be compatible with the direction-finding algorithm in the sense that it must decrease along the search direction. The line search objective function is usually a sum of the objective function and a penalty term that becomes positive when the constraints are violated. The absolute-value penalty function and quadratic penalty function are compatible with the recursive quadratic programming methods using a modified Hessian matrix.

The Absolute-Value Penalty Function

For the nonlinear problem NP (A.1), Han (1977) recommended the merit function with the following form

$$V(x) = F(x) + \sum_{i=1}^{m'} r_i |c_i(x)| + \sum_{i=m'+1}^{m} r_i \max[0, c_i(x)] \tag{A.23}$$

where each penalty parameter r_i is positive. Coleman and Conn (1980a and 1980b) proposed a similar line search function with one penalty parameter as follows

$$V(x) = F(x) + r\left[\sum_{i=1}^{m'} |c_i(x)| + \sum_{i=m'+1}^{m} \max[0, c_i(x)]\right] \tag{A.24}$$

In order to have global convergence, each new vector in the sequence $\{x_k\}$ is calculated to satisfy an inequality that at least obeys the condition

$$V(x_{k+1}) < V(x_k) \tag{A.25}$$

Condition (A.25) is a weak condition. In some methods, x_{k+1} satisfies the strong condition of minimizing the merit function. Han (1977) analyzed a recursive quadratic programming algorithm that obtains x_{k+1} by searching from x_k along a direction d_k and the step length is chosen to give the reduction (A.25). The search direction d_k is the solution of the inequality constrained quadratic programming subproblem IQP (A.11). Han assumed that the matrices $\{B_k;\ k = 0, 1, ...\}$ are uniformly bounded away from singularity and that the linearized constraints in IQP are compatible. Under these assumptions and some other conditions, he proved that limits of the sequence $\{x_k\}$ are Kuhn-Tucker points of the optimization problem NP.

Let $\{\lambda_i; i = 1, ..., m\}$ be the Lagrange multipliers at the solution of the IQP. One of the conditions of Han's analysis is that the penalty parameters $\{r_i; i = 1, ..., m\}$ in the merit function (A.23) have lower bounds as follows

$$r_i \geq |\lambda_i| \qquad i = 1, ..., m \tag{A.26}$$

Coleman and Conn (1980b) and Luenberger (1989) showed the same results for the merit function (A.24) and proved that the recursive quadratic programming method with the absolute-value merit function $V(x)$ in Eqn. (A.24) is globally convergent if

$$r \geq \max_i(\lambda_i) \tag{A.27}$$

and the step length β_k is computed by minimizing the univariate function $V(x_k + \beta_k d_k)$ where d_k is the solution for the IQP subproblem.

The recursive quadratic programming, in conjunction with the absolute-value penalty function, is an attractive technique for nonlinear constrained optimization problems. However, there are some difficulties to be kept in mind. First, the computation of a step length requires a one-dimensional search with respect to a nondifferentiable function. This difficulty can be relaxed by using the weak condition (A.25) or line search procedures which do not need derivatives of the merit function such as the golden section method. Second, the absolute-value function requires an estimate for the upper bound of the Lagrange multipliers to select the penalty parameters such that they satisfy conditions (A.26) or (A.27).

The Quadratic Penalty Function

Another line search objective function that is compatible with the recursive quadratic programming method is the standard quadratic penalty function. For the NP problem (A.1) this differentiable quadratic function is defined as follows

$$Q(x) = F(x) + \tfrac{1}{2}r\left[\sum_{i=1}^{m'} c_i^2(x) + \sum_{i=m'+1}^{m} \left[\max[0, c_i(x)]\right]^2\right] \tag{A.28}$$

Murray (1969) showed that the minimum of $Q(x)$ is approximated with the solution to a certain quadratic programming problem, and suggested that the NP problem (A.1) might be solved very efficiently via a sequence of such problems so as to approach the solution along a trajectory resembling the sequence of penalty function minima. This procedure proved very successful in practice and it was further developed into an EQP approach for the RQP method (Biggs 1972 and 1975; Murray and Wright 1978). For the equality constrained problem (A.4), the standard quadratic penalty function takes the form

$$Q(x) = F(x) + \tfrac{1}{2}r\sum_{i=1}^{l} c_i^2(x) \tag{A.29}$$

Minimizing the function $Q(x)$ in Eqn. (A.29) will not yield an exact solution to the equality constrained problem (A.4) and $rc(x)$ converges to the Lagrange multipliers of problem (A.4) as the penalty number increases. Therefore, to make the quadratic subproblem compatible with the quadratic line search function, it can be stated as follows

$$\text{(EQPP)} \qquad \begin{aligned} &\underset{d_k \in R^n}{\text{minimize}} && \nabla F(x_k)d_k + \tfrac{1}{2}d_k^T B_k d_k \\ &\text{subject to} && \nabla c(x_k)d_k + c(x_k) = \tfrac{1}{r}\hat{\Lambda} \end{aligned} \tag{A.30}$$

where $\hat{\Lambda}$ is an estimate of the Lagrange multipliers for the original nonlinear problem and might be computed using the update formulae discussed in Section A.2. Similarly, Biggs (1982) suggested that for the quadratic merit function in Eqn. (A.28), a new IQP subproblem should be considered for the NP problem as follows

$$\text{(IQPP)} \qquad \begin{aligned} &\underset{d_k \in R^n}{\text{minimize}} && \nabla F(x_k)d_k + \tfrac{1}{2}d_k^T B_k d_k \\ &\text{subject to} && A_k^{eq} d_k + c_k^{eq} = \tfrac{1}{r}\hat{\Lambda} \\ & && A_k^{in} d_k + c_k^{in} \le \tfrac{1}{r}\hat{\Gamma} \end{aligned} \tag{A.31}$$

where $\hat{\Lambda}$ and $\hat{\Gamma}$ are estimates of the Lagrange multipliers for the original problem. The IQPP subproblem (A.31) can be solved using active set strategy to develop a sequence of the EQPP subproblems. Numerical computations have identified cases where subproblem (A.31) is superior to the IQP subproblem (A.11) and, just as for the equality constrained problems, there are seldom any serious disadvantages in including the r-term (Biggs 1982). A good recursive quadratic programming algorithm might include the penalty term in the subproblem at points far from the solution and switch to $1/r=0$ at a suitable stage near the solution to obtain the most rapid ultimate convergence. Another advantage of the subproblems EQPP and IQPP with respect to the subproblems (A.10) and (A.11) is the compatibility of their constraints.

A.4. The Fletcher Active Set Strategy for Solving the QP Subproblem

The Fletcher algorithm is an iterative method based on an active set strategy (Fletcher 1971). At each iteration, there is a working set W_k which is to be treated as the active set. The algorithm generates a sequence of equality constrained quadratic programs which differ only in active constraints. Usually in each iteration one constraint is added or removed from the working set. Consider a general quadratic program with inequality constraints as follows

$$\begin{aligned} &\underset{d \in R^n}{\text{minimize}} && b^T d + \tfrac{1}{2}d^T G d \\ &\text{subject to} && a_i^T d = c_i \qquad i = 1,\ldots,m' \\ & && a_i^T d \le c_i \qquad i = m'+1,\ldots,m \end{aligned} \tag{A.32}$$

The matrix G is symmetric and positive semidefinite. The Fletcher algorithm for solving problem (A.32) can be stated as follows (Fletcher 1971; Luenberger 1989):

Step 1: Start with a working set W_o. Set $k=0$ and find a feasible initial solution d_o lying in the intersection of active constraints.

Step 2: Solve the equality constrained quadratic program (A.34) to obtain search direction p_k, use Eqn. (A.35), if p_k is zero go to *Step 4*.

Step 3: Set $d_{k+1} = d_k + \beta_k p_k$ where

$$\beta_k = \underset{a_i^T p_k > o}{minimum} \left[1, \frac{c_i - a_i^T d_k}{a_i^T p_k}\right] \tag{A.33}$$

If $\beta_k < 1$, then add the minimizing index in (A.33) to W_k to form W_{k+1}. Update matrices D_q and C_q using relations (A.39) and (A.40) . Set k=k+1 and return to *Step 2*.

Step 4: Compute the Lagrange multipliers of the problem (A.34) using Eqn. (A.36) or the formulae given in Section A.2. Then calculate the minimum of the Lagrange multipliers λ_t associated with the inequality constraints in the working set. If λ_t is nonnegative, stop and d_k is the optimal solution. Otherwise, remove t from W_k to form W_{k+1} and update matrices D_q and C_q using relations (A.41) and (A.42). Set k=k+1 and return to *Step 2*.

In *Step 2* the following equality constrained quadratic program must be solved to compute the increment vector p_k

$$\begin{aligned} &\underset{p_k \in R^n}{minimize} \quad g_k^T p_k + \tfrac{1}{2} p_k^T G p_k \\ &subject\ to \quad a_i^T p_k = 0 \qquad i \in W_k \end{aligned} \tag{A.34}$$

where $g_k = b + Gd_k$ is the gradient of the objective function for problem (A.32). The explicit solution for problem (A.34) can be written as

$$p_k = -D_q g_k \tag{A.35}$$

$$\Lambda_{k+1} = -C_q g_k \tag{A.36}$$

where q is the number of active constraints in the working set W_k and matrices $D_q(n \times n)$ and $C_q(q \times n)$ are defined as follows

$$D_q = \left[I - G^{-1}A_q[A_q^T G^{-1} A_q]^{-1} A_q^T\right] G^{-1} \tag{A.37}$$

$$C_q = [A_q^T G^{-1} A_q]^{-1} A_q^T G^{-1} \tag{A.38}$$

where A_q is a matrix whose columns are the vectors a_1 to a_q. Fletcher (1971) introduced the recurrence relations for updating matrices D_q and C_q when a constraint is added to or removed from the working set. These updating formulae make the algorithm very efficient.

Adding a constraint. Suppose that we wish to add the (q+1)th constraint, whose coefficients vector is a_{q+1}, to the working set, the recurrence relations are stated as

$$D_{q+1} = D_q - \frac{vv^T}{v^T a_{q+1}} \tag{A.39}$$

$$C_{q+1} = \begin{pmatrix} C_q \\ 0 \end{pmatrix} + \begin{pmatrix} -C_q a_{q+1} \\ 1 \end{pmatrix} \frac{v^T}{v^T a_{q+1}} \tag{A.40}$$

where $v = D_q a_{q+1}$.

Removing a constraint. To remove the qth constraint from the working set, the recurrence relations take the forms as

$$\begin{pmatrix} C_{q-1} \\ 0 \end{pmatrix} = C_q - C_q \frac{G h h^T}{h^T G h} \tag{A.41}$$

$$D_{q-1} = D_q + \frac{h h^T}{h^T G h} \tag{A.42}$$

where h^T is the qth row of C_q corresponding to the constraint being removed. Permutation of columns of C_q enables the same formula to be used to remove any constraint from the working set. It should be noted that for n active constrains, $D_n = 0$ and $C_n = A_n^{-1}$.

A.5. References

Biggs, M. C. (1972). Constrained minimization using recursive equality quadratic programming. *Numerical Methods for Nonlinear Optimization,* (Lootsma, F. A., ed.). Academic Press, London. 411-428.

Biggs, M. C. (1975). Constrained minimization using recursive quadratic programming: some alternative subproblem formulations. *Towards Global Optimization,* (Dixon, L. C. W., and Szego, G. P., eds.). North-Holland Publishing Co., Amsterdam, North-Holland.

Biggs, M. C. (1982). Recursive quadratic programming methods for nonlinear constraints. *Nonlinear Optimization 1981,* (Powell, M. J. D., ed.). Academic Press, New York. 213-221.

Coleman, T. F., and Conn, A. R. (1980). Nonlinear programming via an exact penalty function method: asymptotic analysis. *Mathematical Programming.* **24.** 123-136.

Coleman, T. F., and Conn, A. R. (1980). Nonlinear programming via an exact penalty function method: global analysis. *Mathematical Programming.* **24.** 137-161.

Fletcher, R. (1971). A general quadratic programming algorithm. *Journal of Institute of Mathematics and its Applications.* **7.** 76-91.

Fletcher, R. (1973). An exact penalty function for nonlinear programming with inequalities. *Mathematical Programming.* **5.** 129-150.

Fletcher, R. (1975). An ideal penalty function for constrained optimization. *Journal of Institute of Mathematics and its Applications.* **15.** 319-342.

Han, S. P. (1977). A globally convergent method for nonlinear programming. *Journal of Optimization Theory and Applications.* **22.** 297-309.

Luenberger, D. G. (1989). *Linear and Nonlinear Programming.* Addison-Wesley Publishing Co.

Murray, W. (1969). An algorithm for constrained minimization. *Optimization,* (Fletcher, R., ed.). Academic Press, London. 247-258.

Murray, W., and Wright M. H. (1978). Projected Lagrangian methods based on the trajectories of penalty and barrier functions. *Report SOL 78-23*, Department of Operations Research, Stanford University. Stanford, California.

Murray, W., and Wright M. H. (1982). Computation of the search direction in constrained optimization algorithm. *Mathematical Programming Study.* **16.** 62-83.

O'Leary, D. P. (1980). A generalized conjugate gradient algorithm for solving a class of quadratic programming problems. *Linear Algebra and Its Applications.* **34.** 371-399.

Powell, M. J. D. (1978). A fast algorithm for nonlinearly constrained optimization calculation. *Numerical Analysis, Dundee, 1977,* (Watson, G. A., ed.). Springer-Verlag, Berlin. 144-157.

Tapia, R. A. (1977). Diagonalized multiplier methods and quasi-Newton methods for constrained optimization. *Journal of Optimization Theory and Applications.* **22.** 135-194.

Van der Hoek, G. (1980). *Reduction Methods in Nonlinear Programming.* Mathematish Centrum, Amsterdam.

Wilson, R. B. (1963). A simplical algorithm for concave programming. Ph.D. Thesis, Graduate School of Business, Administration, Harvard University.

Appendix B

Element Sensitivity Matrices

In this appendix we shall show that the sensitivity of the element mass, damping, and stiffness matrices with respect to the unknown constitutive parameters, one of the primary computational steps in parameter estimation, can be generated in an elegant and straightforward procedure. Since we have assumed that the topology and the geometry of the structure are known, computation of the global sensitivity matrices can be accomplished on an element-by-element basis and combined with the standard assembly process. Here, we derive the relationships for computing the element sensitivity matrix $\boldsymbol{U}^e$ (or $\boldsymbol{U}_K^e$, $\boldsymbol{U}_M^e$, and $\boldsymbol{U}_C^e$ for stiffness, mass, and damping, respectively) specifically for finite elements that are computed by numerical quadrature. The procedure can consider elements with kinematic or material nonlinearity and covers a wide range of finite element models using one dimensional to three (or higher) dimensional elements. For some elements the element stiffness, damping, and mass matrices can be expressed explicitly. The element sensitivities for these elements are straightforward to compute, as we will show for frame elements later in this appendix.

For the sake of the present discussion, let us assume that the geometry of the element is described in a coordinate system with local spatial coordinates z. Transformation to a global coordinate system is standard and will not be included in these derivations. Let Ω^e designate the spatial domain (volume) of the element. In most cases, the context will be sufficient to distinguish between stiffness, mass, and damping parameters. Thus, we will simply designate the parameters associated with an element as $\boldsymbol{x}^e$, unless the ambiguity of the context demands that we refer to them more specifically as mass, $\boldsymbol{x}_M^e$, damping, $\boldsymbol{x}_C^e$, and stiffness $\boldsymbol{x}_K^e$ parameters. Generally the stiffness matrix depends only on stiffness parameters, the mass matrix only on mass parameters, and the damping matrix only on damping parameters. We discuss Rayleigh damping as a special exception to this rule.

B.1. Sensitivity Matrices for Numerically Integrated Elements

Element Stiffness Sensitivity Matrix. Starting from the principle of virtual work, one generally expresses the element stiffness matrix $\boldsymbol{K}^e(\boldsymbol{x}^e)$ as an integral over the domain of the element as follows

$$\boldsymbol{K}^e(\boldsymbol{x}^e) = \int_{\Omega^e} \boldsymbol{B}^{eT}(z)\boldsymbol{E}^e(z,\boldsymbol{x}^e)\boldsymbol{B}^e(z)\,dz \tag{B.1}$$

where $\boldsymbol{x}^e$ is the vector of element constitutive parameters. The matrix $\boldsymbol{B}^e(z)$ has dimension $(n_\varepsilon^e \times n_d^e)$ and represents the strain-displacement operator and the matrix $\boldsymbol{E}^e(z,\boldsymbol{x}^e)$ has dimension $(n_\varepsilon^e \times n_\varepsilon^e)$ and represents the material constitutive properties, both for the eth element. The matrix dimensions are indexed as follows: n_d^e is the number of displacement degrees of freedom associated with the element and n_ε^e is the number of

strain measures defined for the eth element. For example, a two noded planar truss element has n_d^e equal to four (two components of translation at each end) and n_ε^e equal to one (axial strain); a two noded planar beam element has n_d^e equal to six (two components of translation and one rotation at each end) and n_ε^e equal to three (axial strain, shear strain, and flexural curvature).

Let $\boldsymbol{d}^e(z)$ have dimension $(n_{df}^e \times 1)$ and let it designate the continuous displacement field associated with the eth element. Further, let $\boldsymbol{\varepsilon}^e(z)$ have dimension $(n_\varepsilon^e \times 1)$ and let it designate the strain field. The relationship between displacement and strain can then be written as

$$\boldsymbol{\varepsilon}^e(z) = \boldsymbol{L}^e(\boldsymbol{d}^e(z)) \tag{B.2}$$

The differential operator $\boldsymbol{L}^e$ has dimension $(n_\varepsilon^e \times n_{df}^e)$, where n_{df}^e is the number of quantities required to characterize the displacement field for the eth element. We approximate the continuous displacement field by interpolating the nodal displacements $\boldsymbol{u}^e$ (in local coordinates) with appropriately selected element shape functions, $\boldsymbol{N}^e(n_{df}^e \times n_d^e)$. The displacement field is then approximated as

$$\boldsymbol{d}^e(z) = \boldsymbol{N}^e(z)\boldsymbol{u}^e \tag{B.3}$$

Substituting Eqn. (B.3) into (B.2), the strain field can be expressed in terms of the local displacements $\boldsymbol{u}^e$ as follows

$$\boldsymbol{\varepsilon}^e(z) = \boldsymbol{B}^e(z)\boldsymbol{u}^e \tag{B.4}$$

where the strain-displacement matrix $\boldsymbol{B}^e(z)$ depends only on the geometric characteristics of the element, and is defined by substituting Eqns. (B.2) and (B.3) into Eqn. (B.4):

$$\boldsymbol{B}^e(z) = \boldsymbol{L}^e(\boldsymbol{N}^e(z)) \tag{B.5}$$

The differential operator matrix $\boldsymbol{L}^e$ can be either linear or nonlinear. Therefore, for a finite element model which is kinematically nonlinear, the present formulation can be used with only slight modification.

In general, the element stiffness matrix $\boldsymbol{K}^e$ can be implicitly computed by numerically integrating Eqn. (B.1) using Gauss quadrature. To wit

$$\boldsymbol{K}^e(x^e) = \sum_{m=1}^{n_{GP}^e} w_m \boldsymbol{B}^{eT}(z_m)\boldsymbol{E}^e(z_m, x^e)\boldsymbol{B}^e(z_m) \tag{B.6}$$

where w_m is the weight associated with the mth Gauss station z_m, and n_{GP}^e is the number of Gauss points in the eth element needed to integrate the element stiffness matrix $\boldsymbol{K}^e$. From these definitions one can easily see that

$$\frac{\partial[\boldsymbol{K}^e(x^e)\boldsymbol{u}^e]}{\partial x^e} = \sum_{m=1}^{n_{GP}^e} w_m \boldsymbol{B}^{eT}(z_m)\left[\frac{\partial[\boldsymbol{E}^e(z_m, x^e)]}{\partial x^e}\right]\boldsymbol{B}^e(z_m)\boldsymbol{u}^e \equiv \boldsymbol{U}_K^e \tag{B.7}$$

The ijth component of the element sensitivity matrix $\boldsymbol{U}_K^e$ is given by

$$[U_K^e]_{ij} = \left[\frac{\partial[K^e(x^e)u^e]}{\partial x^e}\right]_{ij} = \frac{\partial[K^e(x^e)u^e]_i}{\partial x_j^e} \tag{B.8}$$

In general, the element sensitivity matrix $\boldsymbol{U}_K^e$ is a function of displacements $\boldsymbol{u}^e$ and constitutive parameters $\boldsymbol{x}^e$. If the explicit form of the stiffness matrix is known, one can use Eqn. (B.8) to compute $\boldsymbol{U}_K^e$ explicitly, just as we have done for the Timoshenko beam element in Section B.2. However, for most elements (*e.g.* shell, plane stress, block, and plate elements), $\boldsymbol{K}^e$ is numerically generated. The matrix $\boldsymbol{E}^e$ which defines the relations between strains and stresses is a function of unknown constitutive parameters for each element $\boldsymbol{x}^e$. If the members of the material matrix are linear in constitutive parameters, which many elements are, then the derivative is particularly simple to express. Often this matrix is also diagonal. For example, for the truss element EA (axial stiffness) is the only member of $\boldsymbol{E}^e$, and for a planar beam element $\boldsymbol{E}^e$ is a diagonal matrix of the axial stiffness EA, flexural stiffness EI and shear stiffness GA.

Element Mass Sensitivity Matrix. There are basically two categories of mass that are important to us: *(a)* mass associated with structural elements, and *(b)* mass associated with non-structural elements. The former mass is associated with the nodes of the mathematical model, while the later is associated with the elements. The mass matrix of a structural element can be modeled as either a consistent mass matrix or a lumped mass matrix. We shall discuss the former.

The consistent mass matrix for an element of mass density $\varrho^e(z, \boldsymbol{x}^e)$ can be expressed as

$$M^e(x^e) = \int_{\Omega^e} \varrho^e(z, x^e) N^{eT}(z) N^e(z) dz \tag{B.9}$$

where $\boldsymbol{N}^e(z)$ is the matrix of element shape functions used to approximate the acceleration field (usually the same as those used for the displacement field) for the eth element. The mass matrix can be computed by Gaussian quadrature as follows

$$M^e(x^e) = \sum_{m=1}^{n_{GP}^e} w_m \varrho^e(z_m, x^e) N^{eT}(z_m) N^e(z_m) \tag{B.10}$$

where w_m is the weight associated with the mth Gauss station z_m, and n_{GP}^e is the number of Gauss points in the eth element needed to integrate the element mass matrix. From these definitions one can easily see that

$$\frac{\partial[M^e(x^e)\ddot{u}^e]}{\partial x^e} = \sum_{m=1}^{n_{GP}^e} w_m \left[\frac{\partial \varrho^e(z_m, x^e)}{\partial x^e}\right] N^{eT}(z_m) N^e(z_m) \ddot{u}^e \equiv U_M^e \tag{B.11}$$

The ijth component of the element sensitivity matrix $\boldsymbol{U}_M^e$ is

$$[U_M^e]_{ij} = \frac{\partial[M^e(x^e)\ddot{u}^e]_i}{\partial x_j^e} \tag{B.12}$$

For the consistent element mass matrix the number of parameters is unity.

Element Damping Sensitivity Matrix. Among stiffness, damping, and mass, damping is the most poorly understood. According to our model problem, damping is velocity dependent, implying some sort of viscous damping mechanism. In reality, however, we generally associate many different phenomena with damping. Among these we find dry friction, slip mechanisms, and hysteretic energy loss. The absence of a compelling physical basis for damping complicates its mathematical modeling. Here we discuss only the standard viscous model and the case of Rayleigh damping.

A parametrically linear, consistent viscous damping model gives rise to the following element damping matrix.

$$C^e(x^e) = \int_{\Omega^e} \mu^e(z,x^e) N^{eT}(z) N^e(z)\, dz \tag{B.13}$$

where $N_e(z)$ is the matrix of element shape functions used to approximate the velocity field, $\mu^e(z,x^e)$ is the material damping field, analogous to viscosity, for the eth element. The damping matrix can be computed by Gaussian quadrature as follows

$$C^e(x^e) = \sum_{m=1}^{n^e_{GP}} w_m \mu^e(z_m,x^e) N^{eT}(z_m) N^e(z_m) \tag{B.14}$$

where w_m is the weight associated with the mth Gauss station z_m, and n^e_{GP} is the number of Gauss points in the eth element needed to integrate the element damping matrix. From these definitions one can easily see that

$$\frac{\partial[C^e(x^e)\dot{u}^e]}{\partial x^e} = \sum_{m=1}^{n^e_{GP}} w_m \left[\frac{\partial \mu^e(z_m,x^e)}{\partial x^e}\right] N^{eT}(z_m) N^e(z_m)\dot{u}^e \equiv U^e_C \tag{B.15}$$

The ijth component of the element sensitivity matrix U^e_C is

$$[U^e_C]_{ij} = \frac{\partial[C^e(x^e)\dot{u}^e]_i}{\partial x^e_j} \tag{B.16}$$

For consistent element damping matrix the number of parameters is unity. Although, consistent damping matrix C^e has a strong physical basis for a Newtonian fluid, viscous damping is less popular in structural mechanics than dry friction and hysteresis loss.

There are other interesting damping models. For example, one model often used in structural dynamics is the two parameter Rayleigh damping model. In this model the damping is assumed to be proportional to the mass and stiffness matrix

$$C(\mu_1,\mu_2,x_K,x_M) = \mu_1 K(x_K) + \mu_2 M(x_M) \tag{B.17}$$

Clearly, for this model, the damping matrix is not only a function of the damping parameters μ_1 and μ_2, but also a function of the mass and stiffness parameters x_M and x_K. The computation of the gradient of the damp-

ing matrix with respect to constitutive parameters is straightforward, but must reflect the couping of the parameters. The main motivation for using the Rayleigh damping model in direct analysis problems is that it is diagonalized by the normal modes of vibration. Orthogonality with respect to the normal modes is not important to the inverse problem, and hence the Rayleigh damping model may be unnecessarily complicated and overly restrictive.

Assembly of Global Sensitivity Matrices. The global sensitivity matrix consists of three structural sensitivity matrices $\boldsymbol{U}_K$, $\boldsymbol{U}_C$, and $\boldsymbol{U}_M$ computed by assembling element sensitivity matrices. The rows of the element sensitivity matrices $\boldsymbol{U}_K^e$, $\boldsymbol{U}_C^e$, and $\boldsymbol{U}_M^e$ are assembled into rows of the structural sensitivity matrices $\boldsymbol{U}_K$, $\boldsymbol{U}_C$, and $\boldsymbol{U}_M$ according to the connectivity of elements (just like the assembly of element stiffness matrices into the global stiffness matrix). The columns of the element sensitivity matrices are assembled into the columns of the structural sensitivity matrices according to their parameter group index. For example, if stiffness parameters of two elements belong to the same stiffness parameter group, the columns of their stiffness sensitivity matrices are assembled in the same column of the matrix $\boldsymbol{U}_K$. These two elements might have different mass and damping properties, putting them in different mass and damping parameter groups.

B.2. Sensitivity Matrices for Frame Elements

In this section we derive the sensitivity matrices for a truss bar element, a Bernoulli-Euler beam element, and a Timoshenko beam element. The mass, and damping matrices of these three element are linear with respect to their mass, $\boldsymbol{x}_M^e$, and damping parameters, $\boldsymbol{x}_C^e$. The stiffness matrices of the truss bar and the Bernoulli-Euler beam element are also linear with respect to their stiffness parameters $\boldsymbol{x}_K^e$ (*EA*, or *EA* and *EI*, respectively). The stiffness matrix for the Timoshenko beam element is nonlinear with respect to its parameters *EA*, *EI*, and *GA*.

Truss Bar. To implement the procedure developed in Section B.1, first, we implicitly compute the stiffness element sensitivity matrix and then we use the explicit mass and damping matrices and compute the mass and damping element sensitivity matrices.

For a planar truss bar with three degrees of freedom at each end, there is only one deformation field, axial deformation $u(z)$, one strain field, axial strain $\varepsilon(z)$, and one stiffness parameter *EA*. Using the notations defined in the earlier sections, for a truss element we have the following properties: number of degrees of freedom associated with the element, $n_d^e = 6$, number of strain measures, $n_\varepsilon^e = 1$, number of quantities required to describe the displacement field, $n_{df}^e = 1$, and number of constitutive parameters, $n_p^e = 1$. The displacement field is completely described by the axial displacement, hence $d^e(z) = u(z)$. For a truss element axial strain is the only possible deformation, hence $\varepsilon^e(z) = \varepsilon(z)$. Figure B.1 shows the nodal displacements $u^{eT} = [u_1 \;\; v_1 \;\; \theta_1 \;\; u_2 \;\; v_2 \;\; \theta_2]$ for a general one-dimensional, planar element in the element local coordinate system.

The deformation field along the truss element can be approximated using linear Lagrangian shape functions $N = [1-z/l \;\; 0 \;\; 0 \;\; z/l \;\; 0 \;\; 0]$ as follows

$$u(z) \;=\; N(z)u^e \;=\; (1-z/l)u_1 + (z/l)u_2 \tag{B.18}$$

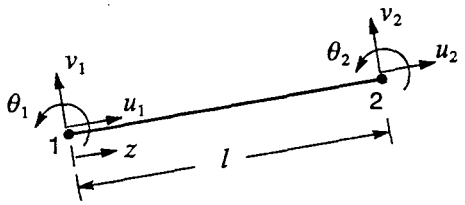

Fig. B.1 Geometric deformation of planar truss and beam elements

Using Eqn. (B.2) the strain-displacement relation in element local coordinates can be written as

$$\varepsilon(z) = \frac{\partial}{\partial z}[u(z)] \tag{B.19}$$

where $\boldsymbol{L}^e \equiv \partial/\partial z$ is the differential operator defined in Eqn. (B.2). The strain-displacement matrix $\boldsymbol{B}^e$ based on Eqn. (B.5) will be

$$\boldsymbol{B}^e = [-\tfrac{1}{l} \quad 0 \quad 0 \quad \tfrac{1}{l} \quad 0 \quad 0] \tag{B.20}$$

The material matrix $\boldsymbol{E}^e$ and the vector of parameters $\boldsymbol{x}_K^e$ each has only one member, the axial stiffness EA. Using Eqn. (B.1) we compute the element stiffness matrix which is a (6×6) sparse matrix with only four nonzero members as follows

$$K_{11} = K_{44} = -K_{14} = -K_{41} = \frac{EA}{l} \tag{B.21}$$

The stiffness element sensitivity matrix $\boldsymbol{U}_K^e(6 \times 1)$ can simply be computed using Eqn. (B.8)

$$\boldsymbol{U}_K^{eT} = [\frac{u_1 - u_2}{l} \quad 0 \quad 0 \quad \frac{u_2 - u_1}{l} \quad 0 \quad 0] \tag{B.22}$$

Since the stiffness matrix of a truss bar is linear in its parameters, the stiffness element sensitivity matrix $\boldsymbol{U}_K^e$ is only a function of the nodal displacements.

One can also compute the mass matrix from the shape functions. Let us assume that the density per unit of length is constant. Using Eqn. (B.9) and the linear Lagrangian shape functions defined previously, the consistent mass matrix for a truss element takes the following form

$$\boldsymbol{M}^e(\varrho^e)\ddot{\boldsymbol{u}}^e = \frac{\varrho^e l}{6}\begin{bmatrix} 2 & 0 & 0 & 1 & 0 & 0 \\ 0 & 2 & 0 & 0 & 1 & 0 \\ 0 & 0 & 0 & 0 & 0 & 0 \\ 1 & 0 & 0 & 2 & 0 & 0 \\ 0 & 1 & 0 & 0 & 2 & 0 \\ 0 & 0 & 0 & 0 & 0 & 0 \end{bmatrix}\begin{bmatrix} \ddot{u}_1 \\ \ddot{v}_1 \\ \ddot{\theta}_1 \\ \ddot{u}_2 \\ \ddot{v}_2 \\ \ddot{\theta}_2 \end{bmatrix} \tag{B.23}$$

where $\ddot{u}^e$ is the vector of nodal accelerations in the element local coordinates system. The consistent mass matrix is only a function of the mass density ϱ^e, therefore the mass element sensitivity matrix $U_M^e(6 \times 1)$ is a vector which can explicitly be computed as follows

$$U_M^{e\,T} = \frac{l}{6}\left[2\ddot{u}_1 + \ddot{u}_2 \quad 2\ddot{v}_1 + \ddot{v}_2 \quad 0 \quad \ddot{u}_1 + 2\ddot{u}_2 \quad \ddot{v}_1 + 2\ddot{v}_2 \quad 0\right] \tag{B.24}$$

From Eqns. (B.9) and (B.13), the consistent mass and damping matrices for a truss element have the same form and consequently, the sensitivity matrices also have the same form. Using Eqn. (B.24) and replacing the vector of the nodal accelerations $\ddot{u}$ with the vector of the nodal velocities $\dot{u}$ the damping sensitivity matrix U_C^e will be

$$U_C^{e\,T} = \frac{l}{6}\left[2\dot{u}_1 + \dot{u}_2 \quad 2\dot{v}_1 + \dot{v}_2 \quad 0 \quad \dot{u}_1 + 2\dot{u}_2 \quad \dot{v}_1 + 2\dot{v}_2 \quad 0\right] \tag{B.25}$$

where l is the length of the truss bar and the nodal velocities are defined the same as nodal displacements shown in Fig. B.1.

Bernoulli-Euler Beam Element. The explicit stiffness matrix for a Bernoulli-Euler beam element, which is linear with respect to its constitutive parameters EA and EI, is given by the following

$$K^e(x^e)u = \frac{1}{l^3}\begin{bmatrix} l^2EA & 0 & 0 & -l^2EA & 0 & 0 \\ 0 & 12EI & 6lEI & 0 & -12EI & 6lEI \\ 0 & 6lEI & 4l^2EI & 0 & -6lEI & 2l^2EI \\ -l^2EA & 0 & 0 & l^2EA & 0 & 0 \\ 0 & -12EI & -6lEI & 0 & 12EI & -6lEI \\ 0 & 6lEI & 2l^2EI & 0 & -6lEI & 4l^2EI \end{bmatrix}\begin{bmatrix} u_1 \\ v_1 \\ \theta_1 \\ u_2 \\ v_2 \\ \theta_2 \end{bmatrix} \tag{B.26}$$

Using the element stiffness matrix given in Eqn. (B.26) one can explicitly compute the stiffness sensitivity matrix U_K^e as follows

$$U_K^e = \frac{1}{l^3}\begin{bmatrix} l^2(u_1 - u_2) \\ 12(v_1 - v_2) + 6l(\theta_1 + \theta_2) \\ 6l(v_1 - v_2) + 2l^2(2\theta_1 + \theta_2) \\ l^2(u_2 - u_1) \\ 12(v_2 - v_1) - 6l(\theta_1 + \theta_2) \\ 6l(v_1 - v_2) + 2l^2(\theta_1 + 2\theta_2) \end{bmatrix} \tag{B.27}$$

The consistent mass matrix for a Bernoulli-Euler beam element is

$$M^e(\varrho^e)\ddot{u}^e = \frac{\varrho^e l}{420}\begin{bmatrix} 140 & 0 & 0 & 70 & 0 & 0 \\ 0 & 156 & 22l & 0 & 54 & -13l \\ 0 & 22l & 4l^2 & 0 & 13l & -3l^2 \\ 70 & 0 & 0 & 140 & 0 & 0 \\ 0 & 54 & 13l & 0 & 156 & -22l \\ 0 & -13l & -3l^2 & 0 & -22l & 4l^2 \end{bmatrix}\begin{bmatrix} \ddot{u}_1 \\ \ddot{v}_1 \\ \ddot{\theta}_1 \\ \ddot{u}_2 \\ \ddot{v}_2 \\ \ddot{\theta}_2 \end{bmatrix} \tag{B.28}$$

The element mass matrix, Eqn. (B.28), is linear with respect to the mass density ϱ^e and one can easily and explicitly compute the mass element sensitivity matrix for the Bernoulli-Euler beam element as

$$U_M^e = \frac{l}{420}\begin{bmatrix} 70(2\ddot{u}_1 + \ddot{u}_2) \\ (156\ddot{v}_1 + 54\ddot{v}_2) + l(22\ddot{\theta}_1 - 13\ddot{\theta}_2) \\ l(22\ddot{v}_1 + 13\ddot{v}_2) + l^2(4\ddot{\theta}_1 - 3\ddot{\theta}_2) \\ 70(\ddot{u}_1 + 2\ddot{u}_2) \\ (54\ddot{v}_1 + 156\ddot{v}_2) + l(13\ddot{\theta}_1 - 22\ddot{\theta}_2) \\ -l(13\ddot{v}_1 + 22\ddot{v}_2) - l^2(3\ddot{\theta}_1 - 4\ddot{\theta}_2) \end{bmatrix} \tag{B.29}$$

Since the consistent element mass and damping matrices are constructed in the same way, their sensitivity matrices also have the same form. Replacing the vector of the nodal accelerations $\ddot{u}$ with the vector of the nodal velocities $\dot{u}$ we can compute the damping sensitivity matrix U_C^e as follows

$$U_C^e = \frac{l}{420}\begin{bmatrix} 70(2\dot{u}_1 + \dot{u}_2) \\ (156\dot{v}_1 + 54\dot{v}_2) + l(22\dot{\theta}_1 - 13\dot{\theta}_2) \\ l(22\dot{v}_1 + 13\dot{v}_2) + l^2(4\dot{\theta}_1 - 3\dot{\theta}_2) \\ 70(\dot{u}_1 + 2\dot{u}_2) \\ (54\dot{v}_1 + 156\dot{v}_2) + l(13\dot{\theta}_1 - 22\dot{\theta}_2) \\ -l(13\dot{v}_1 + 22\dot{v}_2) - l^2(3\dot{\theta}_1 - 4\dot{\theta}_2) \end{bmatrix} \tag{B.30}$$

Timoshenko Beam Element. For a Timoshenko beam element the vector of parameters x_K^e consists of axial stiffness, *EA*, flexural stiffness, *EI*, and shear stiffness, *GA*, thus $n_p^e = 3$. Figure B.1 shows the nodal displacements for this element. Again there are six element displacement degrees of freedom $n_d^e = 6$, but there are three quantities required to describe the displacement $n_{df}^e = 3$ (axial displacement, transverse displacement, and rotation of the normal to the cross section), and three strain quantities $n_\varepsilon^e = 3$ (axial stretch, shearing, and flexural curvature). For a planar Timoshenko beam, one could follow the procedure used for the truss element and implicitly compute the stiffness matrix. It turns out to be nonlinear in its parameters. We will, however, simply use the explicit form of the stiffness matrix to compute its stiffness sensitivity matrix. for this element. The stiffness matrix for this element can be written as

$$K^e(x^e)u = \frac{1}{l^3}\begin{bmatrix} l^2EA & 0 & 0 & -l^2EA & 0 & 0 \\ 0 & 12a_1 & 6la_1 & 0 & -12a_1 & 6la_1 \\ 0 & 6la_1 & 2l^2(2a_1+a_2) & 0 & -6la_1 & 2l^2(a_1-a_2) \\ -l^2EA & 0 & 0 & l^2EA & 0 & 0 \\ 0 & -12a_1 & -6la_1 & 0 & 12a_1 & -6la_1 \\ 0 & 6la_1 & 2l^2(a_1-a_2) & 0 & -6la_1 & 2l^2(2a_1+a_2) \end{bmatrix}\begin{bmatrix} u_1 \\ v_1 \\ \theta_1 \\ u_2 \\ v_2 \\ \theta_2 \end{bmatrix} \tag{B.31}$$

where the scalars $a_1 = EI/(2a_3 + 1)$, $a_2 = a_1a_3$, and $a_3 = 6EI/(GAl^2)$. Using Eqn. (B.8) we can compute the stiffness element sensitivity matrix U_K^e, and it has the following form

$$U_K^e = \begin{bmatrix} d_{11}^e & 0 & 0 \\ 0 & d_{22}^e b_1 & d_{22}^e b_2 \\ 0 & d_{32}^e b_1 + d_{33}^e b_3 & d_{32}^e b_2 + d_{33}^e b_4 \\ d_{41}^e & 0 & 0 \\ 0 & d_{52}^e b_1 & d_{52}^e b_2 \\ 0 & d_{62}^e b_1 + d_{63}^e b_3 & d_{62}^e b_2 + d_{63}^e b_4 \end{bmatrix} \tag{B.32}$$

where scalars d_{ij} and b_i are defined as follows

$$\begin{cases} d_{11}^e = d_{41}^e = \frac{1}{l}(u_1 - u_2) \\ d_{22}^e = -d_{52}^e = \frac{12}{l^3}(v_1 - v_2) + \frac{6}{l^2}(\theta_1 + \theta_2) \\ d_{32}^e = \frac{6}{l^3}(v_1 - v_2) + \frac{2}{l}(2\theta_1 + \theta_2) \\ d_{33}^e = -d_{63}^e = \frac{2}{l}(\theta_1 - \theta_2) \\ d_{62}^e = \frac{6}{l^3}(v_1 - v_2) + \frac{2}{l}(\theta_1 + 2\theta_2) \end{cases}$$

$$\begin{cases} \beta = 12EI + l^2GA \\ b_1 = \frac{\partial a_1}{\partial(EI)} = \frac{(GAl^2)^2}{\beta^2} \\ b_2 = \frac{\partial a_1}{\partial(GA)} = \frac{12(EAI)^2}{\beta^2} \\ b_3 = \frac{\partial a_2}{\partial(EI)} = \frac{72(EI)^2 + 12(GA)(EI)l^2}{\beta^2} \\ b_4 = \frac{\partial a_2}{\partial(GA)} = \frac{-6(EI)^2l^2}{\beta^2} \end{cases} \tag{B.33}$$

The mass and damping element sensitivity matrices for a Timoshenko beam element are the same as for a truss element, except that the terms corresponding to the rotational degrees of freedom are not zero. The mass and damping element sensitivity matrices will be as follows

$$U_M^{e\,T} = \frac{l}{6}\left[2\ddot{u}_1 + \ddot{u}_2 \quad 2\ddot{v}_1 + \ddot{v}_2 \quad 2\ddot{\theta}_1 + \ddot{\theta}_2 \quad \ddot{u}_1 + 2\ddot{u}_2 \quad \ddot{v}_1 + 2\ddot{v}_2 \quad \ddot{\theta}_1 + 2\ddot{\theta}_2\right] \tag{B.34}$$

and

$$U_C^{e\,T} = \frac{l}{6}\left[2\dot{u}_1 + \dot{u}_2 \quad 2\dot{v}_1 + \dot{v}_2 \quad 2\dot{\theta}_1 + \dot{\theta}_2 \quad \dot{u}_1 + 2\dot{u}_2 \quad \dot{v}_1 + 2\dot{v}_2 \quad \dot{\theta}_1 + 2\dot{\theta}_2\right] \tag{B.35}$$

Bibliography

A

Agbabian, M. S., Masri, S. F., Miller, R. K., and Caughey, T. K. (1991). System identification approach to detection of structural changes. *ASCE Journal of Engineering Mechanics.* **117**(2). 370-390.

Aktan, A. E. and Ho, I.-K. (1990). Seismic vulnerability evaluation of existing buildings. *Earthquake Spectra.* **6**(3). 439-472.

Arapostathis, A. and Marcus, S. I. (1990). Analysis of an identification algorithm arising in the adaptive estimation of Markov chains. *Math. Control Signals Systems.* **3**. 1-29.

Archer, J. S. (1965). Consistent matrix formulations for structural analysis using finite-element techniques. *AIAA J.*, 3(10). 1910-1918.

B

Banan, M. R., Banan, M. R., and Hjelmstad K. D. (1992). Parameter estimation in linear complex structures. *ASCE Especial Conference: Probabilistic mechanics and Structural & Geotechnical Reliability.* July 8-10. Denver, Colorado. 571-574.

Baruch, M. (1978). Optimization procedure to correct stiffness and flexibility matrices using vibration tests. *AIAA J.*, 16(11). 1208-1210.

Baruch, M. and Bar-Itzhack, I. Y. (1979). Optimal weighted orthogonalization of Measured Modes. *AIAA J.*, **16**. 346-351.

Baruch, M. (1979). Selective optimal orthogonalization of measured modes. *AIAA J.*, **17**. 120-121.

Baruch, M. (1980). Proportional optimal orthogonalization of measured modes. *AIAA J.*, **18**. 859-861.

Baruch, M. (1981). Reply by author to W. Rodden. *AIAA J.*, **19**. 544.

Baruch, M. (1982). Optimal correction of mass and stiffness matrices using measured modes. *AIAA J.*, **20**(11). 1623-1626.

Baruch, M. (1984). Methods of reference basis for identification of linear dynamic structures. *AIAA J.*, **22**(4). 561-564.

Baruh, H. and Silverberg, L. M. (1986). Identification of external excitations in self-adjoint distributed systems using modal filters. *Journal of Sound and Vibration.* **108**(2). 247-260.

Baruh, H. and Choe, K. (1987). Sensor-failure detection method for flexible structures. *AIAA Journal of Guidance.* **10**(5). 474-482.

Baruh, H. and Khatri, H. P. (1988). Identification of modal parameters in vibrating structures. *Journal of Sound and Vibration.* **125**(3). 413-427.

Baruh, H. and Boka, J. (1992). Issues in modal identification of flexible structures. *AIAA J.*, **30**(1). 214-225.

Batill, S. M. and Hollkamp, J. J. (1989). Parameter identification of discrete-time series models for structural response prediction. *AIAA J.*, **27**(11). 1636-1643.

Beck, J. L. and Jennings, P. C. (1980). Structural identification using linear models and earthquake records. *Earthquake Engineering and Structural Dynamics.* **8**. 145-160.

Beck, J. L. (1982). System identification applied to strong motion records from structures. From *Earthquake Ground Motion and its Effects on Structures* (S.K. Dhatta, ed.) AMD -Vol. 53. Proceedings of ASME Winter Annual Meeting. November.

Bekey, G. A. (1970). System identification -an introduction and a survey. *Simulation.* **15**: 151-166.

Beliveau, J.-G. (1976). Identification of viscous damping in structures from modal information. *Journal of Applied Mechanics. Transaction of the ASME.* 335-339.

Beliveau, J.-G. (1977). Eigenrelations in structural dynamics. *AIAA J.*, **15**. 1039-1041

Beliveau, J.-G. (1987). System identification of civil engineering structures. *Canadian Journal of Civil Engineering.* **14**. 7-18.

Bendat, J. S. and Piersol, A. (1971). *Random data analysis and measurement procedures.* Wiley Interscience.

Ben-Haim, Y. (1990). Detecting unknown lateral forces on a bar by vibration measurement. *Journal of Sound and Vibration.* **140**(1). 13-29.

Berman, A. and Flannelly, W. (1971). Theory of incomplete models of dynamic structures. *AIAA J.*, **9**(8). 1481-1487.

Berman, A. (1979). Mass matrix correction using an incomplete set of measured modes. *AIAA J.*, **17**(10). 1147-1148.

Berman, A. (1979). Parameter identification techniques for vibrating structures. *Shock and Vibration Digest.* **11**(1). 13-16.

Berman, A. (1979). Comment on optimal weighted orthogonalization of measured modes. *AIAA J.*, **17**. 927-928.

Berman, A., Wei, F., and Rao, K. (1980). Improvement of analytical dynamic models using modal test data. *AIAA Paper No. 80-0800.* Seattle, Washington.

Berman, A. and Nagy, J. (1983). Improvement of a large analytical model using test data. *AIAA J.*, **21**(8). 1168-1173.

Berman, A. and Fuh, J.-S. (1990). Structural system identification using multiple tests. *AIAA Dynamics Specialist Conference.* April 5-6. Long Beach, California. 99-104.

Bowels, R. L. and Straeter, T. A. (1972). System identification computational considerations. From *System Identification of Vibrating Structures* (Pilkey and Cohen, eds.). ASME. New York, N. Y., 23-44.

Brandon, J. A. (1988). On the robustness of algorithms for the computation of the pseudo inverse for modal analysis. *6th IMAC.* 397-400.

Braun, S. G. and Ram, Y. M. (1991). Predicting the effect of structural modification: upper and lower bounds due to modal truncation. *The International Journal of Analytical and Experimental Modal Analysis.* **6**(3). 201-213.

Brown, D., Allemang, R., and Zimmerman, R. (1979). Parameter estimation techniques for modal analysis. *Society of Automotive Engineers.* Paper No. 790221.

Burke, B. G., Sundararajan, C., and Safaie, F. M. (1980). Characterization of ambient vibration data by response shape vectors. *The 12th Annual Offshore Technology Conference.* May 5-8. Houston, Texas. Paper No. OTC 3862. 63-76.

C

Carasso, A. S. and Simiu, E. (1989). Identification of dynamic Green's functions in structural networks. *AIAA J.*, **27**(4). 492-499.

Caravani, P. and Thomson, W. T. (1974). Identification of damping coefficients in multidimensional linear systems. *Journal of Applied Mechanics. Transaction of the ASME.* 379-382.

Cawley, P. and Adams, R. D. (1979). The location of defects in structures from measurements of natural frequencies. *Journal of Strain Analysis.* **14**(2). 49-57.

Cawley, P. (1985). Non-destructive testing of mass produced components by natural frequency measurements. *Proc Instn Mech Engrs.*, **199**(B3). 161-168.

Chen, J.-C. and Wada, B. K. (1975). Criteria for analysis-test correlation of structural dynamic systems. *Journal of Applied Mechanics. Transaction of the ASME.* **42**. 471-477.

Chen, J.-C. and Wada, B. K. (1977). Matrix perturbation for structural dynamic analysis. *AIAA J.*, **15**(8). 1095-1100.

Chen, J.-C. and Garba, J. A. (1980). Analytical model improvement using modal test results. *AIAA J.*, **18**(6). 684-690.

Chen, J.-C., Kuo, C., and Garba, J. A. (1983). Direct structural parameter identification by model test results. *Proceedings of the AIAA/ASME/ASCE/AHS 24th Structures, Structural Dynamics and Materials Conference, Collection of Tech. Papers Part 2*. May 2-4. Lake Tahoe, Nevada. AIAA Paper No. 83-0812.

Chen, J.-C. and Garba, J. A. (1987). On orbit damage assessment for large space structures. *Proceedings of the AIAA/ASME/ASCE/AHS 28th Structures, Structural Dynamics and Materials Conference*. April. AIAA. New York, N. Y., 714-721.

Chen, S.-Y. and Fuh, J.-S. (1984). Application of the generalized inverse in structural system identification. *AIAA J.*, **22**(12). Technical Notes. 1827-1828.

Chen, T.-Y. and Wang, B. P. (1988). Finite element model refinement using modal analysis data. *Proceedings of the AIAA/ASME/ASCE/AHS 29th Structures, Structural Dynamics and Materials Conference, Part 3*. April. 18-20. AIAA. Williamsburg, Virginia. 1219-1229.

Chou, C.-M. and Wu, C-H. (1990). System identification and damage localization of dynamic structures. *AIAA Dynamics Specialist Conference*. April. Long Beach, California. 99-104.

Cividini, A., Jurina, L., and Gioda, G. (1981). Some aspects of "characterization" problems in geomechanics. *Int. J. Rock Mech. Min. Sci. & Geomech. Abstr.*, **18**. 487-503.

Clough, R. and Penzien, J. (1975). *Dynamics of Structures*. McGraw-Hill Book Company. New York, N. Y.

Cole, Jr., H. A. (1973). On-line failure detection and damping measurements of aerospace structures by random decremental signatures. *NASA CR-2205*.

Collin, N. and Natke, H. G. (1985). Updating mathematical models on basis of vibration and modal test results -a review of experience. *Proceedings of International Symposium on Aeroelasticity*. Achen.

Collin, N. and Natke, H. G. (1986). On the parameter identification of elastomechanical systems using weighted input and modal residuals. *Ing. Archive*. **56**. 106-113.

Collins, J. D., Young, J. P., and Kiefling, L. (1972). Methods and application of system identification in shock and vibration. From *System Identification of Vibrating Structures* (Pilkey and Cohen, eds.). ASME. New York, N. Y., 45-72.

Collins, J. D., Hart, G. C., Hasselman, T. K., and Kennedy, B. (1974). Statistical identification of structures. *AIAA J.*, **12**(2). 185-190.

Coppolino, R. N. and Rubin, S. (1980). Detectability of structural failures in offshore platforms by ambient vibration monitoring. *The 12th Annual Offshore Technology Conference*. May 5-8. Houston, Texas. Paper No. OTC 3865. 101-110.

Courage, W. M. G., Schreurs, P. J. G., and Janssen, J. D. (1990). Estimation of mechanical parameter values of composites with the use of finite element and system identification techniques. *Computers & Structures*. **34**(2). 231-237.

Cuschieri, J. M. (1987). The relation between dynamic and static response of a structure. *Noise Control Engineering*. **29**(2). 45-53.

D

D'Cruz, J., Crisp, J. D. C., and Ryall, T. G. (1990). Determining a force acting on a plate -an inverse problem. *AIAA J.*, **29**(3). 464-470.

Dennis, J. E. Jr. and Schnabel, R. B. (1983). *Numerical methods for unconstrained optimization and nonlinear equations*. Prentice-Hall, Inc., Englewood Cliffs, New Jersey.

DiPasquale, E. and Cakmak, A. S. (1990). Detection of seismic structural damage using parameter-based global damaged indices. *Probabilistic Engineering Mechanics*. **5**(2). 60-65.

Distefano, N. and Rath, A. (1975). System identification in nonlinear structural seismic dynamics. *Computer Methods in Applied Mechanics and Engineering*. **5**. 353-372.

Distefano, N. and Pena-Pardo, B. (1976). System identification of frames under seismic loads. *ASCE Journal of the Engineering Mechanics Division*. **102**(EM2). 313-330.

Dobbs, M. and Nelson, R. (1983). Parameter identification of large structural models - concept and reality, part of AMD -Vol. 59 Modal Testing and Model Refinement (D. Chu, ed.) *ASME App. Mech. Div.*, 119-133.

Douglas, B. M. and Reid, W. H. (1982). Dynamic tests and system identification of bridges. *ASCE Journal of Structural Division*. **108**(10).

Duggan, D. M., Wallace, E. R., and Caldwell, S. R. (1980). Measured and predicted vibrational behavior of gulf of Mexico platform. *The 12th Annual Offshore Technology Conference*. May 5-8. Houston, Texas. Paper No. OTC 3864. 91-100.

Dunker, K. R. and Rabbat B. G. (1993). Why America's bridges are crumbling. *Scientific American*. March. 66-72.

E

Ellis, J. H., Zimmerman, J. J., and Corotis, R. B. (1990). Stochastic Programs for identifying critical structural collapse mechanisms. *Applied Mathematical Modelling*.

Ewins, D. J. (1975). Measurement and application of mechanical impedance data. *JSEE*. Dec. 1975-June 1976.

Ewins, D. J. and Gleeson, P. (1982). A method for modal identification of lightly damped structures. *Journal of Sound and Vibration*. **84**(1). 57-79.

Ewins, D. J. (1984). *Modal testing: theory and practice*. John Wiley & Sons, Inc., New York, N. Y.

Eykhoff, P. (1974). *System identification, parameter and state estimation*. John Wiley & Sons, Inc., New York, N. Y.

Eykhoff, P. (1981). Trends and progress in system identification. *IFAC Series for Graduates, Research Workers and Practising Engineers, Volume 1*. Pergamon Press.

F

Fassois, S. D. (1990). A fast rational model approach to parametric spectral estimation-Part I: The algorithms. *Journal of vibration and Acoustics*. **112**. 321-327.

Fassois, S. D. (1990). A fast rational model approach to parametric spectral estimation-Part II: Properties and performance evaluation. *Journal of vibration and Acoustics*. **112**. 328-336.

Fassois, S. D., Eman, K. F., and Wu, S. M. (1990). A linear time-domain method for structural dynamics identification. *Journal of vibration and Acoustics*. **112**. 98-106.

Finigan, B. M. and Rowe, I. H. (1974). Strongly consistent parameter estimation by the introduction of strong instrumental variables. *IEEE Transactions on Automatic Control*. **AC-19**(6). 825-830.

Fissette, E., Stavrinidis, C., and Ibrahim, S. R. (1988). Error location and updating of analytical models using a force balance method. *Proceedings of the 6th International Modal Analysis Conference*. Orlando, Florida. 1063-1070.

Flannelly, W. and Berman, A. (1983). The state of the art of system identification of aerospace structures, part of AMD Vol. 59 Modal Testing and Model Refinement, (D. Chu, *ed.*). *ASME App. Mech. Div.*, 121-131.

Flanigan, C. (1987). Test/analysis correlation of the STS CENTAUR using design sensitivity and optimatization methods. *Proc. of the 5th Int'l Modal Analysis Conf.*, London, England.

Flanigan, C. (1988). Test/analysis correlation using design sensitivity and optimization. *SAE Paper No. 871743*. 6.834-6.841.

Flesch, R. G. and Kernbichler (1988). A dynamic method for safety inspection of large prestressed bridges. *Proceeding of International Workshop on Nondestructive Evaluation for Performance of Civil Structures.* University of Souther California. Los Angeles, California.

Foster, C. D. and Mottershead, J. E. (1990). A method for improving finite element models by using experimental data: application and implications for vibration monitoring. *Int. J. Mech. Sci.*, **32**(3). 191-203.

Friswell, M. I. (1990). Candidate reduced order models for structural parameter estimation. *Journal of vibration and Acoustics.* **112**. 93-97.

Fritzen, C.-P. (1986). Identification of mass, damping, and stiffness matrices of mechanical systems. *ASME Journal of Vibration, Acoustics, Stress, and Reliability in Design.* **108**. 9-16.

Fuh, J.-S. and Berman, A. (1986). Comment on: stiffness matrix correction from incomplete test data. *AIAA J.*, **24**(8). 1405-1406.

Fuh, J.-S., Gustavson, B., and Berman, A. (1986). Error estimation and compensation in reduced dynamic models of large space structures. *AIAA Paper No. 86-0837.* 1-9.

G

Garba, J. and Wada, B. (1977). Application of perturbation methods to improve analytical model correlation with test data. *SAE Paper No. 770959.* Los Angeles, California.

Gersch, W. (1974). On the achievable accuracy of the structural system parameter estimates. *Journal of Sound and Vibration.* **34**(1). 63-79.

Gersch, W. and Foutch, D. A. (1974). Least squares estimates of structural system parameters using covarience function data. *IEEE Transactions on Automatic Control.* **AC-19**(6). 898-903

Ghaboussi, J. (1987). Generalized differences in direct integration methods for analysis. *Proceeding of the International Conference on Numerical Methods in Engineering: Theory and Applications (NUMETA 87).* July. Swansea, U.K.

Ghaffar-Zadeh, M. and Chapel, F. (1983). Frequency-independent impedances of soil-structure system in horizontal and rocking modes. *Earthquake Engineering and Structural Dynamics.* **11**. 523-540.

Gladwell, G. M. L. (1986). *Inverse problems in vibration.* Martinus Nijhoff, Dordrecht.

Gladwell, G. M. L. and Dods, S. R. A. (1987). Examples of reconstruction of vibrating rods from spectral data. *Journal of Sound and Vibration.* **119**(2). 267-276.

Gladwell, G. M. L., England, A. H., and Wang, D. (1987). Examples of reconstruction of a euler-bernoulli beam from spectral data. *Journal of Sound and Vibration.* **119**(1). 81-94.

Glaser, R. J., Kuo, C. P., and Wada, B. K. (1992). Improvement of structural models using covarience analysis and nonlinear generalized least squares. *AIAA J.*, **30**(1). 226-233.

Golub, G. H. and Van Loan, C. F. (1983). *Matrix computations.* The Johns Hopkins University Press. Baltimore, Maryland.

Goodwin, G. C. (1984). *Adaptive filtering prediction and control.* Prentice-Hall Inc., Englewood Cliffs, N. J.

Goyder, H. (1978). *ISVR. Ph. D. Thesis.* University of Southampton.

Gravitz, S. (1958). An automated procedure for orthogonalization of experimentally measured modes. *Journal of Aerospace Sciences.* **25**. 721-722.

Grossman, D. (1982). An automated technique for improving model test/analysis correlation. *AIAA Paper No. 82-0640.* New Orleans.

Gundy, W. E., Scharton, T. D., and Thomas, R. L. (1980). Damping measurements on an offshore platform. *The 12th Annual Offshore Technology Conference.* May 5-8. Houston, Texas. Paper No. OTC 3863. 77-90.

Gysin, H. (1986). Critical application of the error matrix for localization of finite element modeling inaccuracies. *Proceedings of the 4th International Modal Analysis Conference.* 1339-1351.

H

Hac, A. and Spanos, P. D. (1990). Time domain method for parameter system identification. *Journal of vibration and Acoustics.* **112.** 281-287.

Hajela, P. and Soeiro, F. J. (1988). Structural damage assessment as an identification problem. *Proceedings of the NASA/Air Force Symposium on Multidisiplinary Analysis and Optimization.* September. 1507-1520.

Hajela, P. (1990). Genetic search -An approach to the nonconvex optimization problem. *AIAA J.*, **28**(7). 1205-1210.

Hajela, P. and Soerio, F. J. (1990). Recent developments in damage detection based on system identification methods. *Structural Optimization.* **2.** 1-10.

Hajela, P. and Soeiro, F. (1990). Structural damage detection based on static and modal analysis. *AIAA J.*, **28**(6). 1110-1115.

Hall, B. (1970). Linear estimation of structural parameters from dynamic test data. *Proceedings of AIAA/ASME 11th Structures, Structural Dynamics and Materials Conference.* 193-197.

Hart, G. C. and Torkamani, M. A. M. (1974). Structural system identification. from *Stochastic problems in mechanics.* University of Waterloo Press, Waterloo. 207-228.

Hart, G. C. and Yao, J. T. P. (1977). System identification in structural dynamics. *ASCE Journal of the Engineering Mechanics Division.* **103**(EM6). 1089-1104.

Hashemi-Kia, M. (1988). Investigation of dynamic characteristics of an elastic wings model by using corrections of mass and stiffness matrices. *Journal of Sound and Vibration.* **121**(1). 67-76.

Hashin, Z. (1983). Analysis of composite materials -a survey. *Journal of Applied Mechanics. Transaction of the ASME.* **50.** 481-505.

Hasselman, T. K. (1972). A perspective on dynamic model verification. *ASME Winter Annual Meeting.* 101-117.

Heylen, W. and Vanhonacker, P. (1983). An automated technique for improving model matrices by means of experimentally obtained data. *AIAA Paper 83-0881.*

Heylen, W., Sas, P., and Leuven, K. U. (1987). Review of model optimization techniques. *The 5th International Modal Analysis Conference.* 1177-1182.

Hjelmstad, K. D., Wood, S. L., and Clark, S. J. (1990). Parameter estimation in complex linear structures. *Report No. SRS 557, UILU-ENG-90-2015.* University of Illinois at Urbana-Champaign. Urbana, Illinois.

Hjelmstad, K. D., Wood, S. L., and Clark, S. J. (1992). Mutual residual energy method for parameter estimation in structures. *ASCE Journal of Structural Engineering.* **118**(1). 223-242.

Ho, I.-K. and Aktan, A. E. (1989). Linearized identification of buildings with cores for seismic vulnerability assessment. *National Center for Earthquake Engineering Research.* State University of New York at Buffalo. Technical Report NCEER-89-0041.

Hoff, C. (1989). The use of reduced finite element models in system identification. *Earthquake Engineering and Structural Dynamics.* **18.** 875-887.

Hollkamp, J. J. and Batill, S. M. (1989). Noise bias in various formulations of Ibrahim's time domain technique. *AIAA J.*, **27**(8). 1142-1145.

Hollkamp, J. J. and Batill, S. M. (1991). Automated parameter identification and order reduction for discrete time series models. *AIAA J.*, **29**(1). 96-103.

Holmes, J. K. (1968). System identification from noise-corrupted measurements. *Journal of Optimization Theory and Applications.* **2**(2). 102-116.

Housner, *et al.* (1990). *Competing Against Time.* Report to Governor George Deukmejian from The Governor's Board of Inquiry on the 1989 Loma Prieta Earthquake.

I

Ibanez, P. (1974). Methods for the identification of dynamic parameters of mathematical structural models from experimental data. *Nuclear Engineering and Design.* **27**. 209-219.

Ibrahim, S. R. and Mikulcik, E. (1973). A time domain modal vibration test technique. *The Shock and Vibration Bulletin.* 43(4).

Ibrahim, S. R. and Mikulcik, E. (1976). The experimental determination of vibration parameters from time response. *The Shock and Vibration Bulletin.* 46.

Ibrahim, S. R. (1977). Random decrement technique for modal identification of structures. *AIAA Journal of Spacecraft and Rockets.* **14**. 696-700.

Ibrahim, S. R. and Mikulcik, E. (1977). A method for the direct identification of vibration parameters from the free response. *The Shock and Vibration Bulletin.* 47(4). 183-198.

Ibrahim, S. R. (1978). Modal confidence factor in vibration testing. *AIAA Journal of Spacecraft and Rockets.* **15**. 313-316.

Ibrahim, S. R. and Pappa, R. S. (1982). Large survey testing using the Ibrahim time domain (ITD) modal identification algorithm. *AIAA Journal of Spacecraft and Rockets.* **19**. 459-465.

Ibrahim, S. R. (1983). Computation of normal modes from identified complex modes. *AIAA J.*, **21**(3). 446-451.

Ibrahim, S. R. (1984). Time domain quasi linear identification of nonlinear dynamic systems. *AIAA J.*, **22**. 817-823.

Ibrahim. S. R. (1986). Double least squares approach for use in structural modal identification. *AIAA J.*, **24**. 499-503.

Ibrahim, S. R. and Saafan A. (1987) Correlation of analysis and test in modeling of structures assessment and review. *The 5th International Modal Analysis Conference.* 1651-1660.

Ibrahim. S. R., Stavrinidis, C., Fissette, E., and Brunner, O. (1990). A direct two response approach for updating analytical dynamic models of structures with emphasis on uniqueness. *Journal of Vibration and Acoustics.* **112**. 107-111.

IFAC (1981). Identification and system parameter estimation. *Automatica.* **17**(1).

IFAC (1982). Identification and system parameter estimation, volume 1. *Proceeding of the Sixth IFAC Symposium.* June 7-11. Washington, D. C..

IFAC (1982). Identification and system parameter estimation, volume 2. *Proceeding of the Sixth IFAC Symposium.* June 7-11. Washington, D. C.

IFAC (1990). Identification and system parameter estimation. *Automatica.* **26**(1).

Ismail, F., Ibrahim, A., and Martin, H. R. (1990). Identification of fatigue cracks from vibration testing. *Journal of Sound and Vibration.* 140(2). 305-317.

J

Janter, T. and Sas, P. (1990). Uniqueness aspects of model-updating procedures. *AIAA J.*, **28**(3). 538-543.

Jiang, J.-S., Gu, S.-N., Wang, Y.-J., and Yao, Q.-H. (1990). A modal parameter identification technique and its application to large complex structures with multiple steady sinusoidal excitation. *Journal of Sound and Vibration.* 138(2). 221-231.

K

Kabe, A. M. (1985). Constrained adjustment of analytical stiffness matrices. *Structural Dynamic Testing and Analysis, SAE Aerospace and Technology Conference and Exposition.* October 14-17. Long Beach, California. Paper No. 851932.

Kabe, A. M. (1985). Stiffness matrix adjustment using mode data. *AIAA J.*, **23**(9). 1431-1436.

Kabe, A. M. (1990). Mode shape identification and orthogonalization. *AIAA J.*, **28**(4). 711-716.

Kammer, D., Jensen, B., and Mason, D. (1988). Test-analysis correlation of the space shuttle solid rocket motor center segment. *Proceedings of the AIAA/ASME/ASCE/AHS 29th Structures, Structural Dynamics and Materials Conference, Part 3*. AIAA. April 18-20. 1474-1486.

Kay, S. M. and Marple, S. L. (1981). Spectrum analysis -a modern perspective. *IEEE proceedings*. **69**(11).

Kendal, M. G., and Stuart, A. (1961). *The advanced theory of statistics, Vol. 2*. Griffen, London.

Kenley, R. M. and Dodds, C. J. (1980). West sole we platform: detection of damage by structural response measurements. *The 12th Annual Offshore Technology Conference*. May 5-8. Houston, Texas. Paper No. OTC 3866. 111-118.

Klosterman, A. (1971). On the experimental determination and use of modal representation of dynamic characteristics. Ph.D. Dissertation. University of Cincinnati, Cincinnati, Ohio.

Klosterman, A. L. and McClelland, W. A. (1973). Combining experimental and analytical techniques for dynamic system analysis. *Structural Dynamics Research Corporation*. Cincinnati, Ohio.

Kuo, C. P. and Wada, B. K. (1990). Truss space structures system identification using the multiple boundary condition test method. *AIAA J.*, **28**(7). 1246-1249.

L

Lee, A.-C. and Chen, J.-H. (1989). Modal analysis for randomly excited structural system with unmeasured input. *Journal of Sound and Vibration*. **132**(1). 101-113.

Lee, C.-K. and Moon, F. C. (1990). Modal sensors/actuators. *Transactions of the ASME*. **57**. 434-441.

Leonard, J. W. and Khouri, B. R. (1985). System identification using a standard finite element program. *Engng. Struct.*, **7**. 190-197.

Liang, Z. and Inman, D. J. (1990). Matrix decomposition methods in experimental modal analysis. *Transactions of the ASME*. **112**. 410-413.

Lim, T. W. (1990). Submatrix approach to stiffness matrix correction using model test data. *AIAA J.*, **28**(8). 1123-1130.

Link, M. and Vollan, A. (1978). Identification of structural system parameters from dynamic response data. *Z. Flugwiss. Weltraumforsch.* **2**(3). 165-175.

Link, M. (1985). Theory of a method for identifying incomplete system matrices from vibration test data. *Z. Flugwiss. Weltraumforsch.* **9**(2). 76-82.

Ljung, L. and Glover, K. (1981). Frequency domain versus time domain methods in system identification. *Automatica*. **17**(1). 71-90.

Loland, O. and Dodds, C. J. (1976). Experiences in developing and operating integrity monitoring systems in the north sea. *The 8th Annual Offshore Technology Conference*. May 3-6. Houston, Texas. Paper No. OTC 2551. 313-319.

Luengerger, D. G. (1969). *Optimization by vector space methods*. John Wiley & Sons, Inc., New York, N. Y.

Luenberger, D. G. (1984). *Linear and nonlinear programming* (second edition). Addison-Wesley Publishing Co., Reading, Massachusetts.

Luk, Y. and Mitchell, L. (1983). System identification via modal analysis, part of AMD -Vol 59 Modal Testing and Model Refinement (D. Chu, ed.). *ASME App. Mech. Div.*, 31-49.

Lytton, R. L., Germann, F. P., Chou, Y. J., and Stoffels, S. M. (1990). determining asphaltic concrete pavement structural properties by nondestructive testing. *National Cooperative Highway Research Program*. Report No. 327. Texas Transportation Institute, The Texas A&M University System, College Station, Texas.

M

Maguire, J. R. and Severn, R. T. (1987). Assessing the dynamic properties of prototype structures by hammer testing. *Proc. Instn. Civ. Engrs. Part 2.* 83. 769-784.

Marczyk, J. (1987). Time-variable reduced order models: an approach to identification and active shape-control of large space structures. *Proceedings of the VPI & AIAA 6th Symposium on Dynamics and Control of Large Structures.*

Masri, S. F., Miller, R. K., Saud, A. F., and Caughey, T. K. (1987). Identification of nonlinear vibrating structures: Part I -formulation. *Journal of Applied Mechanics. Transaction of the ASME.* 54. 918-922.

Masri, S. F., Miller, R. K., Saud, A. F., and Caughey, T. K. (1987). Identification of nonlinear vibrating structures: Part II -applications. *Journal of Applied Mechanics. Transaction of the ASME* 54. 923-929.

Matko, D. and Schumann, R. (1982). Comparative stochastic convergence analysis of seven recursive parameter estimation methods. *Proceeding of the Sixth IFAC Symposium.* June. Washington, D. C.

Maybeck, P. S. (1982). *Stochastic models, estimation, and control.* Volume 2. Academic Press. New York, N. Y.

McGrew, J. (1969). Orthogonalization of measured modes and calculation of influence coefficients. *AIAA J.*, 7. 774-776.

McLamore, V. R., Hart, G. C., and Stubbs, I. R. (1971). Ambient vibration of two suspension bridges. *ASCE Journal of Structural Division.* 97(10).

Meirovitch, L. and Baruh, H. (1985). The implementation of modal filters for control of structures. *AIAA Journal of Guidance.* 8(6). 707-716.

Meirovitch, L. and Norris, M. A. (1987). An iterative approach to parameter identification in structures. *Experimental Mechanics and Manufacturers exhibition.* June 14-19. Houston, Texas.

Meirovitch, L., Norris, M. A., and Williams, J. P. (1987). A Rayleigh-Ritz approach to structural parameter identification. *Proceedings of the VPI & SU/AIAA 6th Symposium on Dynamics and Control of Large Structures.* 171-183.

Minas, C. and Inman, D. J. (1990). Matching finite element models to modal data. *Journal of Vibration and Acoustics.* 112. 84-92.

Mook, D. J. and Lew, J. (1988). A combined ERA/MME algorithm for robust system realization/identification. *Proceedings of the 29th SDM conference.* Williamsburg, Virginia. 1556-1564.

Mottershead, J. E. (1990). Theory for the estimation of structural vibration parameters from incomplete data. *AIAA J.*, 28(3). 559-561.

Mottershead, J. E., Tee, T. K., Foster, C. D., and Stanway, R. (1990). An experiment to identify the structural dynamics of a portal frame. *Journal of Vibration and Acoustics.* 112. 78-83.

N

Natke, H. G. and Yao, J. T.-P. (1988). Structural safety evaluation based on system identification approaches. *Proceedings of the Workshop at Lambrecht/Pfaltz.* Friedr. Vieweg & Sohn. Braunschweig.

Natke, H. G. (1989). Identification approaches in damage detection and diagnosis. *Diagnostics '89.* Politechnika Poznanska, Rydzyna.

Netravali, A. N., Huang, T. S., Krishnakumar, A. S., and Holt, R. J. (1989). Algebraic methods in 3-D motion estimation from two-view point correspondences. *International Journal of Imaging Systems and Technology.* 1. 78-99.

Neidbal, N. and Klusowski, E. (1990). Optimal exciter placement and force vector tuning required for experimental modal analysis. *AIAA Dynamics Specialist Conference.* April 5-6. Long Beach, California. 130-141.

Norris, M. and Meirovitch, L. (1989). On the problem of modelling for parameter identification in distributed structures. *International Journal for Numerical Methods in Engineering.* 28. 2451-2463.

O

O'Callahan, J. C., Avitable, P., Lieu, I. W., and Madden, R. (1986). An efficient method for determining rotational degrees of freedom from analytical and experimental data. *Proceedings of the 4th International Modal Analysis Conference*. Los Angeles, California. 50-58.

O'Callahan, J. C. and Chou, C.-M. (1988). Localization of model changes for optimized system matrices using modal test data. *6th IMAC*. 49-55.

O'Callahan, J. C. and Chou, C.-M. (1989). Localization of model errors in optimized mass and stiffness matrices using modal test-data. *Journal of Modal Analysis*. 8-14.

Oppenheim, A. V. and Shafer, R. W. (1975). *Digital signal processing*. Prentice-Hall. Engelwood Cliffs, N.J.

Otnes, R. L. and Enochson, L. (1978). *Applied time series analysis. Volume 1*. John Wiley and Sons, Inc., New York, N. Y.

Ozaki, T. (1989). Statistical identification of nonlinear random vibration systems. *Transactions of the ASME*. **56**. 186-191.

P

Papageorgiou, A. S. and Lin, B.-C. (1989). Influence of lateral-load-resisting system on the earthquake response of structures -A system identification study. *Earthquake Engineering and Structural Dynamics*. **18**. 799-814.

Papageorgiou, A. S. (1991). Analysis of recorded earthquake response and identification of a multi-story structure accounting for foundation interaction effects. *Journal of Soil Dynamics and Earthquake Engineering*. **10**(1). 55-64.

Pappa, R. S. and Ibrahim, S. R. (1981). A parametric study of the Ibrahim time domain modal identification algorithm. *Journal of Shock and Vibration*. **51**. 43-72.

Park, S. K. and Miller, K. W. (1988). Random number generators: good ones are hard to find. *Communications of the ACM.*, **31**(10). 1192-1201.

Park, S. K. and Jensen D. (1989). A systematic determination of lumped and improved consistent mass matrices for vibration analysis. *Proceedings of the AIAA/ASME/ASCE/AHS 30th Structures, Structural Dynamics and Materials Conference, Part 3*. AIAA. 1532-1540.

Peng, C. (1987). Generalized modal identification of linear and nonlinear dynamic systems. *Report No. EERL 87-05*. California Institute of Technology. Pasadena, California.

Pentland, A. (1990). Dynamic surface estimation using wavelet bases. *M.I.T. Media Lab Vision and Modeling Group*. Technical Report No. 142.

Pentland, A. and Horowitz, B. (1990). Recovery of non-rigid motion and structure. *M.I.T. Media Lab Vision and Modeling Group*. Technical Report No. 136.

Pi, Y.-L. and Mickleborough, N. C. (1989). Modal identification of a vibrating structure in the time domain. *Computers & Structures*. **32**(5). 1105-1115.

Pilkey, W. and Cohen, R., eds. (1972). Mathematical Models from Test Data. From *System identification of vibrating structures*. (Pilkey and Cohen, eds.). ASME. New York, N. Y.

Potter, R. and Richardson, M. (1974). Mass, stiffness, and damping matrices from measured modal parameters. *Advances in Instrumentation*. **29**(Part 2). Proceedings of ISA International Instrumentation-Automation Conference. October 28-31. New York, N. Y.

Press, W., Flannery, B., Teukolsky, S., and Vetterling, W. (1986). *Numerical Recipes*. Cambridge University Press.

Q

Qunli, W. and Fricke, F. (1991). Determination of the size of an object and its location in a rectangular cavity by eigenfrequency shifts: first order approximation. *Journal of Sound and Vibration*. **144**(1). 131-147.

R

Raghavendrachar, M. Shelley, S. J., and Aktan, A. E. (1991). Modal test by impact for bridge diagnosis. Unpublished.

Richardson, M. (1989). Can structural mass, stiffness, and damping be obtained from vibration measurements? *21st Midwestern Mechanics Conference*. August 13-16. Houghton, MI.

Ricles, J. M. and Kosmatka, J. B. (1990). Damage detection in elastic structures using vibratory residual forces and weighted sensitivity. *AIAA Dynamics Specialist Conference*. April 5-6. Long Beach, California. 99-104.

Rizos, P. F., Aspragathos, M., and Dimarogonas, A. D. (1990). Identification of crack location and magnitude in a cantilever beam from the vibration modes. *Journal of Sound and Vibration*. **138**(3). 381-388.

Rodden, W. (1967). A method for deriving structural influence coefficients from ground vibration tests. *AIAA J.*, **5**. 991-1000.

Rodden, W. (1977). Comment on orthogonal check and correction of measured modes. *AIAA J.*, **15**. 1054.

Rodden. W. (1981). Comment on proportional optimal orthogonalization of measured modes. *AIAA J.*, **19**. 543-544.

Ross, R. G. (1971). Synthesis of stiffness and mass matrices from experimental vibration modes. *SAE Transactions*. 80(4). 2627-2635.

S

Sage, A. P. (1972). System identification -history, methodology, future prospects. From *System Identification of Vibrating Structures* (Pilkey and Cohen, eds.). ASME. New York, N. Y.

Salane, H. and Baldwin, J. (1990). Changes in modal parameters of a bridge during fatigue testing. *Experimental Mechanics*. 30(2). 109-113.

Sanayei, M. and Nelson, R. B. (1986). Identification of structural element stiffnesses from incomplete static test data. *SAE Technical Papers Series No. 861793*. 7.1237-7.1248.

Sanayei, M. and Onipede, O. (1991). Damage assessment of structures using static test data. *AIAA J.*, **29**(7). 1174-1179.

Sanayei, M. and Scampoli, S. F. (1991). Structural element stiffness identification from static test data. *Journal of Engineering Mechanics*. **117**(5). 1021-1036.

Sanayei, M. (1992). Pre-test selection of static force and displacement measurement locations for damage assessment. *ASCE Special Conference: Probabilistic mechanics and Structural & Geotechnical Reliability*. July 8-10. Denver, Colorado. 567-570.

Sanayei, M., Onipede, O., and Babu, S. (1992). Selection of noisy measurement locations for error reduction in static parameter identification. *AIAA J.*, **30**(9). 2299-2309.

Sheena, Z., Unger, A., and Zalmanovich, A. (1982). Theoretical stiffness matrix correction by using static test results. *Israel Journal of Technology*. **20**. 245-253.

Shepard, G. (1987). Spatial distribution of model error based on analytical/experimental frequency discrepancies. *Proceedings of the 5th International Modal Analysis Conference*. 1665-1668.

Sidhu, J. and Ewins, D. (1984). Correlation of finite element and model test studies of a practical structure. *Proceedings of the 2nd International Modal Analysis Conference*. Orlando, Florida. 756-762.

Soderstrom, T. and Stocia, P. (1981). Comparison of some instrumental variables methods -consistency and accuracy aspects. *Automatica*. **17**(1). 101-115

Soeiro, F. J. and Hajela, P. (1990). Damage detection in composite materials using identification techniques. *AIAA Paper No. 90-0917-CP*. 950-960.

Stavrinidis, C., Clinckemaillie, J., and Dubois, J. (1989). New concepts for finite-element mass matrix formulations. *AIAA J.*, **27**(9). 1249-1255.

Strang, G. (1986). *Introduction to applied mathematics.* Wellesley Cambridge Press. Wellesley, Massachusetts.

Strejc, V. (1981). Trends in identification. *Automatica.* **17**(1). 7-21.

Stubbs, N., Broome, T.H., and Osegueda, R. (1989). Nondestructive construction error detection in large space structures. *AIAA J.,* **28**(1). 146-152.

Surana, K. S. and Huels, C. R. (1989). A least squares finite element solution of the inverse problem of aquifer transmissivity. *Computers & Structures.* **31**(2). 249-268.

T

Ta'asan, S. and Dutt, P. (1990). Parameter estimation problems for distributed systems using a multigrid method. *Quart. Appl. Math.,* **XLVIII** (2). 387-396.

Tan, R. Y. and Cheng, W. M. (1993). System identification of a non-classically damped linear system. *Computers & Structures.* **46**(1). 67-75.

Tan, R. Y. and Wang, G. (1989). Safety evaluation of a tall building. *The 5th International Conference on Structural Safety and Reliability.* San Francisco, California. **2**. 1451-1458.

Targoff, W. (1976). Orthogonal check and correction of measured modes. *AIAA J.,* **14**. 164-167.

Targoff, W. (1977). Reply to author W. Rodden. *AIAA J.,* **15**. 1054-1056.

Thoren, A. R. (1972). Derivation of mass and stiffness from dynamic test data. *AIAA/ASME/SAE 13th Structures, Structural Dynamics, and Materials Conference.* April 10-12. San Antonio, Texas. AIAA Paper No. 72-346.

Torkamani, M. A. M and Ahmadi, A. K. (1988). Stiffness identification of two- and three-dimensional frames. *Earthquake Engineering and Structural Dynamics.* **16**(8). 1157-1176.

Torkamani, M. A. M. and Ahmadi, M. K. (1988). Stiffness identification of a tall building during construction period using ambient tests. *Earthquake Engineering and Structural Dynamics.* **16**. 1177-1188.

Torkamani, M. A. M. and Ahmadi, M. K. (1988). Stiffness identification of framed using simulated ground excitation. *ASCE Journal of Engineering Mechanics.* **114**(5). 753-776.

Trenkler, G. (1981). Mathematical systems in economics. Gunn & Hain, Publication, Inc., Germany

Tsai, H.-C. and Kelly, J. M. (1989). Dynamic parameter identification for non-linear isolation systems in response spectrum analysis. *Earthquake Engineering and Structural Dynamics.* **18**. 1119-1132.

Tsen, F.-M. and Mook, D. J. (1987). Linear system identification using matrix exponential sensitivities. *Proceedings of the VPI & SU/AIAA 6th Symposium on Dynamics and Control of Large Structures.* 119-126.

Tustin, W. and Mercado, R. (1985). Machinery health monitoring -an application of spectrum analysis. *Journal of Society of Environmental Engineers.* 17-22.

U

Udwadia, F. E. and Sharma, D. K. (1978). Some uniqueness results related to building structural identification. *SIAM Journal of Applied Mathematics.* **34**(1). 104-118.

Udwadia, F. E., Sharma, D. K., and Shah, P. C. (1978). Uniqueness of damping and stiffness distributions in the identification of soil and structural systems. *Journal of Applied Mechanics. Transaction of the ASME.* **45**. 181-187.

Ujihara, B., Dosoky, M., and Tong, E. (1982). Improving a NASTRAN dynamic model with test data using LINWOOD. *10th Nastran Users Colloquium, NASA conf.,* Pub. No. 2249. 74-86.

V

Vandiver, J. K. (1975). Detection of structural failure on fixed platforms by measurement of dynamic response. *The 7th Annual Offshore Technology Conference.* May 5-8. Houston, Texas. OTC 2267. 243-252.

Van Loan, C. F. (1978). Computing integrals involving the matrix exponential. *IEEE Transaction on Automatic Control*. AC-23(3). 395-404.

Veletsos, A. S. and Ventura, C. E. (1986). Modal analysis of non-classical damped linear systems. *Earthquake Engineering and Structural Dynamics*. 14. 217-243.

Vold, H., Kundrat, J., Rocklin, T., and Russel, R. (1982). A multi-input modal estimation algorithm for minicomputers. *SAE Paper No. 820194*.

W

Wada, B., Garba, J., and Chen, J. (1983). Modal test and analysis correlation. AMD Vol. 59: *Modal Testing and Model Refinement* (D.Chu, ed.). ASME. 85-99.

Wada, B., Kuo, C., and Glaser, R. (1985). Multiple boundary conditions test (MBCT) approach to update mathematical models of large flexible structures. *SAE Aerospace and Technology Conference and Exposition*. October 14-17. Long Beach, California. SAE Paper No. 851933.

Wada, B. K., Fanson, J. L., and Crawley, E. F. (1990). Adaptive structures. *Mechanical Engineering*. 41-46.

Wang, B. P., and Chu, F. H. (1983). Structure model refinement using reanalysis techniques. AMD Vol. 59: *Modal Testing and Model Refinement* (D.Chu, ed.). ASME. 135-141.

Wang, B. P., Chu, F. H., and Trundle, C. (1983). Reanalysis techniques used to improve local uncertainties in model analysis. *Proceedings of the 3rd International Modal Analysis Conference*.

Wang, B. P., Chen, T., and Chu, F. H. (1986). Model refinement using test data. *Proceedings of the 4th International Modal Analysis Conference*. 1052-1057.

Wang, B. P. (1991). Closed form solution for minimum weight design with a frequency constraint. *AIAA J.*, 29(1). 152-154.

Wang, J.-H. (1988). Mechanical parameters identification, with special consideration of noise effects. *Journal of Sound and Vibration*. 125(1). 151-167.

Wang, J.-H. (1990). Prediction of vibration at inaccessible points using measurable data. *Journal of Sound and Vibration*. 138(2). 305-319.

Wang, M.-L., Paez, T. L., and Ju, F. (1987). System identification of nonlinear damaged structure. *International Journal of Analytical and Experimental Modal Analysis*. 2(3). 128-135.

Weaver Smith, S. and Hendricks, S. L. (1987). Evaluation of two identification methods for damage detection in large space trusses. *Proceedings of the VPISU/AIAA 6th Symposium on Dynamics and Control of Large Structures*. 127-141.

Weaver Smith, S. and Beattie, C. A. (1991). Secant-method adjustment for structural models. *AIAA J.*, 29(1). 119-126.

Wei, F.-S. (1980). Stiffness matrix correction from incomplete test data. *AIAA J.*, 18(10). 1274-1275.

Wei, F.-S. (1990). Analytical dynamic model improvement using vibration test data. *AIAA J.* 28(1). Technical Notes. 175-177.

Wei, M. L. and Janter, T. (1988). Optimization of mathematical model via selected physical parameters. *Proceedings of the 6th International Modal Analysis Conference*.

Weng, J., Huang, T. S., and Ahuja, N. (1987). 3-D motion estimation, understanding, and prediction from noisy image sequences. *IEEE Transactions on Pattern Analysis and Machine Intelligence*. 9(3). 370-387.

Werner, S. D., Douglas, B. M., and Course, C. B. (1989). System identification of Meloland road overcrossing. *Seismic Engineering: Research and Practice, Proceeding of Sessions Related to Seismic Engineering at Structures Congress*. San Francisco, California.

Werner, S. D., Nisar, A., and Beck, J. L. (1992). Assessment of UBC seismic design provisions using recorded building motions from Morgan Hill, Mount Lewis, and Loma Prieta Earthquakes. *Prepared for National Science Foundation. Grant No. BCS-9011136*. Dames & Moore.

White, C. W. and Maytum, B. D. (1976). Eigensolution sensitivity to parameter model perturbations. *Shock and Vibration Bulletin.* **46**(5). 463-470.

Wicks, A. L. and Han, M.-C. (1989). The estimation of the frequency response function using angular acceleration measurements. *Experimental Techniques.* 32-34.

Wilkinson, J. H. (1965). *The algebraic eigenvalue problem.* Oxford University Press. London, England.

Wilson, E. L. and Penzien, J. (1972). Evaluation of orthogonal damping matrices. *International Journal for Numerical Methods in Engineering.* **4**. 5-10.

Wong, K. Y. and Polak, P. (1967). Identification of linear discrete time systems using the instrumental variable method. *IEEE Transactions on Automatic Control.* **AC-12**(6). 707-718.

Y

Young, P. C. (1970). An instrumental variable method for real-time identification of a noisy process. *Automatica.* **6**. 271-287.

Young, P. C. (1981). Parameter estimation for continuous-time models-a survey. *Automatica.* **17**(1). 23-29.

Yurkovich, S. (1987). System identification experiments for flexible structure control. *Proceedings of the VPI & SU/ AIAA 6th Symposium on Dynamics and Control of Large Structures.* 143-157.

Z

Zadeh, L. A. (1962). From circuit theory to system theory. *Proc. IRE.* **50**. 856-865.

Zak, M. (1983). Discrete model improvement by eigenvector updating. *ASCE Journal of Engineering Mechanics.* **109**(6). 1437-1445.

Zhang, N. and Hayama, S. (1990). Identification of structural system parameters from time domain data (identification of the global modal parameters of a structural system by the improved state variable method). *JSME Int. J., Series III.* **33**(2). 168-175.

Zhang, Q. and Lallement, G. (1987). Dominant error localization in a finite element model of a mechanical structure. *Mechanical Systems and Signal Processing.* **1**(2). 141-149.

Zhang, Q. Lallement, G., Fillod, R., and Piranda, J. (1987). A complete procedure for the adjustment of a mathematical model from the identified compels modes. *Proceedings of the 5th International Modal Analysis Conference.* 1183-1190.

Zhang, W. C. and Evans, K. E. (1988). Numerical prediction of the mechanical properties of anisotropic composite materials. *Computers & Structures.* **29**. 413-422.

Zienkiewicz, O.C. (1977). A new look at the Newmark, Houbolt, and other time stepping formulas. A weighted residual approach. *Earthquake Engineering and Structural Dynamics.* **5**. 413-418.

Zienkiewicz, O.C. and Zhu, J. Z. (1987). A simple error estimator and adaptive procedure for practical engineering analysis. *International Journal for Numerical Methods in Engineering.* **24**. 337-357.

Zimoch, Z. (1987). Sensitivity analysis of vibrating systems. *Journal of Sound and Vibration.* **115**(3). 447-458.